

**DETERMINATION OF CO AND MN IN
MARINE WATERS USING FLOW
INJECTION WITH CHEMILUMINESCENCE
DETECTION.**

by

Vincenzo Cannizzaro

A thesis submitted to the University of Plymouth in partial fulfilment for the degree

of:

DOCTOR OF PHILOSOPHY

Department of Environmental Sciences

Faculty of Science

October 2001

90 0506528 2



UNIVERSITY OF PLYMOUTH	
Item No.	9005065282
Date	28 FEB 2002 S
Class No.	T 551.4601 CAN
Cont. No.	X 704384220
PLYMOUTH LIBRARY	

REFERENCE ONLY

LIBRARY STORE

ACKNOWLEDGEMENTS

I would like to express my thanks to my supervisors for their advice throughout my Ph.D. research and for their critical comments on this thesis. To Eric Achterberg, who has given me intuitive advice and guidance during my studies (and a few kicks on the football pitch) and who has been a friend as good as Paul Worsfold, who has been an extremely supportive supervisor throughout this Ph.D.

Many thanks also to the crew and officers of the *R.R.S Challenger* during the IMPACT cruise. I would like to thank Tim Fileman (at PML) for his support during the cruise. A big thank to the creator of *Sturgeon* tablets that helped me to survive during the worst moments.

Thanks to all members of the Université Libre de Bruxelles (Prof. E. Vander Donckt, Sebastian and Sami) and Universidad de Oviedo (Prof. A. Sanz-Medel) partners of the project.

Thanks to Prof. Frank Millero for hosting me at the Rosenstiel School of Marine and Atmospheric Science (RSMAS), University of Miami, and to all members of his research group for the support and collaborative help during my exchange study: Sherwood, Zhou, Valentina, Paco, Gay and Denise.

Thanks also to members of the old "112" research group (now 102) and other companions who have provided friendship and support in (and out) of the lab. Cheers to Phil (the computer man), Paulo and Grady for the "post office walks", Andie and Sophie (now Tasmanians), Kate (now known as Kake), Simon (the surfer), Richard, Charlie, Toby, Thierry, Ana, Cyril and to all the new boys and girls, best wishes to all.

A big cheers to all my Italian friends all over Europe. Many thanks to mum and dad (mamma e papà) for your support. And finally a big thanks to Raquel (now known as "chica"), who has made the past year quite unforgettable. Tq, Tf, Tb.

AUTHOR'S DECLARATION

At no time during the registration for the degree of Doctor of Philosophy has the author been registered for any other University award. This study was financed with the aid of a studentship from the University of Plymouth within the Marine Science and Technology MAST project sponsored by the European Community (grant number MAS3 - CT97 - 0143, MEMOSEA).

The field work performed during the IMPACT cruise CH 148 forms part of larger, multi-disciplinary project and the assistance of all those involved is duly and gratefully acknowledged.

A programme of advanced study was undertaken which included guided reading in topics related to environmental analytical chemistry and chemical oceanography, and training in the determination of trace metals using a variety of ultra-clean analytical techniques. Relevant scientific seminars and conferences were regularly attended at which work was often presented. All data presented in this thesis (unless otherwise stated in the text and appendices) was prepared by the author, whom the ownership rests with. Before using this data in any presentation or printed publication, please contact the author and include full acknowledgements. All enquiries regarding the sampling, analysis and data preparation can be directed to:

Vincenzo Cannizzaro
Department of Environmental Sciences
University of Plymouth
Drake Circus
Plymouth PL4 8AA
United Kingdom
Tel +44 1752 233128
Fax +44 1752 233035
E-mail: vcannizzaro@plymouth.ac.uk

Signed: *Vincenzo Cannizzaro*
Date: 10/02/2002

ABSTRACT

DETERMINATION OF CO AND MN IN MARINE WATERS USING FLOW INJECTION WITH CHEMILUMINESCENCE DETECTION.

Vincenzo Cannizzaro

This thesis describes the design, optimisation and shipboard deployment of a flow injection – chemiluminescence (FI-CL) technique for the determination of cobalt (Co) and manganese (Mn) in seawater.

Chapter One presents an overview of the marine environment and the biogeochemistry of Co and Mn. Current analytical methods for the determination of Co and Mn in natural waters are also reviewed.

Chapter Two reports reagent clean-up techniques and the synthesis of an 8-hydroxyquinoline resin used for in-line matrix elimination and preconcentration. The resin is also characterised in terms of its chelating ability for the transition metals and the earth alkaline metals. A new column design is also presented.

Chapter Three details the optimisation of a FI-CL system for the determination of Co in seawater. The method described is based on a new chemistry whereby CL emission is produced by oxidation of pyrogallol with hydrogen peroxide in alkaline medium in the presence of CTAB and MeOH.

Chapter Four details the optimisation of a FI-CL system for the determination of Mn in seawater. The method chosen involved the luminous oxidation of 7,7,8,8-tetracyanoquinodimethane (TCNQ) by dissolved O₂. The weak chemiluminescence of TCNQ is effectively sensitised by Eosin Y in DDAB.

In Chapter Five the application of the FI-CL method to the shipboard determination of Co in the western North Sea is presented together with results from the determination of Mn in the western North Sea samples after the cruise. Co and Mn profiles are shown for all the geographical area investigated. The data from an entire tidal cycle of the Humber are also shown.

Chapter Six presents the results of an intercomparison exercise. Co and Mn have been measured with different analytical techniques: FI-CL, AdCSV, and ICP-MS. The method developed for Co has been adapted in order to measure the concentration of Co in samples from the Scheldt estuary with an integrated luminometer at the Universite` Libre de Bruxelles.

PUBLICATIONS AND CONFERENCES ATTENDED

5/1999

Short course: National Instruments LabVIEW and Automation (Plymouth)

10/1999

3rd European Conference on Environmental Analytical Chemistry (Greece)

4/1999

36th R&D in Analytical Chemistry - University of Greenwich

9/1999

PICO (Progress In Chem. Oceanography) (Plymouth)

5/2000

37th R&D in Analytical Chemistry - University of Manchester

Marine Sciences and Technology (MAST)

Progress meetings

Oviedo (SP), Brussels (BE), Plymouth (UK)

Cannizzaro V., Bowie A.R., Sax A., Achterberg E.P., Worsfold P.J.

Flow Injection - Chemiluminescence for the Determination of Co and Fe in Estuarine and Coastal Waters.

The Analyst, 2000, **125**, p. 51

P.J. Worsfold, E. Achterberg, A. Bowie, V. Cannizzaro, S. Charles, J.M. Costa, F. Dubois, R. Pereiro, B. San Vicente, A. Sanz-Medel, R. Vandeloise, E. Vander Donckt, P. Wollast, S. Yunus.

An Integrated Luminometer for the Determination of Trace Metals in Seawater Using Fluorescence, Phosphorescence and Chemiluminescence Detection.

Journal of Automated Methods and Management in Chemistry.

Submitted.

Worsfold P.J., Achterberg E.P., Bowie A.R., Cannizzaro V., Sandford R., Gardolinski P.

Flow Injection techniques for the in-situ monitoring of marine processes. Marine Geochemistry.

Submitted.

CONTENTS

CONTENTS

Copyright	I
Title page	II
Acknowledgements	III
Author's Declaration	IV
Abstract	V
Publications and Conferences Attended	VI
Contents	VII
List of Figures	XII
List of Tables	XVII

CHAPTER 1: INTRODUCTION

1.1	SEAWATER	1
1.1.1	Input and recycling of trace elements within the oceans	2
1.1.2	Types of distribution of trace elements in the water column	5
1.1.2.1	Conservative metals	5
1.1.2.2	Nutrient-type (surface-depletion-depth-enrichment)	5
1.1.2.3	Scavenging-type (surface-enrichment-depth-depletion)	6
1.1.2.4	Elements showing hybrid distributions	7
1.1.3	Speciation	10
1.2	COBALT	13
1.2.1	Origin and nature	13
1.2.2	Cobalt in marine environments	16
1.3	MANGANESE	19
1.3.1	Origin and nature	19
1.3.2	Manganese in marine environments	21
1.4	ANALYTICAL METHODS FOR THE DETERMINATION OF COBALT AND MANGANESE	24
1.4.1	Spectrophotometry	24
1.4.2	Atomic Spectrometry	25
1.4.3	Stripping Voltammetry	26
1.5	CHEMILUMINESCENCE	27
1.5.1	Chemiluminescence detection at sea	27
1.5.2	Theory of chemiluminescence	29
1.6	FLOW INJECTION ANALYSIS (FIA)	37
1.7	RESEARCH OBJECTIVES	41

CHAPTER 2: SYNTHESIS AND CHARACTERISATION OF A CHELATING 8-HYDROXYQUINOLINE RESIN FOR TRACE METAL PRECONCENTRATION.

2.1	INTRODUCTION	42
2.2	EXPERIMENTAL	44
2.2.1	Reagents	44
2.2.2	Cleaning protocol	45
2.2.2.1	The laboratory	46
2.2.2.2	Plastic labware	47
2.2.2.3	Reagent clean-up procedure	47
2.2.2.4	Instrumentation	51
2.2.3	Resin Synthesis	54
2.2.3.1	Preparation procedure	57
2.3	RESULTS AND DISCUSSION	60
2.3.1	Characteristics of 8-HQ	60
2.3.2	Preliminary considerations in the development of an on-line column preconcentration system	63
2.3.3	Column equilibration and washing	64
2.3.4	Column design	65
2.3.5	pH dependence of chelating process	68
2.3.6	Determination of the breakthrough profile	72
2.3.6.1	Breakthrough curves for Co, Mn and Cu	74
2.3.6.2	Retention of Co on 8-HQ in the presence of Ca and Mg	77
2.3.7	Re-usability of the resin	79
2.4	CONCLUSIONS	80

CHAPTER 3: DETERMINATION OF COBALT IN SEAWATER USING FLOW INJECTION WITH CHEMILUMINESCENCE DETECTION.

3.1	INTRODUCTION	81
3.2	EXPERIMENTAL	81
3.2.1	Reagents	81
3.2.1.1	CL Reagents	81
3.2.1.2	Cobalt Standards	82
3.2.1.3	Acids / Ammonia	82
3.2.1.4	Ammonium Acetate Buffer	82
3.2.1.5	HCl Carrier/Eluent	83
3.2.2	Instrumentation	83
3.2.3	Procedures	86
3.3	RESULTS AND DISCUSSION	88
3.3.1	Trautz-Schorigin chemiluminescence reaction	88
3.3.2	Optimisation	91
3.3.2.1	Different polyhydric phenols	92
3.3.2.2	Minimisation of the dark current noise	95
3.3.2.3	Flow rate	96
3.3.2.4	Temperature	97

3.3.2.5 Reaction coil length	98
3.3.2.6 Sample loop volume	98
3.3.2.7 Reaction pH	99
3.3.2.8 Surfactant	100
3.3.2.9 Water soluble compounds	103
3.3.2.10 Hydrogen peroxide	105
3.3.2.11 Variation of pyrogallol stability over time	106
3.3.2.12 Optimised system	107
3.3.3 Calibration graph and limit of detection (LOD) without the 8-HQ column	108
3.3.4 Interference studies	111
3.3.5 pH dependence of cobalt uptake on the preconcentration column	113
3.3.6 Calibration with the 8-HQ column	114
3.3.7 Standard additions method	115
3.3.8 Analysis of Certified Reference Materials (CRMs)	116
3.4 CONCLUSIONS	118

CHAPTER 4: DETERMINATION OF MANGANESE IN SEAWATER USING FLOW INJECTION WITH CHEMILUMINESCENCE DETECTION.

4.1 INTRODUCTION	119
4.2 EXPERIMENTAL	120
4.2.1 Reagents	120
4.2.1.1 CL reagents for the luminol-hydrogen peroxide system	120
4.2.1.2 CL reagents for the TCNQ-O ₂ -OH-Eosin Y system	121
4.2.1.3 Manganese Standards	122
4.2.1.4 Acids/Ammonia	122
4.2.2 HCl Carrier/Eluent	123
4.2.2.1 Acid wash	123
4.2.3 Instrumentation	123
4.2.4 Operating procedures for the luminol-hydrogen peroxide system	126
4.2.5 Operating procedures for the TCNQ-O ₂ -OH-Eosin Y system	126
4.3 RESULTS AND DISCUSSION	127
4.3.1 Luminol-hydrogen peroxide chemiluminescence reaction	127
4.3.2 TCNQ-O ₂ -OH-Eosin Y chemiluminescence reaction	129
4.3.3 Optimisation of the luminol-hydrogen peroxide system	132
4.3.3.1 Flow rate	133
4.3.3.2 Sample loop volume	134
4.3.3.3 Reaction pH	134
4.3.3.4 Hydrogen peroxide concentration	135
4.3.3.5 Luminol concentration	136
4.3.3.6 TETA concentration	136
4.3.3.7 Variation of Luminol sensitivity over time	137
4.3.3.8 Interference	138
4.3.4 Optimisation of the TCNQ-O ₂ -OH-Eosin Y system	140
4.3.4.1 Flow rate	141
4.3.4.2 Sample loop volume	142

4.3.4.3 DDAB, Eosin Y and TCNQ concentrations	142
4.3.4.4 Reaction pH	145
4.3.4.5 Variation of TCNQ-DDAB-Eosin Y solution stability over time	145
4.3.4.6 Optimised TCNQ-O ₂ -OH-Eosin Y system	146
4.3.4.7 Calibration graph without the 8-HQ for the TCNQ-O ₂ -OH-Eosin Y	147
4.3.4.8 Interference studies for the TCNQ-O ₂ -OH-Eosin Y reaction	149
4.3.4.9 pH dependence of manganese uptake on the preconcentration column	152
4.3.4.10 Calibration graph and LOD with the 8-HQ column using the TCNQ-O ₂ -OH-Eosin Y system	153
4.3.5 Analysis of Certified Reference Materials (CRMs) using the TCNQ-O ₂ -OH-Eosin Y system	153
4.4 CONCLUSIONS	155

CHAPTER 5: DISTRIBUTION AND BEHAVIOUR OF COBALT AND MANGANESE IN THE WESTERN NORTH SEA.

5.1 INTRODUCTION	156
5.2 EXPERIMENTAL	162
5.2.1 Sampling strategy	162
5.2.2 Sampling and Analyses	166
5.3 RESULTS AND DISCUSSION	170
5.3.1 Temperature and salinity profiles	170
5.3.2 Distribution of dissolved Co	176
5.3.2.1 Comparison between shipboard and land-based analysis for Co	182
5.3.3 Distribution of dissolved Mn	184
5.3.4 Co and Mn in North Sea waters	191
5.3.5 Tidal cycle study in the Humber estuary	195
5.4 CONCLUSIONS	198

CHAPTER 6: INTERCOMPARISON OF ANALYTICAL METHODOLOGIES FOR THE DETERMINATION OF COBALT AND MANGANESE IN SEAWATER.

6.1 INTRODUCTION	199
6.1.1 Study Site	201
6.2 EXPERIMENTAL	204
6.2.1 Sampling	204
6.2.2 Reagents	205
6.2.2.1 FI-CL, AdCSV, and ICP-MS Reagents	205
6.2.2.2 Cobalt and Manganese Standards	206
6.2.3 The Luminometer FL/FS 900	206
6.2.4 Methodology	209
6.3 RESULTS AND DISCUSSION	212
6.3.1 CRM results	215

CHAPTER 7: CONCLUSIONS AND FUTURE WORK.

7.1	GENERAL CONCLUSIONS	217
7.2	SUGGESTIONS FOR FUTURE WORK	220
7.2.1	Speciation	220
7.2.2	The preconcentration/matrix removal step	221
7.2.4	In-line Standard Addition(s)	222
7.2.5	Multi-element FI-CL Technique	222
7.2.6	Upgrade of Instrumentation	223
7.2.7	Submersible FI-CL and sampling campaign	223
 REFERENCES		 226

LIST OF FIGURES

Figure 1.1: Representations showing the various processes determining the oceanic distribution of trace metals and nutrients	4
Figure 1.2: Some typical depth profiles	8
Figure 1.3: Example of percentage metal-chelate concentration distribution	11
Figure 1.4: Structure of vitamin B ₁₂	15
Figure 1.5: Concept of energy level and transition	29
Figure 1.6: Simple single channel FI manifold.	38
Figure 1.7: The 6-ways injection valve	39
Figure 2.1: The chelating group of 8-hydroxyquinoline (8-HQ)	45
Figure 2.2: The laminar flow hood	47
Figure 2.3: Schematic diagram of apparatus for sub-boiling distillation	49
Figure 2.4: Purification of ammonia solution by isothermal distillation: a) sub-boiling Teflon bottle still; b) principle setup of isothermal	50
Figure 2.5: Manifold used for (a) adsorption studies and (b) breakthrough studies with the 8-HQ resin	52
Figure 2.6: Reaction scheme for the immobilisation of 8-HQ	56
Figure 2.7: Structure of Chelex 100 and Muromac A-1	60
Figure 2.8: Old micro-column containing 8-HQ resin	65
Figure 2.9: a) the new microcolumn design; b) photograph of the column	67

Figure 2.10: Ionic forms of 8-HQ at acid and basic pH.....	69
Figure 2.11: Typical reaction where M represents a metal reacting with 8-HQ	69
Figure 2.12: Theoretical effect of pH on ratio of metal-oxine (ML) to total metal [T(M)] at 20 °C and 0.1 M ionic strength.....	70
Figure 2.13: pH dependance of the upatke of Mn, Cr, Cu, Co, and Fe onto 8-HQ at different pH value.....	71
Figure 2.14: Typical breakthrough curve for an ion-exchange column	72
Figure 2.15: Breakthrough curve of Co(II) 1 μ M (green curve) and Co(II) 1 μ M in the presence of Cu(II) 1 μ M and Mn(II) 1 μ M (black curve).	75
Figure 2.16: Breakthrough curve of Mn(II) 1 μ M.....	76
Figure 2.17: Breakthrough curve of Cu(II) 1 μ M	76
Figure 2.18: The elution of Co(II) from the 8-HQ resin with HNO ₃ 2% (v/v).....	78
Figure 2.19: Breakthrough curve of Co(II) 1 μ M after acid treatment	79
Figure 3.1: FI-CL manifold for the determination of Co(II)	85
Figure 3.2: Detector output from a series of standard additions	88
Figure 3.3: The mechanism of the Trautz-Schorigin Reaction	89
Figure 3.4: The structure of purpurogalline (PPG).....	90
Figure 3.5: Effect of different polyhydroxyphenols tested.....	94
Figure 3.6: Effect of pyrogallol concentration on CL emission.....	95
Figure 3.7: Results of variation of photomultiplier voltage	96
Figure 3.8: Effect of flow rate on CL emission	97
Figure 3.9: Effect of temperature on CL emission	98

Figure 3.10: Effect of injection loop volume on CL emission.....	99
Figure 3.11: Effect of reaction pH on CL emission	100
Figure 3.12: Effect of the surfactant CTAB on CL emission.....	103
Figure 3.13: Effect of different water-soluble (4% v/v) compounds on the CL signal.....	104
Figure 3.14: Effect of methanol percentage on CL emission	104
Figure 3.15: Effect of hydrogen peroxide concentrations on CL emission.....	106
Figure 3.16: Variation in stability of pyrogallol reagent with time.....	107
Figure 3.17: Recorder trace showing electronic and chemical background noise.....	110
Figure 3.18: Calibration graph in the range 0.85-59.5 nM of Co(II) in acidified UHP water.....	111
Figure 3.19: Calibration graph in the range 0.034-0.850 nM of Co(II) in acidified UHP water.....	114
Figure 3.20: Standard additions curve for Irish seawater sample.....	116
Figure 4.1: FI-CL manifold for the determination of Mn(II) (luminol).....	124
Figure 4.2: FI-CL manifold for the determination of Mn(II) (TCNQ-O ₂ -OH-Eosin Y)....	125
Figure 4.3: Oxidation pathway for Luminol.....	129
Figure 4.4: Reaction scheme of neutral TCNQ with NaOH.....	131
Figure 4.5: Reaction scheme of the TCNQ anion radical, O ₂ (aq), and Mn(II).....	131
Figure 4.6: Effect of flow rate on CL emission.	133
Figure 4.7: Effect of injection loop volume on CL emission.....	134
Figure 4.8: Effect of reaction pH on CL emission.....	135
Figure 4.9: Effect of hydrogen peroxide concentration on CL emission.	135

Figure 4.10: Effect of luminol concentration on the signal and baseline CL intensities...	136
Figure 4.11: Effect of TETA concentration on the signal and baseline CL intensities.....	137
Figure 4.12: Variation in sensitivity of luminol reagent with time.....	137
Figure 4.13: CL response of a) seawater matrix, b) acetate buffer, c) citrate buffer, d) succinate buffer.....	139
Figure 4.14: Effect of flow rate on CL emission.....	141
Figure 4.15: Effect of injection loop volume on CL emission.....	142
Figure 4.16: Effect of DDAB surfactant aggregate on the CL signal.....	144
Figure 4.17: Effect of Eosin Y sensitiser on the CL signal.....	144
Figure 4.18: Effect of TCNQ on the CL emission.....	144
Figure 4.19: Effect of reaction pH on the CL emission.....	145
Figure 4.20: Variation in stability of TCNQ-DDAB-Eosin Y solution with time.....	146
Figure 4.21: Calibration graph in the range 50-1400 nM of Mn(II) in UHP water.....	149
Figure 4.22: Calibration graph in the range 5-100 nM of Mn(II) in UHP water.....	153
Figure 5.1: Schematic of basic physical processes in the North Sea.....	157
Figure 5.2: Subdivision into the North Sea Task Force boxes.....	159
Figure 5.3: The RRS Challenger on the Southampton dock.....	161
Figure 5.4: Study site and station positions.....	163
Figure 5.5: The CTD deployment.....	167
Figure 5.6: The filtration system.....	167
Figure 5.7: The clean container on boardship for trace analysis.....	168
Figure 5.8: Depth profiles at the IMPACT stations (Salinity; Temperature).....	170

Figure 5.9: Surface distribution (4 m depth) of dissolved Co in the North Sea	171
Figure 5.10: Depth profiles at the IMPACT stations	176
Figure 5.11: Depth profiles of dissolved Co (stations 32, 33, and 34).....	177
Figure 5.12: Distribution of dissolved depth averaged Mn in the North Sea	183
Figure 5.13: Surface distribution (4 m depth) of dissolved Mn in the North Sea.	184
Figure 5.14: Depth profiles at the IMPACT stations	185
Figure 5.15: a) concentration of Co, b) (TON) and c) concentration of Mn during a tidal cycle at the Humber mouth.	186
Figure 5.16: a) concentration of Co, b) TON and c) concentration of Mn during a tidal cycle at the Humber mouth.	197
Figure 6.1: Map of the Scheldt Estuary. Lower estuary and Upper estuary.....	202
Figure 6.2: The sampling point	205
Figure 6.3: a) General optical arrangement of the FS900CDT spectrometer; b) photograph of the FS900CDT spectrometer.	208
Figure 6.4: FI-CL manifold for the determination of Co(II) with the luminometer.....	210
Figure 6.5: Mn, Co, Cd and salinity data for the Scheldt estuary samples during tidal cycle: a) Co by AdCSV and FI-CL with luminometer detector; b) Mn by ICP-MS and FI-CL; c) Cd by fluorescence.	214

LIST OF TABLES

Table 1.1: Major constituents of seawater.....	1
Table 1.2: A selection of 'new' data on the speciation, concentration and types of vertical distributions of some elements in seawater ..	12
Table 1.3: The average concentrations of Co in seawater.....	23
Table 1.4: Typical concentrations of Fe, Cu, Co and Mn in coastal and open ocean and coastal waters.....	28
Table 1.5: FI-CL methods for metal ions species.....	33
Table 2.1: Historical data of Fe concentrations	46
Table 2.2: Instrumental ICP-MS conditions and measurement parameters.....	53
Table 2.3: Stability constants of H, Ca, Co, Cu, Fe, Mg, Mn, and Ni with 8-HQ.....	61
Table 2.4: Examples of application of 8-HQ based resin.....	62
Table 2.5: Operating conditions for the breakthrough experiments.....	74
Table 3.1: Optimised parameters for the determination of Co in seawater with 8-HQ column	91
Table 3.2: Structure, common and IUPAC name of the different polyhydric phenols tested.	93
Table 3.3: Structures of most commonly used classes of surfactants	100

Table 3.4: Eluotropic series and physical properties of water-soluble.	105
Table 3.5: Optimised parameters for the system without 8-HQ column for the determination of Co in seawater with pyrogallol	107
Table 3.6: Effect of the addition of metal ions on the CL emission of a 250 pM Co(II) standard.	113
Table 3.7: Signal recovery of Co(II) at different sample pH for an Irish seawater sample.	114
Table 3.8: Results for the determination of Co(II) in seawater CRMs and an Irish Sea sample.	117
Table 4.1: Name and pKa values for buffers used.....	120
Table 4.2: Chemical structure of TCNQ, DDAB and Eosin Y	122
Table 4.3: The triggering of luminol chemiluminescence.....	128
Table 4.4: Optimised parameters for the determination of Mn in seawater with 8-HQ column.....	132
Table 4.5: Optimised parameters for the determination of Mn in seawater with 8-HQ column.....	140
Table 4.6: Effect of surfactant aggregates on the CL signal for Mn(II).....	143
Table 4.7: Optimised parameters for the system without 8-HQ column for the determination of Mn in seawater with TCNQ-O ₂ -OH-Eosin Y	146
Table 4.8: Investigation of the relative catalytic effect of Fe(III), Cu(II) and Mg(II) upon the proposed CL system.....	151

Table 4.9: Effect of the addition of DFAM in the sample on the CL response of Mn(II) and Fe(III).....	152
Table 4.10: Results for the determination of Mn(II) in seawater CRMs.	154
Table 5.1: Time of sampling and position of stations (GMT).....	164
Table 5.2: Co and Mn concentrations in coastal waters.....	192
Table 5.3: Concentrations of Co(II) and Mn(II) in the Central southern North Sea and in the Humber Estuary.	195
Table 5.4: Different states of tide at Station 8.....	196
Table 6.1: Instrumental ICP-MS conditions and measurement parameters.....	211
Table 6.2: Data obtained for Co and Mn for the analyses of the Scheldt samples with the different methods, and salinity.....	213
Table 6.3: Accuracy of applied techniques for the determination of Mn(II) and Co(II) in seawater CRMs with AdCSV, FI-CL, and ICP-MS.....	215

CHAPTER 1

INTRODUCTION

1.1 SEAWATER

The major constituents of seawater that make up >99% by weight of sea-salts are shown in Table 1.1. These major seawater ions act conservatively in contrast to many trace elements (i.e. those with concentrations less than 1 mg kg⁻¹, but excluding radioactive elements) and macro-nutrients, the concentrations of which are strongly influenced by biogeochemical cycling.

Table 1.1: Major constituents of seawater

Ion	Concentration (g l ⁻¹) ^a	Percent by weight ^a
Chloride (Cl ⁻)	19.87	55.07
Sodium (Na ⁺)	11.05	30.62
Sulphate (SO ₄ ²⁻)	2.712	7.72
Magnesium (Mg ²⁺)	1.326	3.68
Calcium (Ca ²⁺)	0.422	1.17
Potassium (K ⁺)	0.416	1.10
Bicarbonate (HCO ₃ ²⁻)	0.142	0.39
Bromide (Br ⁻)	0.0674	0.19
Strontium (Sr ²⁺)	0.0079	0.02
Boron (H ₃ BO ₃)	0.00445	0.01
Fluoride (F ⁻)	0.00128	<0.01
Ionic strength (M)		0.6-0.7
Salinity		~35 (range 32-37)
pH		7.5-8.3

^a Ocean water of salinity = 35; data from Chester (2000)

One of the earliest review of trace elements was published in 1975 (Brewer, 1975). Since then there have been significant advances in our knowledge of the oceanic distributions of trace elements: seawater concentrations have been shown to be factors of 10-1000 lower than those previously reported. Vertical

profiles have been found to be consistent with known biological, physical and/or geochemical processes operating within the ocean and, in many cases, different chemical forms (speciation) of the elements have also been elucidated.

1.1.1 Input and recycling of trace elements within the oceans

Trace elements in seawater have two major external sources: (1) atmospheric and riverine inputs of weathering products from the exposed continents; and (2) inputs resulting from the interactions of seawater with newly formed oceanic crustal basalt at ridge-crest spreading centres via both high temperature hydrothermal activity and low temperature interactions. Hydrothermal activities associated with the formation of new oceanic crust have been shown to exert a great influence on the chemistry of seawater. They are major oceanic sources of the trace elements Fe and Mn, and the minor elements Li and Rb, and major oceanic sinks for Mg and SO_4^{2-} . While the riverine inputs of the major elements to the oceans are known fairly accurately, those of the majority of trace elements are not, primarily because the estimation is so dependent upon the choice of effective river end-member concentrations. Atmospheric inputs are an important way in which significant quantities of both natural and anthropogenically mobilised trace elements are transported to the ocean. Most dissolved trace elements are removed from seawater to marine sediments by adsorption onto sinking particles (so called scavenging) or by incorporation into biological phases via active uptake by phytoplankton followed by sinking of biological detritus. The uptake of trace elements by phytoplankton is very important. The uptake of some trace metal species in the sea can be partly understood in terms of their function as essential micronutrients. Trace elements such as V, Cr, Mn, Fe, Cu, Co, Ni, Zn and Mo play important roles in

nutrient-requirements and metal-activated enzyme systems which catalyse major steps in glycolysis, the tricarboxylic acid cycle, photosynthesis and protein metabolism. The processes result in trace elements being removed from solution in surface waters and then being transported to depth by biogenic carriers, involving the removal from surface waters of dissolved species by some form of particulate matter. However, prior to their ultimate removal, trace elements may undergo various degrees of recycling which can involve chemical desorption reactions or redissolution from particles (regeneration) as the particle carrier phases oxidise and/or dissolve (Figure 1.1 represents schematically the oceanic distribution of trace metals and nutrients).

In a very general sense the vertical distribution of many trace metals can be considered to be controlled by either a *scavenging type* (the adsorptive removal of trace metals occurs onto particles that sink down the water column) or a *nutrient type* mechanism (i.e. biological surface-depletion – subsurface enrichment) (Whitfield and Turner, 1983).

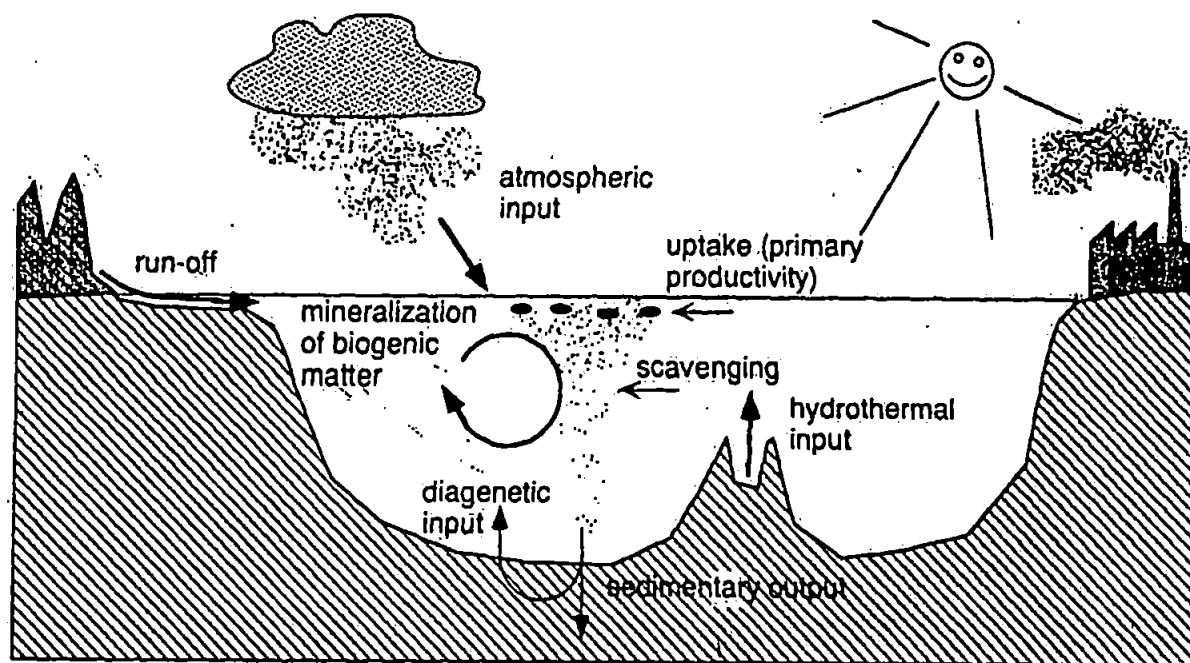


Figure 1.1: Schematic representations showing the various processes determining the oceanic distribution of trace metals and nutrients. External input sources are continental run-off (rivers), atmospheric deposition (rain and dry fall-out), hydrothermal input and diagenetic input. For nutrients and nutrient-type trace metals, diagenetic input is secondary input source. Anoxic sediments may also serve as a sink for these metals and nutrients. Uptake by particle takes place via passive adsorptive removal (scavenging) or active biological uptake. Remineralisation of biogenic matter may take place either predominantly in the water column (organic matter) or at the sediment-water interface. Ultimate output for nutrients and trace metals is by particles surviving diagenesis, permanently buried in the sediment (reproduced from Saager, 1992).

1.1.2 Types of distribution of trace elements in the water column

Surface-water distributions can be extremely useful in identifying the effects that source strengths have on 'fingerprinting' trace-element distributions in the mixed layer. Both the surface and the deep ocean reservoirs are zones of trace-metal reactivity. However, in order to assess the effects that internal oceanic processes have on trace-metal distributions it is necessary to obtain data on their vertical as well as their lateral profiles. There are a number of types of vertical trace-element distribution, profiles in the oceans. These distributions can be summarised as follows (Chester, 2000; Donat et al., 1995; Whitfield et al., 1987).

1.1.2.1 Conservative metals

This group includes monovalent alkali metals such as Na and K, and divalent earth metals such as Ca and Mg, as well as polyvalent metals such as Mo, W, and U which have anionic complexes in seawater. They have generally little affinity for marine particles and their oceanic distributions are therefore very uniform and they have long residence times ($> 10^5$ years) relative to the mixing time of the oceans (ca. 1600 years) (Whitfield, 1979).

1.1.2.2 Nutrient-type (surface-depletion-depth-enrichment)

These elements, including Ni, Zn, Cd, Ba, and to a lesser extent Cu and Fe, exhibit distributions that are remarkably similar to those of the nutrients phosphate, nitrate and silicate. The residence time of the nutrient type elements is intermediate (10^3 to 10^5 years) to those of the conservative and scavenged elements. The characteristic features of the vertical concentration profiles of trace metals with nutrient-type profiles are (a) a depletion in surface waters,

and (b) an enrichment at some depth within the water column. These features arise from the involvement of the elements in the oceanic biogeochemical cycles. Phytoplankton utilises nutrients (phosphate, nitrate, and silicate) in the euphotic zone and as they grow they extract trace elements from the water, thus leading to their depletion in surface waters. As the organisms die and sink down the water column they undergo decay, during which there is a regeneration of the nutrients, and the associated trace elements, back into solution. The most striking examples are Cd and Zn. The vertical distribution of Cd correlates closely with that of phosphate, suggesting that Cd is cycled with the formation and decomposition of organic soft tissues, whilst the vertical distribution of Zn correlates most closely with that of silicate.

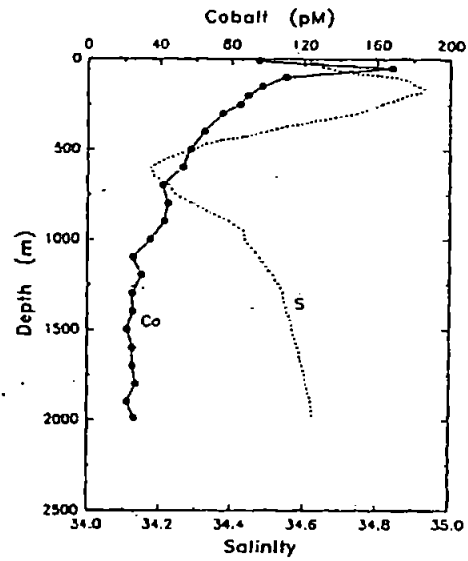
1.1.2.3 Scavenging-type (surface-enrichment-depth-depletion)

Because of their strong interactions with particles, the scavenged elements have very short oceanic residence time ($< 10^3$ years). This group includes Th, Mn, Al, Co (see Figure 1.2a) and Ce amongst many others. Their concentrations are maximum near, and decrease with distance from, their source which include rivers, atmospheric dust, hydrothermal sources and bottom sediments. In general, concentrations of the scavenged elements decrease along the direction of deepwater flows due to continuing particle scavenging.

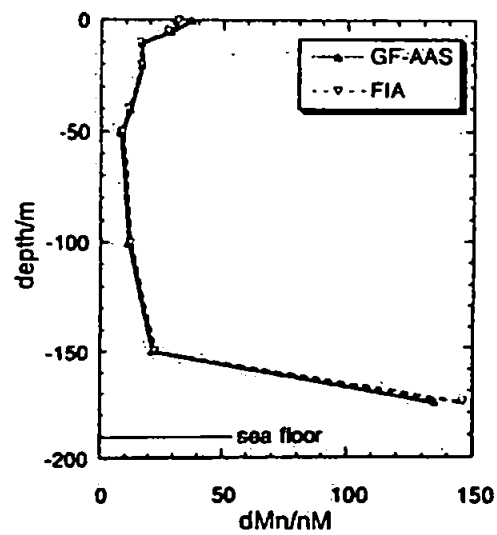
The seawater distributions of Al and Mn (see Figure 1.2b) are maximal in surface waters due to atmospheric input, minimal at mid depths due to particle scavenging and increase towards the seafloor due to benthic sources.

1.1.2.4 Elements showing hybrid distributions.

It has been shown that vertical profiles can provide information on the factors that control the seawater chemistries of individual trace elements. Vertical profiles are therefore useful as process indicators. However, some elements can exhibit 'multishape' profiles because more than one process has affected their seawater chemistries. It is therefore apparent that although the various types of vertical water-column distribution profiles are useful for identifying individual processes, the profiles of some dissolved elements can be influenced by more than one biogeochemical process (that combine features of both the nutrient-type and the scavenging-type profiles). For example, Cu instead of the rapid increase in concentrations with depth shown by recycled elements (see Figure 1.2c), its concentration increase only gradually with depth, due to the combined effect of regeneration and scavenging in deep waters. Iron is another trace element that is now known to have a vertical oceanic profile influenced by both nutrient type and scavenging type processes (see Figure 1.2d).

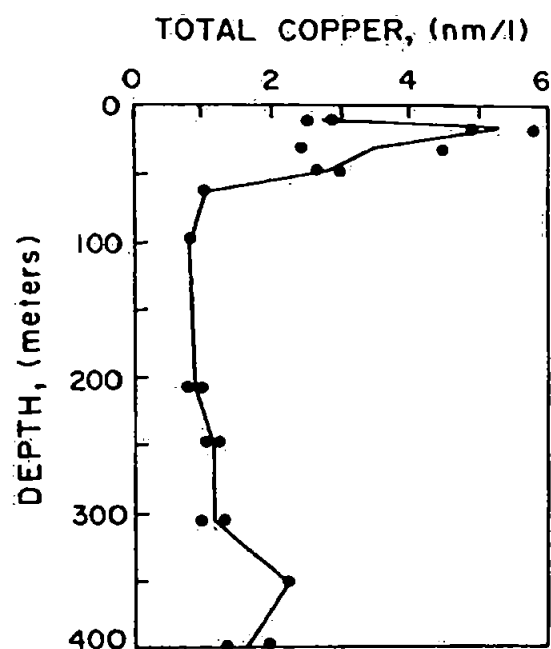


a)

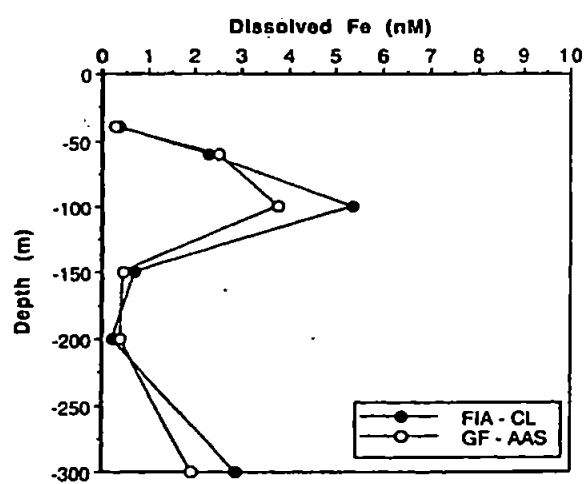


b)

Figure 1.2: Some typical depth profiles: a) Co in the Western Philippine Sea (Wong et al., 1995); b) Mn in the Norwegian Balsfjord (de Jong et al., 2000).



c)



d)

Figure 1.2 (continued): Some typical depth profiles: c) Cu in the North-western Atlantic Ocean (Zuehlke and Kester, 1985); d) Fe in the Atlantic ocean (de Jong et al., 1998).

1.1.3 Speciation

Although the knowledge about the oceanic concentrations and distributions of trace metals has advanced dramatically, it has become increasingly clear that this information alone is insufficient to provide a complete understanding of a trace metal's biological and geochemical interactions. Trace metals dissolved in seawater can exist in different oxidation states and chemical forms (species) including free solvated ions, inorganic complexes (e.g. with SO_4^{2-} , CO_3^{2-} , Cl^- , OH^- , etc), organometallic compounds, and organic complexes (e.g with phytoplankton metabolites, protein, humic substances). Knowledge of the distribution of a trace metal's total dissolved concentration amongst its various forms (speciation) is extremely important because the different oxidation states and chemical forms undergo very different biological and geochemical interactions (Apte and Batley, 1989). For example, Fe(III) and Mn(IV) are much less soluble than their reduced forms Fe(II) and Mn(II). The toxicity and nutrient availability of several transition metals to phytoplankton have been shown to decrease as a result of complexation with ligands such as EDTA, indicating that the toxicity and availability of these metals are proportional to their free metal activities. Organic complexation may greatly decrease or, in some cases even increase (Donat et al., 1995) adsorption of metals onto metal oxide particles. Thus, speciation information is necessary to attempt to fully understand a trace metal's marine biogeochemical cycle (Figure 1.3 is an example of speciation in waste waters at different pH).

Table 1.2 shows the speciation, concentration and types of vertical distributions of some selected elements in seawater (Chester, 2000).

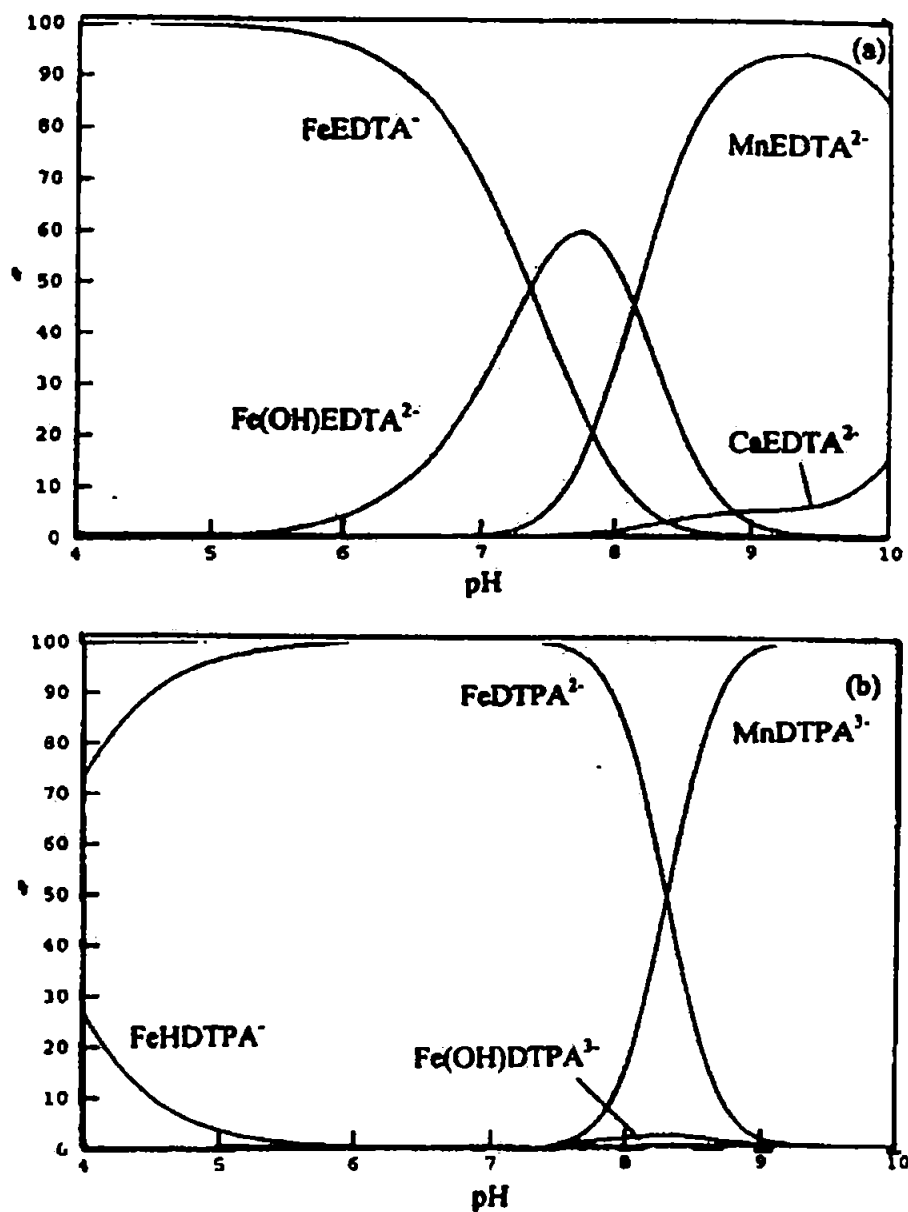


Figure 1.3: Example of percentage metal-chelate concentration distribution of (a) EDTA and (b) DTPA as a function of pH in waste waters for Fe, Mn and Ca (reproduced from Sillanpaa et al., 2001).

Table 1.2: A selection of 'new' data on the speciation, concentration and types of vertical distributions of some elements in seawater (Chester, 2000).

Element	Probable main species in oxygenated seawater	Range and average concentration at 35 salinity*	Type of distribution
Si	H_4SiO_4	<1-180 $\mu\text{mol kg}^{-1}$; 100 $\mu\text{mol kg}^{-1}$	Nutrient type
P	HPO_4^{2-} , NaHPO_4^- , MgHPO_4^0	<1-3.5 $\mu\text{mol kg}^{-1}$; 2.3 $\mu\text{mol kg}^{-1}$	Nutrient type
N	NO_3^- (also as N_2)	<0.1-45 $\mu\text{mol kg}^{-1}$; 30 $\mu\text{mol kg}^{-1}$	Nutrient type
S	SO_4^{2-} , NaSO_4^- , MgSO_4^0	28.2 mmol kg^{-1}	Conservative
Na	Na^+	0.468 mol kg^{-1}	Conservative
Mg	Mg^{2+}	53.2 mmol kg^{-1}	Conservative
Al	$\text{Al}(\text{OH})_4^-$, $\text{Al}(\text{OH})_3^0$	(5-40 nmol kg^{-1} ; 20 nmol kg^{-1})	Mid-depth minima
K	K^+	10.2 mmol kg^{-1}	Conservative
Ca	Ca^{2+}	10.3 mmol kg^{-1}	Slight surface depletion
V	HVO_4^{2-} , H_2VO_4^- , NaHVO_4^-	20-35 nmol kg^{-1} ; 30 nmol kg^{-1}	Slight surface depletion
Cr	CrO_4^{2-} , NaCrO_4^-	2-5 nmol kg^{-1} ; 4 nmol kg^{-1}	Nutrient type
Mn	Mn^{2+} , MnCl^+	0.2-3 nmol kg^{-1} ; 0.5 nmol kg^{-1}	Depletion at depth
Fe	$\text{Fe}(\text{OH})_3^0$	0.1-2.5 nmol kg^{-1} ; 1 nmol kg^{-1}	Surface depletion; depletion at depth
Co	Co^{2+} , CoCO_3^0 , CoCl^+	(0.01-0.1 nmol kg^{-1} ; 0.02 nmol kg^{-1})	Surface depletion; depletion at depth
Ni	Ni^{2+} , NiCO_3^0 , NiCl^+	2-12 nmol kg^{-1} ; 8 nmol kg^{-1}	Nutrient type
Cu	CuCO_3^0 , CuOH^+ , Cu^{2+}	0.5-6 nmol kg^{-1} ; 4 nmol kg^{-1}	Nutrient type and scavenging
Zn	Zn^{2+} , ZnOH^+ , ZnCO_3^0 , ZnCl^+	0.05-9 nmol kg^{-1} ; 6 nmol kg^{-1}	Nutrient type
Mo	MoO_4^{2-}	0.11 $\mu\text{mol kg}^{-1}$	Conservative
Ag	AgCl_2^-	(0.5-35 pmol kg^{-1} ; 25 pmol kg^{-1})	Nutrient type
Cd	CdCl_2^0	0.001-1.1 nmol kg^{-1} ; 0.7 nmol kg^{-1}	Nutrient type

* Parenthesis indicates uncertainty about the accuracy or range of concentration given

1.2 COBALT

1.2.1 Origin and nature

Cobalt has been known for thousands of years for the blue colour it imparts to glass and pottery. Cobalt has been identified in Egyptian pottery dating from around 2600 B.C. Cobalt blue has also been found in early Venetian glass and cobalt bluing was developed to a high degree during the Ming Dynasty. In 1375 the Swedish chemist G. Brandt isolated a very impure metal as the source of the blue colour. The terrestrial abundance of cobalt is only 0.0029% and next to scandium it is the least common element of the first transition series. Cobalt is widely distributed, but only few ores are of commercial value. In nature it always occurs associated with nickel, and commonly also with arsenic. Cobalt is usually obtained as a by-product or co-product from the recovery of copper, nickel and iron from their ores. Most common minerals, which contain cobalt, are arsenides and sulphides such as smaltite, CoAs_2 , cobaltite, CoAsS , and linnaeite, Co_3S_4 . Cobalt is used for example in the production of high-temperatures alloys used in the construction of gas turbines. Like iron and nickel, cobalt is ferromagnetic and is used for the manufacture of magnetic alloys. Cobalt compounds are primarily used in the ceramic and paint industry and are also employed as catalysts in a range of organic reactions (Encyclopaedia, 1995).

Cobalt is a hard, bluish white metal. The metal in large solid pieces is not attacked by air or water at temperatures below approximately 300°C . Cobalt has only one naturally occurring isotope, ^{59}Co . By thermal neutron bombardment this isotope converts to the radioactive ^{60}Co with a half life of 5271 years and it decays by means of β and γ emission to the non radioactive ^{60}Ni . The most common oxidation states of cobalt are +2 and +3. Cobalt(II) is the most stable

form under normal conditions, and production of cobalt(III) compounds demands special circumstances. Cobalt(III) is an extremely powerful oxidising agent in aqueous solution. It oxidises water with the evolution of oxygen. The relative stability of the two oxidation states is altered by the presence of complexing agents, but even so, most cobalt(III) complexes are thermodynamically unstable with respect to cobalt(II). However cobalt(III) forms kinetically inert complexes such as the Co(III)-EDTA complex, which can be boiled in acid or base with little effect. The $\text{Co}(\text{H}_2\text{O})_6^{2+}$ imparts a pink colour to aqueous solutions, but when other ligands are introduced, a number of complexes are formed that produce blue colours, for example CoCl_4^{2-} . A number of organometallic compounds of cobalt have been made, for example cobalt carbonyls, which show valuable catalytic properties.

Cobalt was first shown to be an essential element for cattle and sheep following investigations to find a cure for the disease bush sickness or coast disease. The disease was recognised to be an anaemic condition and was therefore treated with iron compounds. Later it was realised that an impurity (cobalt) in the administered iron salt was responsible for the effective treatment of pernicious anaemia.

The terms vitamin B₁₂ and cobalamin refer to all members of a large group of cobalt-containing corrinoids that can be converted to methylcobalamin or 5'-deoxy-adenosylcobalamin, the two cobalamin coenzymes active in human metabolism (Kendrick et al., 1992). Vitamin B₁₂ is a coenzyme in a number of biochemical processes, the most important of which is the formation of erythrocytes. In the biological processes in which vitamin B₁₂ is involved, it acts as a hydrogen carrier. The structure of vitamin B₁₂ consists of a substituted porphyrin-like corrin ring in which a Co^{2+} ion is coordinated to four nitrogen

atoms with a benzimidazole nitrogen in the fifth position and different ligands, for example, deoxyadenosine, in the sixth coordination position. Cyanocobalamin is the name of the compound where CN^- replaces deoxyadenosine in the sixth position and is the artefact of the isolation procedure. Cyanocobalamin is the commercially available form of vitamin B_{12} . The chemical structure of vitamin B_{12} is shown in Figure 1.4 (Hewitt et al., 1963; Kendrick et al., 1992).

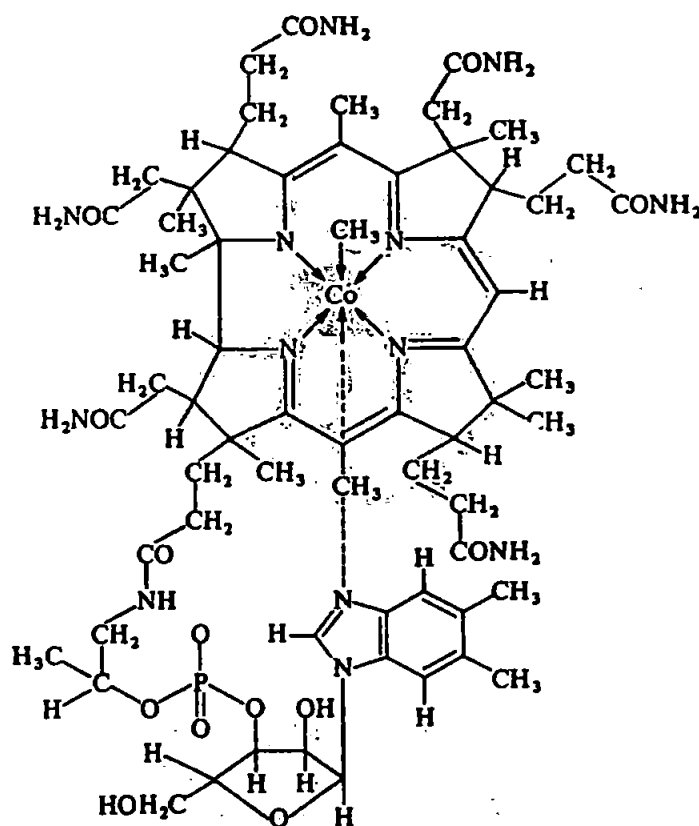


Figure 1.4: Structure of vitamin B_{12}

1.2.2 Cobalt in marine environments

Cobalt can exist as Co(II) or Co(III) within the pH and Eh range of natural waters. Co(III) forms inert complexes or oxides. Co(III) is the thermodynamically favoured state in oxygenated seawater (Garrels et al. 1965), and Co scavenging in the water column may be due to the oxidation of soluble Co(II) to particle reactive or inert Co(III) on surfaces.

Relatively few studies have been carried out on the complexation of Co with organic ligands in open ocean seawaters. Zhang et al. (1990) found that a variable fraction (45-100 %; mean 73 %) of dissolved Co was strongly complexed in the Irish Sea and the Scheldt River estuary. Donat et al. (1988) reported that coastal and open ocean seawater samples had ca. 50% of their total dissolved Co associated with strong organic complexes. Some other workers (Mantoura et al., 1978) reported that Co exists in seawater primarily as the Co(II) ion and as the carbonato complexes and the organic complexes are one of minor importance. Cobalt is a biologically important metal although it is toxic to living organisms at high concentrations ($> 17 \mu\text{M}$) that are rarely, if ever, observed in the environment (Schrauzer, 1991; Williams, 1971). Only a few cobalt metalloproteins are known (Kobayashi et al., 1999). Likewise, even fewer studies have looked at cobalt-enzyme interactions in the marine environment. Cobalt is known to substitute for zinc in the enzyme carbonic anhydrase when marine phytoplankton are cultured under zinc-limiting conditions (Morel et al., 1994; Price and Morel, 1990; Yee and Morel, 1996). More recently, laboratory culture experiments have shown that the relative ratios of concentrations of free Co(II) to free Zn(II) in seawater may be an important influence on the growth of coccolithophores, diatoms and cyanobacteria (Sunda and Huntsman, 1995). The opposite tended to occur under cobalt-limiting conditions. Cyanobacteria, on

the other hand, did not require zinc for growth; however, they did appear to have an absolute requirement for cobalt. Clearly, some microorganisms require free cobalt and its complexation by organic matter may make it biologically unavailable (Ellwood et al., 2001).

Cobalt is also a metal of environmental interest since the radionuclide ^{60}Co is an activation product of radioactive wastes and has been identified as a priority contaminant (Albrecht et al., 1995; Mundschenk, 1996; US Department of Energy, 1994).

Cobalt enrichment in hydrothermal fluids on the sea floor (up to 3.8 nM) has been observed (Sakai et al., 1987). Therefore cobalt is interesting from a geochemical viewpoint as hydrothermal activity may be chemically identified by anomalously high concentrations of Co in deep seawater around hydrothermal fields.

One of the major reasons for the paucity of data on the distribution of cobalt in the oceans is its low concentration, usually less than 0.1 nM, in seawater (Wong et al., 1995). Reliable data, and especially vertical profiles, were not available until the early part of the last decade (Knauer et al., 1982). Previously, the concentrations of cobalt in seawater had been reported as mostly undetectable in some studies (Bewers et al., 1976; Danielsson, 1980) and as unrealistically high and/or widely scattered values in other cases (Fukai, 1967; Robertson 1970). It is now generally recognised that cobalt exists in seawater at concentrations of less than 0.2 nM. In open ocean waters, cobalt has a unique profile (Ellwood et al., 2001). Concentrations are generally low in surface waters (0.01 - 0.04 nM), increase to a maximum in the upper thermocline (0.03 - 0.1 nM), and then decrease to values in deep waters of 0.01 - 0.03 nM (Martin, 1985b; Martin et al., 1989; Martin et al., 1993; Knauer et al., 1982; Johnson et

al., 1988; Ngoc and Whitehead, 1986; Sakamoto-Arnold et al., 1987; Westerlund et al., 1991). Cobalt may be added to the surface oceans from anthropogenic and natural sources via riverine input and atmospheric deposition, especially from the burning of fossil fuels (Arimoto et al., 1989; Donat et al., 1995; Pacyna, 1984). The relative importance of these sources is spatially and temporally variable.

Most of the presently available vertical profiles were obtained in close proximity to major land-masses and the concentration of cobalt increases towards the coast, reaching concentrations as high as nM levels in rivers/estuaries: e.g. Knauer et al. (1982) measured cobalt amount varying between 0.85 and 20.3 nM in north S. Francisco Bay. The source of cobalt in the surface waters has frequently been suggested to be direct run-off from land (Tappin et al., 1993). Johnson et al. (1988) reported that cobalt is removed from the oceans interior by scavenging onto manganese oxide particles. They showed a sub-surface maximum of 0.11 nM at 36 m. The surface concentration of cobalt increased from 0.037 to 0.098 nM. The increase of cobalt at the surface was accompanied by a corresponding increase in nitrate and decreases in oxygen and temperature. Cobalt concentration decreases rapidly with depth below the maximum to values of 0.030 nM between 200 and 600 m. This decrease in cobalt concentration is indicative of removal by scavenging onto particle surfaces. In the bottom waters, the cobalt concentration has been observed to increase with depth towards the water-sediment interface in oxygen-poor basins. It was suggested that under reducing conditions, as manganese oxides are reduced, cobalt is released from the solid phases and subsequently migrates into the bottom water. Thus, the geochemistries of cobalt and manganese may

be interrelated (similar results have been previously reported by Knauer et al., 1982).

1.3 MANGANESE

1.3.1 Origin and nature

Although the common manganese mineral pyrolusite (manganese dioxide) has been used to remove the green colour imparted to glass by iron(II) compounds since the time of the Pharaohs, it was not until 1774 that Scheele recognised that pyrolusite contained a new element. It was the mid 1930s before pure manganese as a silver-white brittle metal was produced by electrolysis. Manganese is the twelfth most abundant element in the earth's crust (0.106% by weight), and is found in some 250 different minerals. The metal occurs as silicates in primary hydrothermal deposits and also it is readily removed by weathering from igneous and metamorphic rocks. Its main commercial ores occur as carbonates or oxides deposited under alkaline conditions in a sedimentary form, as are the major commercial metals iron and aluminium, with which it is often found (Encyclopaedia, 1995). The deposition of manganese as ferromanganese nodules on the deep ocean floor, or as manganese-rich sediments in shallower saline waters and freshwater lakes, has been a matter of extensive study. Such deposits are produced by slow accretion of layers of manganese and iron oxides removed by the weathering of rocks into the aquasphere, contain not only large amounts of iron and manganese (between 10% and 30% by weight in the latter case), but smaller amounts of the commercially attractive metals cobalt, nickel and copper. It is estimated that 10^{12} tonnes of ferromanganese nodules are present on the ocean floor, with some further 10^7 tonnes deposited annually.

There is little industrial demand for manganese metal and virtually all ore produced is used to manufacture ferromanganese. This product, containing approximately 78% manganese, is obtained by the reduction of pyrolusite and ferric oxide (Fe_2O_3) with coke in a blast furnace. It is used to scavenge oxygen and sulphur during the production of steel. As well as acting as a deoxidizer, large amounts (up to 12%) of manganese are alloyed in steel to produce toughness. Manganese is also used in relatively large percentages in both copper and aluminium alloys to yield greater strength and hardness. Other uses for manganese compounds are found in the production of dry cell batteries (pyrolusite), in dyes, paint dryers, catalysts, wood preservatives, glass and ceramic production and pharmaceutical products; it is also added as an essential trace element to fertilisers and animal foods.

Although manganese activates many enzymes, no single biochemical role has been identified for this metal. Mn resembles magnesium in activating a number of phosphate transferases and decarboxylases, notably those used in the Krebs cycle. It appears to remain in the divalent state (Kendrick, 1992).

In public water supplies, manganese causes such difficulties as staining of clothes and plumbing fixtures, "black water", and encrustation of mains. In industrial supplies, it causes severe economic losses through discoloration of products, specks in finished goods, and reduction in pipeline carrying capacities. Although manganese is of little direct toxicological significance, with the exception of the purple-coloured permanganates, which have bactericidal properties, it may have a protective effect and control the concentration of other elements, including toxic heavy metals in surface waters. The current World Health Organisation (WHO) guideline for manganese levels is 0.5 mg l^{-1} on health grounds and 0.1 mg l^{-1} to avoid staining problems. The EC Directive and

UK regulations set a maximum admissible concentration of 0.05 mg l^{-1} (Twort, 1994).

1.3.2 Manganese in marine environments

The concentration of manganese found in natural waters is generally quite low, although the concentration in certain reservoirs has at times become as high as 10 mg l^{-1} , average concentrations usually lie in the range $0.1\text{-}1.0 \text{ mg l}^{-1}$. The use of manganese as a tracer has improved our understanding of eolian, coastal, and riverine inputs to the ocean (Martin and Knauer, 1985). The observed values for dissolved Mn(II) in open ocean waters are normally between 0.2 nM and 3 nM (Jickells et al., 1987). In recent years, it has also been found that a large amount of manganese is injected into the deep waters by hydrothermal emanations through active oceanic crust (Heggie et al., 1987). In natural waters, manganese is found in the +II, +III, and +IV oxidation states. In the oxidising, alkaline conditions of the ocean environment Mn can be found predominately in the form of particulate MnO_2 (Bruland et al., 1983; Stumm et al., 1996). The primary dissolved form of Mn is thought to be Mn(II). Although recent work (Kostka et al., 1995) suggests that there may be soluble Mn(III) complexes in natural waters, which are likely to be present only as meta-stable intermediates, most of the Mn(III) is present as particulate oxides. Dissolved Mn is very reactive in marine environments. The geochemical distribution of Mn in seawater is erratic and strongly influenced by the redox fluctuations. Because of redox influence trends in Mn distribution with respect to seawater depth are variable (Quinby-Hunt and Wilde, 1986; Statham et al., 1985). According to Burton and Statham (1988) the dominant factor that affects the aquatic geochemistry of Mn is the change of oxidation state between reducing and

oxidising environments, coupled with a marked difference in the reactivity of the metal between the two oxidation states; the Mn(II) form, which is the stable state under reducing conditions, is more soluble and geochemically mobile than the Mn(IV) state. Dissolved Mn(II) is supplied to the surface of the ocean mainly via river run-off and diffusion from shelf sediments at the ocean basin margins, and by dissolution from atmospheric particulates over all regions. The dissolved Mn is extremely particle reactive and originally it was thought that the uptake on to suspended particles occurred via microbial oxidation (Sunda and Huntsman, 1988). According to Moffett (1997), although microbial oxidation is found in the Sargasso Sea, a non-oxidative, and biologically mediated uptake occurs in the equatorial Pacific; i.e. the geochemical cycling of Mn is different in the two environments. Relatively high concentrations of dissolved Mn are maintained in surface waters by atmospheric deposition and *in situ* photochemical reduction and photoinhibition of microbial oxidation, processes that do not occur in the lower euphotic layer, where an increase in particulate Mn can sometimes be observed. Dissolved Mn is scavenged throughout the water column on a time-scale of 10-100 years, and once scavenged, this form of Mn is regenerated only under reducing conditions. As a result of these input and removal processes, vertical profiles of dissolved Mn in a 'typical' oceanic water column show a generally consistent overall pattern in which the concentrations are highest in the surface waters and decrease rapidly to low values, which usually are maintained to the bottom. Major perturbations to the typical down column dissolved Mn profiles can be found in regions of hydrothermal activity. Hydrothermal emanations originating at mid-ocean ridges have been thought to provide a substantial source of manganese to the ocean but the evidence supporting this hypothesis is indirect. Anomalous manganese concentrations

have been measured in naturally occurring systems where seawater is in direct contact with lava flows, and laboratory studies have shown that seawater tends to leach manganese from basalt at elevated temperatures and pressures (Bender et al., 1977; Klinkhammer and Bender, 1980; Klinkhammer and Bender, 2000; Klinkhammer et al., 1991; Landing and Bruland, 1989; Murray et al., 1983). Manganese affects trace metals equilibria in marine environments in three ways: (a) adsorption of metals on the Mn oxide surface; (b) coprecipitation of trace metals with Mn solid phases and (c) involvement in redox reactions. For example, several investigators have reported a strong association between Mn nodules and cobalt (Baturin, 1988; Baturin et al., 1989; Manheim, 1986). Co is strongly enriched in marine Mn oxides phases, such as Mn nodules and ferromanganese crusts. X-ray absorption studies have shown that Co is in the trivalent state in these phases. Cobalt adsorption and oxidation could occur on the surfaces of Mn oxides in the water column, which could form a significant mechanism for Co removal (Table 1.3) (Li, 1991).

Table 1.3: The average concentrations of Co in SW C_{sw} , shale C_{sh} , oceanic pelagic clays C_{op} , manganese nodule C_{Mn} , marine organisms C_{org} .

	C_{sw} 10^{-12} g/g	C_{sh} 10^{-6} g/g	C_{op} 10^{-6} g/g	C_{Mn} 10^{-6} g/g	C_{org} 10^{-6} g/g
Cobalt	1.2	19	74	2700	0.43

Important evidence of the correlation between Mn and Co biogeochemistry in marine environment is the implication of Mn oxidising bacteria in Co(II) oxidation. Microbially mediated precipitation of Co and Mn by oxygen dependent, microbial processes has been shown in two fjords and in

decomposing diatom cultures. More recently, Tebo et al. (1984) and Emerson et al. (1982) have shown that spores of a marine *Bacillus*, which oxidises Mn(II), can also oxidise Co(II) to Co(III) oxide even in the absence of Mn (Tebo and Lee, 1993). Therefore, it is possible that Co and Mn are oxidised in seawater via a common microbial pathway.

1.4 ANALYTICAL METHODS FOR THE DETERMINATION OF COBALT AND MANGANESE

A variety of instrumental analytical techniques have been used for the determination of Co and Mn in environmental, biological and synthetic media. This section summarises the most significant methodologies for the determination of Co and Mn in natural waters.

1.4.1 Spectrophotometry

Spectrophotometric analytical methods are based on the formation of a specific complex with a characteristic absorption wavelength. Spectrophotometric instrumentation generally has the advantage of portability, very good limit of detections and cheap purchase/building costs. Malahoff et al., (1996) reported a limit of detection of 17 pM for cobalt in seawater using the catalytic effect of Co(II) on the oxidation of *N,N*'-diethyl-*p*-phenylenediamine by H₂O₂ in the presence of Tiron as an activator. Resing et al., (1992) reported a limit of detection of 36 pM for manganese in seawater by formation of the malachite green complex obtained from the reaction of leucomalachite green and potassium periodate with Mn(II) acting as a catalyst. However spectrophotometric methods can suffer from interferences especially for

samples with a complex matrix such as seawater (Azubel et al., 1999; Brasil et al., 1996; Chen et al., 1999; Chikhalikar et al., 1998; Gao, 1996; Igarashi et al., 1996; Malahoff et al., 1996; Nakano et al., 1999; Ozturk et al., 2000; Suzuki et al., 1997; Watanabe et al., 1994; Zhang et al., 1994).

1.4.2 Atomic Spectrometry

In the 1970s and 1980s atomic spectrometric techniques became the generally preferred approach for Mn and Co determinations in seawater. These methods generally involve a preconcentration step using solvent extraction or an on-line chelation column with GFAAS and, more recently, with ICP-MS detection. Atomic spectrometric techniques do not allow redox speciation. Furthermore the cost involved in instrument purchase and operation are high. GFAAS and ICP-MS are however frequently used to verify shipboard measurements and are considered to be good laboratory reference techniques (Atanasova et al., 1998; Atanassova et al., 1998; Azeredo et al., 1993; Batterham et al., 1997; Benkhedda et al., 2000; Bloxham et al., 1994; Bradford et al., 1991; Cullen et al., 1999; Falk et al., 1997; Field et al., 1999; Hopkins, 1991; Hughes et al., 1995; Klemm et al., 1999; Kumagai et al., 1998; Li et al., 1996; Nickson et al., 1997; Nickson et al., 1999; Nicolai et al., 1999; Saleh et al., 1999; Steffan et al., 1993; Willie et al., 1998; Blain et al., 1993; Grotti et al., 1999; Kenawy et al., 1996; Koshino et al., 1993; Lamoureux et al., 1994; Lin et al., 2001; Nakamura et al., 1994; Porta et al., 1991; Sengupta et al., 1995; Shimizu et al., 1991; Sperling et al., 1991; Weel and Bruland, 1998; Yebrabiurrun et al., 1995; Yuzeforsky et al., 1994; Zhang et al., 2000; Zhuang et al., 1994).

1.4.3 Stripping Voltammetry

Electrochemical methods have proved to be a useful and powerful investigating tool for trace metal determinations. Among electrochemical techniques typically used by marine chemists, stripping voltammetry is the most common one. The strength of stripping voltammetry is its extremely low detection limits (10^{-10} - 10^{-12} M), its multi-element and speciation capabilities and its suitability for on-line, ship-board and in-situ applications. Adsorption Cathodic Stripping Voltammetry (AdCSV) allows direct measurements (without prior concentration of the sample) of saline solutions such as seawater. It is in this area (for the purpose of monitoring and speciation studies) where voltammetry has an advantage over other techniques such as ICP-MS (by which have the capability of very fast measurement of a large number of elements in aqueous solutions of controlled composition but which currently cannot handle saline solutions without dilution or analyte extraction).

AdCSV suffers from interference from competitive adsorption by surface-active organic compounds and it can require long deposition time. The electrodes can be sensitive to vibration, electrostatic interferences and power surges common on ships, and are less robust compared to automated wet chemistry manifolds (Achterberg et al., 1999; Buckley, 1986; Colombo et al., 1997; Donat and Bruland, 1988; de Jong et al., 2000; Economou et al., 2000; Gassama et al., 1994; Ghoneim et al., 2000; Gledhill et al., 1997; Herreramelian et al., 1994; Nimmo et al., 1993; Nimmo et al., 1997; Nimmo et al., 1998; Qian et al., 1998; Roitz et al., 1997; Saito et al., 2001; Tercier et al., 1998; Vega et al., 1997; Yamada and Suzuki, 1984).

1.5 CHEMILUMINESCENCE

Generally speaking, chemiluminescence reactions are oxidation reactions. The use of chemiluminescence (CL) in analytical chemistry suffers from a limited availability of commercial instrumentation, mono-elemental analysis and complex matrices may interfere seriously. However it can offer substantial advantages over other techniques. Compared with other instrumental methods of analysis, CL is simple, rapid, robust, portable, with excellent detection limits (sub-nanomolar levels) and does not require expensive apparatus. The rapid response (seconds) makes it ideally suited to shipboard determinations.

Chemiluminescence is described in more details in Section 1.5.2. For the determination of cobalt and manganese a variety of CL reagents have been used such as gallic acid, pyrogallol, luminol, tiron (Bowie et al., 1995; Cannizzaro et al., 1999; Chapin et al., 1991; Chen et al., 1994; Hirata et al., 1996; Komatsu et al., 1986; Isshiki et al., 1987; Lin et al., 1996; Okamura et al., 1998; Palaroan et al., 2000; Qin et al., 1997; Qin et al., 1998; Sakamoto-Arnold et al., 1987; Tsukada et al., 1998; von Langen et al., 1997; Xie et al., 1998; Zhou et al., 1997).

1.5.1 Chemiluminescence detection at sea

Reported methods for use of CL for trace metals analysis at sea are shown in Table 1.4 together with the typical levels of Cu, Fe, Co, and Mn in marine waters and the analytical figures of merit. All methods have used the Flow Injection (FI) technologies for rapid and reproducible sample handling. The principal CL reagents for the Fe and Co reactions generate the required sensitivity to measure the analyte at sub-nanomolar concentrations. The systems for Mn and Cu employ sensitisers and/or micellar surfactant assemblies to provide a micro-environment suitable for enhancing the weak CL reaction.

Table 1.4: Typical concentrations of Fe, Cu, Co and Mn in coastal and open ocean and coastal waters and previously reported CL reaction systems.

Element	Typical surface levels in coastal waters	Typical surface levels in open ocean	Principle CL reagent	Other reagents	Oxidant	Linear range	FI-CL Detection limit	Reference
Fe (III)	5 nM	0.8 nM	Luminol	NaOH	Dissolved O ₂	0.04 – 10 nM	40.0 pM	Bowie et al., 1998
Cu (II)	10 nM	1.0 nM	Gallic acid	Methanol, NaOH	H ₂ O ₂	0.4 – 100 nM	0.3 nM	Sakamoto-Arnold et al., 1987
Co (II)	700 pM	100.0 pM	TCNQ	DDAB, Eosin Y	Dissolved O ₂	0.01 – 1 nM	5.0 pM	Chapin et al., 1991
Mn (II)	35 nM	2.0 nM	1,10-phenanthroline	CEDAB, TEPA	H ₂ O ₂	0.1 – 100 nM	0.1 nM	Coale et al., 1992

1.5.2 Theory of chemiluminescence

Luminescence spectrometry is a widely used technique in analytical chemistry (Baeyens et al., 1991) and is defined as *“the emission of UV, visible or NIR radiation from a molecule or an atom resulting from the transition of an electronically excited state to a lower energy state (usually the ground state)”* (Campbell, 1988). Several kinds of luminescence are known, classified on the basis of the kind of energy absorbed, e.g. light, x-rays, heat, ultrasound from chemical reactions, or from biological reactions. Luminescence is a general term applied to the emission of electromagnetic radiation by an atomic or molecular species, originating from the decay of that species from a higher to a lower quantized energy state. Figure 1.5 shows a Jablonski diagram, illustrating processes defined as absorption, fluorescence, internal conversion, intersystem crossing, phosphorescence that can take place for a photon-absorbing molecule excited between the ground state and electronically excited states.

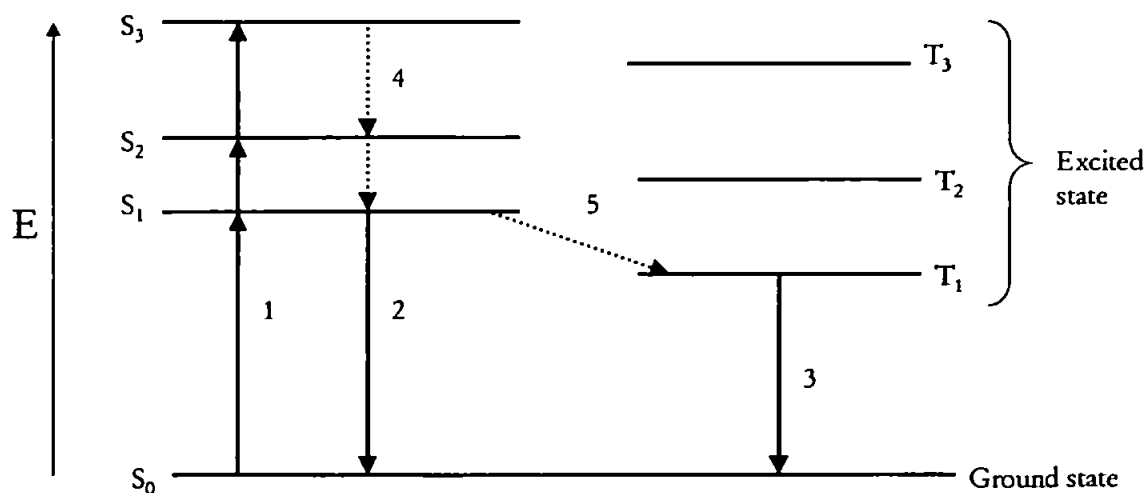
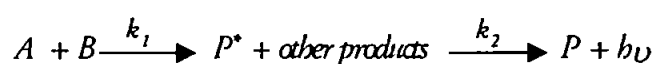


Figure 1.5: Concept of energy level and transition: 1, absorption; 2, fluorescence; 3, phosphorescence; 4, internal conversion; 5, intersystem crossing; E energy; S, singlet state; T, triplet state.

Chemiluminescence (CL) can be defined as the production of electromagnetic radiation (ultraviolet, visible or infrared) by a chemical reaction, the term being first used by Eilhardt Weidemann in 1888. Bioluminescence consists of visible wavelength CL produced by (bio)chemical systems of living organisms. The phenomenon of chemiluminescence has been known for a long time. In 1877 Radziszewski found that lophine emitted green light when it reacted with oxygen in the presence of a base. This is the first example of chemiluminescence using a synthetic organic compound. Since then, a number of chemiluminescent compounds have been synthesised and their chemiluminescence properties studied. Chemiluminescence reactions can be observed in solid, liquid and gas phases and have been exploited for analytical purposes. Chemiluminescence emissions have been identified as direct or indirect (e.g. sensitised) depending on their origin. In a generic, direct chemiluminescence reaction between analyte A and reagent B, a primary electronically excited fluorophore (P^*) is produced, which can subsequently relax to the ground state with the emission of a photon, $h\nu$:



where $k_2 \gg k_1$ and k_1 is therefore the reaction rate limiting value. A higher emission intensity is achieved through a more efficient production of the excited state:

$$I_{CL} = \Phi_{CL} \frac{dP}{dt} = \Phi_{Ex} \Phi_{Em} \frac{dP}{dt}$$

where:

- I_{CL} is the CL emission intensity (photons emitted per second)
- Φ_{CL} is the CL quantum yield (photons emitted per molecule reacted)
- dP/dt is the rate of chemical reaction (molecules reacting per second)
- Φ_{Ex} is the excitation quantum yield (excited states produced per molecule reacted), and
- Φ_{Em} is the emission quantum yield (photons emitted per excited state molecule produced).

The quantum yield (Φ_{CL}) of a reaction is therefore the product of the efficiencies of the excitation and emission steps and values ranging from 0.001 to 0.8 have been observed (Campbell, 1988), higher Φ_{CL} usually being associated with effective biological systems. CL emissions are characterised by their colour, intensity, and rates of production and decay. Since rate constants are usually not known however, CL procedures require empirical standardisation.

Four conditions must be satisfied for CL emissions to occur:

1. The reaction enthalpy must be suitably exothermic, with typically a free-energy change of between 170-300 kJ mol⁻¹.
2. An energetically favourable reaction pathway must exist for generation of an excited state species.
3. The reaction rate must be high enough for detection ($k_2 \gg k_1$).
4. A favourable deactivation pathway must exist to allow CL emission.

Such guidelines are general and in many cases CL behaviour cannot be predicted. The advantages of CL reactions for analysis include their high sensitivities, wide linear dynamic ranges and speeds of response, all of which can be achieved with relatively simple instrumentation. The absence of an emission source (as in e.g. fluorescence spectrophotometry) eliminates noise due to Raman or Rayleigh scattering and detection systems can therefore be

operated at extreme photomultiplier voltages for improvement in signal-to-noise ratios. Femtomole detection limits have been attained for the detection of certain enzymes (Birks, 1989). Novel CL systems, primarily based on the oxidation of organic compounds that are more selective towards the analyte in question, despite often having lower CL quantum yields. The utilisation of reversed micelles and surfactant assemblies as suitable reaction media (Saitoh et al., 1998) has improved the characteristics of many CL reactions, and weak emissions have been enhanced through non-radiative transfer to sensitizer molecules (Segawa et al., 1994).

The potential of CL-based analytical techniques in environmental, biomedical, toxicological and related areas has been documented in detail in a number of recent reviews, covering various aspects of its application (Bowie et al., 1996; Lewis et al., 1993; Robards et al., 1992). In solution-phase, CL has recently found many applications in analytical chemistry for the determination of metal ions, inorganic anions and biomolecules, in a variety of environmental and clinical matrices. Many such systems employ flow injection (FI) (see Section 1.6) as a means of mixing sample and reagent solutions. The rapid and transient nature of solution-phase CL requires a means of rapid and reproducible mixing of sample and reagent streams. Luminescent detection systems have therefore received an increased interest since the advent of flow injection (FI), a powerful methodological innovation for sample handling that has been established over more than two decades of research.

To show the research interest in FI-CL over the last 10 years, in Table 1.5 are reported applications of the technique for the determination of metal ions in different sample matrices.

Table 1.5: FI-CL methods for metal ions species.

Species	CL reaction	Sample matrix	LOD	Reference
Co(II)	Catalyzed oxidation of dibromoalizarin violet by H ₂ O ₂ in alkaline solution; enhanced using cationic surfactant	Natural waters	68 pM	Chen et al., 1994
Co(II)	Gallic acid – H ₂ O ₂ reaction; preconcentration column containing 8-hydroxyquinoline immobilized on silica gel, fluoride containing metal alkoxide glass (8HQ-MAF)	Sea water	11 pM	Hirata et al., 1996
Co(II), Mn(II)	Luminol oxidation by potassium periodate	Fresh, polluted waters, vitamin B ₁₂	0.2 nM Co(II) 0.4 nM Mn(II)	Lin et al., 1993
Co(II), Fe(II)	Decomposition of peroxymonosulfate; use of brilliant sulfoflavin sensitizer in micellar solution	Pepperbush, pond sediment	5.0 nM Co(II) 6.0 nM Fe(II)	Makita et al., 1994
Co(II), Fe(II)	Transition metal ion decompositions of peroxymonosulfate ion	Synthetic	10 nM Co(II) 0.2 µM Fe(II)	Makita et al., 1993
Cu(II)	Oxidation of copper(II) - 1,10-phenanthroline chelates by H ₂ O ₂ at alkaline pH	Sea water	0.05-0.10 nM	Sunda and Huntsman, 1991
Cu(II)	Oxidation of copper - 1,10-phenanthroline complex by H ₂ O ₂ ; separation of copper from matrix on immobilized 8-hydroxyquinoline	Sea water	0.4 nM	Coale et al., 1992
Cu(II)	Oxidation of 1,10-phenanthroline; copper complexation and ligand titration measurements	Seawater	0.1 nM	Zamzow et al., 1998

Table 1.5 (continued): FI-CL methods for metal ions species.

Species	CL reaction	Sample matrix	LOD	Reference
Cu(II)	Fluorescein - hydroxylamine - OH ⁻ system; potassium fluoride acts as masking agent for Fe(II,III) and Co(II)	Serum	7.9 nM	Lin and Hobo, 1995
Cr(III)	Luminol - H ₂ O ₂ system	Distilled, drinking, mineral, waste waters, food samples	0.2 nM	Escobar et al., 1993
Cr(III)	Oxidation of pyrogallol with periodate at neutral pH; increased intensity with 3-(N- morpholno) propanesulphonic acid	Synthetic	19 nM	Nakano et al., 1993
Cr(III)	Catalysed luminol oxidation by H ₂ O ₂ ; using rate of binding to inhibitory ligand (EDTA) to gain specificity	Urine, blood serum, hair	0.2 nM	Escobar et al., 1998
Cr(III), Cr(IV)	Separation by anion-exchange column; reduction by sulfur dioxide solution; detection by luminol oxidation	Fresh water	1.0 nM Cr(III) 1.9 nM Cr(IV)	Beere and Jones, 1994
Cr(III), Cr(VI)	Cr(III)-catalyzed oxidation of luminol by H ₂ O ₂ ; Cr(VI) reduction using H ₂ O ₂ in acidic medium	Waste water	<1.0 nM	Escobar et al., 1995
Au(III)	Tetrachloroaurate(III) - luminol system in reversed micellar system	Chloroform	51 pM	Imdadullah et al., 1991
Au(III)	Tetrachloroaurate(III) with luminol in reversed micellar medium	Silver based alloy	0.05 fM	Imdadullah, 1994

Table 1.5 (continued): FI-CL methods for metal ions species.

Species	CL reaction	Sample matrix	LOD	Reference
Fe(II), Fe(III)	Reaction of luminol – H ₂ O ₂ – Fe(III)oxine complex; enhancement using reversed micellar solution (CTAC) in chloroform-cyclohexane; on-line solvent extraction; reversed FI manifold	Synthetic	90 nM	Kyaw et al., 1998
Fe(II), total dissolved Fe	Brilliant sulfoflavin - H ₂ O ₂ in neutral medium; preconcentration on 8-hydroxyquinoline column	Sea water	0.5 nM	Elrod et al., 1991
Fe(II), total Fe	Luminol – H ₂ O ₂ reaction; use of citric acid as activating and masking agent; micelle enhancement using cationic surfactant; silver reductant column	Human hair, natural waters	5 nM	Saitoh et al., 1998
Fe(II), total dissolved Fe, Mn(II), total dissolved Mn	Catalysed luminol oxidation using potassium periodate; reversed FI manifold; in-situ monitoring	Underground water treatment, drinking water	54 pM Fe(II) 91 pM Mn(II)	Zhou and Zhu, 1997
Fe(III)	Luminol - aqueous ammonia - H ₂ O ₂ reaction; selective column extraction using 8-HQ chelating resin; natural oxidation of sample to measure dissolved Fe	Sea water	50 pM	Obata et al., 1993
Fe(II+III)	Luminol – dissolved oxygen – Fe(II) reaction; in-line matrix elimination and preconcentration on 8-hydroxyquinoline column; Fe(III) reduction using sulphite; shipboard analysis	Sea water	40 pM	Bowie et al., 1998
Fe(III)	Luminol chemistry; in-line preconcentration; shipboard analysis	Sea water	21 pM	de Jong et al., 1998

Table 1.5 (continued): FI-CL methods for metal ions species.

Species	CL reaction	Sample matrix	LOD	Reference
Mn(II)	Oxidation of 7,7,8,8-tetracyanoquinodimethane in alkaline solution; preconcentration on immobilized 8-hydroxyquinoline	Sea water	0.1 nM	Chapin et al., 1991
Mn(II)	Oxidation of 7,7,8,8-tetracyanoquinodimethane in alkaline solution; eosin Y sensitization in surfactant bilayer vesicles	Raw, processed water	82 nM	Bowie et al., 1995
Mn(II)	Luminol – H ₂ O ₂ reaction; removal of Fe interference using 8-hydroxyquinoline column	Sea water	29 pM	Okamura et al., 1998
Mn(II)	Kinetic study of the oxidation of Mn(II) at nanomolar concentrations; reaction of 7,7,8,8-tetracyanoquinodimethane in alkaline solution	Sea water	Not reported	von Langen et al., 1998
Ag(I)	Hydrophilic cation-exchange resin; detection based on oxidation by luminol with peroxodisulfate	Synthetic	4.6 nM	Jones and Beere, 1995
Ti(IV)	Reaction of Ti(III) with carbonate buffer; on-line Jones reductor column	Synthetic	1.0 µM	Alwarthan et al., 1991
Zn(II)	Micellar enhanced chemiluminescence of 1,10-phenanthroline using trimethylstearylammmonium chloride (TSAC)	Synthetic	23 nM	Watanabe et al., 1999

1.6 FLOW INJECTION ANALYSIS (FIA)

Flow Injection improves the performance of chemiluminescence detectors since it is ideally suited to maximise the analyte signal. Usually the light production is rapid, in the milliseconds range, that quick mixing immediately followed by detection is critical to the sensitivity of the system. Since its development in the mid-1970s, FI has become a routine laboratory technique for sample analysis and on-line sample treatment. FI constitutes the most advanced form of solution manipulation available to analytical chemists for mixing and transporting the reagents and products of a chemical reaction to the point of measurement.

First reported by Ruzicka and Hansen in the 1970s, several texts discuss the theory, instrumentation and practice (Karlberg et al., 1989; Ruzicka et al., 1988; Valcarcel et al., 1987). FI is capable of a fast response (typically 10-120 s) and a high sample throughput (typically 30-120/h) with low reagent consumption (typical flow rates are 0.5-2.0 mL/min) and low operational costs and is easily adapted to automated analysis.

The simplest possible manifold configuration is illustrated in Figure 1.6. The manifold design can vary considerably depending on the conditions defined by the method. During the development stage of a method, it is desirable that manifold modifications can be made rapidly and easily to save time. A manifold typically consists in a single-channel system in which the carrier stream (which can also contain a reagent) transports the sample to the detector. If the method requires more than one reagent, additional streams can be merged with the carrier stream at suitable points in the manifold. Common FI manifolds consist of a propulsion unit (such as a peristaltic pump), a six-port rotary injection valve, and a flow-through detector. Narrow-bore poly(tetrafluoroethylene)

(PTFE) tubing (typically 0.8 mm i.d.) is used for sample and reagent transport, and tightly wound coils are often included to aid mixing (Andrew et al., 1994).

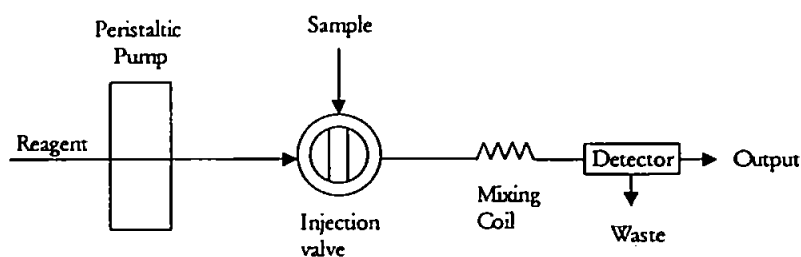


Figure 1.6: Simple single channel FI manifold.

The essential components of a FI manifold, and their characteristics are described below. The liquid delivery or propulsion device is a basic piece of equipment. FI systems are in essence low-pressure systems, with seldom more than a few atmospheres of pressure developed in the conduits. The main features of an ideal liquid delivery device for FIA can be summarised as follows: multi-channel capability, pulse-free fluid delivery, and readily adjustable flow-rates. Owing to its high versatility, the peristaltic pump is undoubtedly the most often used liquid propulsion device in FIA. The main disadvantages of such devices is their flow pulsation, a lack of long term flow-rate stability, and low resistance (of the pump tubes) to organic solvents and high concentrations of strong acids. Transport conduits are an integral component of any flow analysis system. The function of transport conduits is to provide connections between the different components of the flow system. In FIA, PTFE tubings of 0.35-1.0 mm i.d. are used most often for such purposes. Although the outer diameter is

not critical, the tube walls should not be thinner than 0.5 mm to ensure adequate mechanical strength. FI manifolds are essentially made up of a network of T-connections, connecting the different components of the system. Instead of a T-configuration, Y or W-configurations for the merging conduits may also be used for producing not as good mixing effects.

The injection system in FI must be capable of inserting a fixed, precise volume of sample into a carrier stream. The rotary injection valve is based upon a six-port PTFE unit, incorporating a sample loop and/or solid phase column. The unit has two operating positions: the first for loading the loop or column with sample, and the second for eluting the sample from the loop into a carrier stream (Figure 1.7).

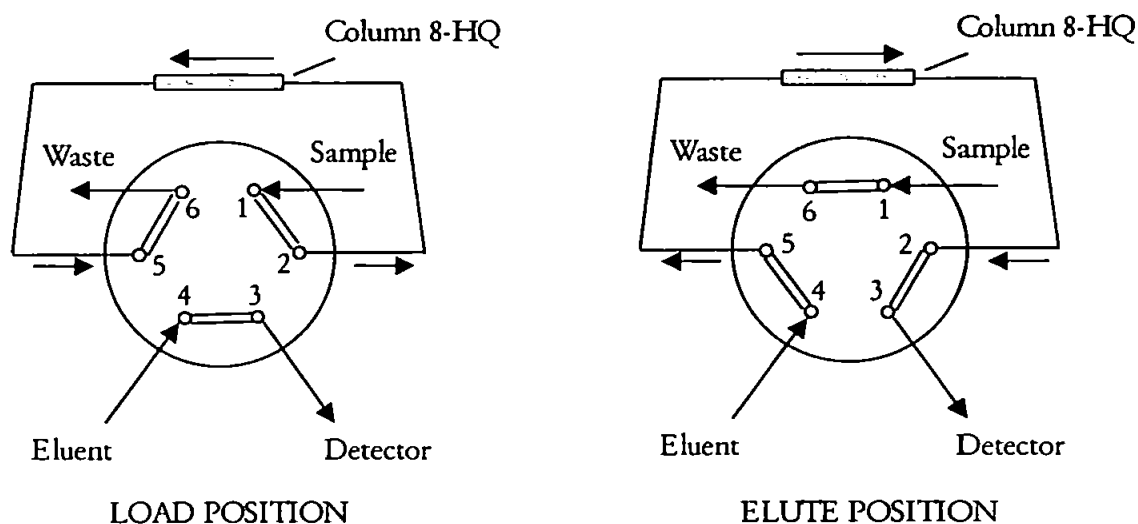


Figure 1.7: The 6-ways injection valve

The flow direction of the eluent should be opposite to the loading. This is necessary to avoid the column becoming more and more tightly packed, which could in turn influence the flow rate and produce leakage problems. With strongly sorbed species (such as Co onto 8-HQ) reversed flow elution is also beneficial in decreasing the dispersion of the concentrate during elution (Fang, 1993).

Pump tubes are made of either PVC, silicone or other related plastic materials. The most commonly used material is Tygon[®], a transparent, PVC-type material. The main function of mixing reactors is to promote the reproducible radial mixing of two or more components merged through a T-piece. The reactor is usually made of PTFE tubing with the same range of dimensions as for the transport conduits. The tubes are coiled, knotted, or knitted.

Another essential component of a FI system is the flow cell. It is normally incorporated within the detector housing. This component should be inert, generate effective mixing and be designed to maximise a property of the analyte (e.g. CL emission) which is continuously monitored by the detector. Some CL reactions are rapid (1-10 s) so it is necessary that solutions enter the flow cell as soon as possible after mixing of sample and reagents. For this purpose an extra 'T' piece can be connected to the cell, so that the sample and reagents can mix inside the cell before passing to waste.

The CL detector in a FI system must respond directly to light to produce an electrical signal that may be sent to a recorder. Three types of detection system are available which are capable of monitoring CL with low photon emission; namely photoelectric devices (e.g. photomultiplier tubes, photon counting modules), photoconductor devices (e.g. photodiodes) and charge transfer devices (e.g. CCD cameras).

A photomultiplier tube (PMT) is commonly used and generates and multiplies electrons from incident photons and thereby enhances the signal. The PMT end-window (10 mm effective diameter, fused silica glass) detects a photon at the photocathode and emits an electron according to the photoelectric effect (primary emission).

1.7 RESEARCH OBJECTIVES

Interest in Fe, Cu, Co, and Mn in open ocean and coastal waters has increased in recent years due to their dual roles as essential nutrients at low concentrations and inhibitors at elevated concentrations (Wells and Bruland, 1998).

As part of the MEMOSEA project (MAS3-CT97-0143) the construction of a flow-injection (FI) - chemiluminescence (CL) monitor for Co and Mn has been realised with special emphasis on new technologies and improvement of existing technologies. The deliverables of the project address the needs for high resolution/quality data and operator friendliness and are clearly relevant to EU legislation covering the aquatic environment and in particular protection of the seas. The research objectives for this PhD project were to:

- investigate the behaviour of 8-HQ in preconcentration/matrix removal columns (Chapter 2)
- investigate chemiluminescence reaction chemistries for the determination of Co(II), design a flow injection manifold based on chemiluminescence detection and develop in-line preconcentration to lower detection limits and remove the sea-salt matrix (Chapter 3)
- investigate chemiluminescence reaction chemistries for the determination of Mn(II), design a flow injection manifold based on chemiluminescence detection and develop in-line preconcentration to lower detection limits and remove the sea-salt matrix (Chapter 4)
- use the FI-CL system in field trials and deploy the system on-board an oceanographic cruise (Chapter 5).
- validate the methods using CRMs and by participation in an intercomparison exercise.

CHAPTER 2

SYNTHESIS AND CHARACTERISATION OF A CHELATING 8-HYDROXYQUINOLINE RESIN FOR TRACE METALS PRECONCENTRATION.

2.1 INTRODUCTION

Cleanup of analytical samples prior to the determination of various metal ions has been a long-standing problem in chemical analysis. This sample pre-treatment has two main goals. One is to separate the target metal ion from a large excess of salts, organic material, dirt, and other matrix components that would interfere in the analytical measurement step. A second goal is to preconcentrate the metal ions to be determined to a point where their analytical determination is facilitated (i.e. above the detection limit of the method). In the past liquid-liquid extraction has played a major role in sample cleanup and preconcentration of the sample components to be measured. However, recovery of sample components by liquid extraction is seldom complete. Liquid extraction tends to be slow and labour-intensive. More stringent environmental concerns are making the use and disposal of large amount of organic solvents more difficult. The popularity and use of solid-phase extraction (SPE) is now well established. SPE is easily automated, faster and in general more efficient than liquid-liquid extraction (Fritz, 1999). The particles used in SPE are non polluting and the amount of liquid solvents use are significant lower than in liquid-liquid extraction. In principle, SPE is analogous to liquid-liquid extraction. As a liquid sample is passed through the SPE column, analytes are

extracted from the sample onto the sorbent material in the column. Interferences can be selectively removed from the column through the correct choice of “wash” solvents. Finally, the desired analytes may be selectively removed from the column by an elution solvent, resulting in a highly purified extract. This extract is often significantly more concentrated than the original sample. Alternatively, an extraction column may be selected which retains the interferences in the sample, but allows the analytes to pass through unretained. Off-line batch methods, either with columns or by static equilibration, can be used and they offer prominent advantages in achieving a large gain in sensitivity as well as separation of the interfering sample matrix, but they are tedious to operate and large amounts of sample are often required for each determination. These shortcomings have largely been overcome by using on-line column preconcentration whilst the advantages of the off-line procedures are preserved. The advantages of the on-line column preconcentration over conventional batch procedures can be summarised as follows. First, the columns offer much greater efficiency (preconcentration is usually higher or a larger numbers of samples can be processed) (Fang et al., 1987). Secondly, sample consumption and reagent consumption is lower than conventional batch procedures. Thirdly the closed preconcentration system decreases the risks of contamination from the laboratory environment. Finally, the continuous monitoring of the baseline provides better checks on column performance.

There are a large number of chelating resins for the removal of various metal ions from solution (Kantipuly et al., 1990; Myasoedova et al., 1986). The correct choice of the chelating agent is critical to ensure a successful SPE extraction procedure. When considering a specific extraction problem, many different aspects influence chelating reagent selection, including the nature of the

analytes and sample matrix, the degree of purity required the nature of major contaminants in the sample and the final analytical procedure. For best results, the chelating reagent should fulfil several criteria:

- the chelating group of the reagent should be selective for the target metal ions. It is preferred that common metal ions such as Na^+ , Mg^{2+} , and Ca^{2+} are not taken up (especially in seawater analysis).
- the rate of formation of the metal-organic chelates must be rapid when the chelating reagent is immobilised on the SPE column (fast kinetics are not so important when the reagent is added to the sample prior to the SPE step).
- an adequate exchange capacity
- little swelling or contraction of the resin on sample load/elution
- low metal blank contamination
- most importantly in a pH specific alkaline CL reaction, ease of elution with a weakly acidic solution.
- tolerance of a wide range of pHs

2.2 EXPERIMENTAL

2.2.1 Reagents

All reagents were analytical grade and used as received unless otherwise specified. Where possible, steps were performed in a laminar flow hood in order to reduce any particulate contamination that would result in high resin column blanks. Sub-boiled, quartz distilled hydrochloric acid (Q-HCl, 9 M) and acetic acid (Q-acetic acid, 17.5 M) were prepared by a single distillation of the analytical grade acids. Q-NH₃, (ca. 6 M) was purified using isothermal distillation (see Section 2.2.1) and nitric acid (HNO₃, Aristar; Merck BDH, 15.5

M) was used as received. Ammonium acetate and phosphate buffers were used to adjust the pH ranges 3.5 – 6.0 and 6.8 – 8.0 respectively, wherever necessary. The TSK 75 (F) resin was obtained from TosoHaas. Ethanol, acetone and dichloromethane were HPLC grade (Rathburn). p-nitrobenzoylchloride was provided by Fluka (puriss. p.a.). Sodium nitrite (AnalaR grade), sodium dithionite (GPR grade), 8-hydroxyquinoline (AnalaR grade) (also known as 8-quinolinol or oxine, and hereafter referred to as 8-HQ; the chemical structure of the 8-HQ is shown in Figure 2.1), triethylamine (AnalaR grade) and sodium hydroxide (Aristar grade) were provided by BDH, Merck. Certified 1000 ppm trace metal solutions (Fisher Scientific) were used to prepare working standard solutions for Co(II), Mn(II), Cr(III), Fe(III) and Cu(II).

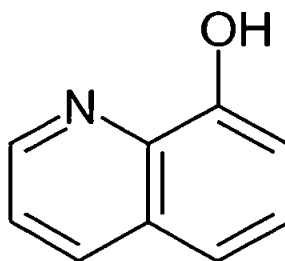


Figure 2.1: The chelating group of 8-hydroxyquinoline (8-HQ)

2.2.2 Cleaning protocol

Trace elements are present in seawater at concentrations of nanomols to picomoles per litre and lower. Such low concentrations pose extreme analytical problems. It is known, for example, that contamination and the lack of sufficiently precise analytical techniques have led to reported concentration data

that for some trace elements were too high by factors as great as 10^3 (Table 2.1 reports the historical data of Fe concentrations; Nolting et al. 1994).

Table 2.1: Historical data of Fe concentrations

Year	Concentration (nM)
1924	25000
1931	500-1400
1935	100-800
1954	60
1989	0.2-2.0
1996	0.6-0.7 (deep ocean)

In FI-CL systems the flow of the CL reagent streams in front of the PMT end-window generates a continuous background CL emission due to trace levels of metals (e.g. Co(II) or Mn(II)) present in the CL reagents. An elevated background seriously degrades the detection limit of the method.

2.2.2.1 The laboratory

Contamination of samples and reagents by aerosol particles is a severe problem in ultratrace analysis. The determination of Co requires good protocols in order to avoid contamination, which may result in erroneous results. Wherever possible, experimental work was carried out in a class-100 (< 100 particles m^{-3}) laminar flow bench (Figure 2.2). In this special hood the air is filtered through a high-efficiency particulate filter, reducing the dust level by 3-4 orders of magnitude compared with the air of a normal laboratory. Samples and reagent handling was done wearing polythene gloves. Samples and reagents bottles and

flasks were always closed and double sealed within plastic bags, except when solutions were being manipulated.

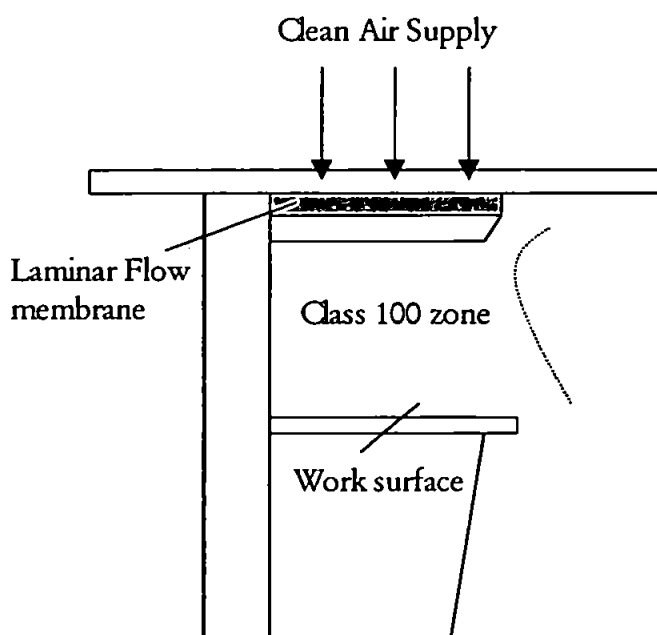


Figure 2.2: The laminar flow hood

2.2.2.2 Plastic labware

All plasticware had to be cleaned by first soaking in hot 5% (v/v) micro detergent (DECON®) for 24 h, followed by one week in 50% (v/v) hydrochloric acid and one week in 50% (v/v) nitric acid. Labware was thoroughly rinsed with ultra high purity (UHP) de-ionised water ($18.2 \text{ M}\Omega \text{ cm}^{-1}$). All the bottles were high-density polyethylene (HPDE) (Merck, BDH).

2.2.2.3 Reagent clean-up procedure

To take full advantage of the sensitivity and accuracy of an analytical method, the reagent blank should be no more than few per cent of the amount being

determined. Most analytical-reagent grade chemicals are not pure enough to be used for trace element analysis without further purification. Some commercial suppliers have focussed attention on this problem and have introduced special grades of ultrapure reagents. Although fulfilling many requirements for marine trace element determinations, ultrapure reagents often do not satisfy the standards required for extreme trace analysis (e.g. analysis of open-ocean waters). Methods of preparing ultrapure reagents in the laboratory have been described in detail by Howard (1993). Below are presented the techniques used in this research for purifying hydrochloric acid, ammonia solution and acetic acid.

- Quartz Sub-boiling Distillation Still

A quartz finger, sub-boiling distillation still was utilised for the purification of the following materials: hydrochloric acid, nitric acid and acetic acid (Howard et al., 1993). A schematic diagram of the still is shown in Figure 2.3. Commercially available HCl (11.3M), and acetic acid (17.5M) (all AnalaR, Merck BDH) were cleaned using the distillation still. The stock acids were introduced into the unit until the surface of the liquid touched the rim of the outlet tube. The purification is based upon vaporisation of the liquid by radiative heating of the surface of the liquid to prevent boiling. The violent boiling action typical of a conventional distillation apparatus leads to a significant carry-over of raw solvent with the distillate. The surface evaporation process does not generate such a spray or droplets and the condensate is therefore of higher purity.

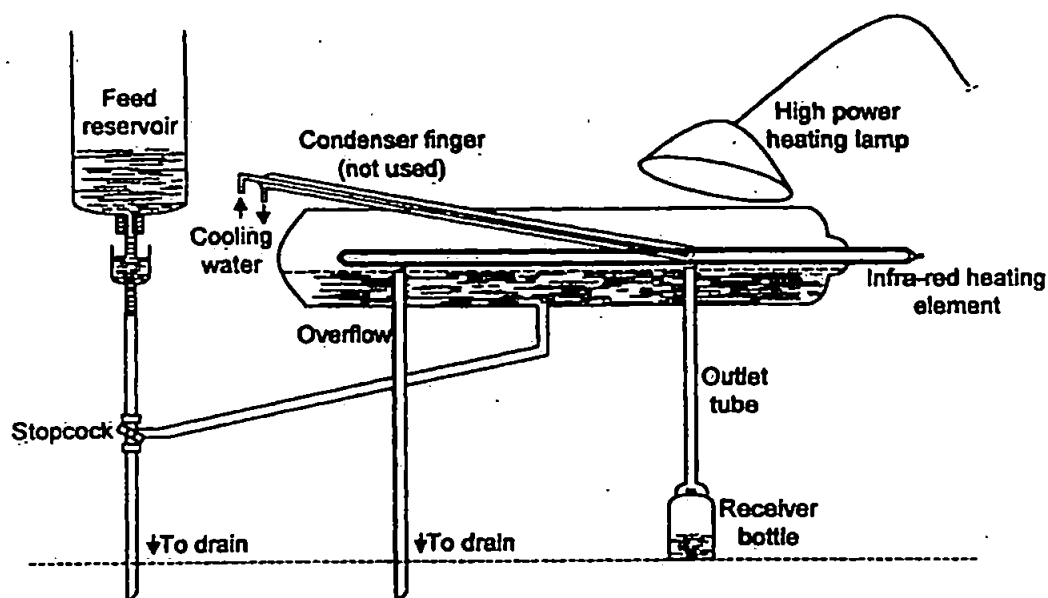


Figure 2.3: Schematic diagram of apparatus for sub-boiling distillation (reproduced from Moody et al., 1982)

Heating was carried out by means of a high power infra-red lamp (250 W), directed onto the surface of the liquid. Care was taken to prevent the stock acids from becoming too hot and starting to boil. An inclined, water-cooled cold finger condensed the acid vapour and led the condensate into a pre-cleaned collecting bottle outside the still. A constant head device was used to feed the still reservoir, which was periodically flushed with fresh acid to prevent the build-up of contaminants. The distillation still was in continual operation and the typical rate for purification of hydrochloric acid was 250 ml d⁻¹. The purified acids resulted in concentrations of Q-HCl (9.2 M), Q-HNO₃ (~12 M) and Q-acetic acid (~17 M).

- Isothermal Distillation

Isothermal (or isopiestic) distillation is a very simple procedure suitable for materials (e.g. ammonia) which possess a high vapour pressure at room temperature. High purity NH_4OH was prepared from 30% NH_4OH by isothermal distillation. As illustrated in Figure 2.4, two wide-mouth 1 l HDPE bottles each containing ca. 800 ml of UHP water were placed in a 5 l wide mouth keg containing ca. 2.5 l of the analytical grade ammonia solution. The keg was sealed and left for 5 days at room temperature, with a single daily stir, allowing the ammonia to equilibrate between the two aqueous solutions. During this period, the ammonia transfers to the UHP water, leaving the involatile trace elements behind and generating a high purity ammonia solution (ca. 5-6 M).

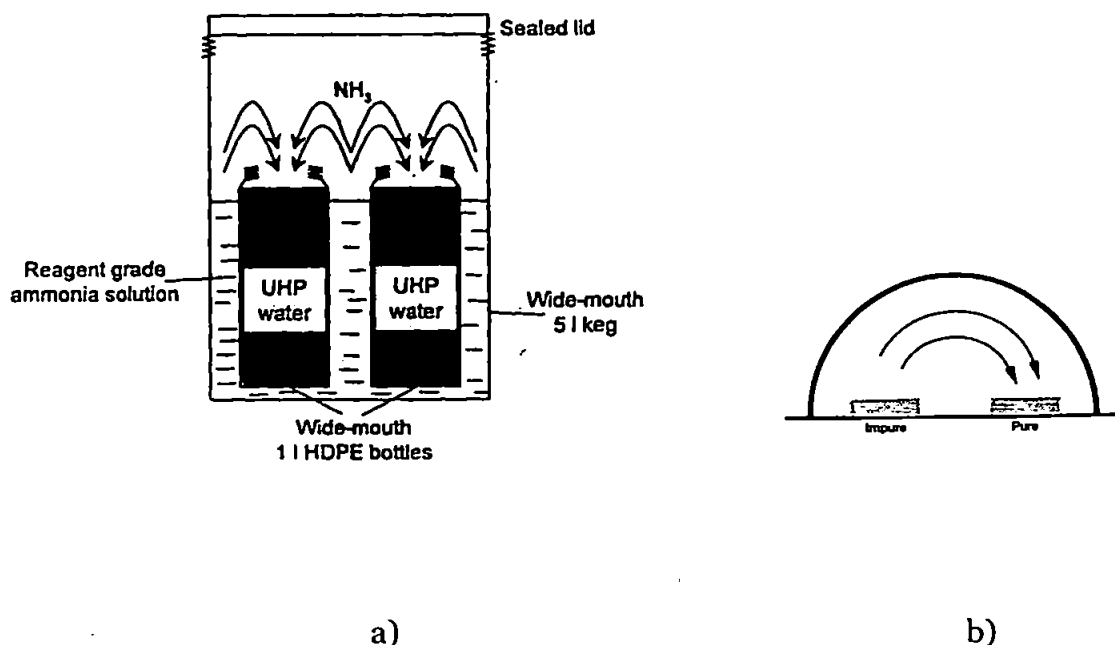


Figure 2.4: Purification of ammonia solution by isothermal distillation: a) sub-boiling Teflon bottle still; b) principle setup of isothermal distillation (reproduced from Grasshoff et al., 1983)

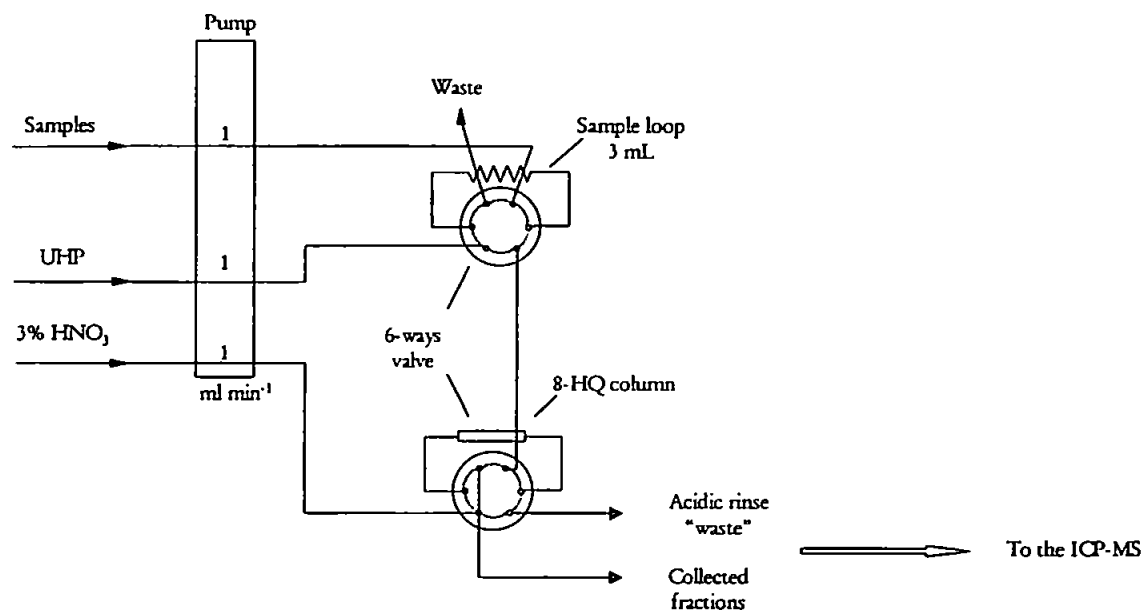
2.2.2.4 Instrumentation

Two flow injection manifolds with ICP-MS as the detector were used. The first was used to study the complexation characteristic of 8-HQ at different pH for Mn(II), Cu(II), Co(II), Cr(III), and Fe(III), and the off-line manifold is shown in Figure 2.5a. The second manifold is shown in Figure 2.5b and it was an on-line system for studying the breakthrough behaviour of the 8-HQ. Both systems were assembled using Gilson Minipuls 3 peristaltic pumps and a six-port rotary injection valve (Rheodyne, HPLC technologies). All manifold tubing was PTFE (0.75 mm i.d., Fisher) except for the peristaltic pump tubing, which was flow-rated PVC ("Accu-rated", Elkay), and the 8-HQ column.

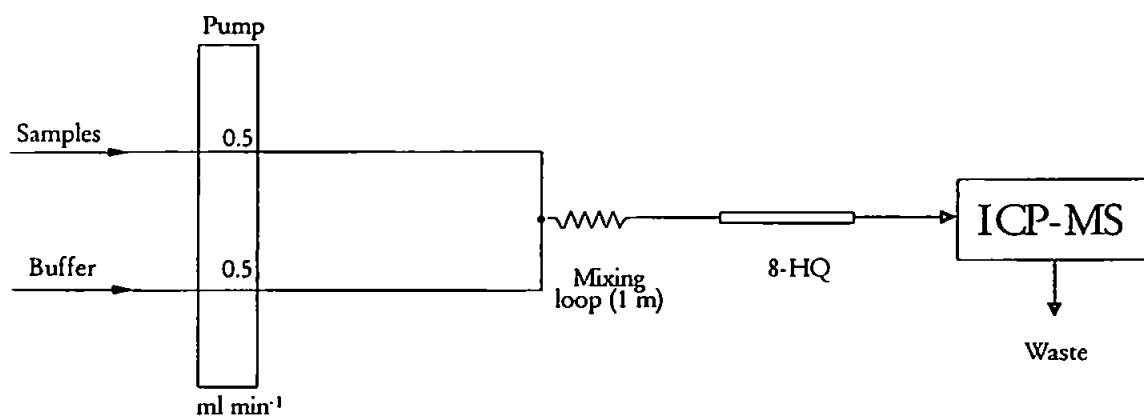
A commercially available ICP-MS instrument was used (Plasmaquad PQ-2). The operating conditions and main acquisition parameters are summarised in Table 2.2.

pH measurements were performed on a Hanna Instruments HI 9021 meter, calibrated in the pH 4-7 or pH 7-10 ranges using standard buffer solutions (Colourkey, BDH Merck), as required.

Prior to use, the FI manifold, the column, the PTFE flow line fittings and connectors were cleaned with 0.5 M Q-HCl and UHP water for several hours.



a)



b)

Figure 2.5: Manifold used for (a) adsorption studies and (b) breakthrough studies with the 8-HQ resin.

Table 2.2: Instrumental ICP-MS conditions and measurement parameters

ICP-MS	Plasmaquad PQ-2
Forward power (W)	1350
Reflected power (W)	4
Gas flow rates:	
Plasma (L/min)	13
Auxiliary (L/min)	1.0
Nebulizer flow rate (L/min)	0.85
Nebulizer pressure (psi)	40
Sample depth	(8-10) mm
Acquisition mode 1 (for pH dependence experiments)	Peak jumping
Acquisition mode 2 (for breakthrough experiments)	Peak jumping time resolved
Sample cone	Ni, 1.0 mm orifice
Skimmer cone	Ni, 0.4 mm orifice
Dwell time(for pH dependence experiments)	320 ms
Dwell time(for breakthrough experiments)	160 ms
Washing solution	HNO ₃ 2% v/v
Flow rate	1 ml/min

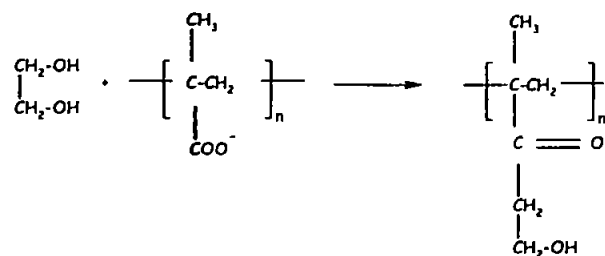
2.2.3 Resin Synthesis

A chelating resin of 8-hydroxyquinoline immobilised on a solid support (TSK gel, Toyopearl HW-75F, 32-63 micron, fine, TosoHaas Co., supplied through Anachem) was prepared following meticulously the modified procedure suggested by Landing et al. (1986). Previous methods have involved the immobilisation of 8-HQ onto silica substrates, which offer the advantages of good mechanical strength, resistance to swelling and rapid overall exchange kinetics in column applications. Such immobilisations are, however, unstable at high pH. This method used the highly porous, chemically stable organic resin gel Toyopearl-TSK as the solid support. Toyopearl TSK is a semi-rigid spherical gel, synthesised by a copolymerisation of ethylene glycol and methacrylate type polymers. The intertwined vinyl polymer agglomerates offer high porosity, mechanical and chemical stability and a high hydrophilicity due to the presence of ether linkages and hydroxyl groups. TSK beads are small and uniform, and show no signs of swelling at high pH values. The numerous surface hydroxyl groups enable relatively simple chemical modification, which is used in the immobilisation of ligands such as 8-hydroxyquinoline *via* phenyl-azo linkages. The polymer solid support itself shows no cation exchange capacity and does not concentrate dissolved humic or fulvic acids. The resin TSK-8HQ is stable in strong acid solutions (2.0 M HCl / 0.1 M HNO₃) and more stable than 8-HQ immobilised on silica gel after same base treatment (the base catalyses the hydrolysis of the resin benzoyl-ester linkage) (Landing et al., 1986).

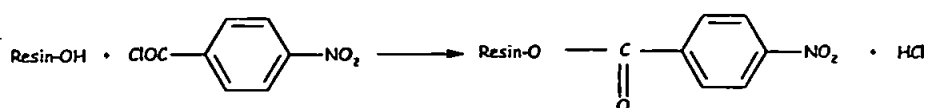
All reagent solutions were filtered (0.45 µm pore size, 47 mm diameter, polycarbonate; Nuclepore) to remove contaminant particles which may end up in the modified resin. The synthesis provided enough resin slurry to pack all the columns used during this research. Figure 2.6 illustrates the reaction scheme for

the 8-HQ immobilisation and in Section 2.2.3.1 the entire preparation procedure is presented.

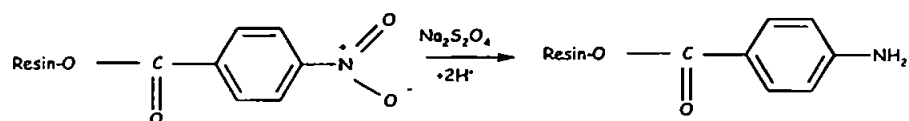
The Resin:



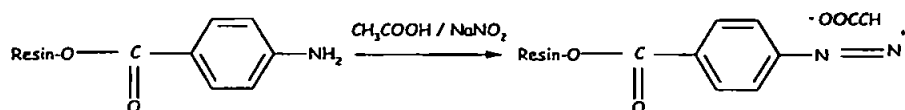
Benzoylation:



Reduction:



Diazotisation:



8-HQ Immobilisation:

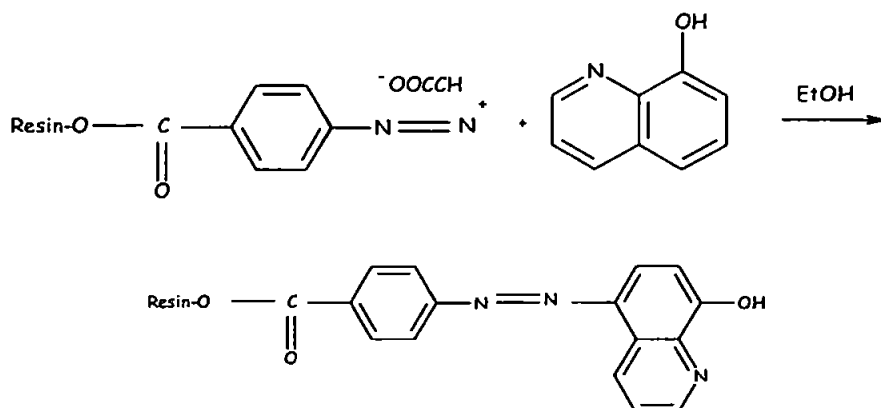


Figure 2.6: Reaction scheme for the immobilisation of 8-HQ

2.2.3.1 Preparation procedure

Toyopearl TSK HW-75 F is the precursor for the benzylation reaction, whereby *p*-nitrobenzoylchloride is attached to the resin. The nitro group is then reduced to an amino group, which is diazotised. By preservation of the two nitrogen atoms, 8-HQ is attached. The total preparation time was 35 hours.

Recently (Dierssen et al., 2001) has been reported a simplified synthesis for 8-HQ covalently bonded to a chemically resistant TosoHaas TSK vinyl polymer resin in a single step reaction).

- Step 1: washing and removing fine particles.

A 50 ml slurry of TSK HW-75 F was suspended in 100 ml of UHP water to wash away the preservative NaN_3 . The beads were allowed to settle down and the supernatant was decanted. Then the slurry was vacuum filtered onto a Whatman glass fibre filter. Care was taken not to scratch out particles of the filter while removing the filter cake. The washing procedure included the following steps: 2 x 50 ml 1.0 M NaOH; 3 x 50 ml MQ water; 2 x 50 ml 0.5 M HCl; 3 x 50 ml UHP water; 2 x 50 ml EtOH; 2 x 50 ml Acetone; 2 x 50 ml CH_2Cl_2 . After the rinse with dichloromethane the resin was placed in a desiccator overnight.

- Step 2: benzylation

As the *p*-nitrobenzoylchloride could react with water the resin was kept dried and all labware was oven-dried (100°C). A quantity of 5 g of dried TSK HW-75 F was put into a 3 necked round bottom flask, 2 g (0.011 mols) of *p*-nitrobenzoylchloride and 5 g (0.036 mol) of triethylamine and 95 ml of dichloromethane were added. Triethylamine worked as a Cl^- scavenger driving

the reaction, dichloromethane (42 °C boiling point) maintained a stable reaction temperature. The under reflux boiling, gently stirred reaction was allowed to continue for 12 h. The benzoylated product was rinsed three times with 50 ml dichloromethane as described in step 1 and filtered to air dryness.

- Step 3: reduction

5 g (0.03 mol) of sodium dithionite were dissolved in 100 ml of UHP water, added to the resin in a HDPE bottle. Periodically the mixture was shaken for a time of 3 hours. As reported by Landing (1986), a change in the colour was observed (it is reported a change from white to yellow). As the reaction is proton consuming, a pH of 7.2 should not be exceeded. The actual pH increased from 5 (start) to 6.5 (after 2.5 hours) (if necessary the pH can be adjusted with HCl / NH₃OH). A rinsing step followed using 3 x 50 ml acetone. Three rinses each with 50 ml UHP water removed the acetone. Landing et al. (1986) suggested 19.5 g sodium sulfide in 100 ml 0.1 M acetic acid instead of sodium dithionite, due to its better reducing capabilities. Degassing the solution with N₂ should also increase the percentage of the reduced nitro groups.

- Step 4: diazotization

The wet resin was ice-cooled and 100 ml of ice-cooled 0.2 M of acetic acid glacial, containing 5 g sodium nitrite (0.073 mol) was added. It was important to maintain the temperature of 0 °C, because the diazonium salt is not stable at higher temperatures (e.g. room temperature). The reaction was allowed to proceed for 45 min, after which the resin was vacuum filtered and rinsed three times with ice-cooled UHP water. The resin was transferred to the ice cold HPDE bottle.

- Step 5: attachment of the 8-HQ group

A pre ice-cooled solution of 8-HQ (2 g in 100 ml, 0.0138 mol) in 95 % ethanol was quickly added to the resin. The slurry was kept for 45 min in ice-cold media and shaken periodically. The colour of the slurry turned from orange to brick red after two h.

- Step 6: washing and storage of the immobilised 8-HQ

The resin was rinsed twice with 0.5 M NaOH, (the resin darkens in colour), three times with UHP water and twice with 1 M HCl (the resin lightens in colour) and again three times with MQ water. Finally the resin slurry was allowed to settle and the supernatant discarded. The immobilised 8-HQ was stored as a slurry, suspended in UHP water in a HDPE bottle at room temperature.

2.3 RESULTS AND DISCUSSION

2.3.1 Characteristics of 8-HQ

A range of ion exchangers based on polymers substrates are available, but their lack of selectivity over alkali and alkaline earth metals, and swelling of the polymer substrate pose limitations on their use. Chelating exchangers that are more selective to heavy metals are commercially available; for example, the use of Chelex 100[®], which has an imminodiacetic functional group (IDA), has been widely reported (Haraldsson et al., 1993; Pesavento et al., 1999; Pyrzynska et al., 2000) with the following lg K: 9.01 for Cu(II), 7.01 for Ni(II), 6.21 for Zn(II), 6.11 for Co(II), and 2.11 for Mg(II) (Hering, 1967) . This however also has a polymer substrate that is affected by swelling. Another commercial resin, Muromac A-1, which has the same functional groups (see Figure 2.7) has been reported to be less effected by swelling (Chang et al., 1999; Hirata et al., 1986; Lin et al., 2001; Rao, 1995; Sung et al., 1997a; Sung et al., 1997b) but still requires a considerable wash time between analyses.

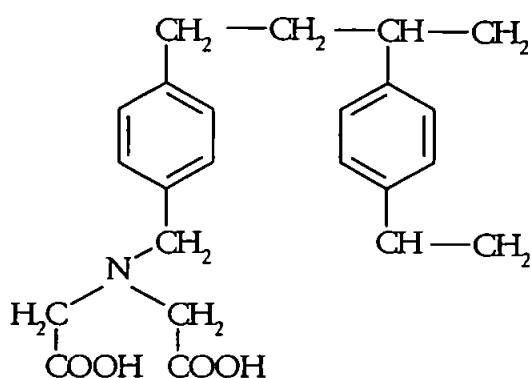


Figure 2.7: Structure of Chelex 100 and Muromac A-1

Since Landing et al. (1986) described the covalent attachment of 8-hydroxyquinoline to stable organic beads, the resin has found widespread use among analytical and marine chemists, especially in flow-injection applications (Bowie et al., 1998; Chapin et al., 1991; Coale et al., 1992a; Dierssen et al., 2001; Elrod et al., 1991; Landing et al., 1991; Lewis et al., 1991; Measures et al., 1995; Orians et al., 1993; Powell, 1998; Sakamoto-Arnold et al., 1987; Shiller, 1998a; Shiller et al., 1998b). 8-HQ can chelate over 60 metals under controlled pH conditions. In Table 2.3 are reported the stability constants of various ions with 8-HQ (Sillen, 1964).

Table 2.3: Stability constants of H, Ca, Co, Cu, Fe, Mg, Mn, and Ni with 8-hydroxyquinoline.

Species	Temp. (°C)	Log of Equilibrium Constants
H ⁺	25	K ₁ 11.19, K ₁₂ 3.76
Ca ²⁺	20	K ₁ 3.27
Co ²⁺	20	K ₁ 9.1, K ₂ 8.1
Cu ²⁺	20	K ₁ 12.29, K ₂ 11.2
Fe ²⁺	20	K ₁ 8.0, K ₂ 7.0
Fe ³⁺	20	K ₁ 12.3, K ₂ 11.3
Mg ²⁺	20	K ₁ 4.5
Mn ²⁺	20	K ₁ 6.8, K ₂ 5.8
Ni ²⁺	20	K ₁ 9.9, K ₂ 8.8

Its application for the preconcentration of trace elements from natural waters, following immobilisation on a suitable support, is demonstrated in Table 2.4.

Table 2.4: Examples of application of 8-HQ based resin

Elements	Matrix	Column	Detection	LOD (pM)	Reference
Cd Cu Fe Mn Ni Pb Zn	Seawater	Complexation with 8-HQ and adsorption on C18 bonded Silica gel	ICP-AES	Cd 444.8 Cu 314.7 Fe 537.1 Mn 364 Ni 851.6 Pb 482.6 Zn 611.6	Watanabe et al., 1981
Ca Co Cu Fe Ni	Aqueous standards	Silica immobilised 8-HQ	FI-FAAS	Not reported	Marshall et al., 1985
Cd Cu Fe Mn Ni Zn	Seawater	Precomplexation with 8-HQ and retention on an Amberlite XAD-2 column	FI-ICP-AES	Cd 106.8 Cu 283.3 Fe 429.7 Mn 72.8 Ni 1020.9 Zn 458.7	Porta et al., 1992
Cd Cu Fe Mn Ni Pb Zn	Seawater	Silica immobilised 8-HQ	Discontinuous FI-GFAAS	In range $5.4 \cdot 10^{-3} - 1.8 \cdot 10^{-1}$	Azeredo et al., 1993
Cd Cu Ni	Open ocean water	Silica immobilised 8-HQ	FI-ICP-AES with continuous flow ultrasonic nebulisation	Cd 0.14 Cu 1.10 Ni 0.92	Lan et al., 1994
Mn	Seawater	8-HQ immobilised onto a vinyl polymer gel	FI-Spectrophotometry	36 for 15 mL sample volume	Resing et al., 1992
Cu	Seawater	Immobilised 8-HQ	FI-CL	400	Coale et al., 1992
Fe	Seawater	Immobilised 8-HQ	Spectrophotometry	25	Measures et al., 1995
Co	Seawater	8-HQ immobilised on silica gel, CL detection with gallic acid and hydrogen peroxide	CL	10.5	Hirata et al., 1996

2.3.2 Preliminary considerations in the development of an on-line column preconcentration system.

The process of sample loading on packed column is a key link in the entire preconcentration procedure. In FI preconcentration systems the sample volume being processed may be determined either by fixing the time interval for sample introduction (loading) onto the preconcentration system under a defined sample flow rate or by using a carrier stream to displace a fixed sample volume, defined by the volume of the sample loop. The former approach is referred to as time-based sampling, and the latter, volume-based sampling. Time-based loading systems usually give higher preconcentration than volume-based systems (Hartenstein et al., 1985; Hirata et al., 1986; Jorgensen et al., 1985; Malamas et al., 1984). Obviously, it is simpler and more straightforward to load the sample directly onto a column without prior introduction into a loop. This also avoids the need for a washing stage to remove the dispersed sample completely from the loop, which is necessary for volume-based loading. However, with volume-based loading, the sample remaining in the pump tube at the end of the loading period will have to be washed out of the tube by the next sample, but this can be done during the elution state and will not require extra time as in the volume-based procedure. Samples can be changed during the elution period so that the next sample loading cycle can be initiated immediately after the elution period without appreciable carry-over. A disadvantage of time-based systems is its larger dependence on the stability of the flow rate. Thus, with time-based loading, regular checks of the sample flow rate are needed, particularly when a new column is used for the first time or when large fluctuations in sensitivity are observed.

2.3.3 Column equilibration and washing

The column should be equilibrated by washing with a buffer solution at the pH required for sample loading before preconcentration. However this procedure requires a more sophisticated manifold. When an equilibration stage is excluded, breakthrough of the analyte cannot be avoided during the initial stage of sample loading, owing to unsuitable pH conditions created during the previous elution. It is, therefore, necessary to consider if the equilibration of the column is really necessary in an on-line column preconcentration system, and whether omitting this step degrades the column performance (details of the operating system are presented in Chapter 3). The column was packed with fresh 8-HQ resin. An ammonium acetate solution (0.4 M, pH 5.5) buffered in-line sample containing 0.425 nM of Co(II) and the resulting mixed solution was pumped onto the column for 60 s at 1.2 ml min⁻¹ immediately after the elution of the previous sample with 0.05 M HCl. The peak height was measured by FI-CL analysis. In another experiment an ammonium acetate buffer solution was pumped first through the column for 30 s at 0.5 ml min⁻¹ in order to condition the column. Then the same buffered sample was pumped through the column for 60 s at 1.2 ml min⁻¹. The recoveries of cobalt differed were complete and differed by only 8% (n=3). The omission of the equilibration sequence does not seriously affect the performance of the column. Sample loading can be used as a sequence for column equilibration, with the same function as equilibrating with a buffer solution. So consequently the advantages gained by simplifying the manual system and improving the overall analytical efficiency are obvious. Washing the 8-HQ column with UHP water after sample loading before elution with HCl did not create loss of Co(II). Moreover the seawater matrix (Ca and Mg) interferes too seriously with the determination of Co and Mn by FI-CL

analysis (see Chapters 3 and 4) and so a washing step with UHP water is absolutely necessary. An UHP water rinsing time of 30 s is normally adopted for alkaline earth metals removal.

2.3.4 Column design

The complexation of metal ions by the chelating resin is influenced by parameters such as sample pH, length and internal diameter (i.d.) of the column. Moreover in a dynamic flow system the exchange times are much reduced and the exchange reaction may not reach equilibrium, although the localised micro-environment may enhance the chelation of analytes. Column performance can depend considerably on the packing of the resin. Initially the columns were constructed using a 2.4 mm i.d. PTFE tubing and a 10 mm length of resin was used, as illustrated in Figure 2.8. The column ends were fabricated using 0.89 mm i.d. Tygon pump tubing, which was connected to the 0.75 mm i.d. PTFE manifold tubing. A plug of quartz wool was placed at either end in order to retain the resin inside the column.

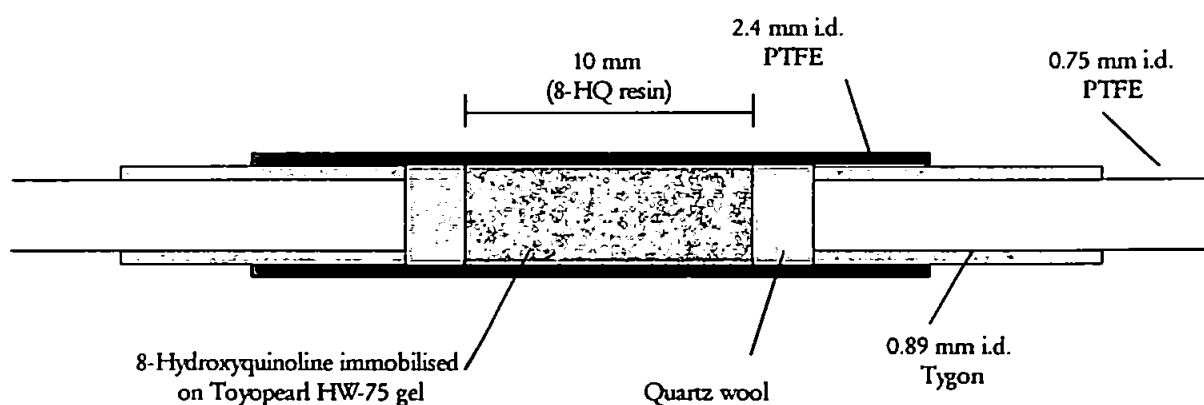
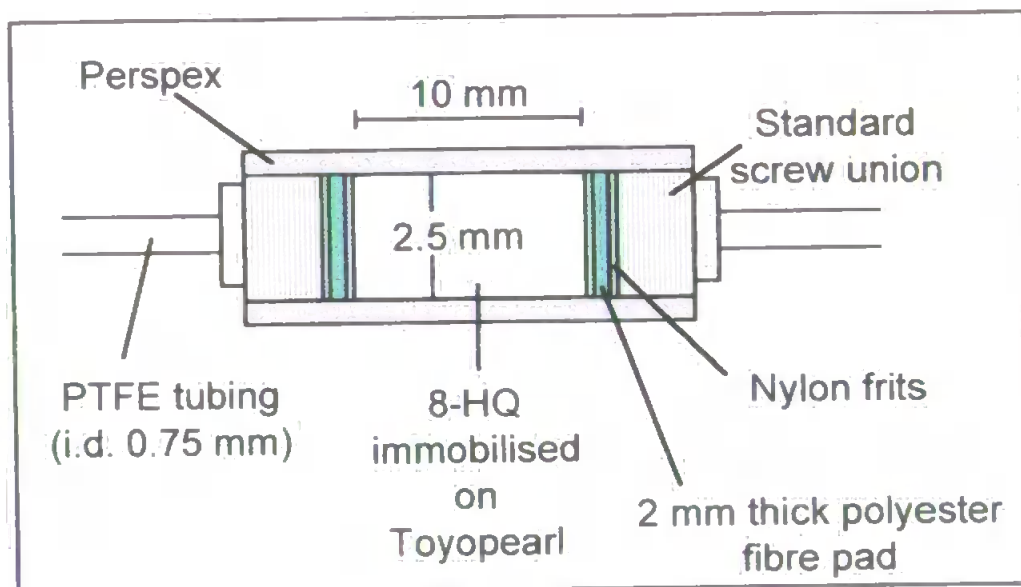


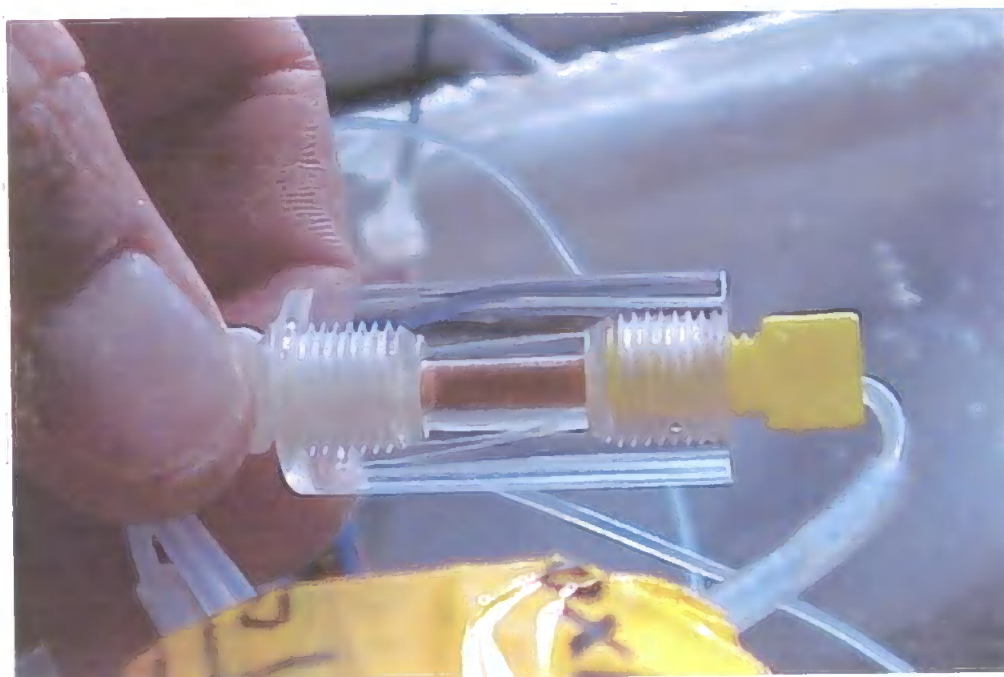
Figure 2.8: Old micro-column containing 8-HQ resin

The performance of these columns was generally good in respect of peak shape and reproducibility, but for shipboard experiments the procedure to prepare the columns was time consuming and tedious. Each column was prepared singularly and destroyed after the resin lost its performance (each column was packed in about 30 min; Bowie, personal communication). A new type of column was designed in order to reduce the preparation time and with the possibility of replacing only the resin inside. This new and robust microcolumn design (Daviron Instruments Ltd., Bere Alston, Devon) was constructed from cast acrylic rod and the TSK-8HQ resin sealed inside using standard screw fittings with flanged tubing and nylon frits sandwiching a 2 mm thick polyester fibre pad at each end (see Figure 2.9). Columns were constructed with the following dimension: length 10 mm with an i.d. of 2.5 mm. Smaller i.d. such as 1.5 mm resulted in increased back-pressure in the FI manifold and a reduced flow rate for loading sample was necessary, increasing the overall analysis time. Increasing the i.d. to 3 mm was not possible due to imperfect fitting of the polyester fibre pad at the top and end of the column.

To prepare the column prior to packing it, the 8-HQ slurry was stirred in order to form a homogenous suspension. A flow line was connected from the PTFE column direct to the resin reservoir. Narrow bore pump tubing was attached downstream of the column and the resin drawn up at low pressure using a peristaltic pump (ca. 0.5-0.8 ml min⁻¹). The columns were cleaned with 1.0 M Q-HCl for at least 6 h, followed by UHP water for 6 h prior to use. The 8-HQ columns were also used for all the required (in-line and/or off-line) chemicals purification.



a)



b)

Figure 2.9: a) the new microcolumn design; b) photograph of the column

2.3.5 pH dependence of chelating process

The structure of the 8-HQ resin at acid and basic pH is presented schematically in Figure 2.10. The hydronium ion (H_3O^+) competes strongly with metal ions for the chelating sites. As a result mineral acid such as hydrochloric acid and nitric acid are effective eluents. At $\text{pH} < 2.5$ the resin will not concentrate transition metals.

8-HQ binds the metal ion through the ring nitrogen and phenolate oxygen. A proton is lost from the phenol group as a result of chelation (see Figure 2.11).

Figure 2.12 (reproduced from Zuehlke and Kester, 1985) shows the theoretical behaviour of Cu(II), Ni(II), Zn(II), Co(II), Fe(II), Cd(II), Mn(II) onto 8-HQ at different pH (Zuehlke and Kester, 1985). The curves were derived from stability constants determined in simple well-defined solution media for each metal; the influences of other cations, both major (e.g. Ca^{2+} and Mg^{2+}) and minor (e.g. trace metals), was neglected. At pH greater than 7 all the metal ions are quantitatively chelated by the ligand. At pH 5.5 Co(II), Zn(II), Ni(II), and Cu(II) are retained completely by the ligand but only about 60% of Fe(II), 10% of Cd(II) and less than 5% of Mn is retained.

In order to verify that the selectivity of 8-HQ for desired metal ions (which can be adjusted by control of pH) the uptake of 182.0 nM Mn(II), 192.3 nM Cr(III), 157.4 nM Cu(II), 169.7 nM Co(II), and 179.0 nM Fe(III) was studied. The column was packed and cleaned as described in 2.2.3.1. A set of solutions was prepared for each metal ion. The pH of each set was varied in the range 2.3 – 6.8. A processing volume of 3 ml was used for this study. The procedure operates by taking a fixed volume of sample (3 ml) then injecting this into the column and all the fractions collected and measured by ICP-MS (see Figure 2.5a). The results are presented in Figure 2.13.

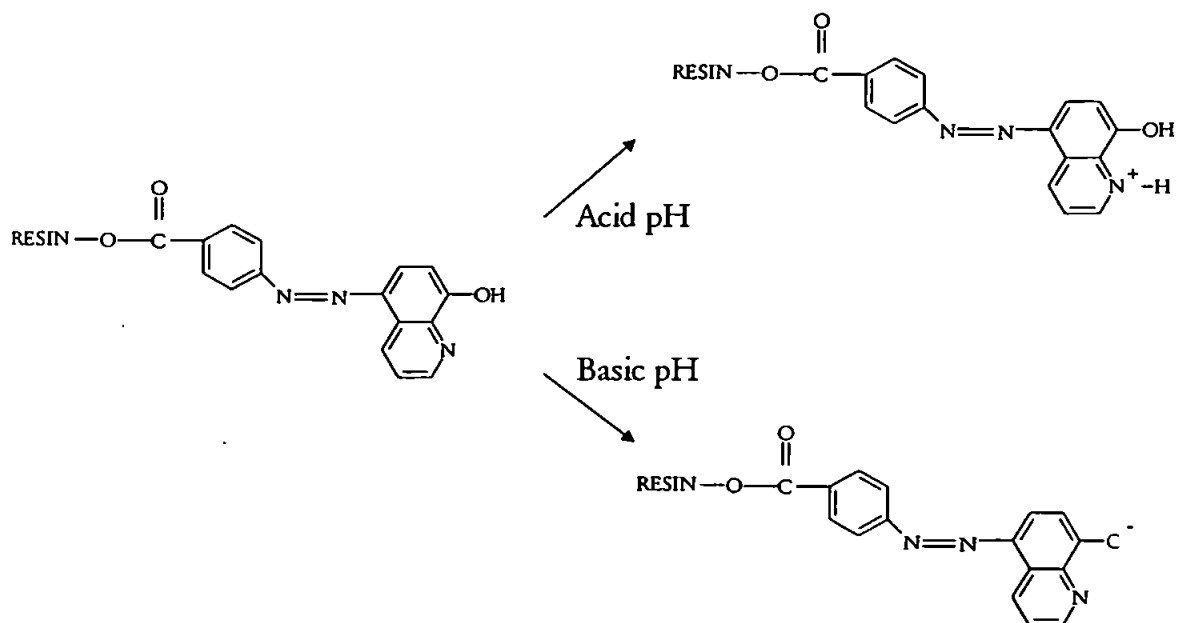


Figure 2.10: Ionic forms of 8-HQ at acid and basic pH

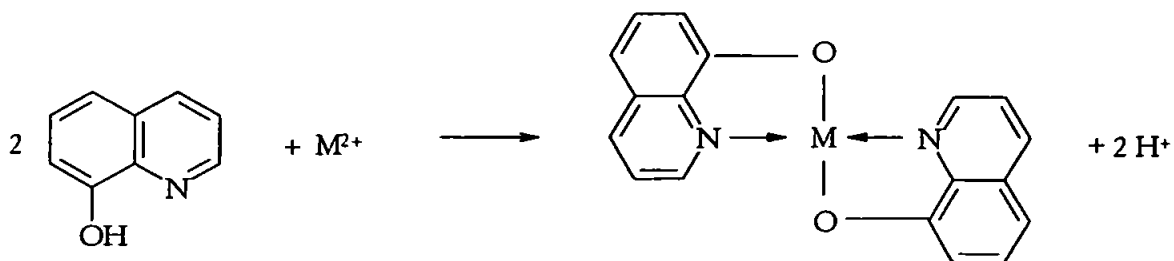


Figure 2.11: Typical reaction where M represents a metal reacting with 8-HQ

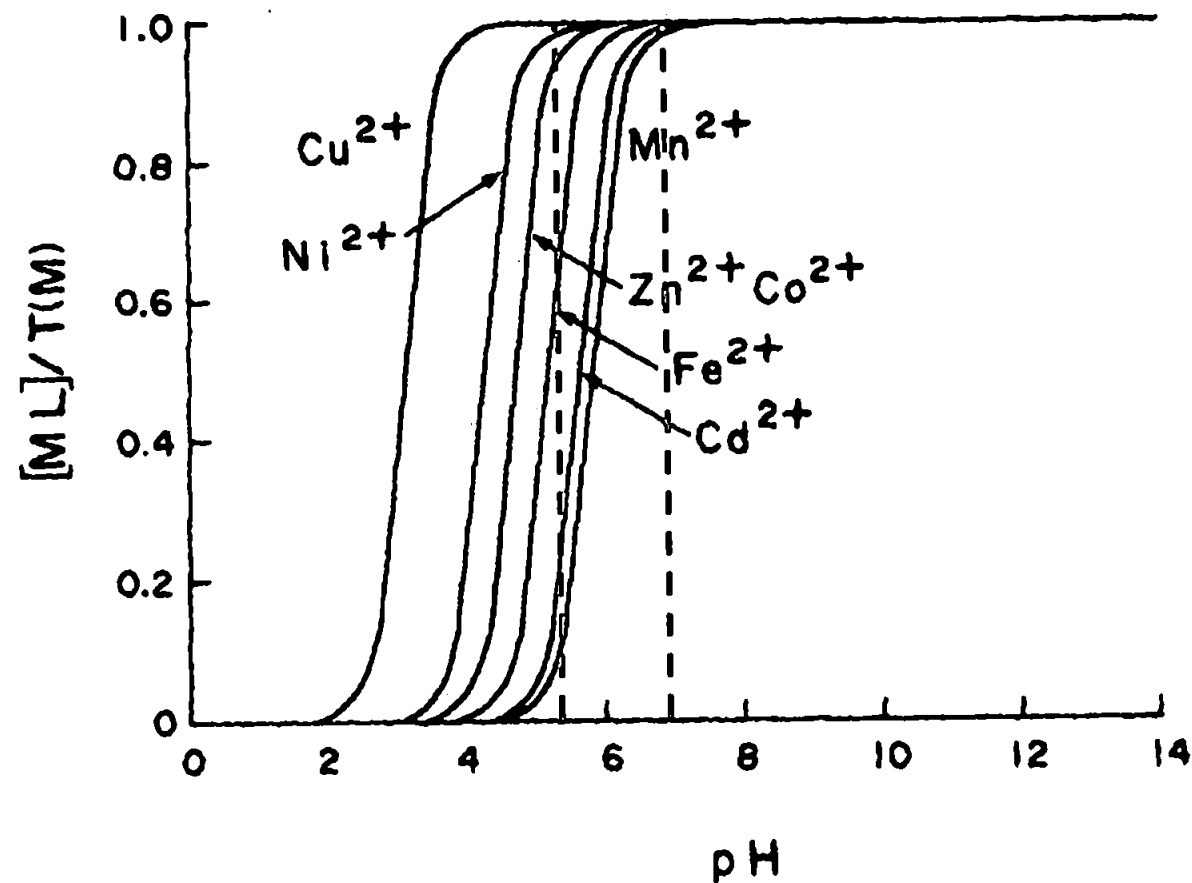


Figure 2.12: Theoretical effect of pH on ratio of metal-oxine (ML) to total metal $[T(M)]$ at 20°C and 0.1-M ionic strength for $Cu(II)$, $Ni(II)$, $Zn(II)$, $Cd(II)$, $Fe(II)$, $Cd(II)$, and $Mn(II)$ (reproduced from Zuehlke and Kester, 1985).

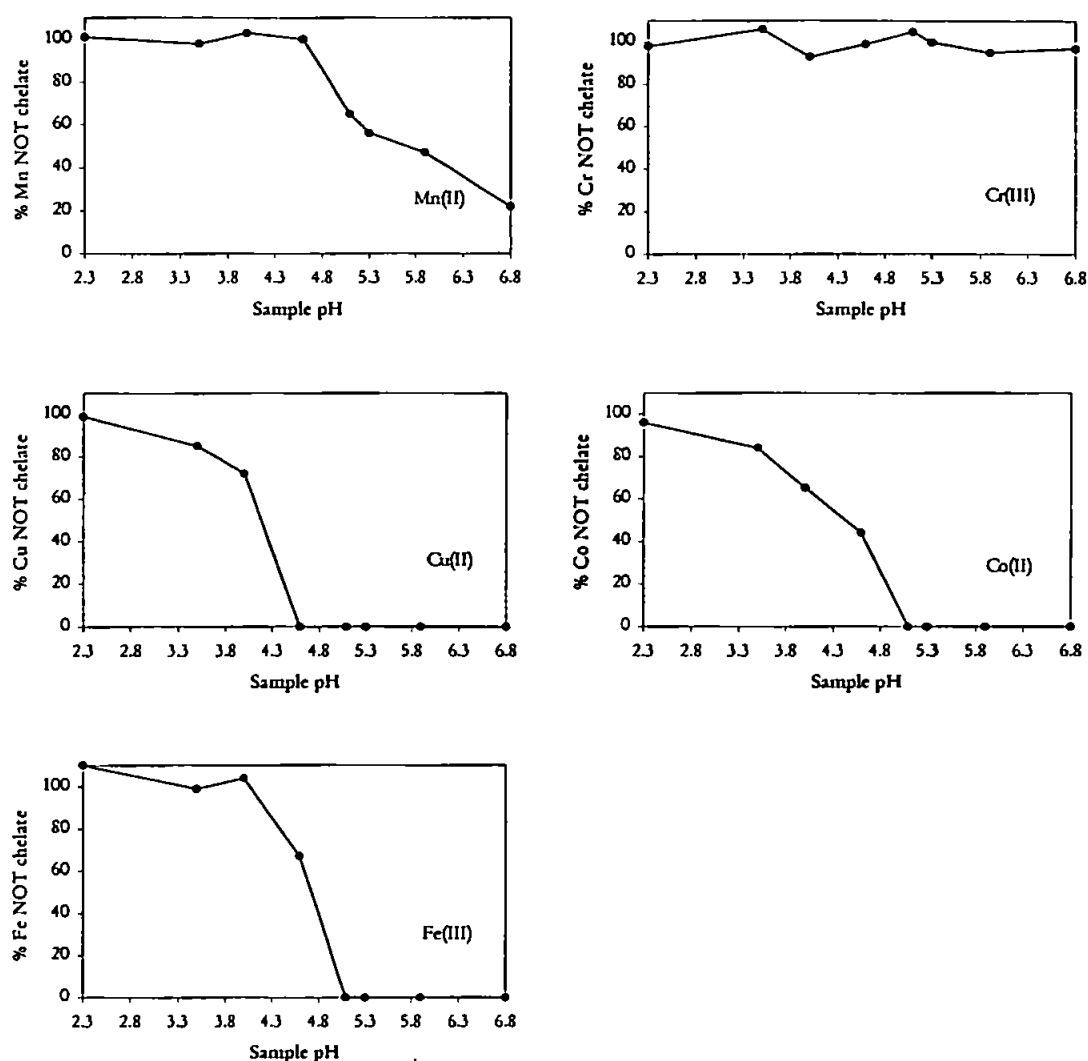


Figure 2.13: pH dependance of the upatke of Mn(II), Cr(III), Cu(II), Co(II), and Fe(III) onto 8-HQ at different pH value

As previously stated the complexation increases with increasing pH (Obata et al., 1993). Three types of complexation could be distinguished: Cu(II), which has the highest complexation constant, starts to be complexed at pH close to 3.5; Mn(II), which has the lowest complexation constant, was partially recovered at pH 6.8 (about 75%). For the other metals the recovery was 100% for pH > 5.5.

It is interesting to note that Cr(III) shows a different behaviour to the other metals. Alexandrova et al. (1993) reported only a partial recovery in the on-line

preconcentration of Cr(III) with 8-HQ. This has been attributed to the inertness of Cr(III) aquo-complexes (Cotton and Wilkinson, 1980).

2.3.6 Determination of the breakthrough profile

When concentrating dilute samples by solid-phase extraction with a short column, the capacity of the column should be well in excess of the total analyte content of the sample. This being the case, the next important question concerns the maximum sample volume that can be passed through the column before breakthrough occurs. When a sample is fed continuously into a column, it is usually assumed that the shape of the eluting front (the breakthrough curve) can be described of a Gaussian peak (Fritz, 1999). Breakthrough is acquired by plotting the volume of solution that is passed through the column versus the concentration of the “breakthrough ion” as it appears in the eluent. If C_0 is the known concentration of M^{n+} entering the column and C is the concentration of M^{n+} that emerges, than a plot of C/C_0 versus the volume of effluent gives a typical breakthrough curve such as is shown in Figure 2.14.

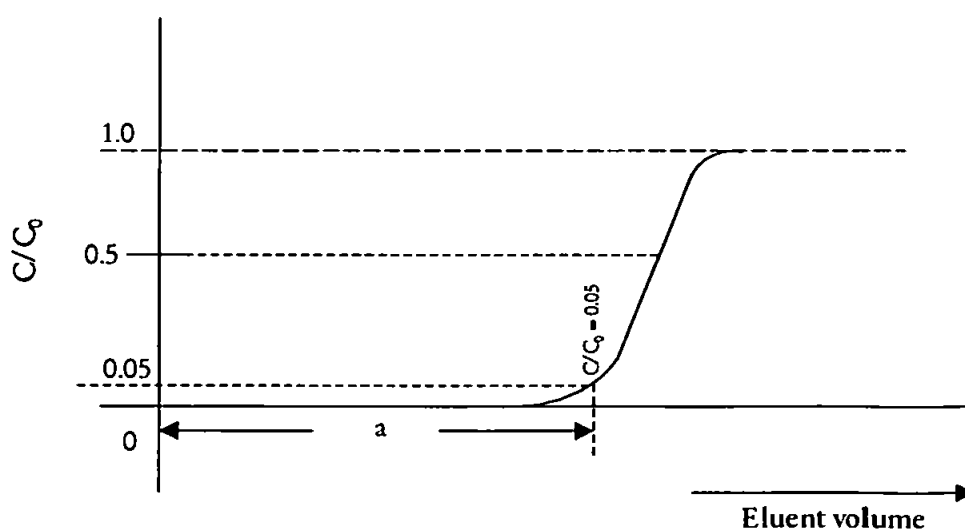


Figure 2.14: Typical breakthrough curve for an ion-exchange column, a =breakthrough capacity

The breakthrough capacity is dependent on several factors such as particle size of the resin beads, the flow rate at which influent passes through the column, the temperature, the sample matrix, and the column dimensions (Samuelson, 1963). Berg (1963) has reported that the breakthrough capacity of a column is greatly increased as the size of the resin particles is decreased. For a given quantity of resin the breakthrough capacity increases with increased column length or decreased column diameter. As the flow rate is decreased, the breakthrough capacity increases. An increase in temperature also speeds up the rate of exchange and increases the breakthrough capacity. Breakthrough was deemed to have occurred when the concentration of analyte in the column effluent had increased to 5% of the concentration of the analyte in the influent solution (Hashemi et al, (1997) have defined breakthrough as occurring when the concentration of analyte in the column effluent had increased to 1% of the concentration of the analyte in the influent solution).

The flow injection manifold (Figure 2.5b) was modified in order to measure the breakthrough capacity of the column. Operating conditions are as outlined in the manifold and given in Table 2.5. A fresh TSK-8HQ column (internal volume = 45 μ l, 56.3 mg of wet resin) was attached directly in-line with the ICP-MS. The sample solutions were buffered in-line with ammonium acetate 0.4 M at pH 5.4 and pumped through the column at 1 ml min⁻¹. Once breakthrough was obtained, HNO₃ 2% was pumped into the column for 120 s in order to clean the column.

Table 2.5: Operating conditions for the breakthrough experiments

Sample	pH	Flow rate	Metal
1 μ M Co(II) in UHP water	5.4	1 ml/min	Co(II)
1 μ M Co(II) + 1 μ M Cu(II) + 1 μ M Mn(II) in UHP water	5.5	1 ml/min	Co(II)
1 μ M Mn(II) in UHP water	5.4	1 ml/min	Mn(II)
1 μ M Cu(II) in UHP water	5.4	1 ml/min	Cu(II)
Atlantic seawater	5.3	1 ml/min	Co(II)
Ca(II) 10 mM + Mg(II) 53 mM in UHP water	5.5	1 ml/min	Co(II)

2.3.6.1 Breakthrough curves for Co, Mn and Cu

Acidified UHP water (pH 2.0) containing 1 μ M Co(II) was buffered in-line (pH 5.4) and passed continuously through the column. Initially, the reading was at the baseline, indicating the effective complexation of the Co ions onto the resin. As Co(II) began to breakthrough the column, the signal increased until a plateau was reached, indicating that chelating sites on the TSK-8HQ column were saturated. The effect of the presence of other trace metal ions (such as Mn and Cu) was also examined. Acidified UHP water (pH 2.0) containing 1 μ M Co(II), 1 μ M Cu(II), and 1 μ M Mn(II), was buffered in-line (pH 5.4) and passed continuously through the column. For comparison the breakthrough curve in the presence of Mn and Cu is reported together with the breakthrough curve of Co alone (see Figure 2.15). Manganese and copper only slightly affect the

complexation capacity of 8-HQ for cobalt (see Table 2.3 for comparison of the stability constants).

Acidified UHP water (pH 2.0) containing $1\ \mu\text{M}$ Mn(II) was buffered in-line (pH 5.4) and passed continuously through the column. The Mn breakthrough curve rose sharply (see Figure 2.16). Acidified UHP water (pH 2.0) containing $1\ \mu\text{M}$ Cu(II) was buffered in-line (pH 5.4) and passed continuously through the column (see Figure 2.17). Cu(II) should show the highest value for the slope of the curve due to its high complexation constants and Mn(II) should show the lowest slope to the low affinity of Mn(II) for the 8-HQ. The breakthrough curve for Cu(II), however, results not particularly neat due to a possible failure in the ICP-MS.

The breakthrough capacity of the resin is $0.124\ \mu\text{mol g}^{-1}$ of wet resin for Co(II).

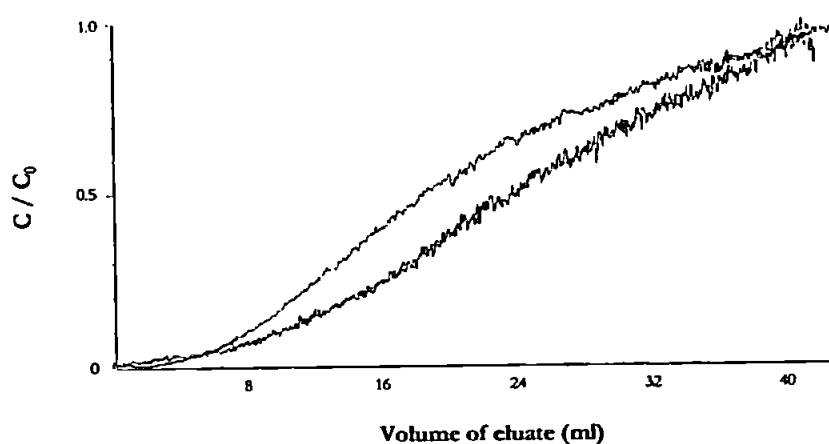


Figure 2.15: Breakthrough curve of Co(II) $1\ \mu\text{M}$ (green curve) and Co(II) $1\ \mu\text{M}$ in the presence of Cu(II) $1\ \mu\text{M}$ and Mn(II) $1\ \mu\text{M}$ (black curve).

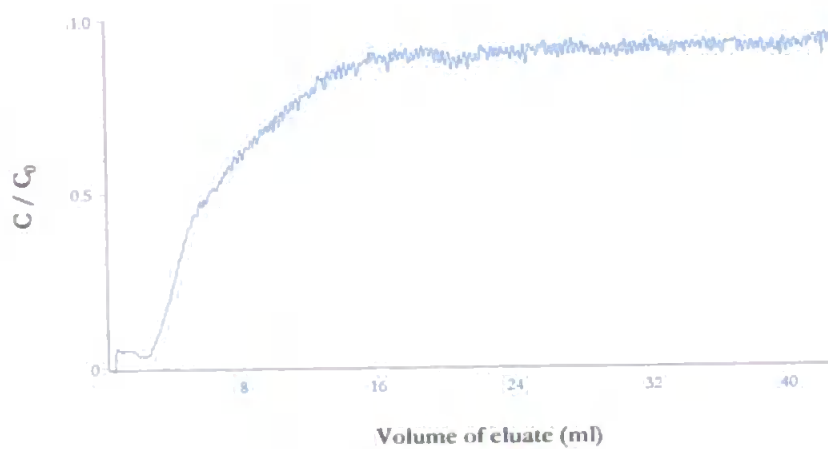


Figure 2.16: Breakthrough curve of Mn(II) 1 μ M.

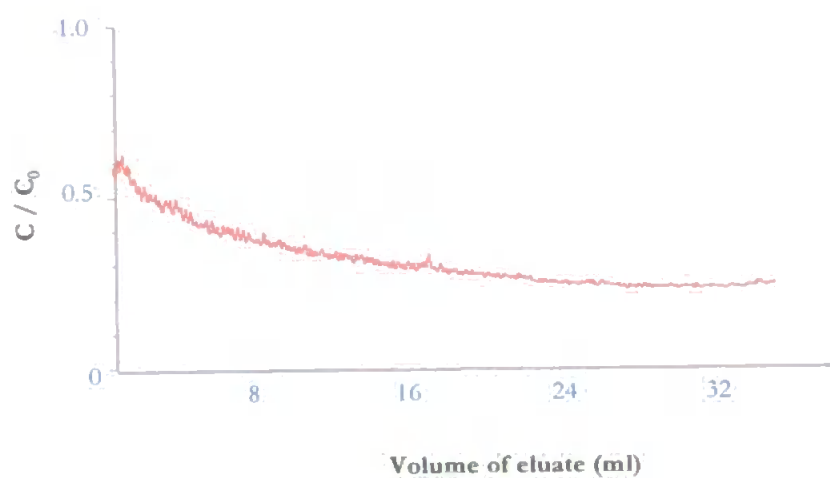
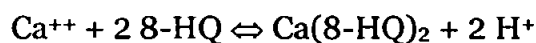


Figure 2.17: Breakthrough curve of Cu(II) 1 μ M.

2.3.6.2 Retention of Co on 8-HQ in the presence of Ca and Mg

The effect of trace metal ions such as Mn and Cu on the breakthrough capacity of 8-HQ is already shown in the previous sections. Here, the focus is on interference problems generated by the sea-salt matrix. The six major components make up more than 98 % by weight of seawater (see Table 1.1). When Ca and Mg are present in large excess with the respect to the transition metals (such as Co(II)), they effectively coat the column, occupying the active sites:



Because of the difference in the binding constants of the calcium and cobalt ions, the latter one preferentially displace the calcium ions:



So Co(II) is still competing successfully for these sites, but retention of Ca and Mg slightly slows down the retention process. Figure 2.18 (solution containing Ca 1.02×10^{-2} M, Mg 5.32×10^{-2} M, and Co 1×10^{-6} M in UHP water at pH 5.4) shows that Co is quantitatively retained even in the presence of Ca and Mg (the slight increase in the background signal is caused by the polyatomic interference of $^{43}\text{Ca}^{16}\text{O}^+$ and $^{42}\text{Ca}^{17}\text{O}^+$).

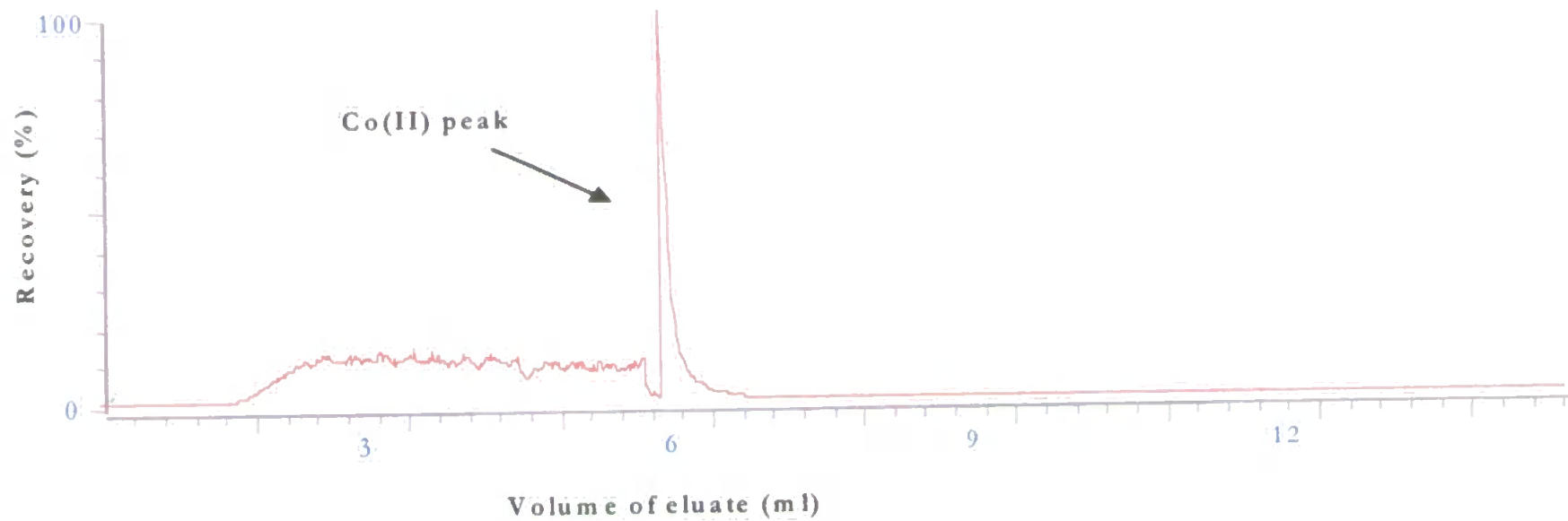


Figure 2.18: The elution of Co(II) from the 8-HQ resin with HNO_3 2% (v/v)

2.3.7 Re-usability of the resin

The beads of 8-HQ change their colour from dark orange to rusty brown at acid and basic pH respectively, but remain physically intact. The re-usability of the resin was tested by treating it with HNO_3 at 2% (v/v) and at a flow rate of 1 ml min^{-1} for several hours. After UHP water rinse, the breakthrough curve was again obtained using a solution containing $1 \mu\text{M}$ of Co(II) in UHP water and buffered in-line at pH 5.4. The solution was passed continuously through the column. The breakthrough profile did not vary significantly as can be seen in Figure 2.19. During the optimisation work for Co and Mn the resin was replaced less than 5 times. Therefore, multiple use of the resin is feasible.

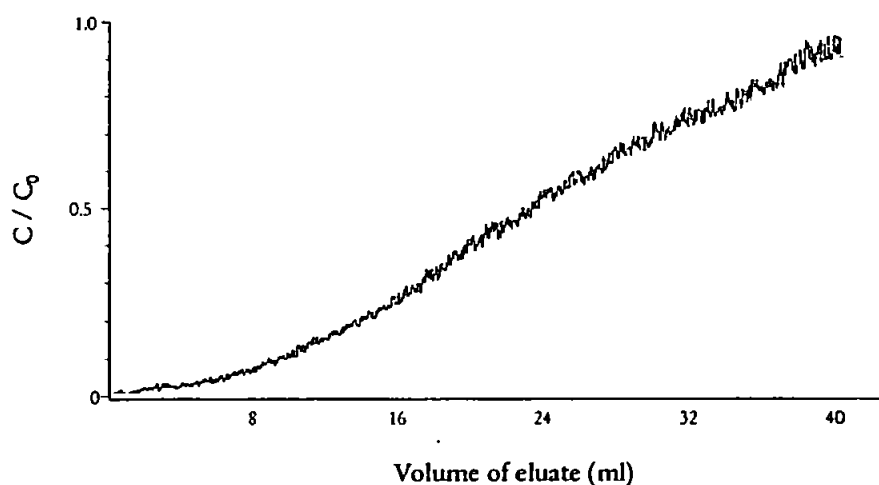


Figure 2.19: Breakthrough curve of Co(II) $1 \mu\text{M}$ after acid treatment of the resin

2.4 CONCLUSIONS

The objective of this study was to understand the effect of the presence of different trace metals and alkaline earth metals on the complexation capacity of the 8-HQ.

- As demonstrated the formation of 8-HQ complexes is strongly pH dependent.
- For the metals of interest, formation and isolation of the complexes at the typical pH of seawater (i.e., about 8) should, in principle, yield complete recovery.
- 8-HQ resin offers a very interesting performance for the preconcentration of trace metals in seawater. Transition metal ions are quantitatively recovered in seawater without any interference of the sea-salt matrix.
- 8-HQ can be successfully applied in the preconcentration and/or matrix removal of trace metals in seawater.

CHAPTER 3

DETERMINATION OF COBALT IN SEAWATER USING FLOW INJECTION WITH CHEMILUMINESCENCE DETECTION.

3.1 INTRODUCTION

This chapter describes the design and validation of a flow injection-chemiluminescence (FI-CL) procedure for the determination of Co in seawater (Cannizzaro et al., 2000). The method described is based on a new chemistry whereby CL emission is produced by oxidation of pyrogallol with hydrogen peroxide in alkaline medium in the presence of cetyltrimethylammonium bromide (CTAB) and methanol. The principal objective was the development of a portable system capable of measuring Co at picomolar levels in seawater.

3.2 EXPERIMENTAL

3.2.1 Reagents

3.2.1.1 CL Reagents

Gallic Acid, pyrogallol, hydroquinone, resorcinol, catechol (ACS grade, Aldrich), 2,3,4-trihydroxybenzoic acid, (all purum ACS, Fluka), 1,3,4-trihydroxybenzene (99%, Acros), methanol, ethanol, propan-2-ol, propanol, acetonitrile (HPLC grade, Rathburn), ethylene glycol (puriss. p.a., Fluka), cetyltrimethylammonium bromide (CTAB, Microselect 99%, Fluka) and hydrogen peroxide 30% v/v (Merck, BDH) were all used without further purification and solutions prepared in UHP water.

The highest purity grades available were used to minimise cobalt contamination in the reagents (and hence minimise the chemical noise). The optimum pyrogallol reagent solution was prepared by dissolving 6.3055 g of pyrogallol and 9.1115 g of CTAB in UHP water, adding 113.4 g of 30% (v/v) hydrogen peroxide (Merck BDH) and making up to 1 l with UHP water. 0.15 M NaOH was prepared in 80% v/v UHP water and 20% v/v MeOH. Silicone oil (Lancaster) was used in the thermostating bath and was stable up to 180 °C.

3.2.1.2 Cobalt Standards

A 179 μM Co(II) stock standard was prepared by dilution of a 1000 mg l^{-1} (17.9 mM) Co(II) atomic absorption standard solution ($\text{Co}(\text{NO}_3)_2$), with 0.5 M nitric acid (SpectrosoL). Other standards were prepared daily in 0.05 M sub-boiled, quartz distilled hydrochloric acid (Q-HCl) by serial dilution.

3.2.1.3 Acids / Ammonia

Sub-boiled, quartz distilled hydrochloric acid (Q-HCl, 9 M) and acetic acid (Q-acetic acid, 17.5 M) were prepared by a single distillation of the analytical grade acids. Q- NH_3 , (ca. 6 M) was purified using isothermal distillation and nitric acid (HNO_3 , Aristar; Merck BDH, 15.5 M) was used as received.

3.2.1.4 Ammonium Acetate Buffer

Ammonium acetate ($\text{NH}_4\text{-O-Ac}$) stock solution (2 M) was prepared by adding 22.2 ml of Q- CH_3COOH to 90 ml of Q- NH_3 solution and diluting to 200 ml with UHP water. A working sample buffer (0.4 M) for in-line pH adjustment of the sample was prepared by diluting 20 ml stock to 100 ml with UHP water, and adjusting to pH 5.5 with Q- CH_3COOH .

3.2.1.5 HCl Carrier/Eluent

The eluent solution (0.05 M) was prepared by diluting 2.8 ml of Q-HCl (9 M) to 500 ml with UHP water.

3.2.2 Instrumentation

A description of the individual components of the FI-CL system is contained in Chapter 1. Figure 3.1 shows the manifold of the optimised FI-CL manifold. Two peristaltic pumps (Gilson Minipuls 3) were used to deliver the UHP water, sample/buffer and reagents solutions, respectively, to the injection valve, preconcentration column and CL detector. All manifold tubing was PTFE (0.75 mm i.d., Fisher) except for the peristaltic pump tubing, which was flow-rated PVC ("Accu-rated", Elkay), and the 8-HQ columns.

A six-port rotary injection valve (Rheodyne, HPLC technology) is based upon a six-port PTFE unit, incorporating a sample loop or an 8-HQ column. This valve has two positions: the first for loading the loop or the column with sample, and the second for eluting the sample from the loop or column into the carrier stream. A quartz glass spiral flow cell positioned in a light-tight housing enabled the CL reaction to be monitored. The quartz glass spiral flow cell consisted of three turns of a tightly wound quartz glass spiral coil (tubing i.d. 1.1 mm; o.d. 3.0 mm; internal volume 130 μ l; diameter 20 mm).

The detection system consisted of an end-window photomultiplier tube (Thorn EMI, 9789QA) contained in a μ -metal shield for magnetic insulation (MS52D), a built-in current-to-voltage amplifier (C634, capable of four different settings "A, B, C & D", x1, x10, x100 and x1000 factors respectively; used setting "C"), an ambient temperature rf shielded housing (B2F/RFI) and a 1.1 kV power supply (Thorn EMI, PM28B). The amplifier was supplied with 15 V from an

independent power supply (BBH products). Once powered, the PMT detection system remained switched on and took <2.5 h to stabilise and give low dark current and dark voltage signals. Peak detection and quantification was achieved using a flat-bed chart recorder (Kipp and Zonen, BD111).

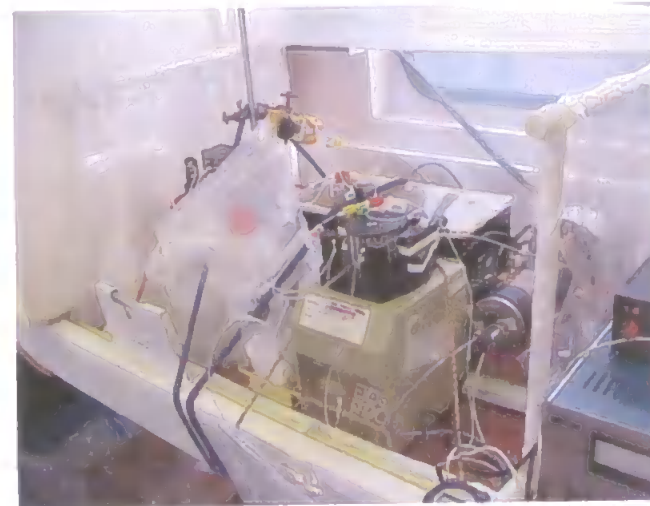
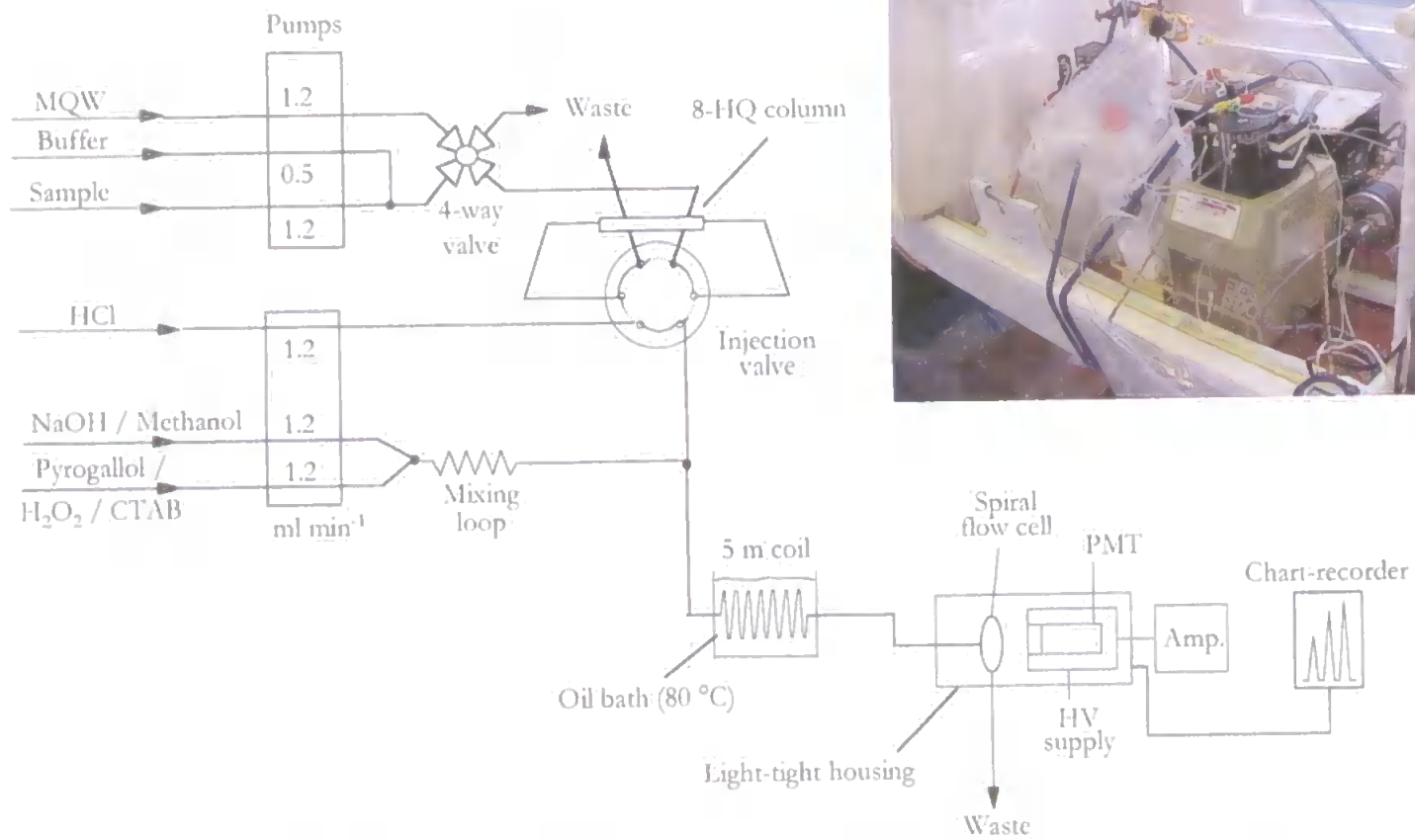


Figure 3.1: FI-CL manifold for the determination of Co(II). Inset: Photograph of the FI-CL manifold

3.2.3 Procedures

The CL detection system remained on throughout method development. After the stabilisation period, the PMT and amplifier gave a low dark current. Injection of a Co(II) standard or sample into the FI-CL resulted in a sharp, repeatable CL peak superimposed on the background CL emission. The signals were sent to a flat-bed chart recorder and the peaks measured manually with a ruler. For each sample, three replicates were obtained and the mean, standard deviation. Due to the nature of the analytical method, it is imperative to ensure high accuracy and precision in the preparation of reagent, standard and sample solutions.

High precision variable volume micropipettes (Finnpipette: 20-50; 50-200; 200-1000 μL and 500-5000 μL) were used throughout the work. These pipettes contain a ceramic piston and possess a minimum of metallic parts. They were regularly re-calibrated using a five-figure analytical balance (Sartorius A 200 S). A unique pipette tip was retained exclusively for each solution, stored in 25 mL sterilin vials or plastic bags and changed if memory effects were noted or if the volume setting was adjusted. pH measurements were performed on a Hanna Instruments HI 9021 meter, calibrated in the pH 4-7 or pH 7-10 ranges using standard buffer solutions (Colourkey, BDH Merck), as required.

Prior to use, the FI manifold, the column, the PTFE flow lines fittings and connectors were cleaned with 0.5 M Q-HCl and UHP water for several hours.

One analytical cycle could be completed in 8 min ($n=3$ or 4) with a 60 s preconcentration time and 55 s for the detection-elution step. The time for sample quantification was therefore 26 min ($n=3$).

1. Initially the 4-way valve (position one) allows the seawater sample to be pumped into the column for 60 s at pH 5.5 (with ammonium acetate buffer). Longer seawater load times would decrease the detection limit although this would require further purification of the sample buffer, and the UHP water in order to reduce the blank signal (Chapin et al., 1991). (The injection valve is in LOAD position).
2. By switching the 4-way valve (into position two) UHP water was subsequently passed through the column (30 s) to remove any residual sea-salt matrix ions present (at the same time the tube was introduced into the new sample to remove the previous solution from the flow line).
3. The injection valve was then switched to the ELUTE position and 0.05 M Q-HCl flowed through the column in a reverse direction (ca. 60 s) carrying the Co to the detection system, where it mixed with the CL reagent stream and generated a CL peak. Reversal of the flow direction between the loading and the elution stages was necessary to avoid the column becoming more and more tightly packed, which could in turn influence the flow rate and produce leakage problems. With strongly sorbed species, reversed flow elution is also beneficial in decreasing the dispersion of the analyte during elution, and improving the enrichment factor.
4. The injection valve was then returned to the load position and UHP water was pumped through the column (30 s) to remove residual hydrochloric acid.
5. Finally the 4-way valve was returned to position one and a new sequence commenced.

A typical detector output for a series of four replicates of the analytical cycle using an Irish seawater sample is shown in Figure 3.2.

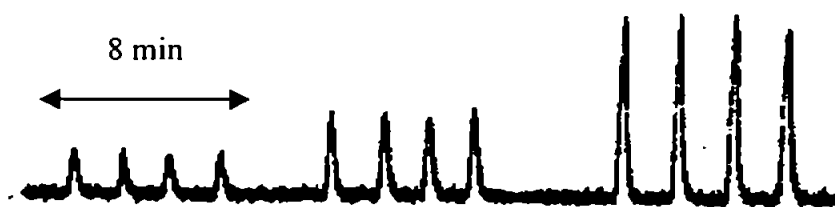


Figure 3.2: Detector output from a series of two standard additions of Co(II) to an Irish seawater sample (operating conditions: standard additions 300 and 600 pM; flow rate 1.2 ml min⁻¹; preconcentration time 60 s; reaction temperature 80° C; CTAB 0.025 mM; Pyrogallol 0.05 M; MeOH 20% v/v; H₂O₂ 1 M).

3.3 RESULTS AND DISCUSSION

3.3.1 Trautz-Schorigin chemiluminescence reaction

In 1905 Trautz and Schorigin reported a chemical system, consisting of formaldehyde and some polyhydric phenols (such as gallic acid) oxidised with aqueous alkaline hydrogen peroxide, that produced relatively strong chemiluminescence in the spectral range 560-850 nm, with an intense band at 643 nm and a weaker band at 478 nm (the Trautz-Schorigin Reaction, TSR). There are some spectrometric (Bowen et al., 1963) and chemical (Kearns, 1971) data suggesting singlet oxygen formation. However details of the mechanism and the exact nature of the emitters are not clear. The classical TSR is not convenient for analytical purposes. The modified TSR involving dilute reagents and gallic acid has been applied to the determination of formaldehyde (Slawinska and Slawinska, 1975) and proteins (Balcerowicz et al., 1970).

In 1977 Stieg et al. (1977) found that the rate of the CL oxidation of gallic acid was affected by trace concentrations of metals ions and other inorganic species. Furthermore, the CL obtained was enhanced by only a few compounds out of some 40 species tested, showing selectivity uncharacteristic of previous CL

reaction rate methods. These previous studies provide a basis for understanding of the light emission process of the TSR (Figure 3.3).

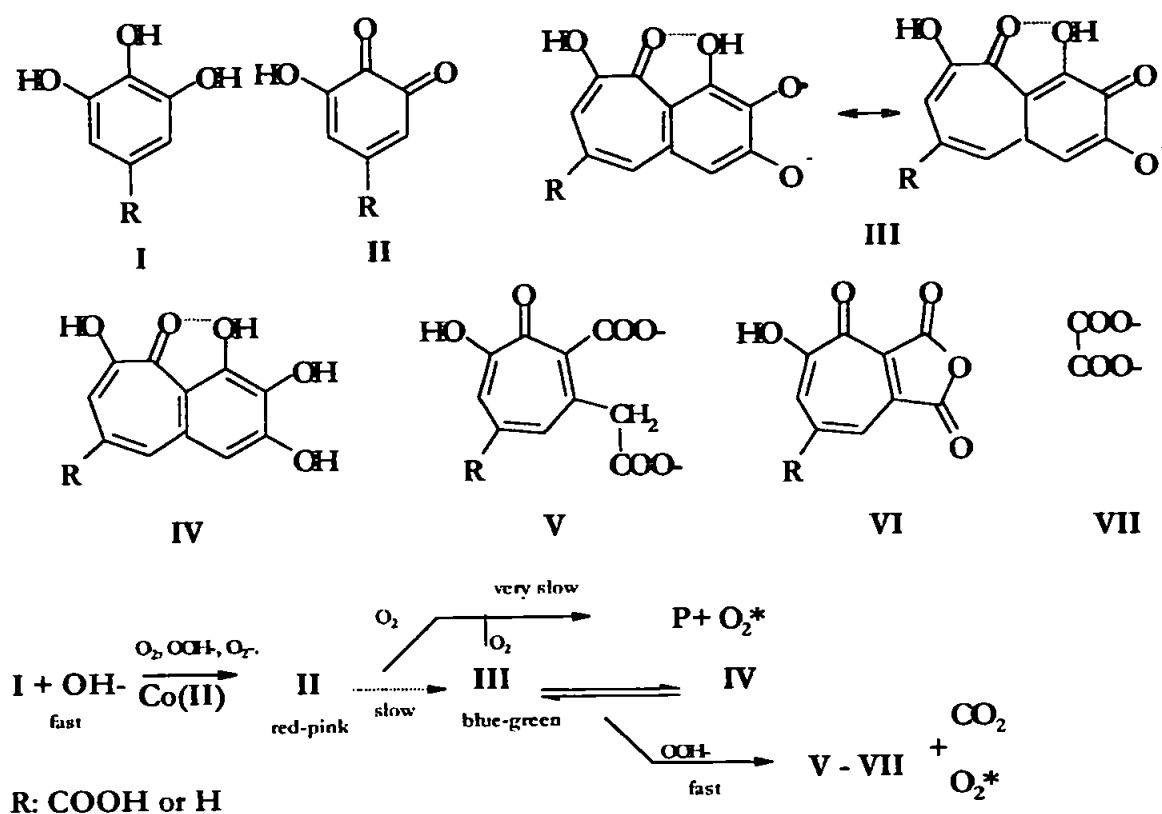


Figure 3.3: The mechanism of the Trautz-Schorigin Reaction

The oxidation of gallic acid (I) (when R is COOH) proceeds gradually in several stages, involving coloured intermediates (II) and (III). Final oxidation products (IV-VIII) are tropolone, oxalate, and a brown, low molecular weight, water soluble polymer (P) of unknown structure. Carbon dioxide and excited singlet oxygen are also generated. Bowen et al. (1963) found a narrow emission band at 630 nm and assigned it to $^1\text{O}_2^*$. Furthermore there is a 50 times weaker blue emission in the range 440-510 nm, with a maximum at 475 nm. These bands

were assigned to the radiative deactivation of $^1\text{O}_2^*$ and the excited anions of carboxylic acids, resulting from the oxidative cleavage of polyphenols.

Miller et al. (1982) detected trace amounts of cobalt by utilising the CL oxidation of pyrogallol, as an alternative polyhydric phenol, with alkaline hydrogen peroxide. However in alkaline solution pyrogallol is less stable than gallic acid due to its rapid autoxidation (some by-products of the autoxidation can also give rise to chemiluminescence). One of the intermediates that has been identified is 2,3,4,6'-tetra-hydroxy-5H-cycloheptabenzene-5-one-purpurogallin (PPG) (Figure 3.4) (Slawinska, 1971; Meluzova and Vassilev, 1970) and this itself undergoes oxidation to produce CL (Figure 3.4).

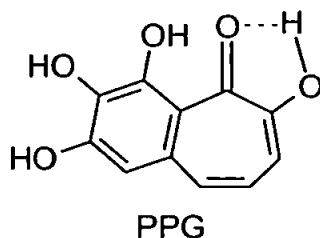


Figure 3.4: The structure of 2,3,4,6'-tetra-hydroxy-5H-cycloheptabenzene-5-one-purpurogallin (PPG)

Presumably, oxidation of PPG plays an important role in the CL mechanism of certain trihydroxybenzenes. Moreover, CL emission from PPG is interesting for other reasons: (a) the structure PPG indicates the existence of two condensed, resonating rings – benzene and tropolone. The question therefore arises as to which of the rings undergoes chemical changes leading to CL. (b) PPG is not only an end-product, but also an intermediate, in the oxidation of pyrogallol. These oxidation reactions, however, are complex and the mechanisms have not yet been fully established.

3.3.2 Optimisation

Sakamoto et al. (1987) used the following parameters for the determination of Co in seawater at picomolar levels (see Table 3.1).

Table 3.1: Optimised parameters for the determination of Co in seawater with 8-HQ column

Variables	Working conditions
PMT	- 20°C
Flow rate sample stream	0.75 ml min ⁻¹
Flow rate CL reagents stream	0.75 ml min ⁻¹
Temperature reaction coil	60°C
Reaction coil length	2 m
Gallic acid	0.02 M
Reaction pH (determined by NaOH)	10.4
Water soluble compound	MeOH (4% v/v)
Hydrogen peroxide	0.4 M
Eluent (HCl)	0.05 M
Preconcentration time	4 min
LOD	8 pM

Due to the many physical and chemical variables, an optimisation procedure was carried out univariately. The optimum values found by Sakamoto et al. (1987) were utilised as a starting point for the optimisation procedure. The concentration of the carrier, HCl 0.05 M, was not considered in the optimisation, due to being reported that a molarity of 0.05 M represents the optimum concentration to elute cobalt from the column in the smallest possible volume of acid (Sakamoto et al., 1987). All the univariate experiments (all parameters except one remain constant) were carried out to achieve the optimum working conditions (Co was 1.7 nM in HCl 0.05 M in all experiments). Each optimum value was recorded for further optimisation experiments. The noise has not been reported in the plots because was constant in all experiments (0.0175 mV).

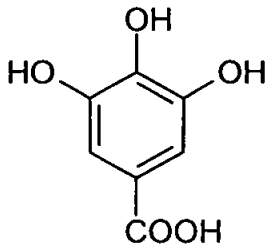
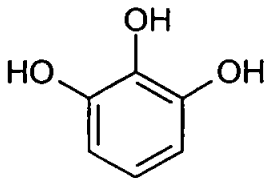
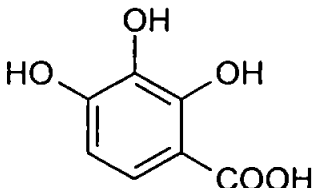
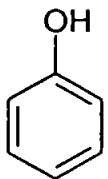
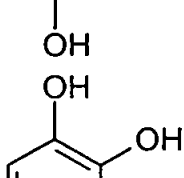
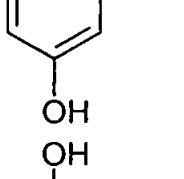
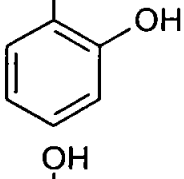
It is often desirable to optimise FI manifolds using simplex optimisation, which is a multivariate optimisation technique designed to locate the summit of the response surface, defined by the system variables. In this case, however, a univariate approach was preferred because the key variables were considered to be the reagent concentrations and it was impractical to prepare the required number of mixed reagent solutions.

All the variables were evaluated without using a preconcentration column. Each variable was optimised sequentially and for subsequent experiments optimised settings were used as found. For all the plots presented in this chapter error bars represent 2s unless stated otherwise.

3.3.2.1 Different polyhydric phenols

In 1982 Miller et al. (1982) used Pyrogallol (Pg) for the determination of Co in a batch system. Therefore in this work seven polyhydroxyphenols were screened to investigate their effect on the CL response (Table 3.2). The effect of different numbers and positions of -OH groups is shown in Figure 3.5 (all the compounds were tested in the range 0.01-1.0 M). Pyrogallol increased the signal by 140% as compared with gallic acid.

Table 3.2: Structure, common and IUPAC name of the different polyhydric phenols tested.

Structure	Chemical Name
	Gallic Acid (3,4,5-trihydroxybenzoic acid)
	Pyrogallol (1,2,3-trihydroxybenzene)
	2,3,4-Trihydroxybenzoic acid
	Hydroquinone (benzene-1,4-diol)
	1,2,4-Trihydroxybenzene
	Catechol (benzene-1,2-diol)
	Resorcinol (benzene-1,3-diol)

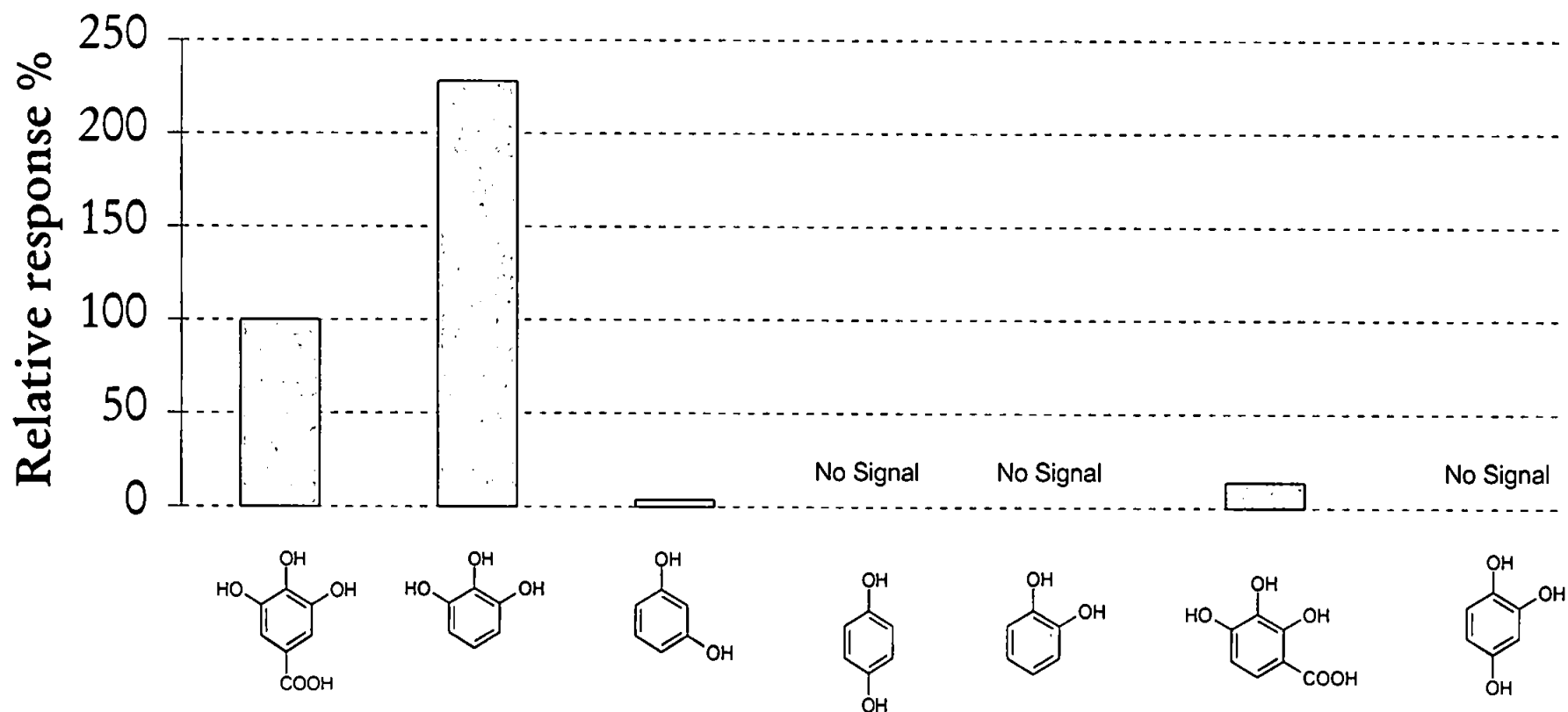


Figure 3.5: Effect of different Polyhydroxyphenols tested on the CL signal (each compound was tested at its optimum concentration: Gallic acid 0.02 M; Pyrogallol 0.05 M; Resorcinol 0.05 ; Catechol 0.02M)

Pyrogallol was chosen in place of gallic acid due to the enhanced sensitivity and the optimum concentration found was 0.050 M as shown in Figure 3.6.

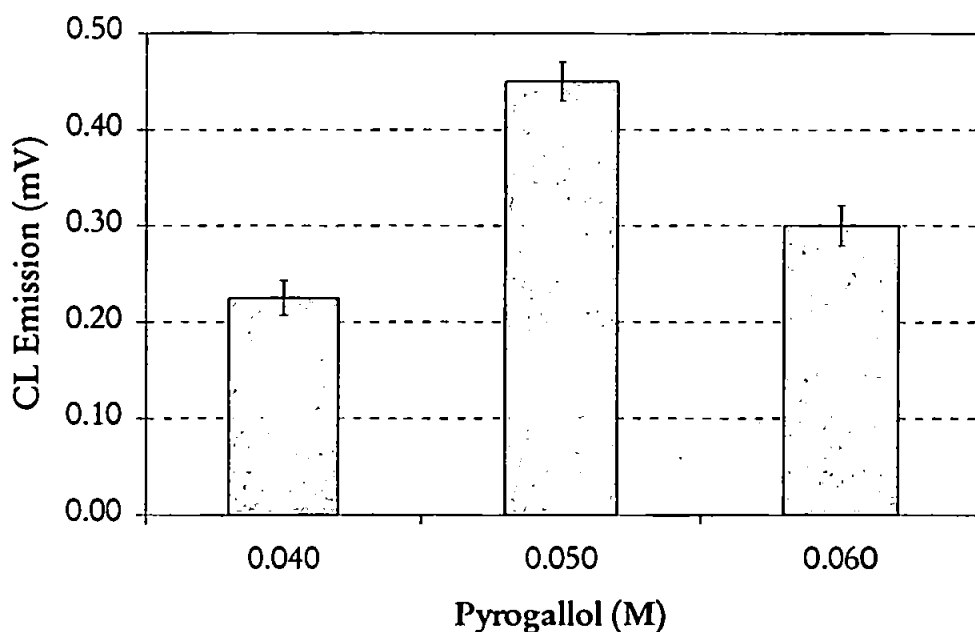


Figure 3.6: Effect of pyrogallol concentration on CL emission (reaction temperature 80° C; CTAB 0.025 mM; MeOH 20% v/v; H₂O₂ 1 M; pH 10.35).

3.3.2.2 Minimisation of the dark current noise

The best method for reducing the dark current is by cooling the photomultiplier down to -20° C, which is not easy or cheap to realise; therefore photomultiplier voltage was optimised by recording replicates of the chemiluminescent emission obtained when different voltages (increments of 50 V) were applied across the photomultiplier tube and a 1.7 nM Co(II) standard was injected. As the voltage was increased the signal increased in proportion. However the noise on the baseline also increased in a similar fashion. The noise was quantified by taking the mean of ten measurements of the noise on the baseline. Figure 3.7 shows

that the optimum signal-to-noise ratio was 1065 V and that was used for all further work.

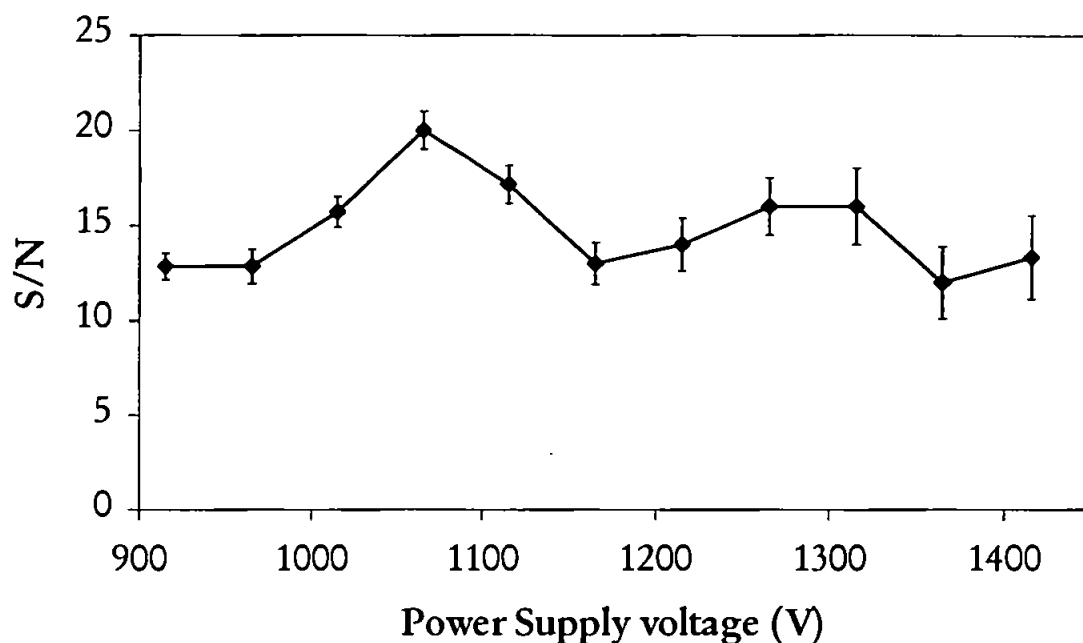


Figure 3.7: Results of variation of photomultiplier voltage

3.3.2.3 Flow rate

A CL emission versus flow rate plot, for the manifold without preconcentration column, is shown in Figure 3.8. The flow in a CL detection system requires careful monitoring because the rate of the CL reaction and the time from mixing of the Co(II) solution and reagents in the spiral flow cell must be matched as closely as possible. The entire emission versus time profile is not observed and the CL intensity detected in a flowing stream is the integrated portion of the emission profile that occurs during the time interval intersected by the observation cell. For the CL reagents it is important to keep the same flow rate for each channel to achieve the best mixing. On the other hand it is not possible to prepare one solution containing all five CL reagents due to incomplete solubilisation of the mixture. In this system the two streams for NaOH/MeOH

and Pyrogallol/CTAB/H₂O₂ were kept at identical flow rates. For method development, an operating flow rate of 1.2 mL min⁻¹ for each channel (sample, CL reagents and UHP) was selected.

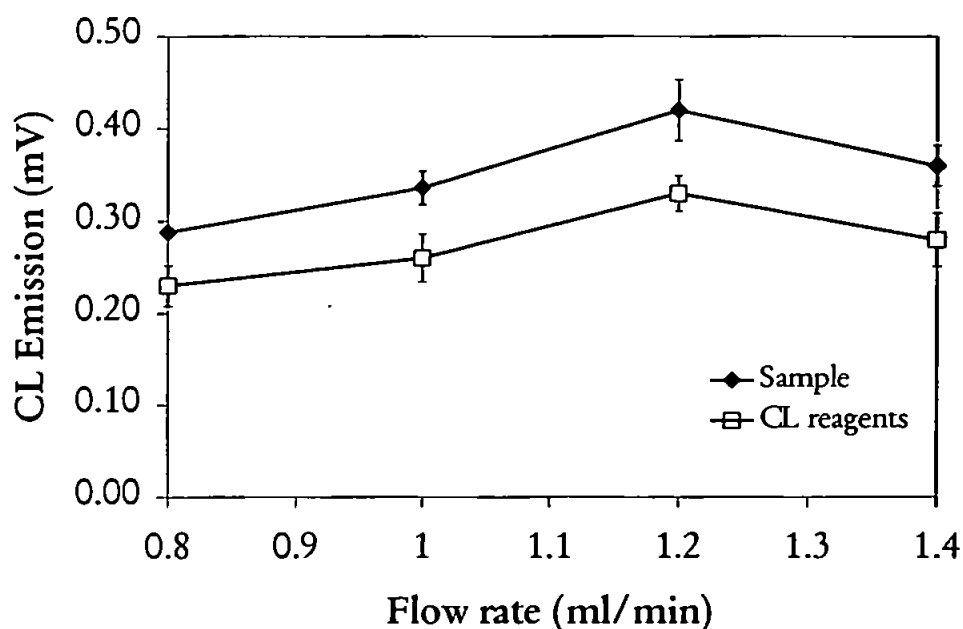


Figure 3.8: Effect of flow rate on CL emission for the sample stream and the CL reagents stream (reaction temperature 80° C; CTAB 0.025 mM; Pyrogallol 0.05 M; MeOH 20% v/v; H₂O₂ 1 M; pH 10.35).

3.3.2.4 Temperature

An increase of the reaction temperature also accelerated the oxidation rate of the TS reaction (Figure 3.9). The temperature was varied from 60 to 80°C using a silicone high temperature oil bath. No bubble formation was observed in spite of exceeding the boiling point of methanol (65°C) and the background noise also remained unchanged.

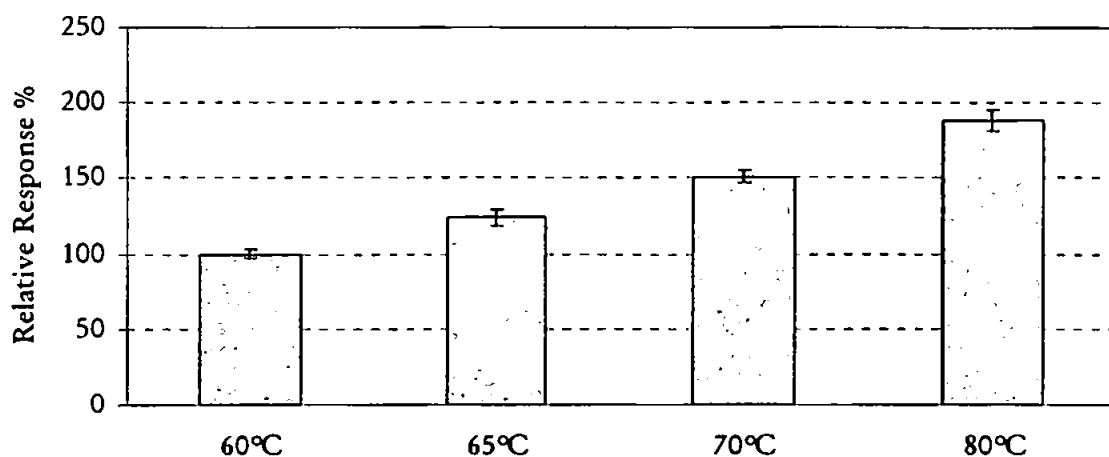


Figure 3.9: Effect of temperature on CL emission (CTAB 0.025 mM; Pyrogallol 0.05 M; MeOH 20% v/v; H₂O₂ 1 M; pH 10.35).

3.3.2.5 Reaction coil length

The intensity of the CL signals of cobalt increased with the length of the reaction coil. Chemiluminescence does not appear immediately after mixing of the reagents but increases gradually, attains a maximum, and then gradually decreases. In comparison with other CL systems (e.g. luminol) this system requires a very long reaction time demonstrating the very slow kinetic (Slawinska and Slawinska, 1975). A 5 m reaction coil (internal volume 2.21 ml; reaction time 60 s) was used because this gave us the required sensitivity without excessively decreasing sample throughput. Silicone oil instead of water was used in the thermostating bath and was stable up to 180 °C.

3.3.2.6 Sample loop volume

The optimisation of sample loop volume is generally not essential. The sample loop is usually replaced by the 8-HQ column in the final operating system. However it is an essential information if the system has to be applied to the

determination of Co(II) in freshwaters where the concentrations are higher and there are no interferences coming from alkaline earth metals. Figure 3.10 shows the optimum CL emission response. The highest value was achieved with a loop of 150 μL . Higher volumes increased the sample dispersion in the CL system generating double peak.

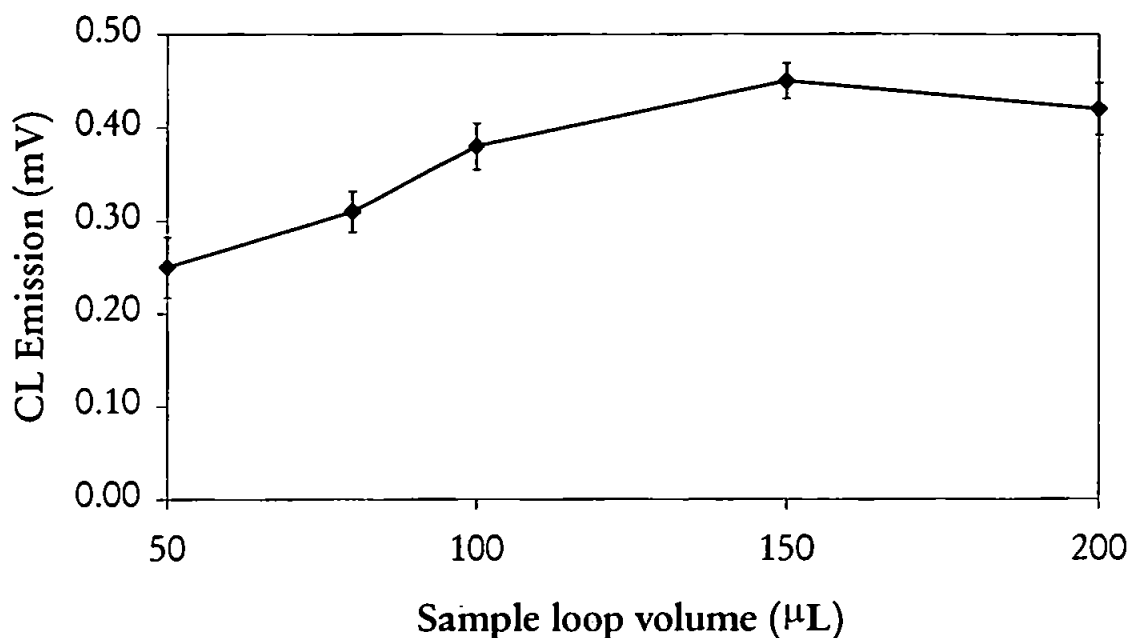


Figure 3.10: Effect of injection loop volume on CL emission (reaction temperature 80° C; CTAB 0.025 mM; Pyrogallol 0.05 M; MeOH 20% v/v; H_2O_2 1 M; pH 10.35).

3.3.2.7 Reaction pH

The optimum reaction pH was determined by varying the NaOH concentration in the alkaline methanol solution. A pH of 10.35 (0.15 M NaOH), measured in the effluent from the flow cell, was found to be optimum and agrees with literature values (Figure 3.11) (Hirata et al., 1996; Sakamoto-Arnold and Johnson, 1987).

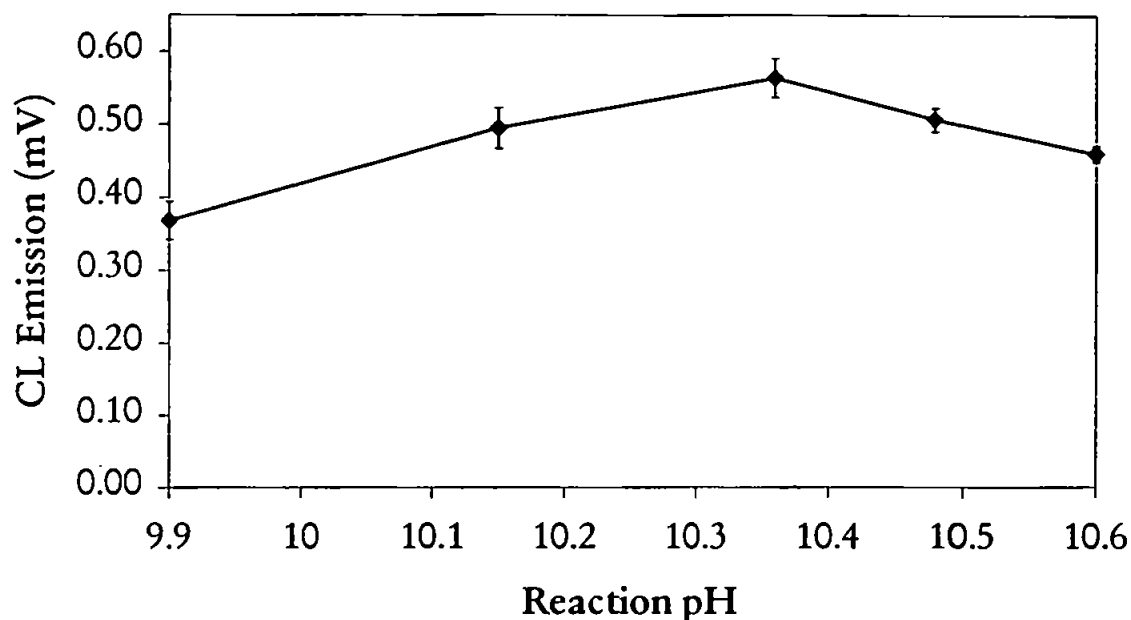


Figure 3.11: Effect of reaction pH on CL emission (reaction temperature 80° C; CTAB 0.025 mM; Pyrogallol 0.05 M; MeOH 20% v/v; H₂O₂ 1 M).

3.3.2.8 Surfactant

A typical simple surfactant has the structure R-X, where R is a long chain hydrocarbon of 8-18 atoms (usually unbranched) and X is the polar (or ionic) head group. Depending on X, surfactants can be classified as non-ionic, cationic, anionic or zwitterionic. Other surfactants consist of two or more hydrophobic chains and can incorporate different functional groups (Table 3.3) (Mittal and Fendler, 1982).

Table 3.3: Structures of most commonly used classes of surfactants

Name	Structural formula	Comments
Sodium dodecyl sulfate (SDS)	$\text{CH}_3(\text{CH}_2)_{11}\text{SO}_4^- \text{Na}^+$	Anionic
Cetyltrimethyl ammonium bromide(CTAB)	$\text{CH}_3(\text{CH}_2)_{15}\text{N}(\text{Br})(\text{CH}_3)_3$	Cationic
Polyoxyethylene(6)dodecyl alcohol	$\text{CH}_3(\text{CH}_2)_{11}(\text{OCH}_2\text{CH}_2)_6\text{OH}$	Non-ionic
4-(Dodecyldimethylammonium) butyrate	$\text{CH}_3(\text{CH}_2)_{11}\text{N}^+(\text{CH}_3)_2(\text{CH}_3)_3\text{COO}^- \text{Na}^+$	Zwitterionic

Depending on their chemical structure and on the nature of the solvent, amphiphilic molecules can give rise to different organised structures, namely aqueous and reversed micelles, microemulsions, monolayers, bilayers and vesicles. These systems are often referred to as organized assemblies and have been shown to exhibit some interesting properties. For example, they can solubilise, concentrate and compartmentalise ions and molecules, they can modify equilibria, acid-base and redox properties, and they can influence reaction rates, modify chemical pathways and influence stereochemistry (Pelizzetti and Pramauro, 1985). Obviously not all the organised structures are useful in all applications. Aqueous micellar solutions are formed by surfactants above their critical micellar concentration (c.m.c.). The surfactant is organised in micelles with diameters of 4-8 nm, by gathering together the hydrophobic non-polar tails of the surfactant molecules. The hydrophobic region is separated from the aqueous phase by a layer containing the surfactant polar heads and a "shell" of strongly retained water molecules (Yamada and Suzuki, 1984; Hinze et al., 1984).

Analytical applications of surfactant aggregates have attracted considerable interest in recent years (Ramis Ramos et al., 1988). Such organised assemblies exhibit unique properties facilitating analytical measurement, e.g. solubilisation, concentration and compartmentalisation of reactants and/or analytes, and alteration of micro-environment, chemical pathways and reaction rates.

In liquid phase CL methods, surfactants affect the microenvironment of fluorescing substances and can thus change their characteristic fluorescence parameters (excitation and emission spectra, fluorescence quantum yield,

energy transfer efficiency). In the determination of metal ions, the two most important properties are the effect of surfactants on the intensity of the fluorescent radiation and the improved selectivity of the CL system. The increase in the quantum yield of fluorescence has been attributed to vesicular solubilisation of the CL reagents and sensitizers, and also to the effect of changes in polarity of the medium, due to the presence of the surfactant (Hinze et al., 1984a; Hinze et al., 1984b).

Observations of enhanced CL in solvent systems consisting of membrane mimetic agents have recently been reported and physico-chemical studies have shown that surfactant CTAB micelles were effective in enhancing the CL efficiency for the determination of cobalt (Safavi and Baezzat, 1998; Xie et al., 1998). When the concentration of CTAB in solution increases gradually (the starting point is a concentration five times higher than the cmc), it starts to enhance the chemiluminescence intensity (Figure 3.12). The optimum concentration was found to be 0.025 M, which was used for all further work (reported cmc for CTAB is 0.002 M at 25°C) (Goto et al., 1982).

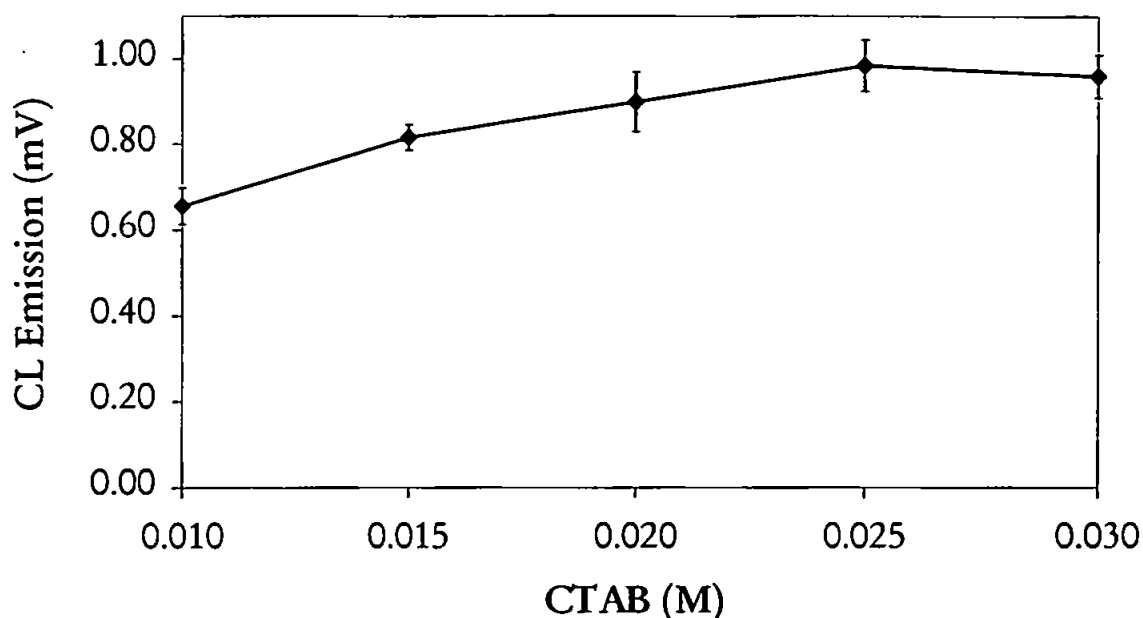


Figure 3.12: Effect of the surfactant CTAB on CL emission (reaction temperature 80° C; Pyrogallol 0.05 M; MeOH 20% v/v; H₂O₂ 1 M; pH 10.35).

3.3.2.9 Water soluble compounds

It is reported that methanol is required to prolong the lifetime of singlet oxygen (Nakahara et al., 1982; Yamada et al., 1983). Sakamoto et al. (1982) reported 4% as the best compromise between maximum signal and lowest noise. Different water-soluble compounds such as methanol, ethanol, ethylene glycol, isopropanol, propanol and acetonitrile were therefore investigated. It is reported that the lifetime (τ) of singlet oxygen in MeOH is 7 μ s, but in MeCN is 30 μ s, so this does not explain the great enhancement of the CL signal in methanol (Figure 3.13). As shown in Figure 3.14 a much higher increase in the chemiluminescence signal was observed at higher percentage of methanol.

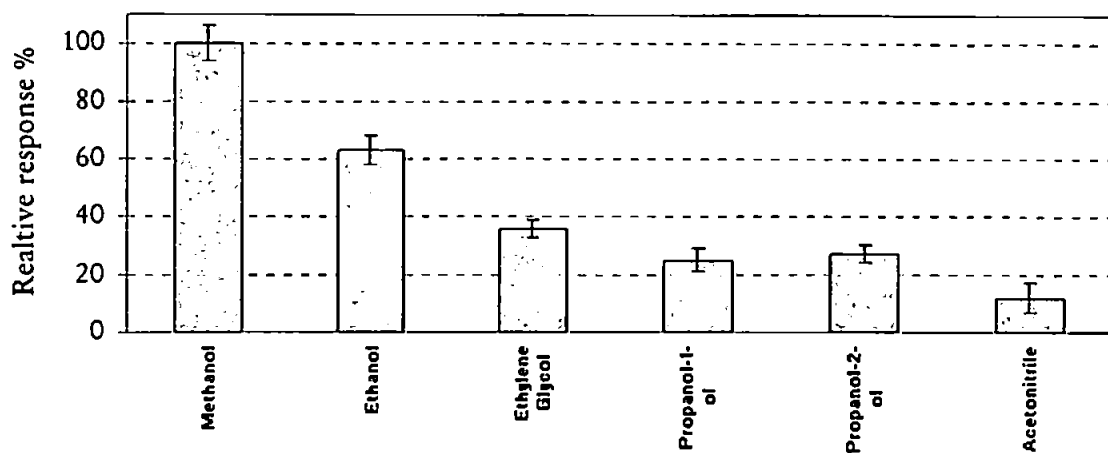


Figure 3.13: Effect of different water-soluble (4% v/v) compounds on the CL signal (signals are normalized to MeOH as 100%).

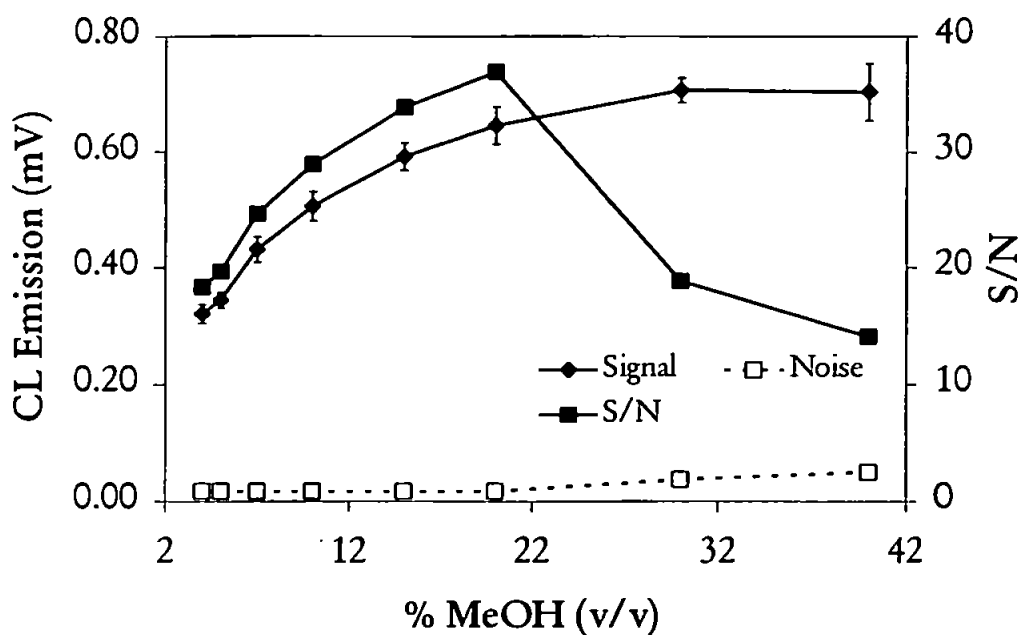


Figure 3.14: Effect of methanol percentage on CL emission (reaction temperature 80°C; CTAB 0.025 mM; Pyrogallol 0.05 M; H₂O₂ 1 M; pH 10.35).

The reason why methanol is the best solvent for the TS reaction is not clear. Aqueous micellar solutions, microemulsions and reversed micelles are thermodynamically stable organised media which form spontaneously when

appropriate amounts of a surfactant and a polar and/or non-polar solvent are mixed. The addition of a cosurfactant, usually an alcohol or an amine, can also be necessary (Mittal and Fendler, 1982). In micellar solutions, surfactant/alcohol/water systems are different from microemulsions mainly in the compactness of the micellar membrane, surface charge density, and extent of water penetration. For example, surfactants with bigger polar head groups, such as CTAB compared to SDS, are more penetrated by water. Addition of alcohol also causes an exclusion of water and a tightening of the micellar membrane. Methanol can be considered a cosurfactant. Moreover the polarity of the compounds does not seem to play any role. The relative response for ethylene glycol, which has 1.17 higher polarity than methanol, is still lower (Table 3.4). MeOH nonetheless plays essential role in the TS reaction.

Table 3.4: Eluotropic series and physical properties of water-soluble compounds (Kearns, 1979; Gollnick and Huhn, 1979).

Solvent	Polarity $\epsilon^\circ(\text{Al}_2\text{O}_3)$	Lifetime τ (μs)	Viscosity (mPa s; 20° C)	Boiling point (°C)
Acetonitrile	0.65	30	0.37	82
Iso-propanol & n-propanol	0.78	Not reported	2.3	82.97
Ethanol	0.88	12	1.20	78
Methanol	0.95	7	0.60	65
Ethylene glycol	1.11	Not reported	19.9	197

3.3.2.10 Hydrogen peroxide

A concentration of 1 M hydrogen peroxide was found to deliver the maximum response (Figure 3.15). This amount of oxidant is much higher than the 0.4 M used by Sakamoto et al., (1987). This is due to the fact that in the case of gallic

acid the optimum reagent concentration was 0.02 M. The optimum value of pyrogallol was almost the double that gallic acid (0.05 M).

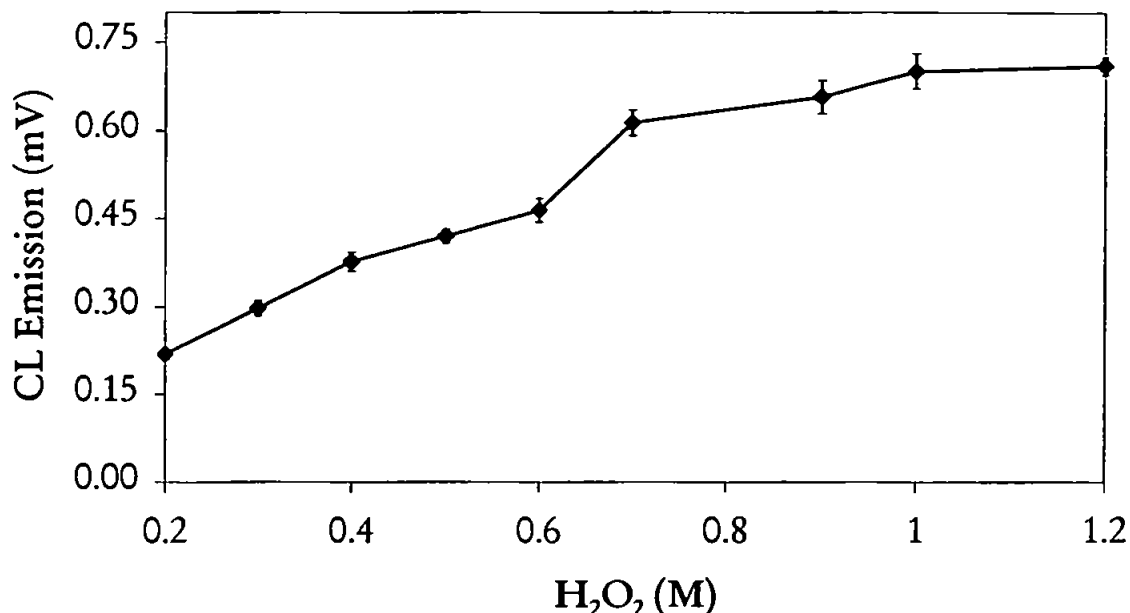


Figure 3.15: Effect of hydrogen peroxide concentrations on CL emission (reaction temperature 80° C; CTAB 0.025 mM; Pyrogallol 0.05 M; MeOH 20% v/v; pH 10.35).

3.3.2.11 Variation of pyrogallol stability over time

In order to assess the stability of pyrogallol reagent over time, the signal obtained by a 1.7 nM Co(II) standard was monitored over a period of 3 d. Optimum reaction conditions were used; the pyrogallol concentration was 0.05 M. Figure 3.16 shows that the pyrogallol solution was stable only for 48 h after preparation. Some workers (Nakano et al., 1993; Slawinska, 1971) found that it was possible to increase the stability of pyrogallol by preparing the solution in 0.01 M of HNO₃; however in order to avoid any further contamination, working solutions were prepared daily without acid.

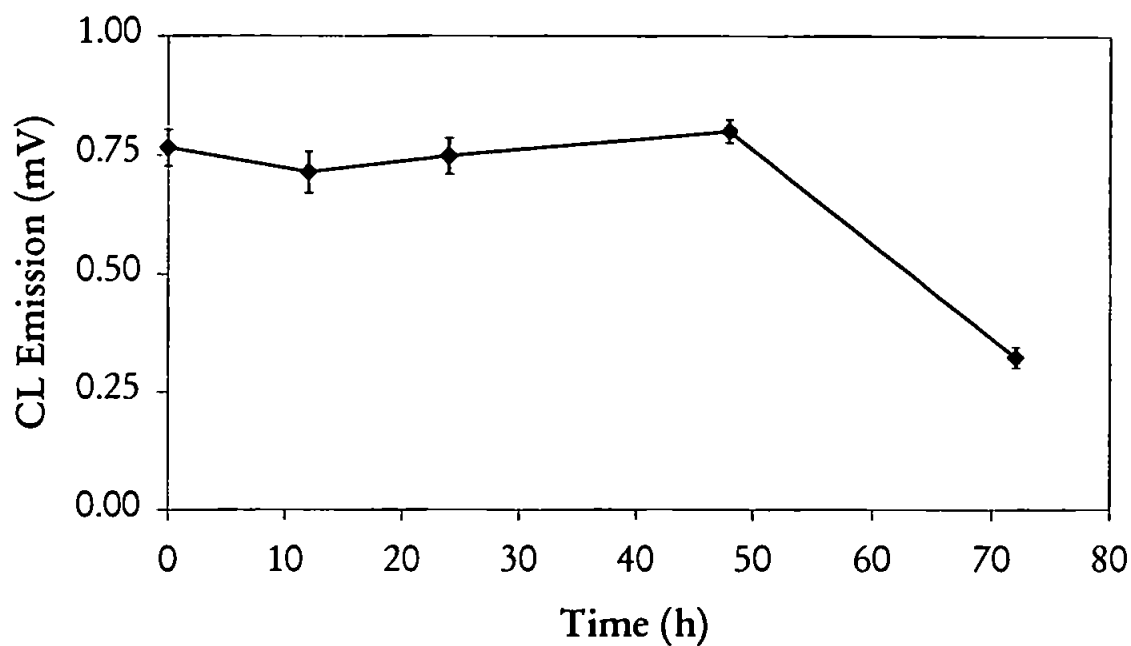


Figure 3.16: Variation in stability of pyrogallol reagent with time

3.3.2.12 Optimised system

Table 3.5 shows the optimised values utilised for further experiments and field trials.

Table 3.5: Optimised parameters for the system without 8-HQ column for the determination of Co in seawater with pyrogallol

Variables	Working conditions
PMT	Room temperature
Flow rate sample stream	1.2 ml min ⁻¹
Flow rate CL reagents stream	1.2 ml min ⁻¹
Temperature reaction coil	80°C
Reaction coil length	5 m
Pyrogallol	0.05 M
Surfactant (CTAB)	0.025 M
Reaction pH (determined by NaOH)	10.35
Water soluble compound	MeOH (20% v/v)
Hydrogen peroxide	1 M
Sample loop volume	150 µl
Carrier (HCl)	0.05 M

3.3.3 Calibration graph and Limit of Detection (LOD) without the 8-HQ column

The IUPAC definition of limit of detection (LOD) is the analyte concentration giving a signal equal to the blank signal plus three times the standard deviation of the blank (Miller and Miller, 1993). This can be related to the calibration graph *via* the equation $y = b + 3s_{y/x}$ where b is the y -axis intercept and $s_{y/x}$ is a standard deviation statistic. Sometimes, in the absence of a blank signal, the background noise has to be used to calculate a LOD, and this can be defined as three times the peak-to-peak noise.

The analytical blank for a calibration graph is defined as: “the signal generated by a solution containing no deliberately added analyte, but containing the sample reagent additions as the other test samples and also subjected to exactly the same sequence of analytical procedures” (Miller and Miller, 1993). All seawater samples were analysed by the method of standard additions (see Section 3.3.7). This is because analytical calibration graphs can only be used if the sample matrix is highly reproducible or if changes in the matrix do not affect the quantitative relationship between measured chemiluminescent power and analyte concentration. If neither of these conditions is fulfilled, then the standard additions technique must be used. This technique relies in principle on a blank solution giving zero signal at zero Co concentration.

In order to accurately quantify the amount of Co(II) from the CL peaks and the LOD, it is necessary to define the components of the peaks and noise. The noise is composed of two contributions as expressed in:

$$N = N_{\text{Electronic}} + N_{\text{CL reagents}}$$

where N_E is the electronic noise of the PMT and $N_{CL \text{ reagents}}$ is the noise due to the Co contained in the CL reagents and/or to the natural chemiluminescence emission of the CL reagents (pyrogallol, H_2O_2 , NaOH, methanol and CTAB). In the case of measurements of metal ions with a high contamination risk such as Fe, Al, or Cu it would be advisable set up a cleaning procedure for the CL reagents (when is feasible; some reagents are difficult to clean) such as recrystallisation.

However in this system for the determination of Co the limiting factor for the LOD is $N_{CL \text{ reagents}}$ (N_E was negligible compare with $N_{CL \text{ reagents}}$ so $N \cong N_{CL \text{ reagents}}$).

The noise baseline showed in Figure 3.17 was 0.0175 mV.

The Co signal (Co^*) superimposed on B_{Signal} , can be expressed as:

$$Co^* = Co_{SW} + Co_{UHP} + Co_{Buffer} + (Co_{HCl})$$

where Co_{SW} is the analyte concentration, Co_{UHP} is the Co contained in the UHP water, Co_{Buffer} is the Co impurity in the buffer, and Co_{HCl} is the Co impurity in the HCl used to acidified any seawater samples stored for later analysis. If we assume that Co_{HCl} is zero (due to the use of Q-HCl), the main efforts to lower the LOD have to be focused on Co_{UHP} and Co_{Buffer} . In the reaction reported here, Co_{Buffer} and Co_{UHP} are negligible due to the low amount of Co present in the purified buffer and in the UHP water. So $Co^* = Co_{SW}$ is the signal due only to the analyte in the sample. ($Co_{UHP} + Co_{Buffer} + Co_{HCl} \cong 0$) and state that the signals obtained are due only to the Co(II) contained in the sample without the interference product by the buffer, the UHP water and the Q-HCl.

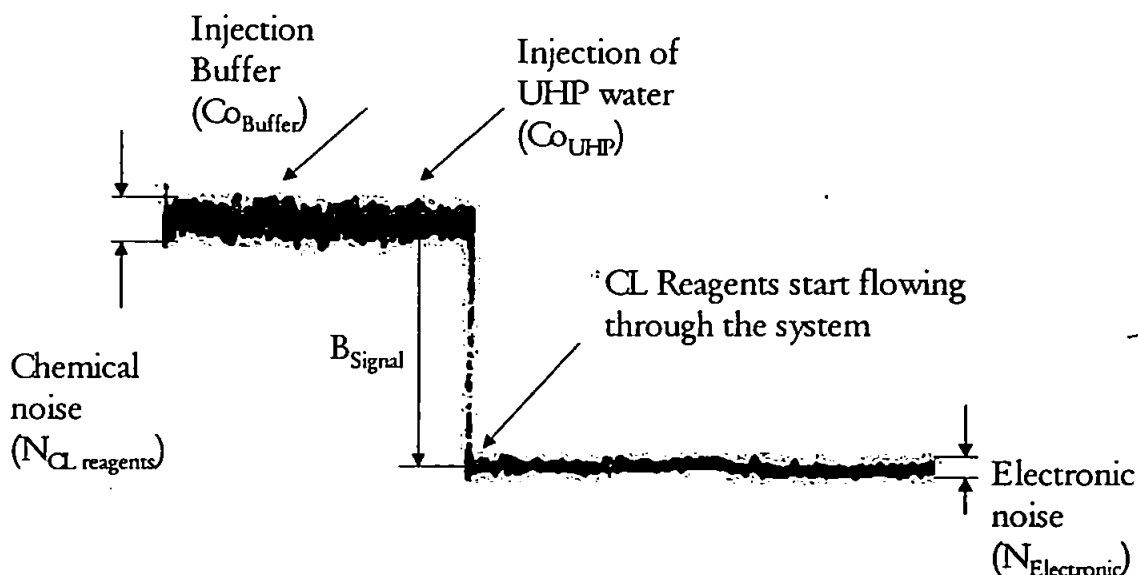


Figure 3.17: Recorder trace showing electronic and chemical background noise.

It is possible to use the value of 0.0175 mV for $N_{CL \text{ reagents}}$ to calculate the LOD of the system and this value was taken as the blank signal.

A calibration graph for the optimised system is shown in Figure 3.18. When a concentration greater than 60 nM Co was used, the calibration graph deviated from a straight line. This is a common phenomenon with concentration versus CL signal plots for the TS reaction for several reasons. It has been shown that in a stopped-flow experiment the rate of the TS reaction depended on the Co(II) concentration (Nakahara et al., 1982); for high cobalt concentrations a water-soluble brown polymer appeared to be the principal end-product and may cause light scattering; examination of the pyrogallol absorption spectrum and the CL spectrum indicates that self-absorption is possible (Ryan et al., 1978). Most likely in the system reported here, the concentration of the CL reagents (pyrogallol and/or hydrogen peroxide) was not high enough to maintain an excess at high Co concentrations.

The calibration graph for Co in the optimised FI manifold system without a column is shown in Figure 3.18 and was linear in the concentration range 0.850-59.5 nM ($r^2 = 0.9983$; RSDs < 6%; $n = 3$ or 4; LOD = 0.2 nM).

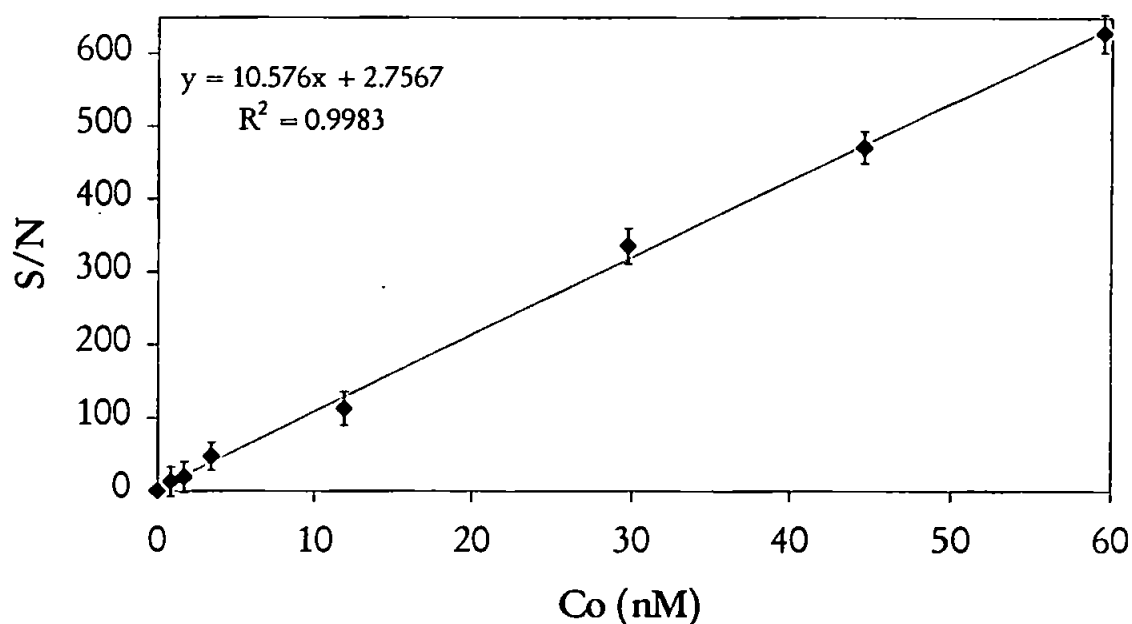


Figure 3.18: Calibration graph in the range 0.85-59.5 nM of Co(II) in acidified UHP water (reaction temperature 80° C; CTAB 0.025 mM; Pyrogallol 0.05 M; MeOH 20% v/v; H₂O₂ 1 M; pH 10.35).

3.3.4 Interference studies

Stieg and Nieman (1977) found that metal ions such as Co(II), Mn(VII), Mn(II), Ag(I), Cd(II) and Pb(II) showed a significant enhancement of the TS reaction, while most other transitions metals (e.g. Ni(II), Fe(II), Fe(III), Cr(III), Cu(II), Zn(II)) showed no enhancement. In view of previous research on the mechanism of trace metal enhancement of the luminol reaction (Burdo and Seitz, 1975) it is possible that these metal species either form a complex with H₂O₂ in solution or form a complex directly with the polyhydric phenol (gallic

acid or pyrogallol). However it has been shown (Elinany et al., 1976) that the latter cannot be the case. It was found that there was no evidence for complexes of gallic acid with Co(II), Mn(II), Pb(II) or Cd(II)-the enhancing species seen for the gallic acid oxidation. Furthermore, definite evidence of gallic acid complexes with As(III), Cr(III), Cu(II), Fe(II) and Mo(VI) (all species which do not enhance gallic acid CL) was found.

These results suggest that at some point in this reaction the free metal ion is needed for enhancement, and that the selectivity of this reaction is, by default, dependent on the complexing characteristics of pyrogallol. It may be, as in the luminol reaction, that a metal - H₂O₂ complex forms; however, it is then difficult to explain why different sets of metal - H₂O₂ complexes react with luminol and gallic acid. Nevertheless Co(II) remains the most effective enhancer in this reaction, Sakamoto et al. (1982) reported that although Mg(II) and Ca(II) have low quantum yields in the reaction, their concentrations are sufficiently high in seawater that they produce a chemiluminescence signal that masks the signal due to Co(II). Moreover the alkaline-earth ions present in seawater also complexed a significant fraction of the pyrogallol, which suppressed the cobalt catalysed chemiluminescence.

The interference of various transition metal ions (Ag(I), Fe(III), Cu(II), Pb(II), Mn(II), Cd(II)) on the determination of Co(II) by pyrogallol CL was conducted on acidified Atlantic seawater samples, spiked with Co(II) to give a ca. 425 pM final concentration. Individual metal ions were added at fifty times their typical concentrations found in open-ocean seawater (Chester, 2000). These samples were buffered in-line with ammonium acetate to pH 5.1 and pH 7.8. Ag(I) was the only cation that showed any detectable interference (Table 3.6) but its

concentration in seawater is typically 0.5 - 35 pM (Chester, 2000) and therefore it is unlikely to interfere in the analysis of real seawater samples.

Table 3.6: Effect of the addition of metal ions (at 50x their average seawater concentration at S=35) on the CL emission of a 425 pM Co(II) standard (data are shown as %, normalised to the response for 425 pM Co(II)).

Sample pH	Fe(III)	Cd(II)	Mn(II)	Ag(I)	Cu(II)	Pb(II)
5.1	103 ± 4	102 ± 6	94 ± 3	212 ± 5	101 ± 3	103 ± 6
7.8	98 ± 5	106 ± 4	97 ± 5	207 ± 7	93 ± 2	100 ± 2

The influence of NO₃⁻, Cl⁻, SO₄²⁻, Br⁻, CH₃COO⁻ was investigated by Stieg et al. (1977). All the CL signals were equal, which suggests that the method is insensitive to the various anions.

3.3.5 pH dependence of cobalt uptake on the preconcentration column

Figure 2.12 in Chapter 2 illustrates the retention of Co ions on a 8-HQ column as a function of sample pH. Co(II) was quantitatively retained from seawater at pH > 5 as shown in Table 3.7. Seawater can therefore be loaded directly from sampling points at natural pH (ca. 8). In order to reduce loss of metals on the walls of the containers (due to adsorption phenomena) samples are often stored at pH 2 or lower, especially for delayed analyses. For acidified seawater samples (pH ca. 2) the pH was adjusted in-line using ammonium acetate buffered at pH 5.5 immediately prior to adsorption onto the 8-HQ column. This resulted in a final sample pH of 5.0.

Table 3.7: Signal recovery of Co(II) at different sample pH for an Irish seawater sample.

pH	Recovery %
3.8	68.3 ± 6.2
5.1	99.8 ± 2.3
7.8	99.5 ± 3.1

3.3.6 Calibration graph and LOD with the 8-HQ column

The calibration graph for the optimised system in UHP incorporating an 8-HQ column was linear in the concentration range 0.034-0.850 nM with RSDs (n=3) of 2.1-5.8% (Figure 3.19). The limit of detection in acidified UHP water (as 3s) was 0.005 nM using a preconcentration time of 60 s.

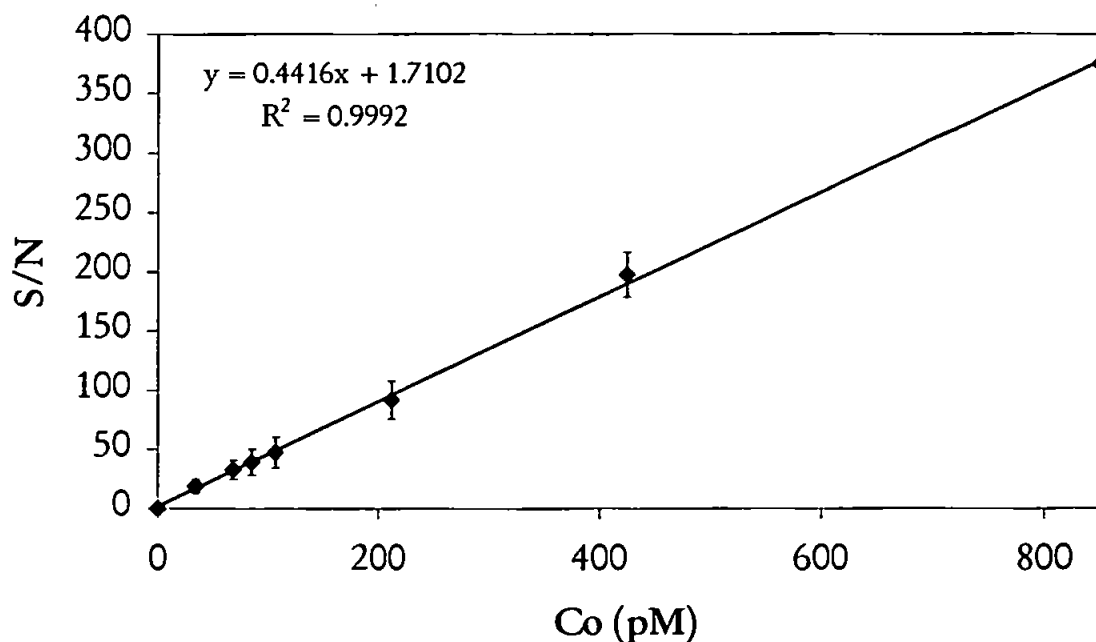


Figure 3.19: Calibration graph in the range 0.034-0.850 nM of Co(II) in acidified UHP water (reaction temperature 80° C; CTAB 0.025 mM; Pyrogallol 0.05 M; MeOH 20% v/v; H₂O₂ 1 M; pH 10.35).

3.3.7 Standard additions method

For this method, the signal for an accurately known volume (or time) of sample solution is recorded. The sample solution is then “spiked” with a known concentration of the species of interest (using as small a volume of spike as possible) and the signal peak recorded again. This process is repeated to obtain a standard additions plot. Once the standard additions graph has been obtained, extrapolation of the straight line back of the x -axis enables the concentration of the analyte in the sample solution to be determined. In statistical terms, the principle disadvantage of the standard additions technique is that it is an extrapolation method, and thus is less precise than interpolation techniques. Quoting determined concentrations with reasonable confidence intervals will introduce large error bands and reduce precision. Ideally, four points should be used in the experiments, and the additions should cover a considerable range in order to improve precision. Spikes should be at similar or double the concentration of the analyte.

Figure 3.20 shows the standard addition graph obtained for the determination of Co in an Irish seawater sample.

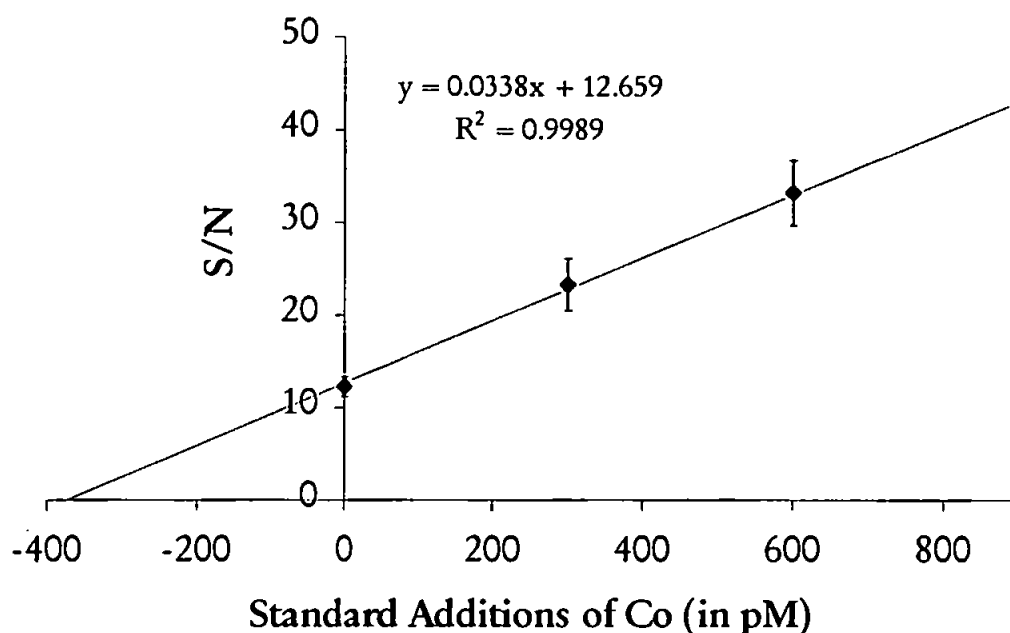


Figure 3.20: Standard additions curve for Irish seawater sample (reaction temperature 80° C; CTAB 0.025 mM; Pyrogallol 0.05 M; MeOH 20% v/v; H₂O₂ 1 M; pH 10.35).

3.3.8 Analysis of Certified Reference Materials (CRMs)

Boyle et al. (1977) stated that results for the determination of trace metals in seawater should not be accepted unless they meet two criteria: interlaboratory agreement and oceanographic consistency. The Canadian seawater trace metal standards NASS-4 (North Atlantic Surface Seawater), CASS-3 (Coastal Atlantic Surface Seawater) and SLEW-2 (St. Lawrence Estuarine Water) were analysed in the laboratory to verify that results obtained with the FI-CL could meet the first of these criteria. These standards have been rigorously analysed by expert laboratories using a number of analytical techniques for many of trace metals including cobalt.

Moreover a Irish seawater samples kindly provided from the Marine Geochemistry Laboratory at the University of Plymouth, where the concentration of Co(II) was ascertained by CSV, has been analysed using the FI-CL method. In Table 3.8 are reported the results of these analyses.

Table 3.8: Results for the determination of Co(II) in seawater CRMs and an Irish Sea sample.

Sample	FI-CL	Certified value	AdCSV ^{a)}
NASS-4 (nM)	0.16 ± 0.01	0.15 ± 0.02	-
CASS-3 (nM)	0.60 ± 0.09	0.68 ± 0.11	-
SLEW-2 (nM)	0.93 ± 0.13	0.87 ± 0.21	-
Irish Seawater (nM)	0.35 ± 0.02	-	0.34 ± 0.01

Error bars represent ±2s; a) sample analysed by Dr. Braungardt.

A way in which the results of a new analytical method may be tested is by comparing them with those obtained using a reference method. The null hypothesis adopted is that the means of the results given by the two methods are equal, we need to test whether \bar{x}_1 and \bar{x}_2 differs significantly from zero. The pooled value of the standard deviation is given by:

$$s^2 = \frac{\{(n_1 - 1)s_1^2 + (n_2 - 1)s_2^2\}}{(n_1 + n_2 - 2)}$$

where \bar{x}_1 and \bar{x}_2 are the two sample means, s_1 and s_2 their corresponding standard deviations and n_1 and n_2 the number of measurements. Hence, in the case of the CASS-3 for example:

$$s^2 = \frac{(2 \times 0.11^2 + 2 \times 0.09^2)}{4} = 0.0162$$

$$s = 0.127$$

The value of t is then given by:

$$t = \frac{(\bar{x}_1 - \bar{x}_2)}{s\sqrt{(1/n_1 + 1/n_2)}}$$

where t has $n_1 + n_2 - 2$ degrees of freedom. So,

$$t = \frac{(0.68 - 0.60)}{0.127\sqrt{(1/2 + 1/3)}} = 0.688$$

Miller (Miller and Miller, 1993) gives the critical value of $|t|$ ($P=0.05$) at 3 degrees of freedom of 3.18. Since the experimental value of $|t|$ is less than the reference value, the difference between the two results is insignificant at the 5% level and the null hypothesis is accepted, confirming the good agreement between experiment results by FI-CL and certified values.

3.4 CONCLUSIONS

The development of a highly sensitive system for the determination of dissolved Co at picomolar level is presented, based on a flow injection technique coupled with pyrogallol (instead of gallic acid) chemiluminescence detection.

- For best results care must be taken to minimise contamination risks during all development work and reagent clean-up procedures must be adopted.
- A chelating resin of 8-hydroxyquinoline is effective for in-line matrix elimination and preconcentration.
- The method permits the selective determination of Co with a practical limit of detection (3s) of 5 pM when 1.1 ml of sample is loaded onto the column, and a relative standard deviation of 4.1 % ($n = 3$) for a 0.85 nM Co sample.
- One analytical cycle (incorporating load, wash and rinse steps) can be completed within 8 min, making this system suitable for real-time analyses.
- The method determination of Co in NASS-4, CASS-3 and SLEW-2 certified reference materials is accurate as shown by Table 3.8.

CHAPTER 4

DETERMINATION OF MANGANESE IN SEAWATER USING FLOW INJECTION WITH CHEMILUMINESCENCE DETECTION.

4.1 INTRODUCTION

This chapter describes the development of a flow injection-chemiluminescence (FI-CL) procedure for the determination of Mn in seawater. The first method chosen involved the oxidation of luminol (5-amino-2,3-dihydro-1,4-phthalazinedione) in alkaline media by hydrogen peroxide with Mn(II) as the catalyst. Luminol is an extremely sensitive CL reagent for trace metals including manganese (reported LOD for this reaction is 29 pM) (Okamura et al., 1998). Therefore no preconcentration is required (the lowest Mn(II) concentration reported in seawater is 200 pM) (Statham et al., 1986). However due to the interference caused by the buffer to the luminol reaction this method is not suitable for the determination of Mn(II) in seawater.

Yamada et al. (1985) demonstrated that the luminous oxidation of 7,7,8,8-tetracyanoquinodimethane (TCNQ) by dissolved O₂ can be utilised for sensitive determination of Mn(II). The weak chemiluminescence of TCNQ is effectively sensitised by Eosin Y in didodecyldimethylammonium bromide (DDAB) bilayer vesicles. Photons are produced at a rate proportional to the concentration of manganese in solution. This second reaction has been optimised for the determination of Mn(II) in seawater.

4.2 EXPERIMENTAL

4.2.1 Reagents

4.2.1.1 CL reagents for the luminol-hydrogen peroxide system

Luminol and TETA (triethylenetetramine) were obtained from Fluka, H_2O_2 and Na_2CO_3 (Merck, BDH) and were not further purified. A 0.1 M sodium carbonate (Na_2CO_3) buffer was prepared by dissolving 5.3 g in 500 ml of UHP water. A stock solution of luminol (10 mM) was prepared by dissolving 0.1772 g in 100 ml of Na_2CO_3 0.1 M followed by sonicating for 30 min. A working luminol reagent solution (1 mM) was prepared by diluting 10 ml of the stock solution in 100 ml of 0.1 M Na_2CO_3 (final pH 12). Luminol solutions provided maximum and stable sensitivity after a storage period of 24 h in the dark and therefore were prepared a minimum of 1 day in advance. Luminol solutions were stable for at least 1 month. The following buffers (see Table 4.1), (Beynon et al., 1996; Harris, 1995) were provided from Fluka and used without any further purification.

Table 4.1: Name and pKa values for buffers used.

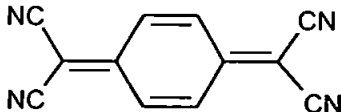
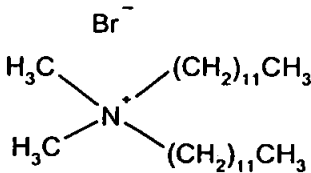
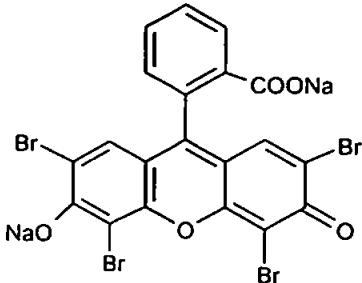
Name	pK _a (25 °C)	Grade
Acetic acid	4.76	puriss. p.a. ACS
Succinic acid	4.21 (pK ₁)	puriss. p.a. ACS
Citric acid	4.76 (pK ₂)	puriss. p.a. ACS
2-(N-Morpholino)ethansulphonic acid (MES)	6.15	puriss. p.a. ACS
N-2-Acetamidoiminodiacetic acid (ADA)	6.60	puriss. p.a. ACS
1,3-Bis[tris(hydroxymethyl)methylamino]propane (BIS-TRIS propane)	6.80	puriss. p.a. ACS
Piperazine-N,N'-bis(2-ethansulphonic acid) (PIPES)	6.80	puriss. p.a. ACS
N-(2-Acetamido)-2-amino ethansulphonic acid (ACES)	6.90	puriss. p.a. ACS

4.2.1.2 *CL reagents for the TCNQ-O₂-OH-Eosin Y system*

All reagents were of analytical grade, supplied by Fluka, unless stated otherwise, and prepared in UHP water. DDAB, Eosin Y, NaOH, and TCNQ were used without further purification. The first CL reagent solution (denominated R₁) was prepared by adding 0.051 g of TCNQ and 1.8506 g of DDAB to a 1000 ml volumetric flask half-filled with UHP water. The solution was first shaken and then sonicated in an ultrasonic bath for 40 min. A 0.2076 g amount of Eosin Y was then added to the flask, which was adjusted to volume and sonicated for a further 40 min to help to solubilize the TCNQ. It is possible prepare R₁ by adding 5 ml of Eosin Y 0.06 M, 0.051 g of TCNQ, and 1.85 g of DDAB to 900 ml of UHP water and adjusting the volume to 1000 ml with UHP water. This solution was shaken occasionally and sonicated for at least 60 min. However the TCNQ does not solubilize completely with this procedure. The chemical structure of TCNQ, DDAB and Eosin Y are shown in Table 4.2.

To obtain a 0.01 M sodium hydroxide solution, 0.4 g of NaOH was diluted to 1000 ml. A stock solution (1 mM) of the masking agent desferrioxamine mesylate (DFAM, C₂₅H₄₈N₆O₈•CH₄O₃S) (Sigma) was prepared by dissolving 0.657 g of DFAM in 1000 ml of UHP water. The effectiveness of DFAM was strongly dependent on its age (Bowie et al., 1995), and for this reason the reagent was stored in a refrigerator and working solutions prepared as required.

Table 4.2: Chemical structure of TCNQ, DDAB and Eosin Y

Chemical structure	Name
	TCNQ
	DDAB
	Eosin Y

4.2.1.3 Manganese Standards

A 182 μM Mn(II) stock standards were prepared by dilution of a 1000 mg l^{-1} (18.2 mM) Mn(II) atomic absorption standard solution ($\text{Mn}(\text{NO}_3)_2$), in 0.5 M nitric acid (Spectrosol). Other standards were prepared daily in 0.05 M Q-HCl by serial dilution.

4.2.1.4 Acids/Ammonia

Q-HCl, 9 M was prepared as specified in Chapter 2. Nitric acid (HNO_3 , Aristar; Merck BDH, 15.5 M) was used as received. A working Q- NH_3 solution (0.6 M) was prepared by diluting 25 ml stock (ca. 6 M) to 250 ml with UHP water.

4.2.1.5 HCl Carrier/Eluent

The eluent solution for the TCNQ-O₂-OH-Eosin Y system (0.0025 M) was prepared by diluting 10 ml of Q-HCl (0.25 M) to 1000 ml with UHP water.

4.2.1.6 Acid wash

An acid wash solution (0.6 M Q-HCl / 0.16 M HNO₃) was prepared by diluting 7 ml of Q-HCl (9 M) and 1 ml of HNO₃ (15.5 M) to 100 ml with UHP water.

4.2.2 Instrumentation

A description of the individual components of the FI systems is contained in Chapter 1. The manifold built for the luminol-hydrogen peroxide reaction is shown in Figure 4.1. Figure 4.2 shows the manifold used for the TCNQ-O₂-OH-Eosin Y system. For both systems two peristaltic pumps (Gilson Minipuls 3) were used to deliver the UHP water, sample/buffer and reagents solutions, respectively, to the injection valve, preconcentration column and CL detector. All manifold tubing was PTFE (0.75 mm i.d., Fisher) except for the peristaltic pump tubing, which was flow-rated PVC ("Accu-rated", Elkay), and the 8-HQ columns.

A six-port rotary injection valve (Rheodyne, HPLC technology) was used to deliver the sample to the PMT. A quartz glass spiral flow cell (identical to the one used for the Co system) positioned in a light-tight housing enabled the CL reaction to be monitored. The detection system has been previously described in Section 3.2.2.

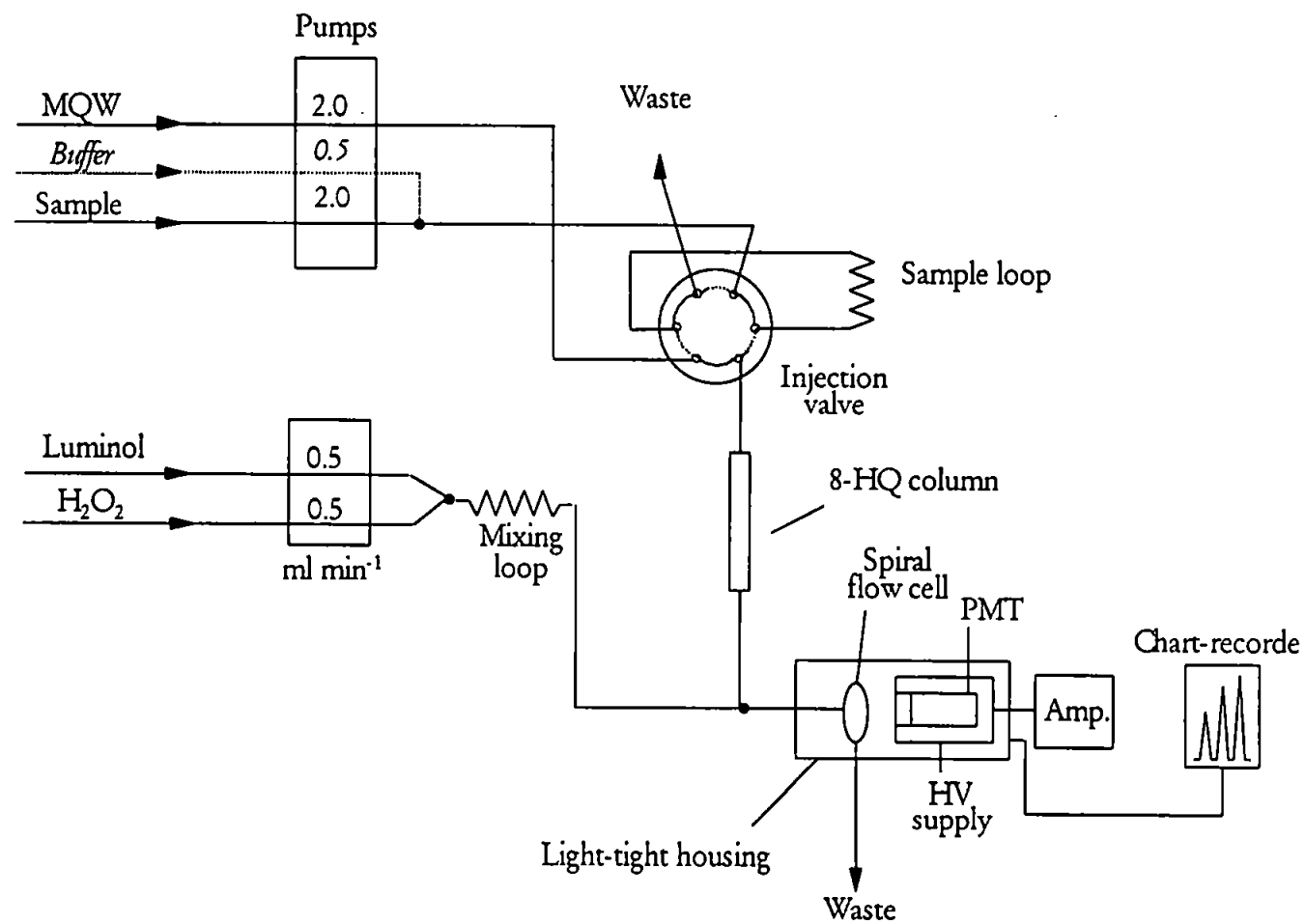


Figure 4.1: FI-CL manifold for the determination of Mn(II) with the luminol-hydrogen peroxide system

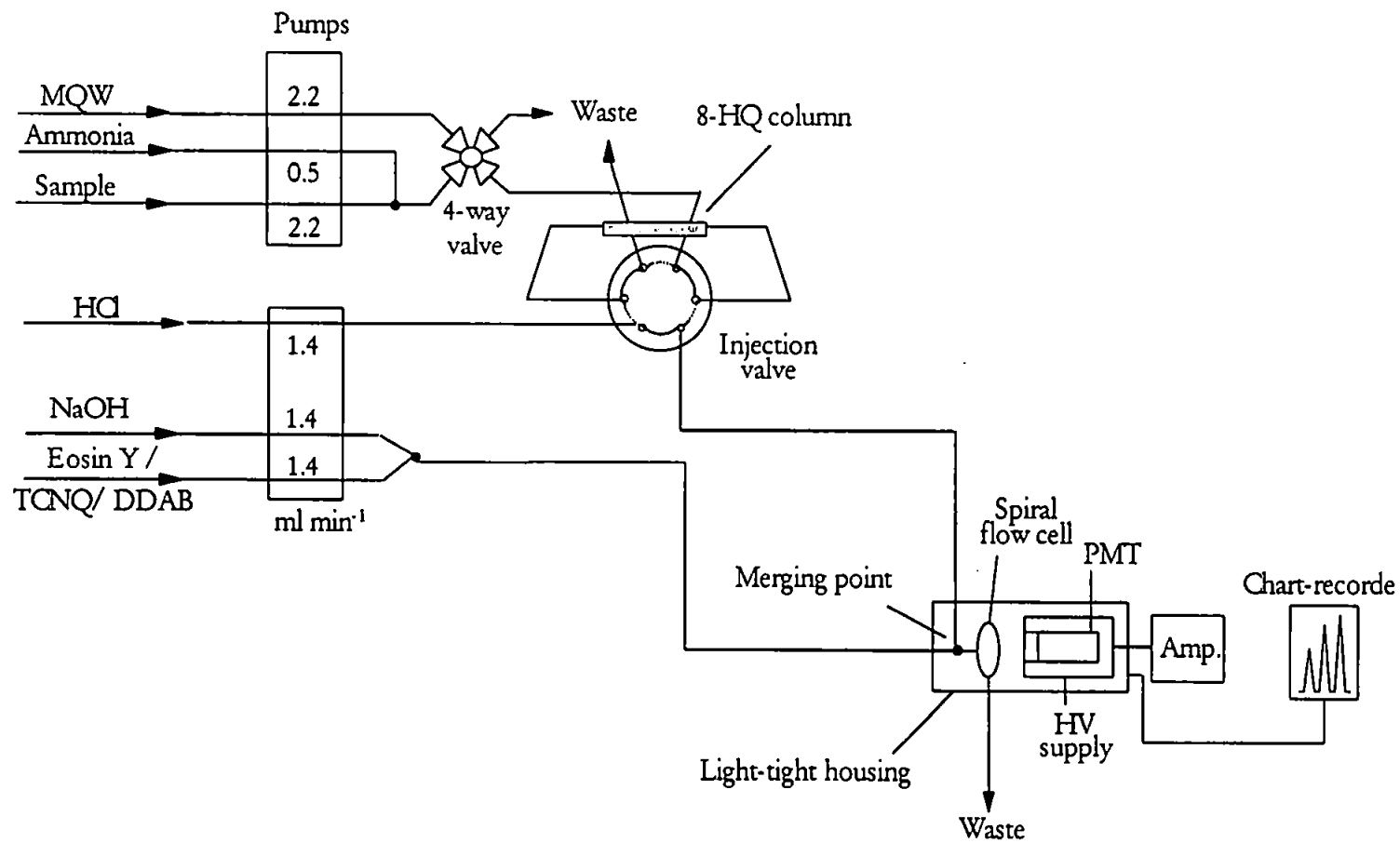


Figure 4.2: FI-CL manifold for the determination of Mn(II) with the TCNQ-O₂-OH-Eosin Y system

4.2.3 Operating procedures for the luminol-hydrogen peroxide system

In this system the operating procedure was different from the usual FI procedure due to the absence of any preconcentration/matrix removal step.

1. Initially the injection valve is in LOAD position. The sample is loaded into the sample loop in less 10 s and the excess is directed into the waste. UHP water runs continuously through the system *via* the injection valve.
2. By switching the injection valve into the INJECTION position (for 30s) UHP water is redirected into the sample loop flushing the sample into the system. The sample passes through the column, which retains all metal ions except Mn(II).
3. The injection valve is then switched to the LOAD position and before a new sequence commences the column is washed with HNO₃/HCl for 15 s and equilibrated for 30 s with the buffer at pH 5.5.

4.2.4 Operating procedures for the TCNQ-O₂-OH-Eosin Y system.

One analytical cycle is completed in 26 min (n=3) with 6 min of preconcentration time and 30 s for the detection-elution period. So the time for sample quantification is ca. 78 min (n=3).

1. Initially the 4-way valve (LOAD position) allows the seawater sample to be pumped into the column for 6 min at pH 8 (by ammonia solution). Longer seawater load times can be used, but this would lead to incomplete recovery.
2. By switching the 4-way valve (into position two) UHP water was subsequently passed through the column (60 s) to remove any residual sea-salt matrix ions present. Interfering metal ions can also be removed by masking agents mixed with the UHP water (at the same time the tube was

introduced into the new sample to remove the previous solution from the flow line).

3. The injection valve was then switched to the INJECT position and 0.0025 M Q-HCl flowed through the column in a reverse direction for 45 s, carrying the Mn(II) to the detection system where it mixed with the CL reagent stream and generated a CL peak.
4. The injection valve was then returned to the load position and UHP water was pumped through the column (60 s) to remove residual hydrochloric acid.
5. Finally the 4-way valve was returned to position one and the column was washed with HNO₃/HCl for 20 s to avoid any memory effect.

4.3 RESULTS AND DISCUSSION

4.3.1 Luminol-hydrogen peroxide chemiluminescence reaction

CL detection using a luminol-hydrogen peroxide system was thought to be a promising method for the sensitive and shipboard determination of various metal ions. The intensity of CL emission with this system is proportional to the concentration of metal ions over a wide range from sub ng l⁻¹ to ng l⁻¹ (Seitz and Hercules, 1973). Luminol was discovered in 1928 by Albrecht. The luminol CL reaction allows the determination of either the oxidising species (most commonly hydrogen peroxide), organic compounds which can generate the oxidising species (e.g. haeme-containing enzymes, peroxidase), the catalyst, which can be a metal ion such as Co(II), Fe(II) or Cu(II), or species which quantitatively suppress the CL emission (e.g. ammonia) (see Table [Error! Not a valid link.](#)).

Table 4.3: The triggering of luminol chemiluminescence (Campbell, 1988)

Condition	Analyte
1. Oxidant alone	O ₂ , O ₃ , H ₂ O ₂ , O ₂ ⁻ , OCl ⁻ , KO ₂ , K ₂ S ₂ O ₈ , NIO ₄ , NOCl, DMSO, OsO ₄ , BO ₄ ⁻
2. Catalyst + O ₂	Fe ²⁺ , Co ²⁺ , t-butoxide, Br ₂ , I ₂ , Fe(CN) ₆ ³⁻ , MnO ₄ ⁻ , DMSO
3. Catalyst + H ₂ O ₂ /OH ⁻ (pH 10-13)	
(a) free transition metal cations	Fe ²⁺ , Fe ³⁺ , Co ²⁺ , Ni ²⁺ , Cu ²⁺ , Hg ²⁺ , Cr ³⁺ , Mn ⁴⁺ , V ⁴⁺
(b) transition metal anion complexes	Fe(CN) ₆ ³⁻ , MnO ₄ ⁻ , AuCl ₄ ⁻ , SbCl ₆ ⁻
(c) transition metal cation complexes	UO ₂ ²⁺ , Cu(NH ₃) ₆ ²⁺ , VO ₂ ⁺
(d) free porphyrins	coproporphyrin
(e) porphyrin Fe ³⁺	protohaem, haematin, deuterio-haematic, other modified haematin
(f) haemoproteins	haemoglobin, myoglobin, catalase, peroxidases, cytochrome c
(g) other Fe ³⁺ proteins	ferritin
(h) corrins	vitamin-B ₁₂
4. Enhancers	benzothiazoles (e.g. firefly luciferin on peroxidase), iodophenol at pH 8
5. Inhibitors	Ce ⁴⁺ , Th, Zr ²⁺ , cysteine, tris, CN ⁻ , bicine, albumin, serum, EDTA

Luminol CL methods for Fe, Co, Mn and Cu have particularly low detection limits, at the low nanomolar level (Alwarthan et al., 1990; Alwarthan and Townshend, 1987; Klopff and Nieman, 1983; Seitz and Hercules, 1973). The commonest oxidant has been hydrogen peroxide in alkaline condition, but added oxidant is not always necessary. Seitz and Hercules (1973) determined Fe(II) by its catalysis of luminol chemiluminescence in the absence of added oxidant, the oxidant being assumed to be dissolved oxygen.

The predicted mechanism of luminol oxidation (Figure 4.3) reported by Merényi et al. (1990a, 1990b) is believed to involve two steps; firstly, a nucleophilic addition to the carbonyl group, followed by breakdown of the formed α -hydroxy hydroperoxide intermediate.

Specifically, Mn(II) catalyses the decomposition of H₂O₂ to produce the hydroxyl radical, HO[•]. The resulting hydroxyl radical is thought to rapidly oxidise luminol in the presence of O₂ and/or active oxygen species to produce

(Muto et al., 1970). The anion radical $\text{TCNQ}^{\cdot -}$ has got characteristic bands at about 420-440, 750 and 850 nm (Muto et al., 1970, Muto et al., 1971). The 470 nm band is caused by the charge transfer complex formed between neutral TCNQ trapped within the hydrophobic bilayer membrane, and the bromide counter anions of the surfactant.

The addition of NaOH to the TCNQ-DDAB solution leads to the appearance of a new absorption band at about 345 nm in place of the disappearance of the 470 nm band (Yamada et al., 1985), but does not affect the $\text{TCNQ}^{\cdot -}$ bands. In the two-step reaction shown in Figure 4.4 the nucleophilic addition of OH^- on the carbon α of TCNQ (which is a strong electron acceptor, as a result of the cumulative electron withdrawal by the four CN groups) produces the hydrolysis product α, α -dicyano-*p*-toluoylcyanide (DCTC^-) (Kryszewski et al., 1981) which readily reacts with dissolved O_2 in alkaline environment to emit light and produce α, α -dicyano-*p*-benzoic acid.

This species is the final reaction product, with the absorption band at 345 nm. In the Mn(II)-catalysed CL reaction the decrease in the $\text{TCNQ}^{\cdot -}$ band intensity also causes an increase in the absorption band at approximately 345 nm; the changes in both band intensities depend on the Mn(II) concentration added. Hence, one can conclude that Mn(II) works catalytically on $\text{TCNQ}^{\cdot -}$ in alkaline solution to ultimately yield α, α -dicyano-*p*-benzoic acid *via* the formation of the α, α -dicyano-*p*-toluoylcyanide anion. The catalytic activity of Mn(II) is due to the stabilisation of the radical species via the vacant d-orbital. This reaction mechanism for the chemiluminescent reaction is illustrated in Figure 4.5 (Bowie et al., 1995).

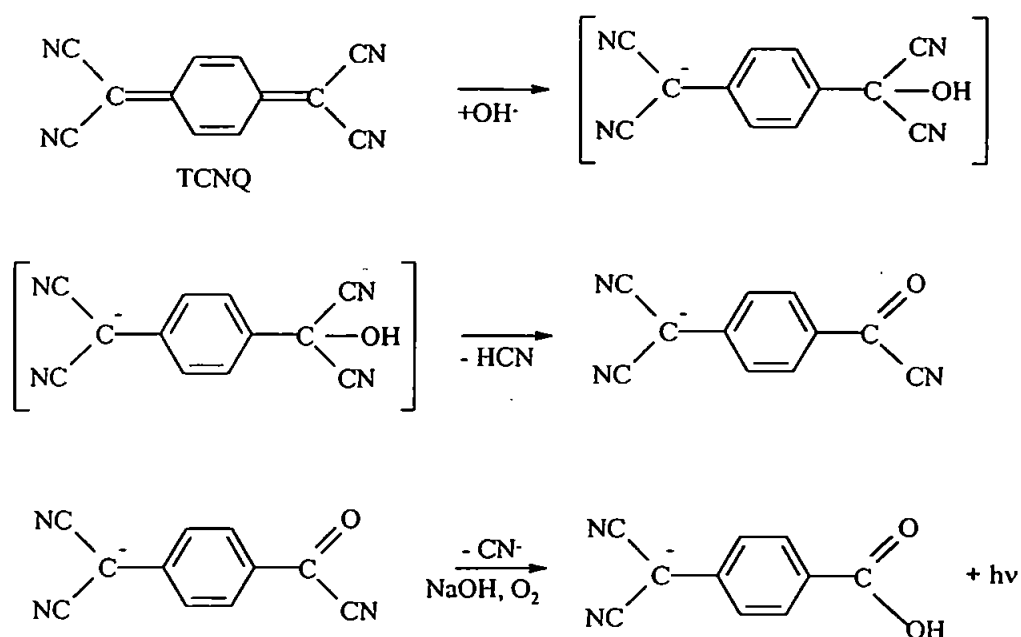


Figure 4.4: Reaction scheme of neutral TCNQ with NaOH

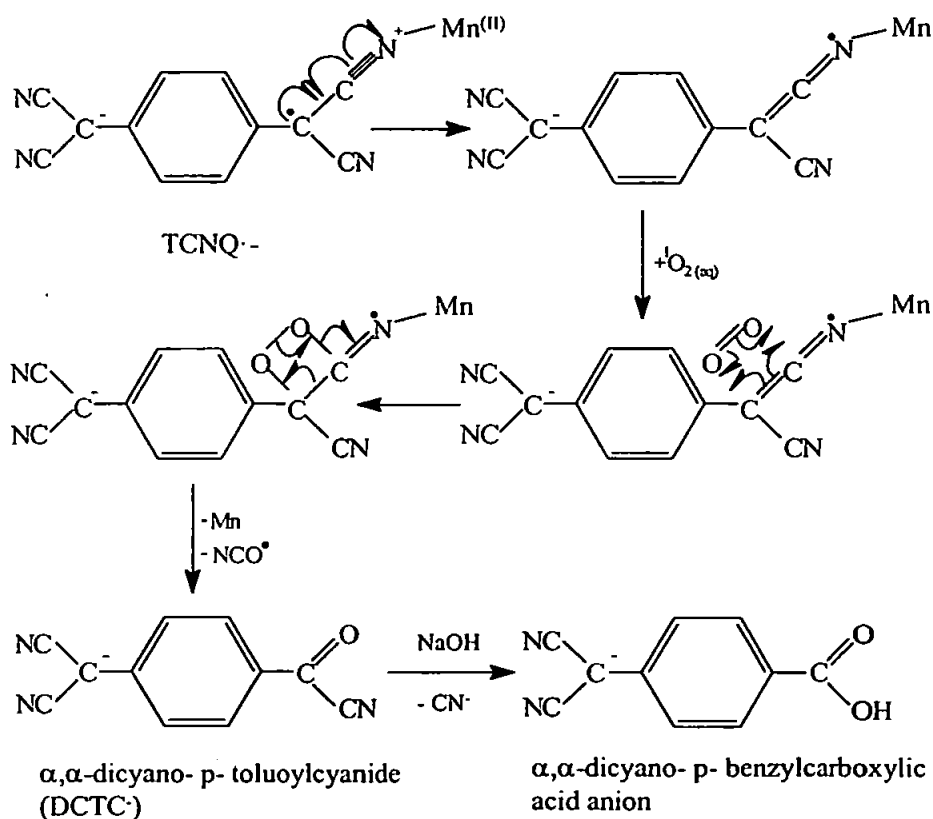


Figure 4.5: Reaction scheme of the TCNQ anion radical, $\text{O}_{2(\text{aq})}$, and $\text{Mn}(\text{II})$.

4.3.3 Optimisation of the luminol-hydrogen peroxide system

Due to the many physical and chemical variables, the optimisation procedure was carried out univariately. The optimum values found in the literature (Chapin et al., 1991; Okamura et al., 1998) were utilised as a starting point for the optimisation procedure. For all the plots error bars represent 2s unless stated otherwise.

Okamura et al., (1988) used the following parameters for the determination of Mn in seawater at nanomolar levels (see Table 4.4).

Table 4.4: Optimised parameters for the determination of Mn in seawater with 8-HQ column

Variables	Working conditions
PMT	Room temperature
Flow rate sample stream	2.4 ml min ⁻¹
Flow rate CL reagents stream	0.6 ml min ⁻¹
Temperature reaction coil	20 °C
Reaction coil length	6.1 m
Luminol	1 mM
Reaction pH	9.5
TETA	1.0 mM
Hydrogen peroxide	1.0 M
Carrier	UHP water
LOD	0.03 nM

Okamura et al. (1998) utilised as a starting point for the optimisation procedure. All the univariate experiments (all parameters except one remain constant) were carried out to achieve the optimum working conditions (Mn was 1.82 nM in all experiments). Each optimum value was recorded for further optimisation experiments. The chemical noise has been reported in all the plots.

All the variables were evaluated without using a preconcentration column. Each variable was optimised sequentially and for subsequent experiments optimised

settings were used as found. For all the plots presented in this chapter error bars represent 2s unless stated otherwise.

4.3.3.1 Flow rate

For the CL reagents it is important to keep the same flow rate for both streams to achieve the best mixing. However it is not possible to prepare one solution containing all CL reagents due to a rapid degradation of the mixture. In this system the luminol and H_2O_2 streams flow rates were matched. For method development, an operating flow rate of 0.8 ml min^{-1} was selected for luminol and H_2O_2 and an operating flow rate of 2.5 ml min^{-1} for the carrier/sample stream (Figure 4.6).

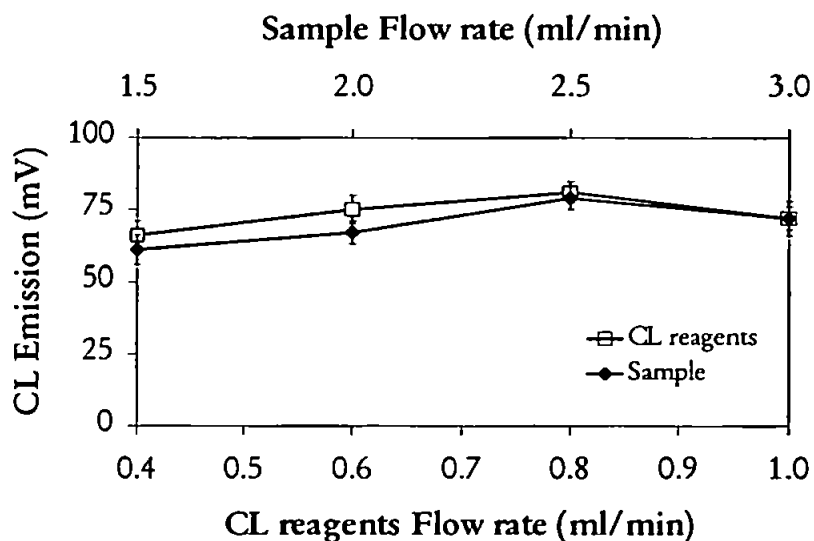


Figure 4.6: Effect of flow rate on CL emission for the sample stream and the CL reagents stream.

4.3.3.2 Sample loop volume

The highest CL emission was achieved with an 80 μL sample loop (182 mm of PTFE tube with 0.75 mm of i.d.) (Figure 4.7). The sample loop has been replaced by the 8-HQ column in the final operating system. Also in this system higher volumes increased the sample dispersion in the CL system generating double peak.

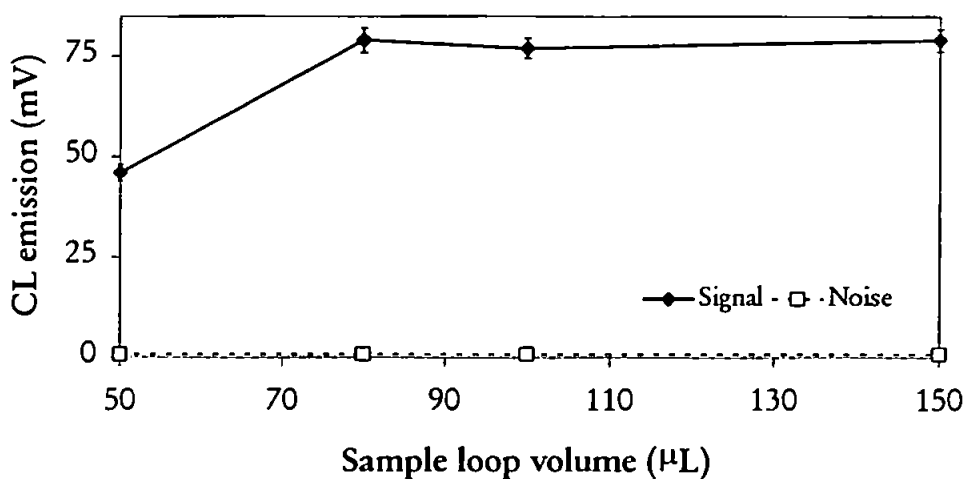


Figure 4.7: Effect of injection loop volume on CL emission

4.3.3.3 Reaction pH

Since luminol CL depends significantly on the reaction pH, it is important to conduct the reaction at the optimum pH. In this system, adjusting the pH of the luminol solution controlled the final reaction pH. Taking into account the fact that Mg(II) deposits as Mg(OH)_2 at pH values > 9.75 , a final pH of 9.3 was chosen as giving the highest CL signal without the risk of precipitation blocking the detector (Figure 4.8).

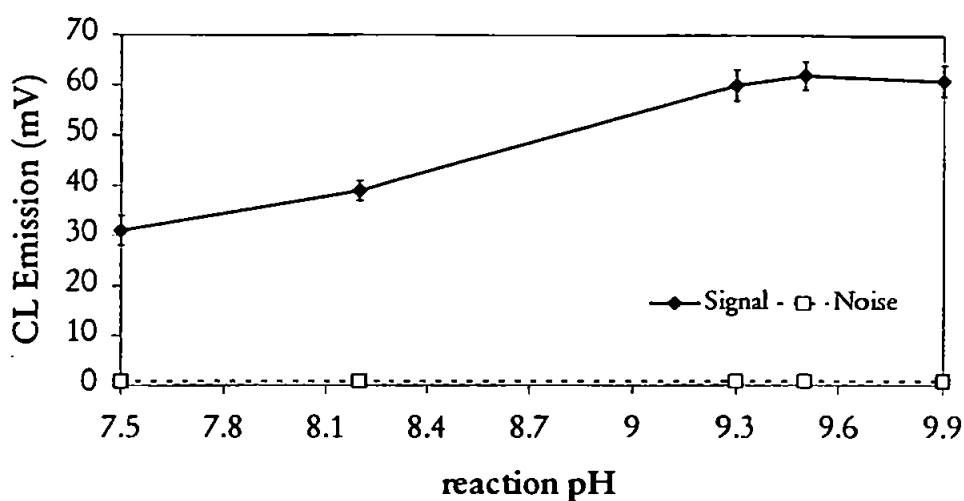


Figure 4.8: Effect of reaction pH on CL emission

4.3.3.4 Hydrogen peroxide concentration

As shown in the plot of CL emission vs. H_2O_2 concentration (Figure 4.9), the signal CL was nearly constant in the range 1-2 M, so a 1 M concentration of hydrogen peroxide was chosen as the optimum in order to compromise between signal intensity and reagent consumption.

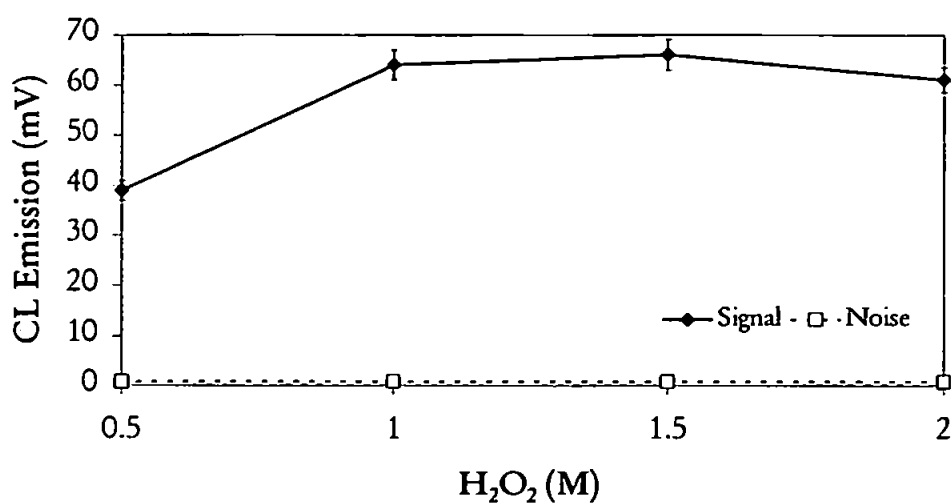


Figure 4.9: Effect of hydrogen peroxide concentration on CL emission.

4.3.3.5 Luminol concentration

Luminol is a critical reagent in this system because an increase in luminol concentration led to an increase in both the signal and baseline CL. The concentration for this system was set at 1 mM where the signal/noise ratio was a maximum (Figure 4.10). Any small variation in luminol concentration led to an evident variation in the noise. To highlight this feature the plot reports S/N.

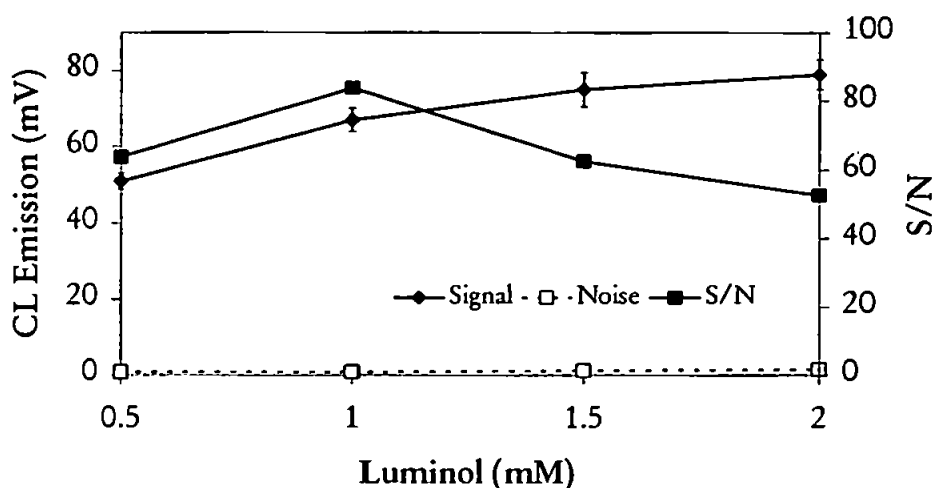


Figure 4.10: Effect of luminol concentration on the signal and baseline CL intensities.

4.3.3.6 TETA concentration

TETA is one of the most common activators of the luminol CL system (Nakayama et al., 1989; Obata et al., 1993). The optimum concentration was found to be 1 mM and was used for routine operation (both signal and baseline CLs were enhanced linearly with increasing TETA concentrations, see Figure 4.11). Again any small variation in luminol concentration led to an evident variation in the noise. To highlight this feature the plot reports S/N.

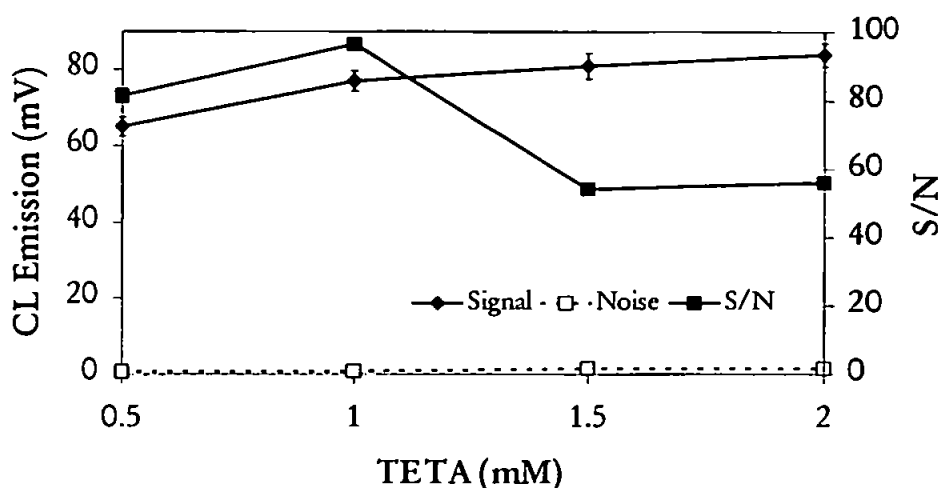


Figure 4.11: Effect of TETA concentration on the signal and baseline CL intensities.

4.3.3.7 Variation of Luminol sensitivity over time

In order to assess the sensitivity of luminol reagent over time, the signal obtained by a 1.82 nM Mn(II) standard was monitored over a period of 4 d. Optimum reaction conditions were used; the luminol concentration was 1 mM in 0.1 M carbonate buffer with a reaction pH = 9.5. Figure 4.12 indicates that the luminol working solution was most active ca. 24 – 45 h after preparation so all working solutions were freshly prepared 1 d prior to use.

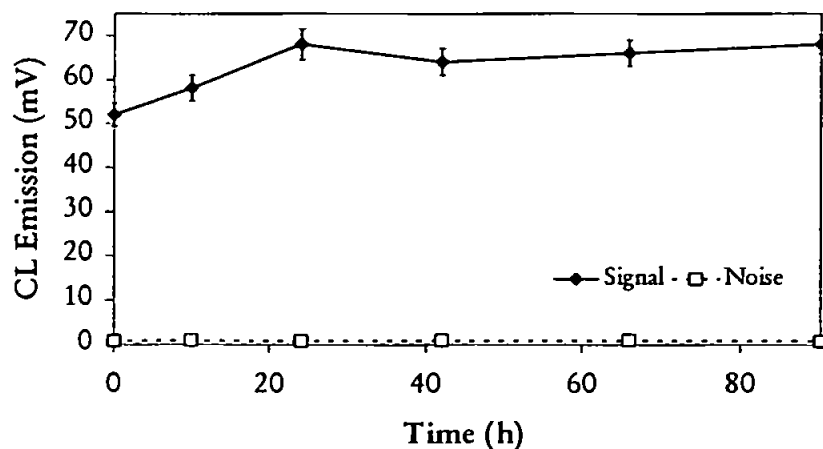


Figure 4.12: Variation in sensitivity of luminol reagent with time

4.3.3.8 Interferences

The luminol hydrogen-peroxide method, however, lacks selectivity and other metals such as Fe, Co, and Cr interfere with the determination of manganese (Nakayama et al., 1989). Therefore, a selective trace metal removal step is required for seawater analysis that can be achieved using an 8-HQ column. However when the method is applied to marine water samples the matrix (the alkaline earth metals) interferes severely with the reaction (see Figure 4.13a), and this manifold configuration does not allow the removal of the seawater matrix. Moreover the buffer necessary to achieve the correct sample pH for trapping all the interfering metals on the column and not retain Mn(II) interferes with the reaction (see Figure 4.13b,c,d). Many buffers have been examined (see Table 4.1) and most of them showed a quenching effect in the luminol emission and the acetate buffer showed a mixed effect: quenching of the reaction and formation of double peaks. The reason of the quenching phenomenon is the ability of the buffer anions to partially complex the transition metal ions (Mn(II) in this case). This will give rise to suppression of CL emission from the luminol reaction by preventing these ions from catalysing the reaction. Figure 4.13 shows an example of the responses obtained for solution containing Ca(II) and Mg(II) at seawater level (a), acetate buffer (b), citrate buffer (c), and succinate buffer (d).

This approach is therefore not suitable for the determination of Mn(II) in seawater and an alternative approach was evaluated using the luminous oxidation of TCNQ by dissolved O₂ sensitised by Eosin Y in DDAB.

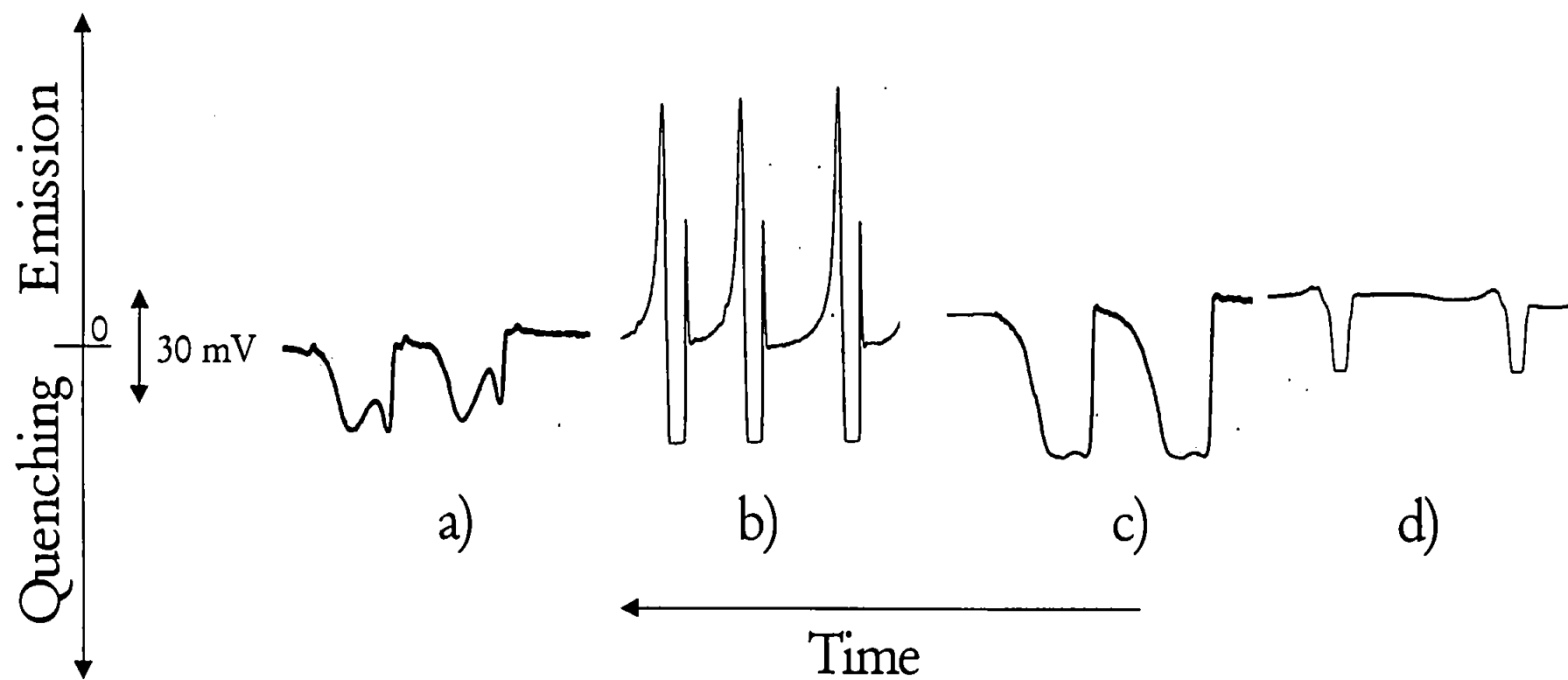


Figure 4.13: CL response of a) seawater matrix, b) acetate buffer, c) citrate buffer, d) succinate buffer.

4.3.4 Optimisation of the TCNQ-O₂-OH-Eosin Y system.

Chapin et al. (1991) used the following parameters for the determination of Mn(II) in seawater at nanomolar levels (see Table 4.5).

Table 4.5: Optimised parameters for the determination of Mn in seawater with 8-HQ column.

Variables	Working conditions
PMT	- 15 °C
Sample stream flow rate	2.7 ml min ⁻¹
CL reagents stream flow rate	1.3 ml min ⁻¹
TCNQ	0.25 mM
Eosin Y	0.3 mM
Surfactant (DDAB)	0.4 mM
Reaction pH (adjusted with NaOH)	> 11
Preconcentration time	4 min
LOD	0.1 nM
Carrier (HCl)	0.0025 M

This FI-CL system has also been optimised univariately. The optimum values found by Chapin et al. (1991) were utilised as a starting point for the optimisation procedure. The concentration of the carrier (HCl 0.0025 M), was not considered in the optimisation, due to it being reported that a molarity of 0.0025 M represents the optimum concentration to elute manganese from the column in the smallest possible volume of acid (Chapin et al., 1991). All the univariate experiments (all parameters except one remaining constant) were carried out to achieve the optimum working conditions (Mn was 50 nM in HCl 0.0025 M in all experiments). Each optimum value was used for subsequent optimisation experiments. The chemical noise has not been reported in the plots because was constant in all experiments (0.0375 mV). All the variables were evaluated without using a preconcentration column. Each variable was optimised sequentially and for subsequent experiments optimised settings were

used as found. For all the plots presented in this chapter error bars represent 2s unless stated otherwise.

4.3.4.1 Flow rate

The optimum flow rates for sample/carrier and CL reagents are shown in Figure 4.14. A flow rate of 2.2 ml min⁻¹ and 1.4 ml min⁻¹ has been chosen for the sample stream and the reagent streams respectively. Even in this system it is not possible to prepare one solution containing all the CL reagents due the instability of the mixture. Four lines have been used: one for the CL reagent denominated R₁ containing TCNQ, DDAB, and Eosin Y one for the NaOH solution and the other two for the eluent and the sample stream.

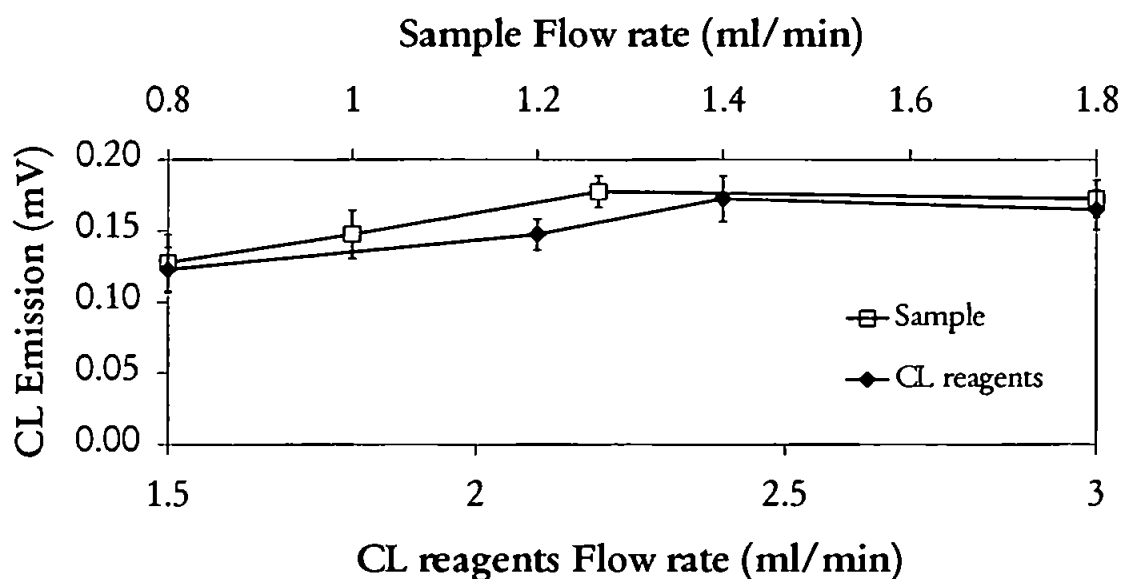


Figure 4.14: Effect of flow rate on CL emission for the sample stream and the CL reagents stream.

4.3.4.2 *Sample loop volume*

An injection volume of 180 μL was selected to deliver the maximum response (Figure 4.15). The 8-HQ column in the final operating system replaced the sample loop.

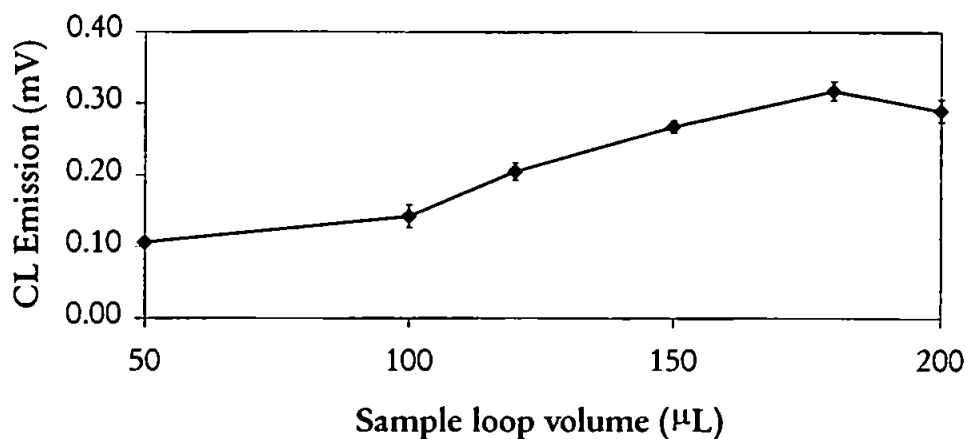


Figure 4.15: Effect of injection loop volume on CL emission

4.3.4.3 *DDAB, Eosin Y and TCNQ concentrations*

Yamada et al. (1985) showed that TCNQ as a CL reagent is only solubilised in organised assemblies which cationic surfactant molecules form. The weak CL arising from the Mn(II)-catalysed oxidation of TCNQ by dissolved O_2 in alkaline condition is sensitised by Eosin Y and this phenomenon is further enhanced by means of bilayer vesicles. Various cationic surfactant aggregates for sensitive detection of Mn(II) were examined by Yamada et al. (1985). They showed that in the absence of a sensitiser (such as Eosin Y), organised assemblies did not yield strong Mn(II)-catalysed CL. However, with some organised assemblies, such as DDAB, the CL signal was considerably enhanced by the presence of Eosin Y in

the CL system. The emission being sensitised by ca. 360 times in the DDAB solution compares with other surfactant such as HEAB (Yamada et al., 1985) (see Table 4.6).

Table 4.6: Effect of surfactant aggregates on the CL signal for Mn(II). (For the experimental conditions see Yamada et al., 1985)

Cationic surfactant	Concentration/ 10 ⁻³ M	CMC/ 10 ⁻³ M	Relative CL signal without any sensitiser	Relative CL signal with Eosin Y
HEAB [C ₁₆ H ₃₃ (C ₂ H ₅)N(CH ₃) ₂]Br	20	Not reported	7.1	36
DDAB [(C ₁₂ H ₂₅) ₂ N(CH ₃) ₂]Br	0.8	0.18	1.0	260

It is known that surfactant molecules with two long-chain alkyl groups such as DDAB form bilayer aggregates (vesicles) rather than micelles (Kunitake et al., 1977). Such vesicular aggregates of the bilayer membrane exhibit higher organisation, stability, and rigidity than micellar aggregates do, resulting in the occurrence of more effective energy transfer to the sensitizer (Nikokavouras et al., 1981).

The optimum concentration for DDAB, Eosin Y and TCNQ are shown in Figure 4.16, Figure 4.17 and Figure 4.18 respectively.

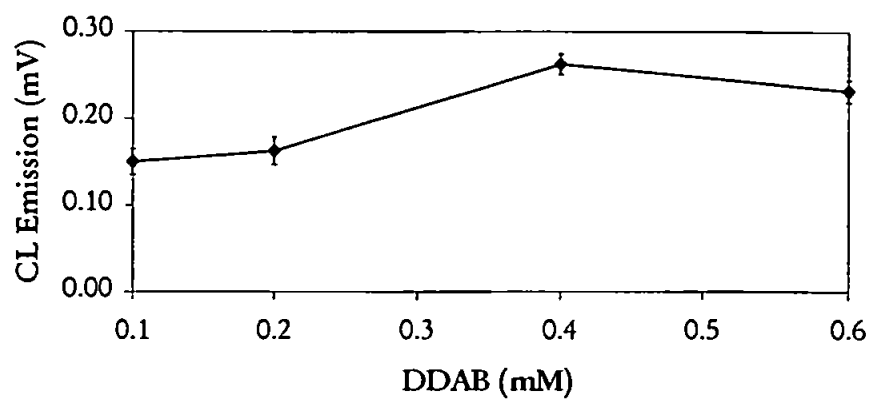


Figure 4.16: Effect of DDAB surfactant aggregate on the CL signal

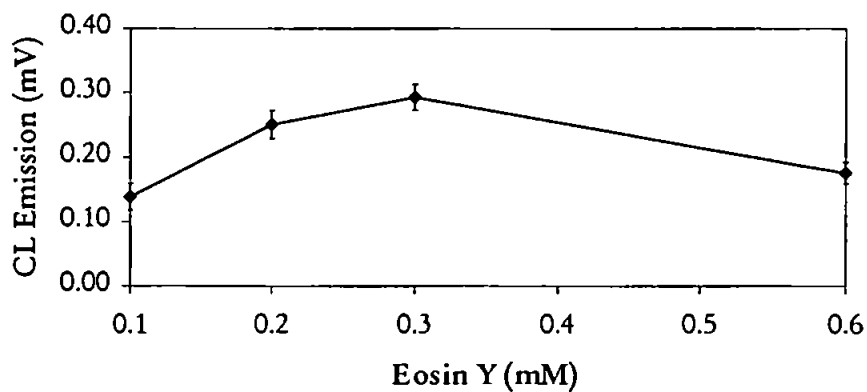


Figure 4.17: Effect of Eosin Y sensitizer on the CL signal

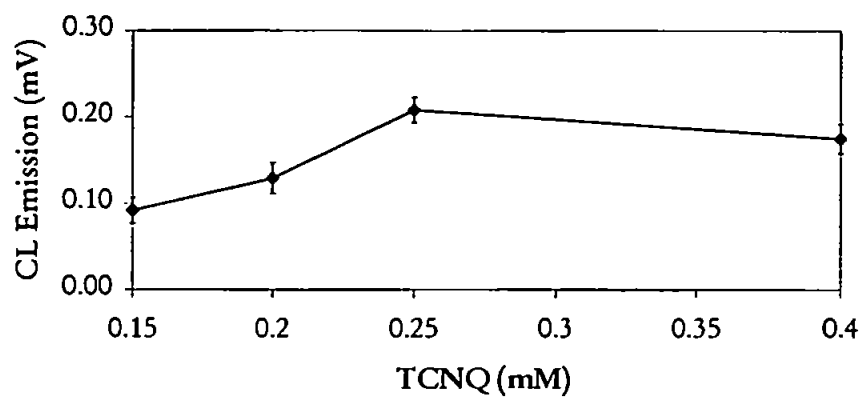


Figure 4.18: Effect of TCNQ on the CL emission

4.3.4.4 Reaction pH

The chemiluminescence efficiency was dependent on the reaction pH. Control of the final reaction pH was achieved by adjusting the sodium hydroxide concentration. As previously reported (Bowie et al., 1995; Chapin et al., 1991) a minimum pH of 11 was required in the flow cell to produce chemiluminescence. The same result has been found in this optimisation work. (Figure 4.19)

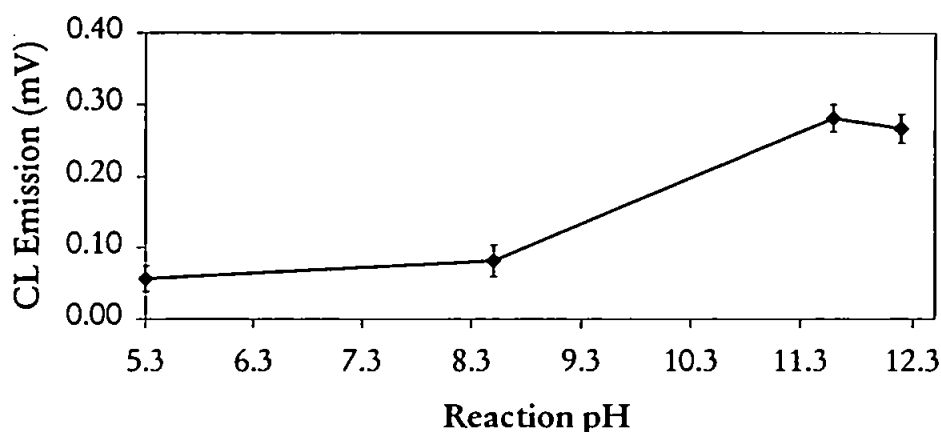


Figure 4.19: Effect of reaction pH on the CL emission

4.3.4.5 Variation of TCNQ-DDAB-Eosin Y solution stability over time

In order to assess the stability of TCNQ-DDAB-Eosin Y solution reagent over time, the signal obtained by a 50 nM Mn(II) standard was monitored over a period of 3 d. Optimum reaction conditions were used; the TCNQ concentration was 0.25 mM; the DDAB concentration was 0.40 mM and the Eosin Y concentration was 0.30 mM. Figure 4.20 shows that the TCNQ-DDAB-Eosin Y solution was stable only for 48 h after preparation. After this period of time a black precipitate was observed in the reaction flask due to the decomposition of the mixture.

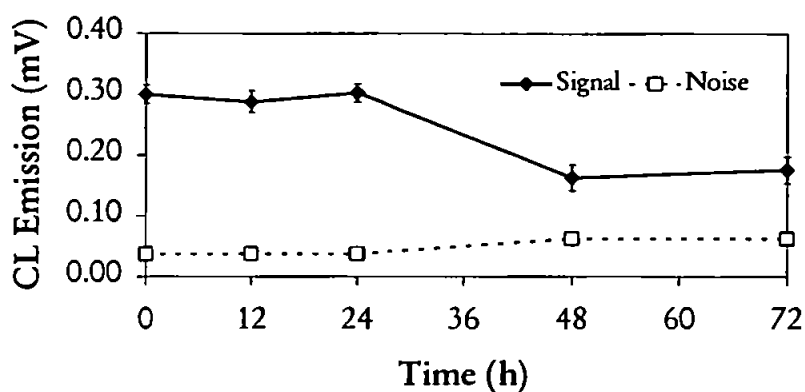


Figure 4.20: Variation in stability of TCNQ-DDAB-Eosin Y solution with time

4.3.4.6 Optimised TCNQ- O_2 -OH-Eosin Y system

Table 4.7 shows the values utilised for further experiments and field trials.

Table 4.7: Optimised parameters for the system without 8-HQ column for the determination of Mn in seawater with TCNQ- O_2 -OH-Eosin Y.

Variables	Working conditions
PMT	Room temperature
Sample stream flow rate	2.2 ml min ⁻¹
CL reagents stream flow rate	1.4 ml min ⁻¹
TCNQ	0.25 mM
Eosin Y	0.3 mM
Surfactant (DDAB)	4 mM
Reaction pH (adjusted by NaOH)	11.3
Sample loop volume	180 µl
Carrier (HCl)	0.0025 M

4.3.4.7 *Calibration graph and Limit of Detection (LOD) without the 8-HQ column for the TCNQ-O₂-OH-Eosin Y system*

The mixing of reagent solutions through the manifold generated a chemical noise emission as already shown in Figure 3.17. In order to accurately quantify the amount of Mn(II) from the CL peaks and the LOD, it is necessary to define the components of the peaks and noise. In the TCNQ-O₂-OH-Eosin Y system the noise is composed of two contributions as expressed in:

$$N = N_{\text{Electronic}} + N_{\text{CL reagents}}$$

where N_E is the electronic noise of the PMT and $N_{\text{CL reagents}}$ is the noise due to the Mn contained in the CL reagents and/or to the natural chemiluminescence emission of the CL reagents (TCNQ, NaOH, DDAB and Eosin Y). For the determination of Mn the limiting factor for the LOD is $N_{\text{CL reagents}}$ (N_E was negligible compare with $N_{\text{CL reagents}}$ so $N \cong N_{\text{CL reagents}}$). The noise baseline due only to the Mn in the CL reagents (and/or to the natural chemiluminescence emission of the CL reagents) was 0.0375 mV.

The Mn signal (Mn^*) can be expressed as:

$$Mn^* = Mn_{\text{SW}} + Mn_{\text{UHP}} + Mn_{\text{Ammonia}} + (Mn_{\text{HCl}}) + Mn_{\text{Masking agents}}$$

where Mn_{SW} is the analyte signal, Mn_{UHP} is the Mn contained in the UHP water, Mn_{Ammonia} is the Mn impurity in the ammonia, and Mn_{HCl} is the Mn impurity in the HCl used to acidify any seawater samples stored for later analysis, and $Mn_{\text{Masking agents}}$ is the Mn impurity in the masking agents that can be used to mask the interference of other trace metals.

If we assume that Mn_{HCl} is zero (as it is for many metals, due to the use of Q-HCl), the main efforts to lower the LOD have to be focused on Mn_{UHP} , $Mn_{Ammonia}$, and $Mn_{Masking\ agents}$. In the TCNQ- O_2 -OH-Eosin Y system reported here, the contributions of Mn_{UHP} , $Mn_{Ammonia}$, and $Mn_{Masking\ agents}$ are negligible due to the low amount of Mn present. So it is possible to assign $Mn^* = M_{NSW}$ signal due only to the analyte in the sample ($Mn_{UHP} + Mn_{Ammonia} + Mn_{HCl} + Mn_{Masking\ agents} \cong 0$) and state that the signals obtained are due only to the Mn(II) contained in the sample. It is possible to use the value of 0.0375 mV for $N_{CL\ reagents}$ to determine the LOD of the TCNQ- O_2 -OH-Eosin Y system and this value was taken as the blank signal.

When a concentration $> 1400\ nM$ Mn(II) was used, the calibration graph deviated from a straight line. This is a common phenomenon with CL signals and in this case is due to the increasing self quenching deep-red coloured Eosin Y (Bowie et al., 1995). The calibration graph for Mn in the optimised system without a column is shown in Figure 4.21 and was linear in the concentration range 50-1400 nM ($r^2 = 0.9977$, RSDs $< 7\%$, $n = 3$, and LOD of 30 nM).

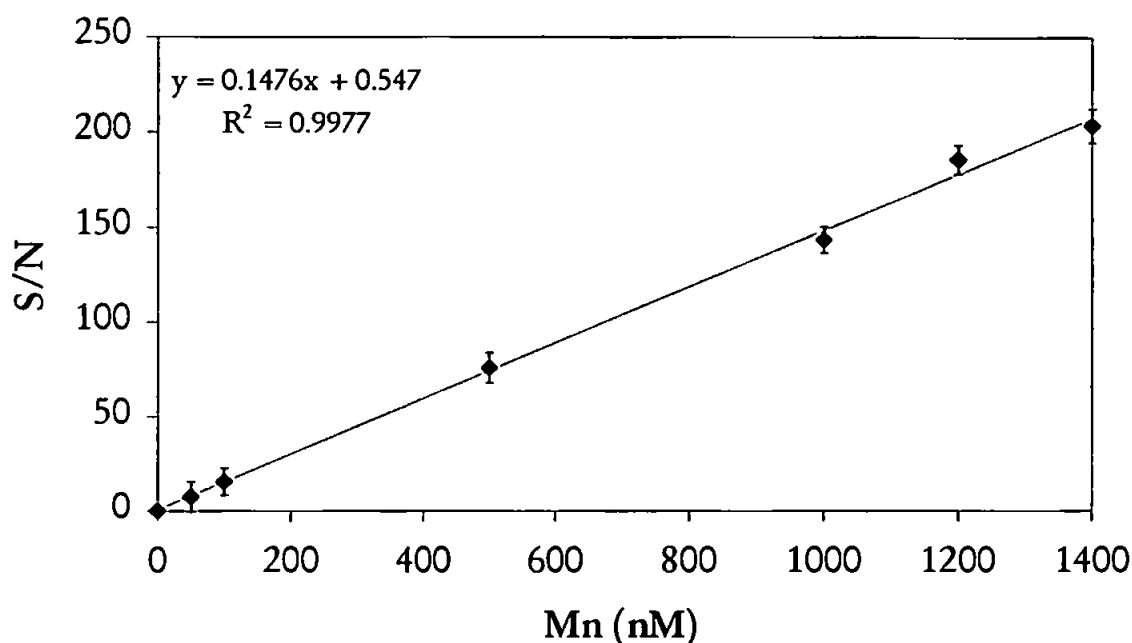


Figure 4.21: Calibration graph in the range 50–1400 nM of Mn(II) in acidified UHP water

4.3.4.8 Interference studies for the TCNQ- O_2 -OH-Eosin Y reaction

Most solution CL methods suffer from poor selectivity. In addition to Mn(II), other trace metals (such as Fe(II), Fe(III), Mg(II), Mo(VI), and Cu(II)) are known to catalyse the TCNQ- O_2 -OH $^\cdot$ system (Bowie et al., 1995; Chapin et al., 1991; Yamada et al., 1985). These interfering species act to alter the apparent quantitative relationship between the observed luminescent power and analyte concentration.

The iron(II) interference in the manganese determination is a common problem due to the similarities of the chemistries of the two transition elements involved. Hydes (1987) suggested that the addition of EDTA to a manganese-formaldoxime complex helps to remove iron interference. 1,10-phenanthroline has also been proposed as a reagent that will selectively complex with the interferents, including Fe(II). However Fe(II) interference is generally not a problem in the analysis of well oxygenated waters because the Fe(II) formed is

rapidly re-oxidised by O_2 , H_2O_2 and other oxidants (half life of the order of 10 min in coastal seawater, pH 8, $T=22\text{ }^\circ\text{C}$; Holland, personal communication). Other researchers (King et al., 1995; Millero et al. 1995a; Millero et al, 1995b; Millero and Sotolongo, 1989) found similar half lives (several minutes, dependent on factors such as pH, temperature, $[Fe]$, $[oxidant]$) in seawater based on model calculations and experimental measurements. Emmenegger et al. (1998) reported even lower values ranging between 7 and 60 s. Chapin et al. (1991) suggested the use of DFAM (a siderophore) to remove the interfering iron(III) from the manganese analyses. The iron-specific chelating agent desferrioxamine was first suggested by Perrin (1970), and used by Chin et al. (1992) in the spectrophotometric determination of manganese in natural waters. Desferrioxamines, or sideramines, occur only naturally in bacteria and have three iron binding sites which occupy all six positions around the ferric ion. They have a powerful Fe(III) chelating ability (the thermodynamic formation constant for the Fe(III)-DFAM complex is $10^{30.6}$) with a very weak affinity for complexing Mn(II) (Morel, 1983; Perrin, 1970). Moreover DFAM is specific for Fe(III) but also might masks Fe(II), probably by shifting the equilibrium between Fe(II) and Fe(III) in solution. Mg(II) is generally not accumulated in the 8-HQ resin due to its low stability constant (see Table 2.3). Chapin et al. (1991) found that Mo(IV) at natural seawater levels had a negligible interference with the method because it shows little variability in seawater (Bruland, 1983b). They also suggested that the interference from Cu(II) can be suppressed using tetraethylenepentamine (TEPA) as a complexing agent. This ligand has an extremely high binding constant for copper, ca. seventeen order of magnitude greater than 8-HQ (Martell et al., 1974). TEPA

may be added directly to the sample or to the UHP water rinse to suppress the copper interference.

In order to assess the production of CL by catalysis of the TCNQ-O₂-OH-Eosin Y system for the suspected interferent metals (Fe(III), Mg(II) and Cu(II)) three sets of solutions were prepared containing each interferent singularly. The responses for Fe(III), Cu(II) and Mg(II) were normalised to the Mn(II) response. In Table 4.8 are reported the responses of Fe(III), Cu(II) and Mg(II) at 3 different ranges of concentrations (Mg has been kept constant). Fe(III) was a serious interferent for concentrations higher than 600 nM, and it resulted almost negligible at concentration of 60 nM. Cu(II) and Mg(II) did not interfere. Table 4.9 shows the effect of the addition of DFAM. A DFAM solution which had a concentration of about 20 times that of the Mn(II) present, effectively masked Fe(III), whilst leaving the Mn(II) signal unchanged.

Table 4.8: Investigation of the relative catalytic effect of Fe(III), Cu(II) and Mg(II) upon the proposed CL system.

Species/Concentration	Relative signal (%)
Mn(II) (1000 nM)	102.1
Fe(III) (1000 nM)	25.9
Mg(II) (53 mM)	1.3
Cu(II) (1000 nM)	3.1
Mn(II) (600 nM)	98.6
Fe(III) (600 nM)	16.5
Mg(II) (53 mM)	1.5
Cu(II) (600 nM)	0.0
Mn(II) (60 nM)	99.8
Fe(III) (60 nM)	5.7
Mg(II) (53 mM)	1.1
Cu(II) (60 nM)	0.0

Table 4.9: Effect of the addition of DFAM in the sample on the CL response of Mn(II) and Fe(III).

	Addition of DFAM (1 $\mu\text{mol L}^{-1}$) to the sample	Addition of DFAM (2 $\mu\text{mol L}^{-1}$) to the sample
Species	Relative signal (%)	Relative signal (%)
Mn(II) (1000 nM)	96	93
Fe(III) (1000 nM)	5	0

4.3.4.9 *pH dependence of manganese uptake on the preconcentration column*

Figure 2.12 in Chapter 2 illustrates the retention of Mn ions on a 8-HQ column as a function of sample pH. Mn(II) was quantitatively retained from seawater at pH 7.8, consistent with a theoretical treatment for the effect of pH on metal – 8HQ complexes (Zuehlke and Kester, 1985). Seawater can therefore be loaded directly from sampling points at natural pH (ca. 8). For acidified seawater samples (pH ca. 2) the pH was adjusted in-line using ammonia immediately prior to chelation onto the 8-HQ column. This resulted in a final sample pH of 8.0.

4.3.4.10 Calibration graph and LOD with the 8-HQ column using the
TCNQ-O₂-OH-Eosin Y system

The calibration graph for the optimised system in UHP incorporating an 8-HQ column was linear in the concentration range 5-100 nM with RSDs (n=3) of 3.4-5.9% (Figure 4.22). The limit of detection in acidified UHP water (as 3s) was 3 nM using a preconcentration time of 6 min.

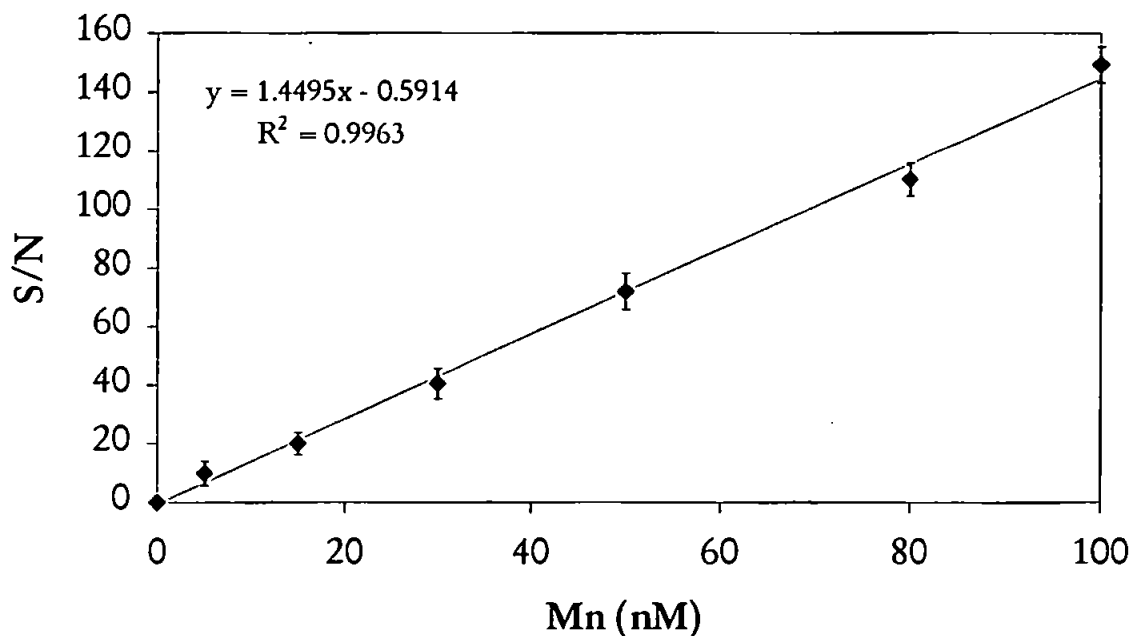


Figure 4.22: Calibration graph in the range 5-100 nM of Mn(II) in acidified UHP water.

4.3.5 Analysis of Certified Reference Materials (CRMs) using the
TCNQ-O₂-OH-Eosin Y system

The Canadian seawater trace metal standards CASS-3 (Coastal Atlantic Surface Seawater) and SLEW-3 (St. Lawrence Estuarine Water) were analysed in the

laboratory to verify the results obtained with the FI-CL and in Table 4.10 are presented the results.

Table 4.10: Results for the determination of Mn(II) in seawater CRMs.

Sample	FI-CL	Certified value
CASS-3 (nM)	47.9 ± 5.7	45.68 ± 6.55
SLEW-2 (nM)	73.2 ± 4.9	70.98 ± 5.46

Error bars represent $\pm 2s$

In order to evaluate if the results differ significantly it is possible to use the t test. The null hypothesis adopted is that the means of the results given by the two methods are equal, we need to test whether \bar{x}_1 and \bar{x}_2 differs significantly from zero. Hence, in the case of the CASS-3 for example s^2 is 61.09, s is 7.81 and t results -0.34 . The critical value of $|t|$ ($P=0.05$) at 3 degrees of freedom is 3.18. Since the experimental value of $|t|$ is less than the reference value, the difference between the two results is insignificant at the 5% level and the null hypothesis is accepted, confirming the good agreement between experiment results by FI-CL and certified values.

4.4 CONCLUSIONS

The development of a sensitive method for the determination of dissolved Mn at nanomolar level is presented. Mn can be determined by FI-CL by exploiting the Mn(II) catalysis of the oxidation of 7,7,8,8- tetracyanoquinodimethane (TCNQ)-O₂-OH-Eosin Y in presence of didodecyldimethylammonium bromide (DDAB).

- For best results care must be taken to minimise contamination risks during all development work.
- A chelating resin 8-hydroxyquinoline is effective for in-line matrix elimination and preconcentration.
- A chelating agent such as desferrioxamine mesylate (DFAM) can be used in-line to selectively complex with interferents (such as Fe(III)).
- The CL system permits the selective determination of Mn(II) with a practical limit of detection (3s) of 3 nM when 13.2 ml of sample is loaded onto the column, and a relative standard deviation ranging between 3.2 and 6.7% (n=5).
- One analytical cycle (incorporating load, wash and rinse steps) can be completed in 26 min.
- The method determination of Mn in SLEW-2 and CASS-3 certified reference materials is accurate as shown in Table 4.10.

CHAPTER 5

DISTRIBUTION AND BEHAVIOUR OF COBALT AND MANGANESE IN THE WESTERN NORTH SEA.

5.1 INTRODUCTION

Like many other coastal seas around the world, the waters around England (mainly North Sea and English Channel) are under strong environmental pressure. The countries surrounding the North Sea are densely populated, with approximately 164 million people living within the North Sea catchment area. The catchments of the rivers Elbe, Weser, Rhine, Meuse, Scheldt, Humber and Thames, which drain into the North Sea, have particular high population densities and are highly industrialised and intensively farmed. The coastal waters around England have important ecological, economic (e.g. fishing, oil/gas exploration) and amenity values, and often various demands on the system are in conflict with each other (Jarvie et al., 1997). A proper management of the coastal waters requires a good understanding of biogeochemical processes (Achterberg et al., 1999). The hydrography of the North Sea has been described in several publications (Carruthers, 1925; FTNS, 1983; Lee, 1980; Laevastu, 1963). Figure 5.1 presents the schematic of basic physical processes in the North Sea (Charnock et al., 1994). The two major types of saline water flowing into the North Sea are Atlantic water entering from the north between Scotland and Norway, and from the south via the Dover Straits and low salinity Baltic water. The largest freshwater inputs are from the Rhine

and Elbe rivers. The Rhine contribute approximately 37% of the fresh water inflow (van Paguee and Postma, 1987).

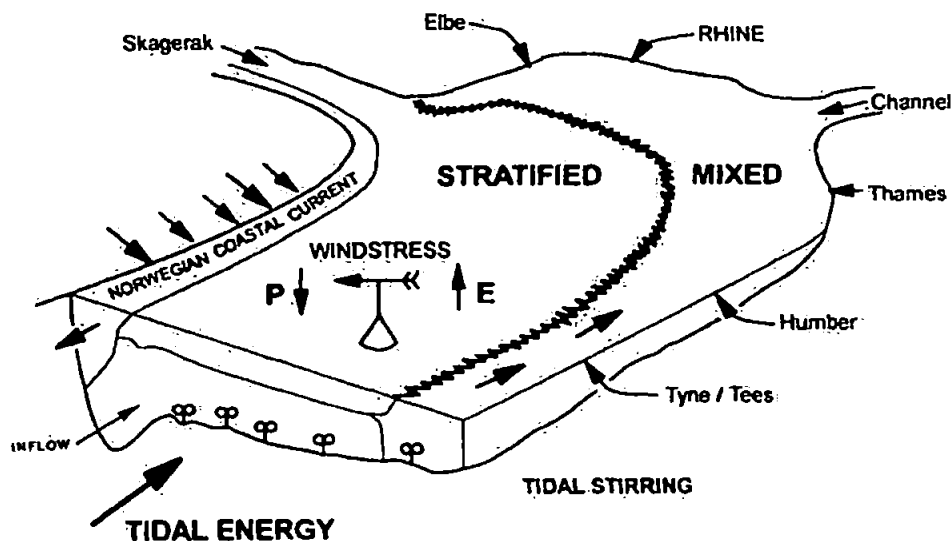


Figure 5.1: Schematic of basic physical processes in the North Sea (reproduced from Charnock et al., 1994).

The general pattern of water flow is anti-clockwise with the principal outflow of water being along the coast of Norway in the Norwegian Current. This circulation pattern leads to an accumulation of relatively low salinity water in the German Bight. During winter, the major part of the North Sea is vertically well mixed. In summer, a seasonal thermocline forms in large part of the central and northern regions.

While advances in sampling and analytical techniques have greatly improved our knowledge of the distribution of dissolved trace metals in the deep oceans, there is more doubt about the nature of the dominant process in coastal waters. Coastal waters are complex systems in which a range of processes change the concentration of a dissolved metal on relatively short time and space scales. The

processes are often superimposed. The likely processes that need to be quantified include: inputs from rivers (Balls, 1985; Morris et al., 1982); atmosphere (Dedeurwaeder et al., 1985); bottom sediments (Sundby et al., 1986; Westerlund et al., 1986); exchange with ocean waters and circulation (Prandle, 1984), removal mediated by biological processes (Morris, 1974; Hydes, 1989); and exchange reactions with particles (van Beusekom, 1988; Balls, 1989). The importance of these processes will depend on the biogeochemical pathways and reactivity of the different metals, but the general view is that the coastal shelf system acts as a significant removal filter in the transfer of metals to the open ocean (Martin and Windom, 1991). These coastal cycling and removal processes thus have important implications for the transport and long-term fate of natural and anthropogenic metals introduced from the land.

To aid the study of the North Sea (Hydes et al., 1999) have divided it into areas that are considered to have distinguishable water mass properties. The four areas are shown in Figure 5.2, and comprise of Boxes 7b, 4 and 5 which are areas of shallow coastal water and are generally considered well mixed all year around. Box 3b is the English coastal area.

The English coastal area receives a river discharge of $13 \text{ km}^3 \text{ year}^{-1}$ (9% of total freshwater discharge into the southern North Sea). This is the region with the highest suspended sediment concentration, which is the result of coastal erosion (Eisma and Kalf, 1987). Box 4 is the region of French, Belgian and Dutch coasts. This area receives the largest fresh water input to the North Sea from the river Rhine ($81 \text{ km}^3 \text{ year}^{-1}$, 60% of total). The discharge of the Rhine occurs at five points along the coast and is controlled by sluices. Box 5 is the region of the German and Danish coasts.

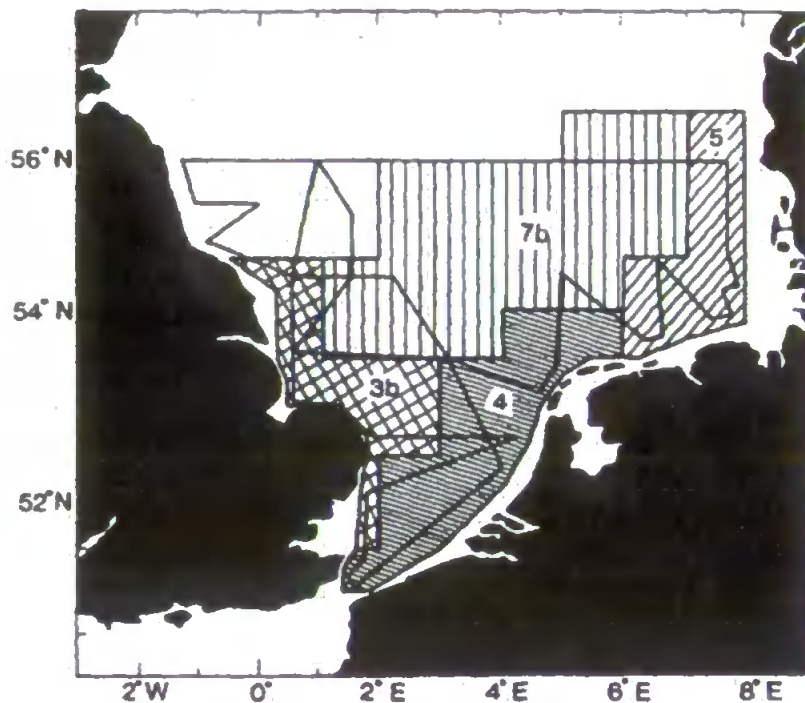


Figure 5.2: Subdivision into the North Sea Task Force boxes. Areas and volumes of the boxes are 3b, 910.7 km³, 32544 km²; 4, 1196.1 km³, 44208 km²; 5, 781.6 km³, 36576 km²; 7b, 3085.8 km³, 77616 km². The line across the boxes represents the cruise track (reproduced from Hydes et al., 1999).

This box is the region of lowest average salinity due to the combined influence of the river Rhine and Elbe (Elbe discharge 25 Km³ year⁻¹, 18% of total). Box 7b is the southern central area. This is the region most directly influenced by inflow from the Atlantic Ocean. The southern central area is seasonally stratified, with water depths of up to 90 m. In the south west of the area is the Dogger Bank where depths are as shallow as 10 m and water is sufficient clarity for a low level of biological production to continue through the winter months.

In order to assess practicality of shipboard operation of the manual FI-CL analyser and to validate the analytical method, the cobalt method has been tested at the North Sea IMPACT cruise 1 on-board the RRS Challenger (CH 148) between 16th – 27th September 1999 in the North Sea. All equipment and scientific personnel joined the Challenger at the port of Southampton on the 15th

of September and set sail on the 16th of September at 8.30 hrs. The RRS Challenger (Figure 5.3) is a 54.3 m research vessel with accommodation for up to 14 scientific staff. In order to validate the analytical method for the determination of Mn in seawater the cruise samples (acidified at pH 2 and stored in the dark at room temperature for 22 months) have been analysed at the University of Plymouth using the TCNQ-O₂-OH-Eosin Y reaction.



Figure 5.3: The RRS Challenger on the Southampton dock.

5.2 EXPERIMENTAL

5.2.1 Sampling strategy

The IMPACT cruise station plan was designed with the following objectives:

- to investigate pollutant behaviour in the three main geographical areas (Humber, Flamborough Front and Dogger Bank) and many topographical features (e.g. Silver Pit, Outer Silver Pit, Leman and Indefatigable Banks)
- to study pollution gradients in the outflow region of the Humber, and to assess pollutant inputs and fluxes to the North Sea from Humber whilst accounting for the Wash, Dogger Bank and other potential inputs.

Account was also taken of potential contaminant inputs from the numerous Gas Platforms operating in the area. Station positions for the survey are given in Figure 5.4. Exact details of locations are shown in Table 5.1. Logistical problems meant that stations 30 and 35 were not sampled, and in addition station 12 was sampled twice and 5 more stations were added to the original cruise plan. The cruise set out to provide data on the concentrations and distributions of dissolved Fe, Co, Mn, Mo, V, Cr, U, trace metals in SPM and dissolved nutrients (Si, PO₄, NO₃).

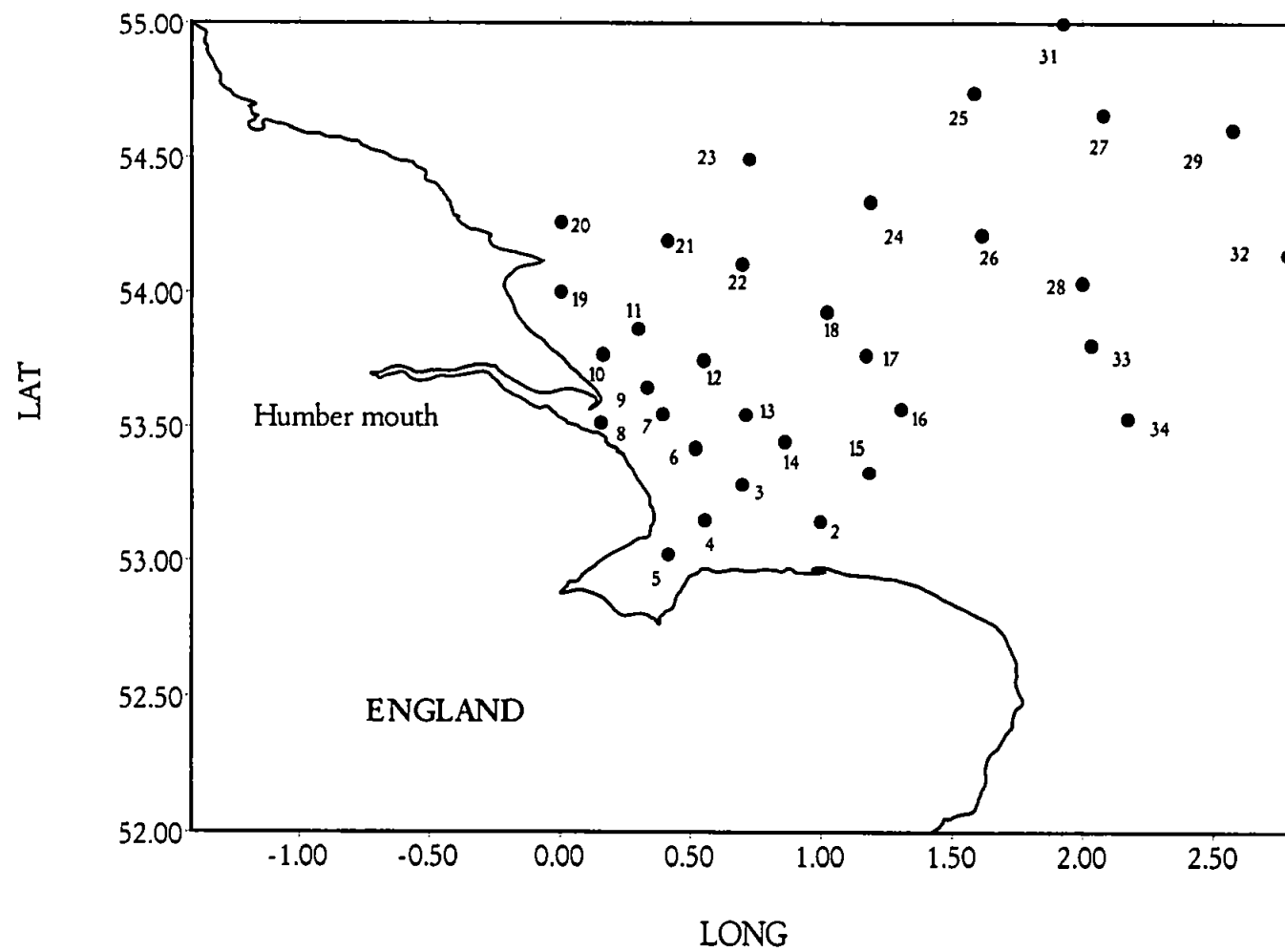


Figure 5.4: Study site and station positions

Table 5.1: Time of sampling and position of stations (GMT)

Date	Time	Lat	Lon	Station	Name	Event
16/09/99	0900				Southampton	Depart Southampton
17/09/99	1246 - 1630	52 35.6N	2 15.5E	1		CTD, Sediments
	2216	53 08.7N	0 59.8E	2	The Well	CTD, Sediments
18/09/99	0049					Complete St. 2
	0259 - 0400	53 16.9N	0 41.9E	3	Burnham Flats	CTD, Sediments
	0551 - 0640	53 09.1N	0 33.3E	4	Protector overfalls	CTD, Sediments
	0806 - 0841	53 01.3N	0 24.8E	5	N. Docking	CTD, Sediments
	1200 - 1453	53 25.1N	0 31.1E	6	Bell S. Race	CTD, Sediments
	1600 - 1643	53 32.7N	0 23.5E	7	Yarmouth	CTD, Sediments
	1827 - 2048	53 38.8N	0 19.9E	9	Cromer Knoll	CTD, Sediments
	2214 - 2246	53 46.1N	0 09.8E	10	E. of Spurn light	CTD, Sediments
19/09/99	0005 - 0047	53 51.8N	0 17.9E	11	Silver Pit 2	CTD, Sediments
	0218 - 0304	53 44.8N	0 33.0E	12	Malory Field	CTD, Sediments
	0514 - 0611	53 32.6N	0 42.7E	13	West Sole	CTD, Sediments
	0708 - 1104	53 26.6N	0 39.4E	14	Outer Silver Pit	CTD, Sediments
	1350 - 1606	53 19.7N	1 11.0E	15	NW. Whilst Humber	CTD, Sediments
	1806 - 2033	53 33.9N	1 18.3E	16	SE. Rough Gas Field	CTD, Sediments
	2213	53 45.9N	1 10.3E	17	S. of Ravenspurn	CTD, Sediments
20/09/99	0052					Complete St. 17
	0231 - 0503	53 55.7N	1 01.4E	18	S. Dogger Bight	CTD, Sediments
	1000 - 1318	54 00.0N	0 00.1E	19	Ravenspurn	CTD, Sediments
	1532 - 1622	54 15.6N	0 00.2E	20	Dimlington	CTD, Sediments
	1930 - 2215	54 11.5N	0 24.7E	21	NW. of Rough	CTD, Sediments

Table 5.1 (continued): Time of sampling and position of stations (GMT)

Date	Time	Lat	Lon	Station	Name	Event
21/09/99	0035 - 0314	54 06.2N	0 42.0E	22	NW. of Cleeton Gas Field	CTD, Sediments
	0600 - 0644	54 29.6N	0 43.6E	23	S. of Flamborough	CTD, Sediments
	0936 - 1013	54 11.6N	1 07.6E	24	N. of Flamborough	CTD, Sediments
	1414 - 1444	54 44.4N	1 35.0E	25	Dogger North Ground	CTD, Sediments
	1808 - 1900	54 12.7N	1 36.7E	26	Dogger North Shoal	CTD, Sediments
22/09/99	0812 - 0851	54 39.4N	2 04.7E	27	N. of South West Patch	CTD, Sediments
	0908 - 1032					Inflatable boat collecting metals, microlayer and nutrient samples
23/09/99	1518 - 1721	54 02.0N	1 59.9E	28	N. of Easternmost Shoal	CTD, Sediments, microlayer
	2135 - 2213	54 36.1N	2 34.4E	29	Easternmost Shoal	CTD, Sediments
	0809 - 0842	54 59.9N	1 55.6E	31		CTD, Sediments
	1546 - 1623	54 08.3N	2 46.9E	32		CTD, Sediments
	2037	53 48.2N	2 01.9E	33		CTD, Sediments
24/09/99	2037	53 48.2N	2 01.9E	33		CTD, Sediments
	0034					Complete St. 33
	0255 - 0400	53.35.6N	2 03.4E	34		CTD, Sediments
	1134 - 1549	53 44.9N	0 29.9E	12a	Malory Field	CTD, Grab
25/09/99	1818			8	Silver Pit 1	Arrive St. 8
	1403	53 44.9N	0 29.9E	8		CTDs, Sediments
27/9/99						Complete St. 8;
	0900					Proceed to Southampton Dock Southampton

5.2.2 Sampling and Analyses

A total of 130 samples were collected during the IMPACT cruise. Sample bottles (250 ml and 500 ml in high-density polyethylene, HDPE) had been cleaned by first soaking in hot 5% (v/v) micro-detergent (DECON, Merck BDH) for 24 h, followed by 1 week in 6 M hydrochloric acid (AnalaR, Merck BDH) and one week in 2 M nitric acid (AnalaR, Merck BDH), and were subsequently stored in 0.01 M Q-HCl. UHP water ($18.2 \text{ } \Omega\text{m cm}^{-1}$, Elgastat Maxima) was used throughout the work. All the reagents for the shipboard determination of cobalt were used as specified in Chapter 3, and prepared at the University of Plymouth (UoP) before travelling and the FI-CL system and support equipment for the cruise was securely packed and loaded on the transport van to join the RRS Challenger. Reagents for the laboratory analysis of Co and Mn were used as specified in Chapter 3 and 4.

Contamination control procedures were used throughout all trace metal sampling and analytical steps employed in this work. Sampling was performed in close liaison with other participants of the cruise. Samples were taken from three depths (occasionally four) deploying the stainless steel Conductivity-Temperature-Detector (CTD) rosette frame (Figure 5.5), with acid cleaned modified lever-action 10 l Niskin water samples attached (Morley et al., 1988). This approach allowed the collection of water samples from a selection of sampling depths, with the associated master variable data (salinity, temperature, transmissometer, fluorimetry). Seawater samples from each depth were pressure filtered through 37 mm diameter, $0.4 \text{ } \mu\text{m}$ poresize Nuclepore polycarbonate filters (acid cleaned) (Figure 5.6).

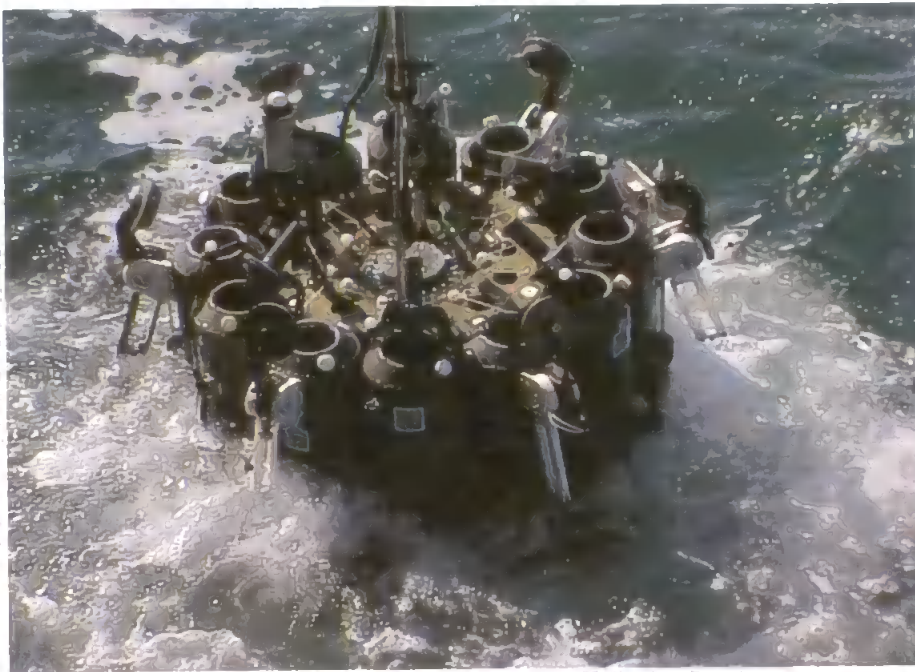


Figure 5.5: The CTD deployment



Figure 5.6: The filtration system

The filtrate was collected in the acid cleaned bottles. Prior to use, the bottles were thoroughly washed with UHP water and rinsed with the seawater sample. After the shipboard FI-CL analysis of Co(II) the samples were acidified at pH 2 using 25 μ l of Q-HCl (9 M) per 250 ml of sample and stored in re-sealable plastic bags for the subsequent land-based analysis of Co(II) and Mn(II). Filtration of samples, sample handling and determination of Co at sea was carried out in a clean container (Figure 3) supplied by NERC (National Environment Research Council). Critical sample handling procedures were conducted in a class-100 laminar flow hood.



Figure 5.7: The clean container on board ship for trace analysis

Cobalt was measured in unacidified samples at sea with pyrogallol as the luminescent reagent, using the method of standard additions. Three 20 ml aliquots of sample were transferred to 25 ml polystyrene screw-capped vials (Sterilin, Merck BDH). Sub-sample 1 was left, whilst sub-samples 2 and 3 were spiked with a small volume (20–50 μ l of Co(II) standard; variable

concentrations) to achieve standards additions ranging from 0.15–1.5 nM. Prior to use, the FI manifold, the PTFE flow lines fittings and connectors were cleaned with 0.5 M Q-HCl and UHP water for one hour. The pump tubing was suitable for at least 4 days of near continuous shipboard analyses, after which all tubing was changed. Over a 10 days cruise period, the use of one 8-HQ resin column for preconcentration of Co from seawater showed no deterioration in performance or reduction in chelating ability.

The accuracy of the FI-CL measurements was ascertained by regular analysis of Irish reference seawater sample during the cruise (which had previously been found to contain 0.35 ± 0.02 nM of Co by CL and 0.34 ± 0.01 nM by Adsorptive Cathodic Stripping Voltammetry, AdCSV). Manganese was measured in acidified samples at the UoP by exploiting the Mn(II) catalysis of the oxidation of 7,7,8,8-tetracyanoquinodimethane (TCNQ) in presence of DDAB, Eosin Y. The method of standard additions was applied. Prior to use, the FI manifold, the PTFE flow lines fittings and connectors were cleaned with 0.5 M Q-HCl and UHP water for one hour. Over a period of analysis during the cruise it was necessary repack the column with fresh resin only one time, due to a supposed deterioration in performance or reduction in chelating ability of 8-HQ resin.

5.3 RESULTS AND DISCUSSION

In Figure 5.8 is reported the distribution of salinity (S) (4 m depth) in the western North Sea. The large input of freshwater from the Humber (S = 30.1) and can be observed, with salinity values ranging between 33.8 and 34.7 away from the immediate influence of the Humber.

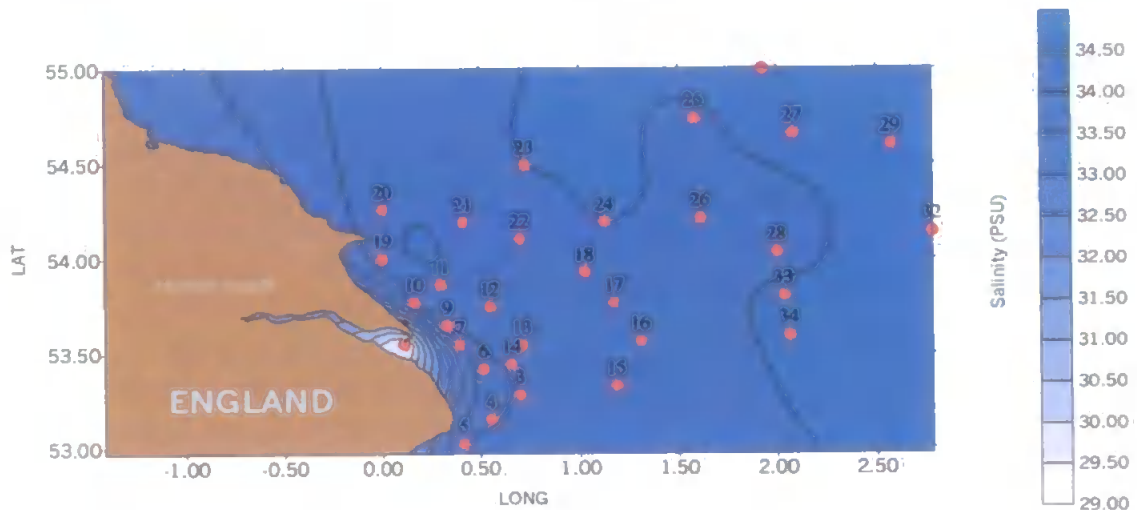


Figure 5.8: Surface distribution (4 m depth) of salinity in the North Sea

5.3.1 Temperature and salinity profiles

Figure 5.9 shows T-S depth profiles for stations visited during the IMPACT cruise (station 4 is not reported due to a malfunction of the CTD). The profiles show that the inshore waters (e.g. stations 5 and 10) are well mixed with constant T-S depth profiles. Some offshore stations with a shallow water column were well mixed too (e.g. station 31), whereas deep offshore stations (bottom depth 50-85 m) were stratified during the IMPACT cruise with a thermocline depth between 20-30 m (e.g. stations 22, 26, 28, 32).

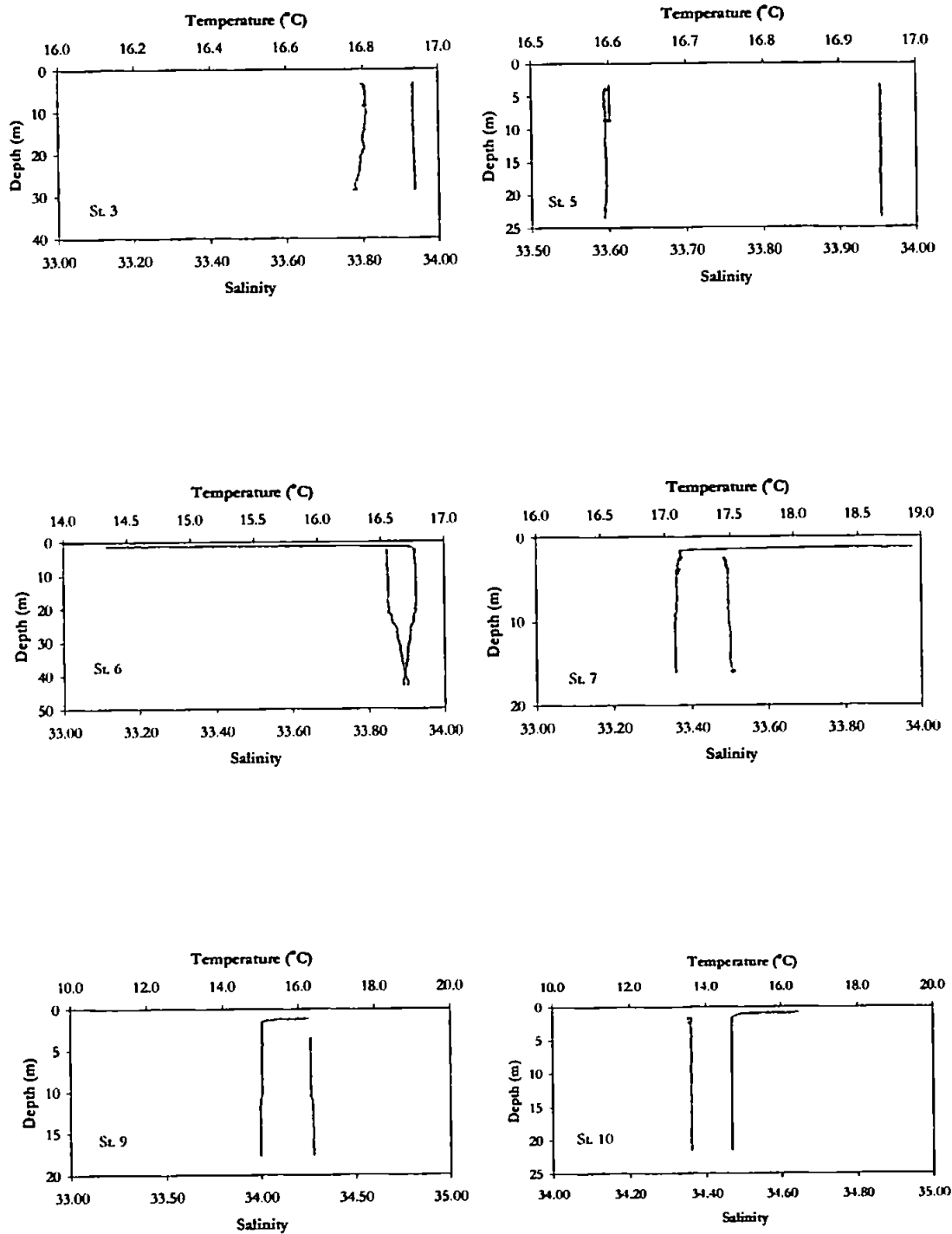


Figure 5.9: Depth profiles at the IMPACT stations (Salinity; Temperature)

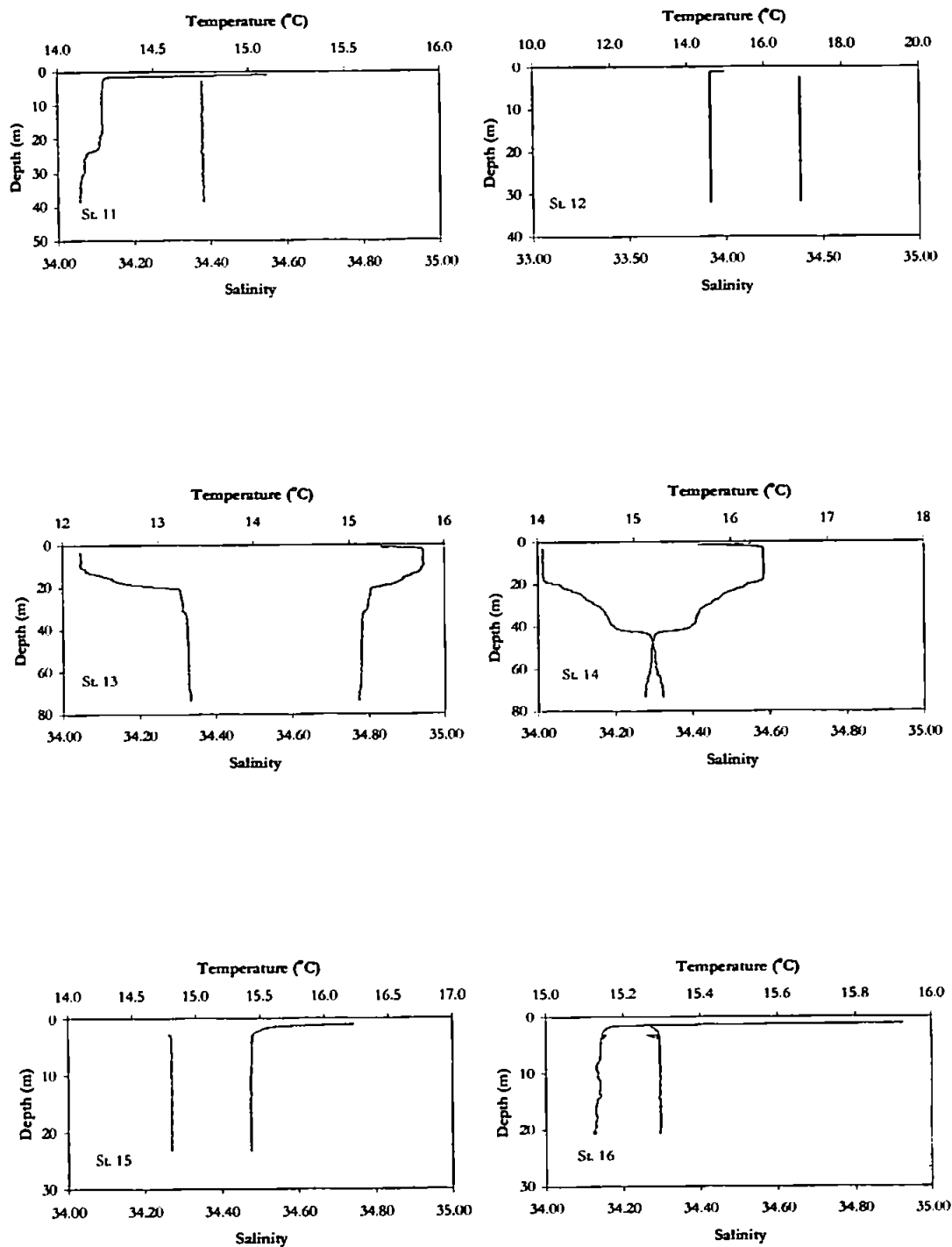


Figure 5.9 (continued): Depth profiles at the IMPACT stations (Salinity; Temperature)

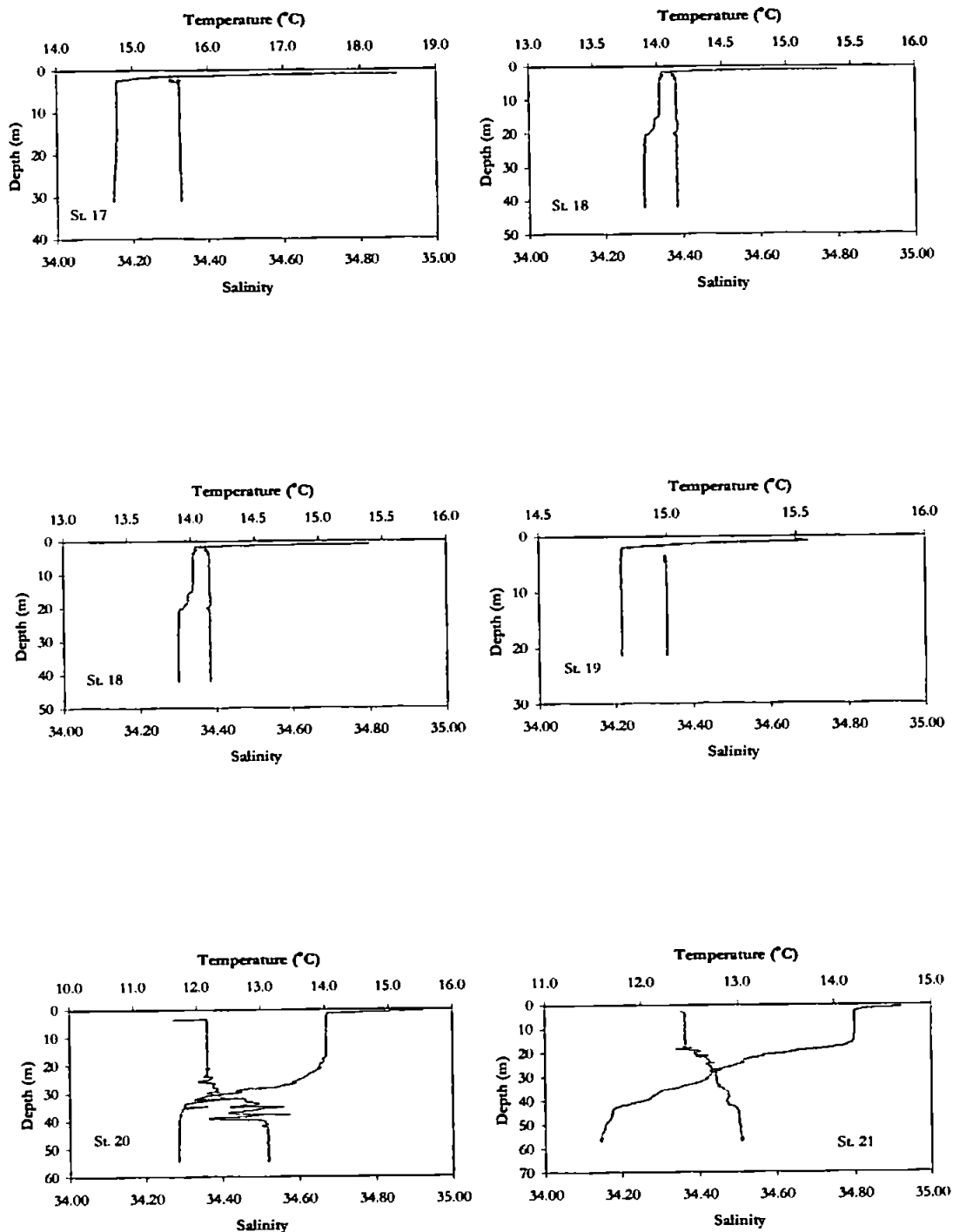


Figure 5.9 (continued): Depth profiles at the IMPACT stations (Salinity: Temperature)

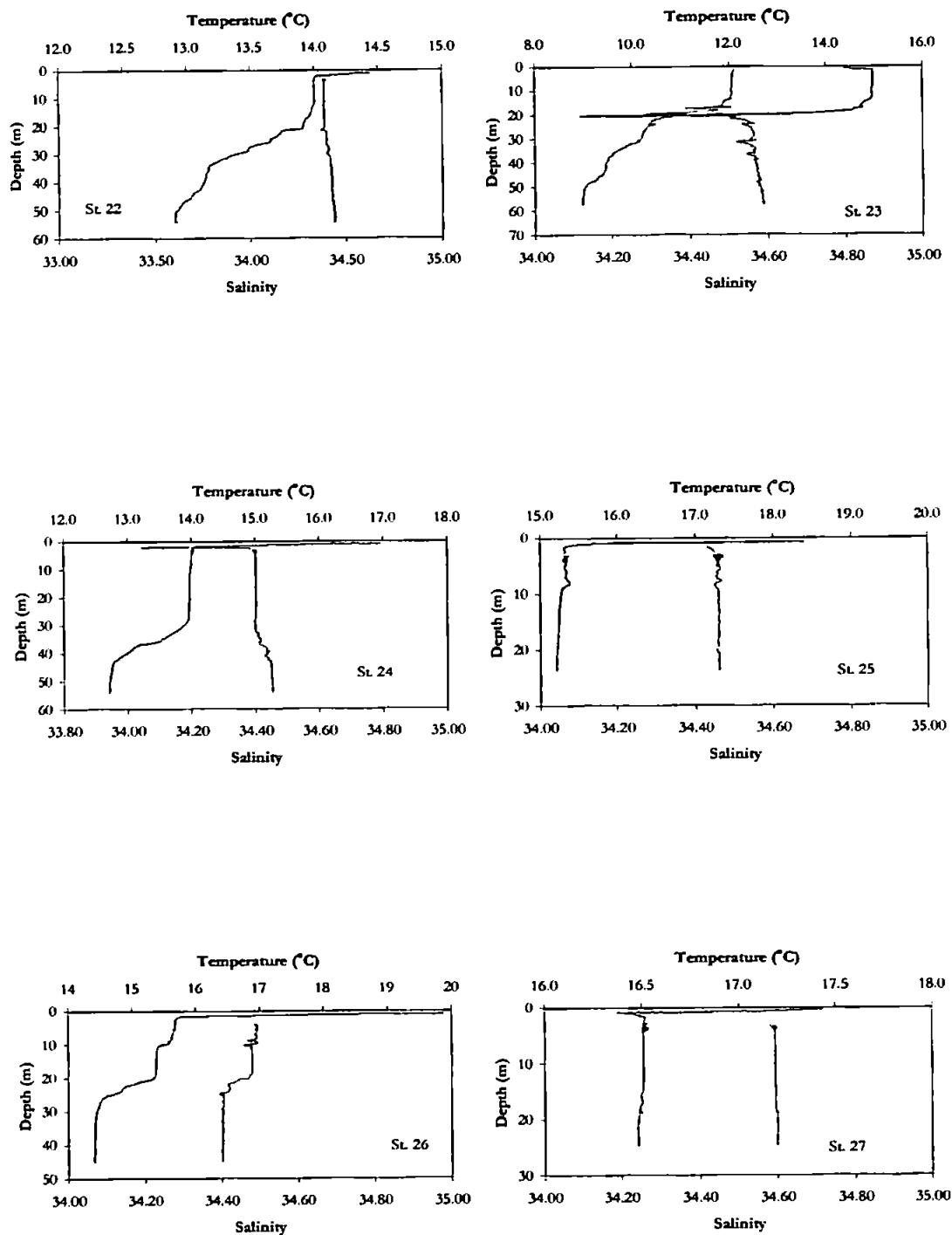


Figure 5.9 (continued): Depth profiles at the IMPACT stations (Salinity; Temperature)

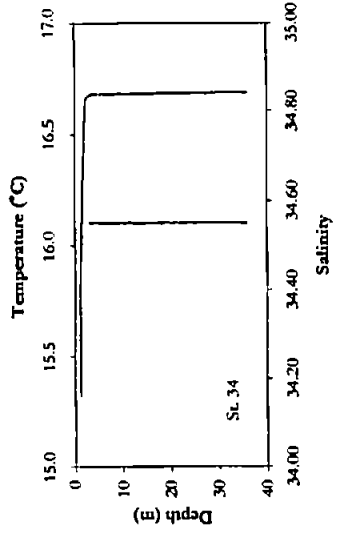
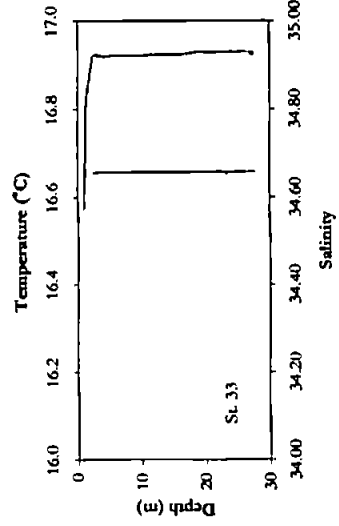
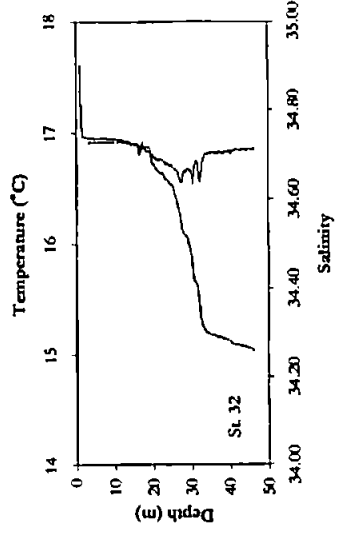
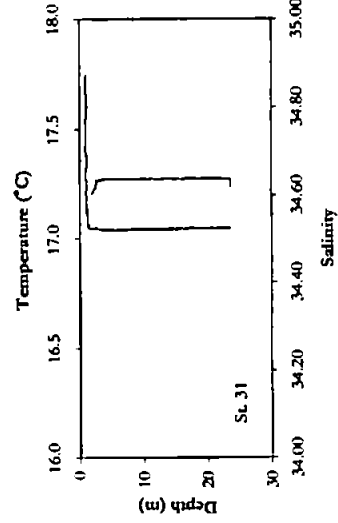
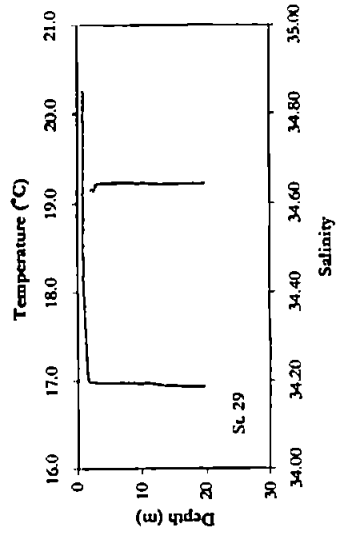
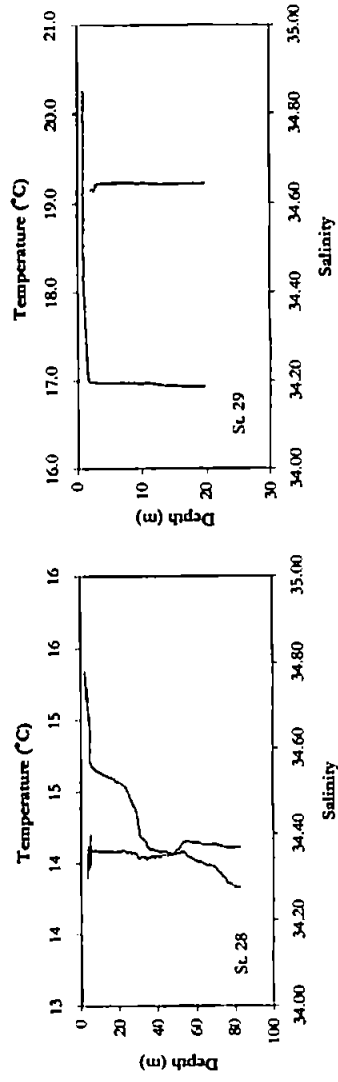


Figure 5.9 (continued): Depth profiles at the IMPACT stations (Salinity: Temperature)

5.3.2 Distribution of dissolved Co

The surface (4 m depth) distribution of Co can be evaluated using Figure 5.10. Enhanced concentrations of Co(II) (>800 pM) were observed near the plume of the Humber estuary. A decrease in dissolved Co concentration (100-300 pM) was evident away from the coast (further than 28 nautical miles off-shore), and can be explained by biological uptake, particle scavenging and mixing of coastal Co enhanced waters with cleaner Atlantic seawaters. Figure 5.10 has been generated using the software package Surfer 6.0. The disadvantage of this software is that the distribution of Co concentrations is automatically averaged among all the points. The output is an arbitrary assignment of concentration even in area not sampled during the cruise.

In Figure 5.11 are reported the depth profiles for all the stations for cobalt. The concentration values for Co(II) ranged from a minimum of 76 pM at 3 m depth at station 18 to a maximum of 434 pM at 11.4 m depth at station 34.

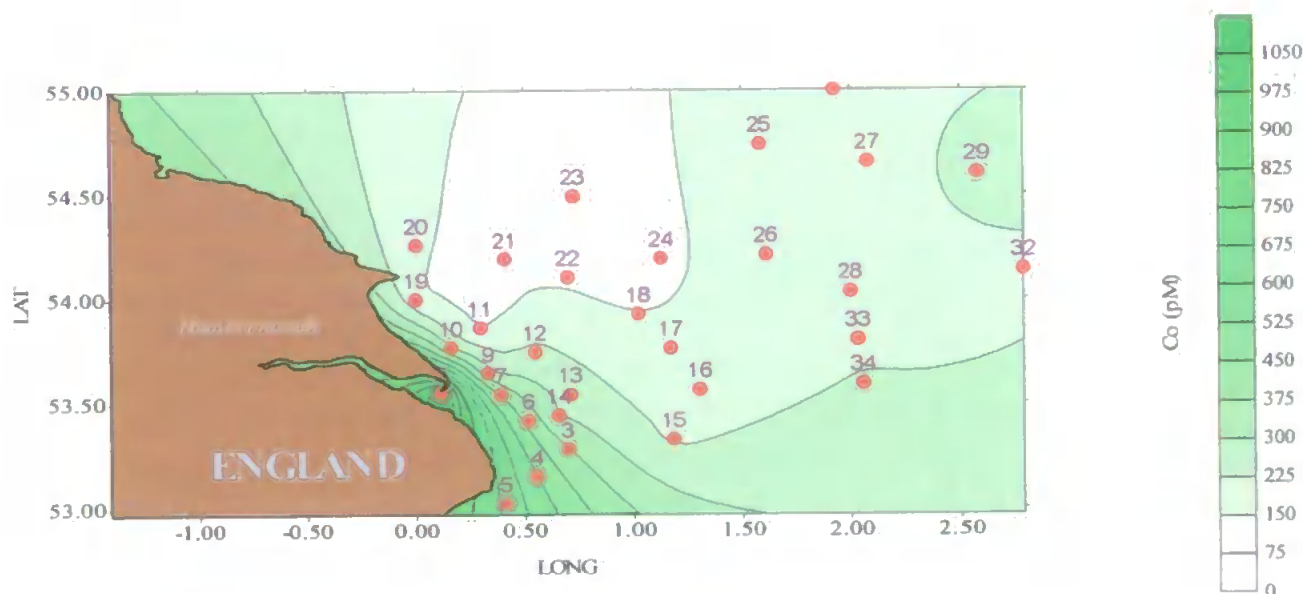


Figure 5.10: Surface distribution (4 m depth) of dissolved Co in the North Sea (Stations 1 and 2 have not been considered due to suspected contamination; the value for dissolved Co at station 8 was the value at ebb tide)

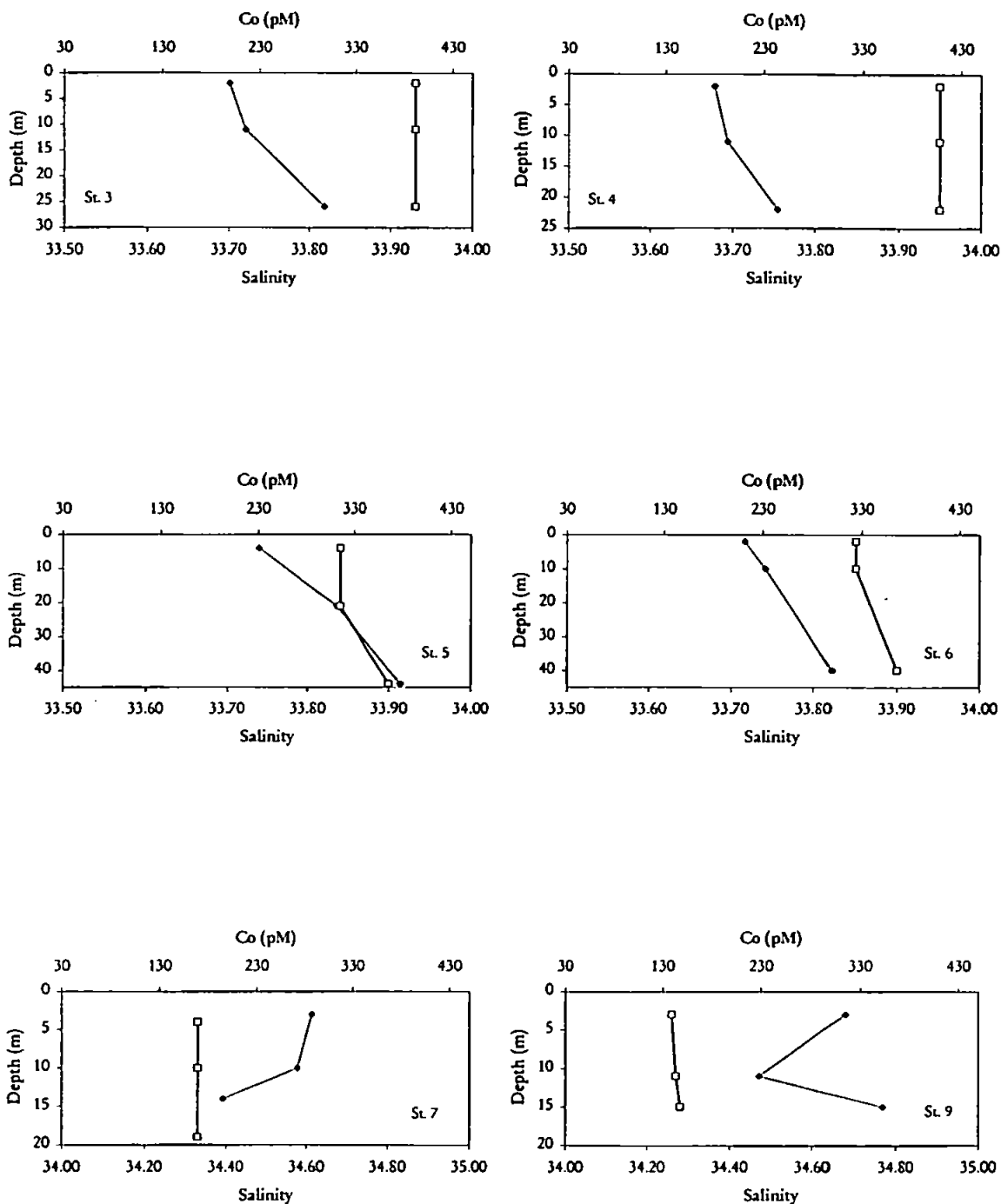


Figure 5.11: Depth profiles at the IMPACT stations (-- represents Salinity; -◆- represents Co; RSD comprises between 5.3 and 7.2 %)

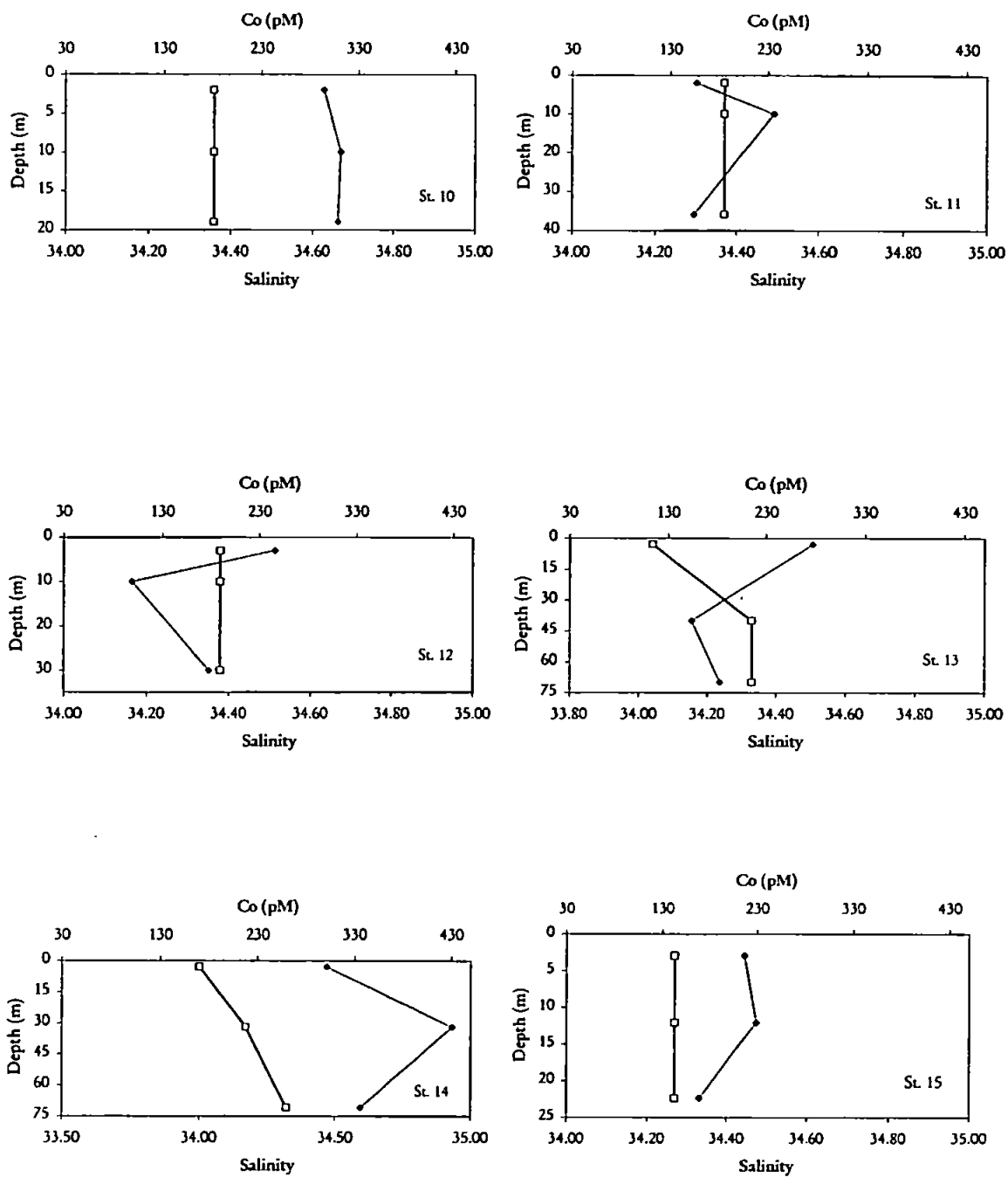


Figure 5.11 (continued): Depth profiles at the IMPACT stations (--- represents Salinity; -◆- represents Co; RSD comprises between 5.3 and 7.2 %)

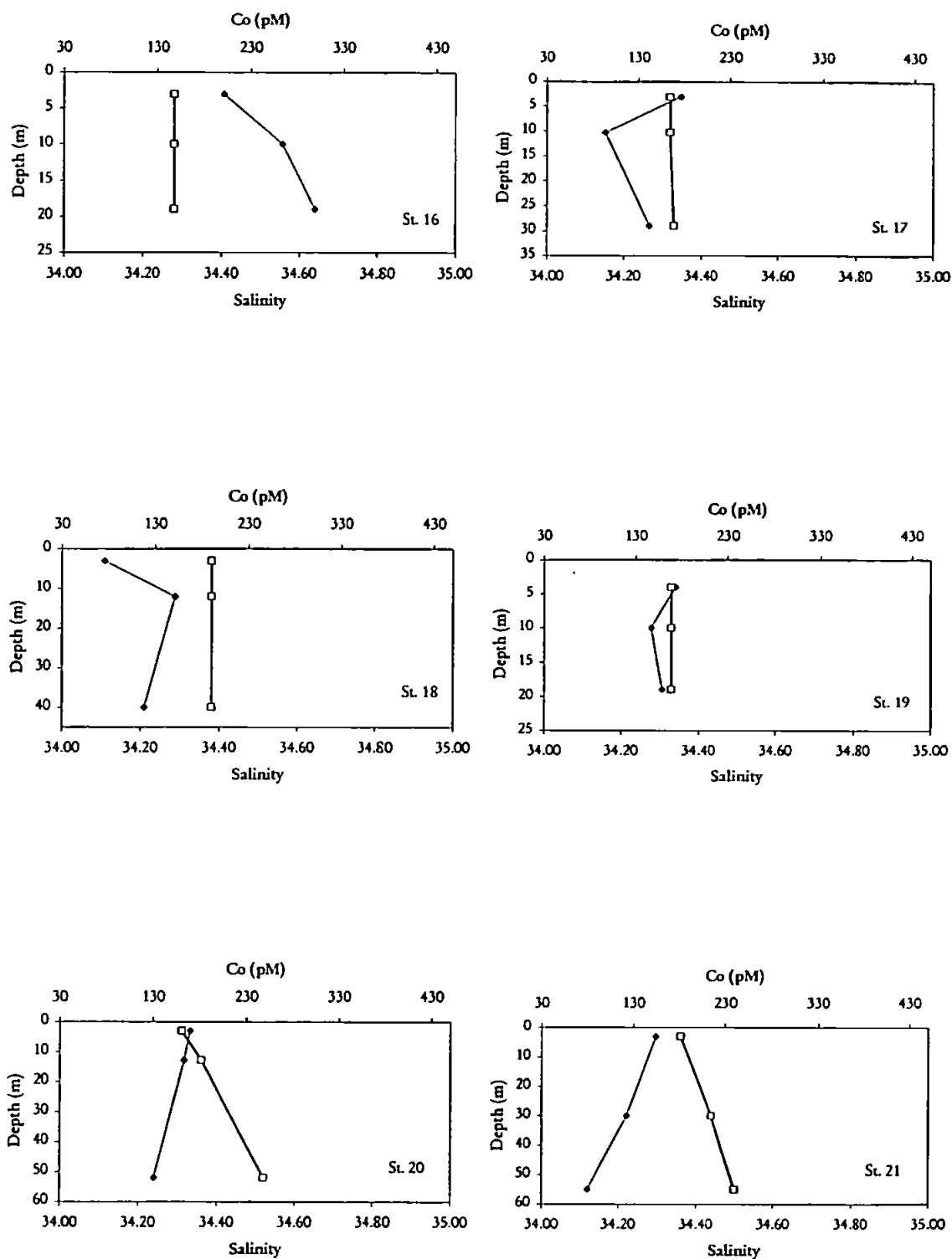


Figure 5.11 (continued): Depth profiles at the IMPACT stations (--- represents Salinity; -◆- represents Co; RSD comprises between 5.3 and 7.2 %)

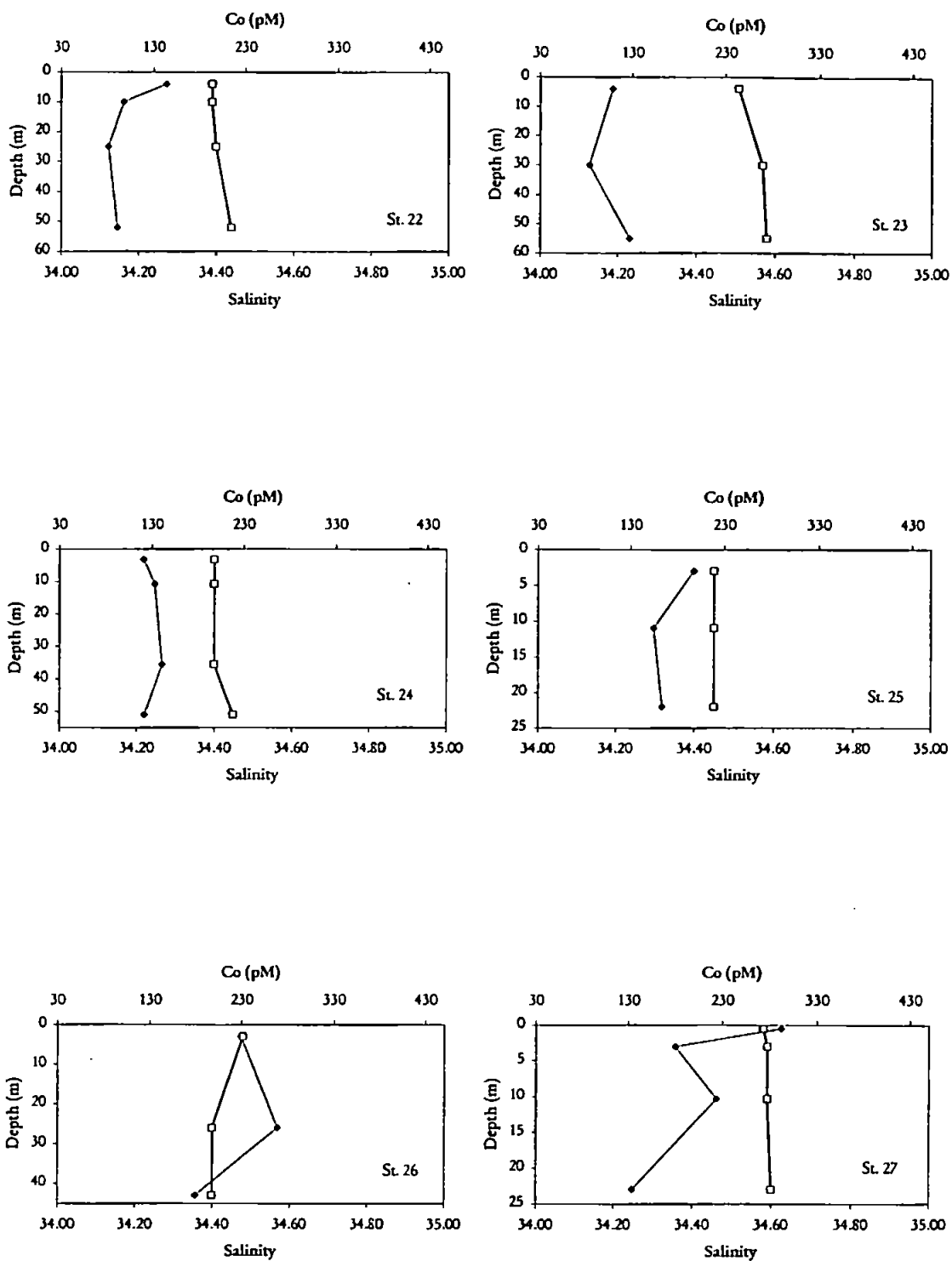


Figure 5.11 (continued): Depth profiles at the IMPACT stations (--- represents Salinity; -◆- represents Co; RSD comprises between 5.3 and 7.2 %)

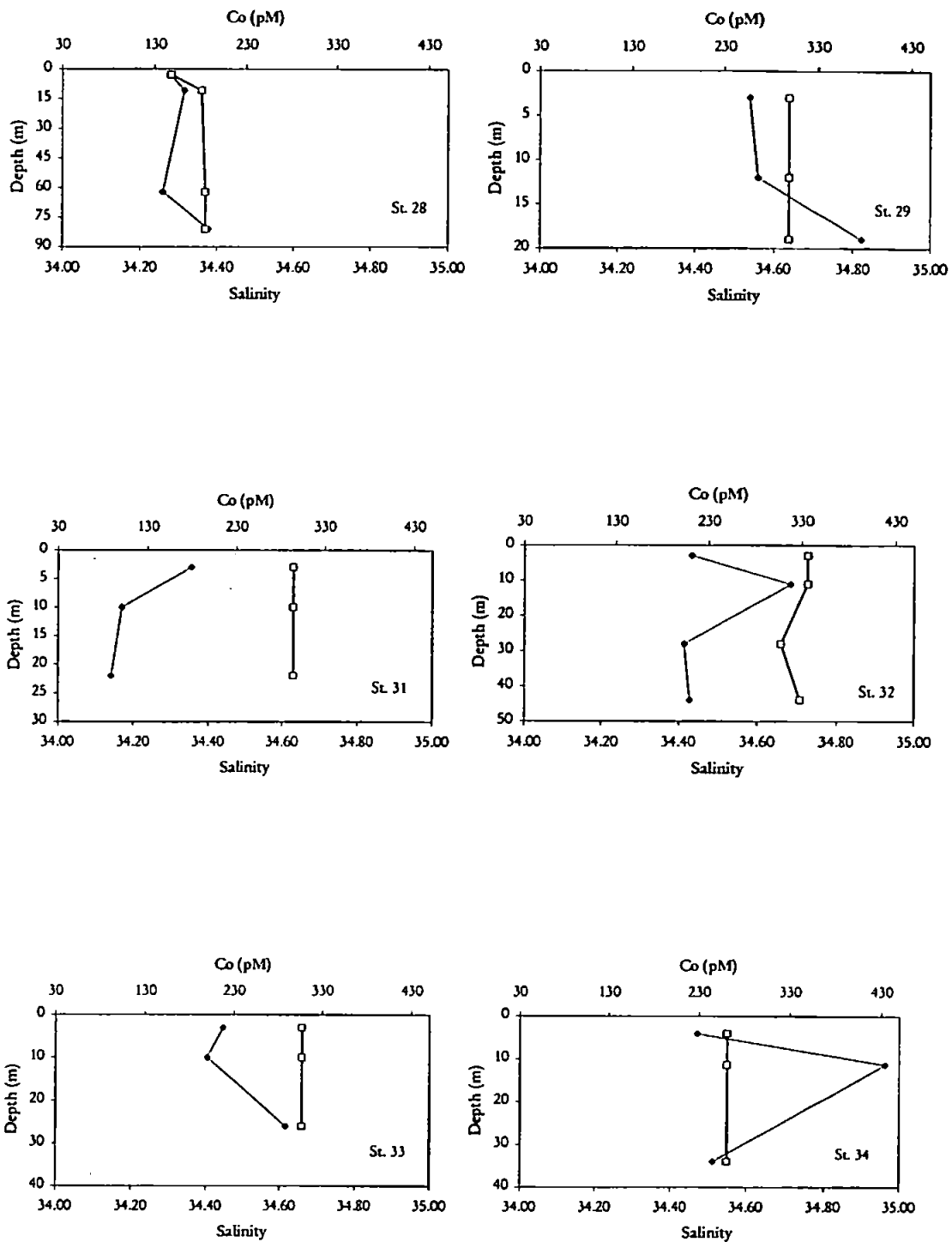


Figure 5.11 (continued): Depth profiles at the IMPACT stations (--- represents Salinity; -◆- represents Co; RSD comprises between 5.3 and 7.2 %)

5.3.2.1 Comparison between shipboard and land-based analysis for Co

An important fraction of Co is reported to be complexed by natural organic ligands in seawater (Nimmo and Chester, 1993; Zhang et al., 1990). The organic complexation is thought to prevent metal scavenging by suspended particulate matter and formation of insoluble inorganic metal complexes (Achterberg et al., 2001), thereby maintaining enhanced dissolved Co concentrations in seawater. The metal-organic complexes are strong, with reported stability constants of $\log K_{CoL}$ varying between 15.6 – 17.5 (Zhang et al., 1990). The profiles obtained for shipboard samples analysis (stations 32, 33, and 34) (neutral pH) and land-based (acidified samples to pH 2 with Q-HCl) analysis are shown in Figure 5.12. Sample handling in the laboratory in Plymouth was carried out in a class-100 laminar flow hood. There was no detectable signal from the ammonium acetate buffer used to adjust the pH of the acidified samples. Figure 5.12 shows that there was no systematic difference between the shipboard and land-based Co(II) profiles. This observation indicates that acidification to pH 2 did not release additional Co from the possible organic Co complexes. The implication of this observation is that either Co-organic complexes are not as strong as reported in the literature, with our 8-HQ column being able to complex all the Co present in the sample, or that Co(II) is mainly present as (weak) inorganic complexes in seawater. The main inorganic Co complex is free Co^{2+} (50%) and $CoCl_2$ (30%) according to Chester (2000) and Turner and Whitfield (1981).

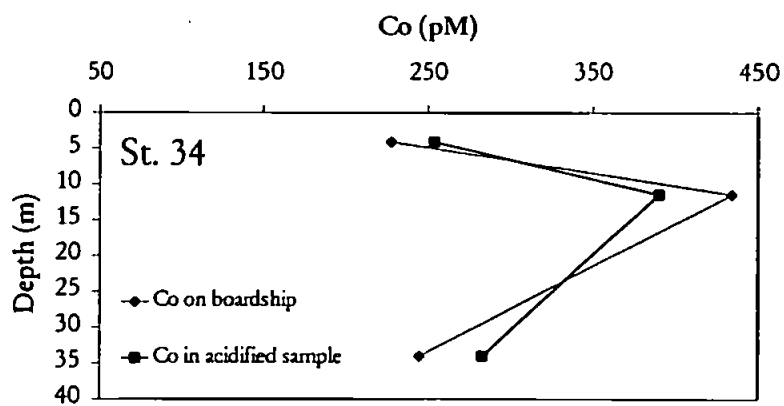
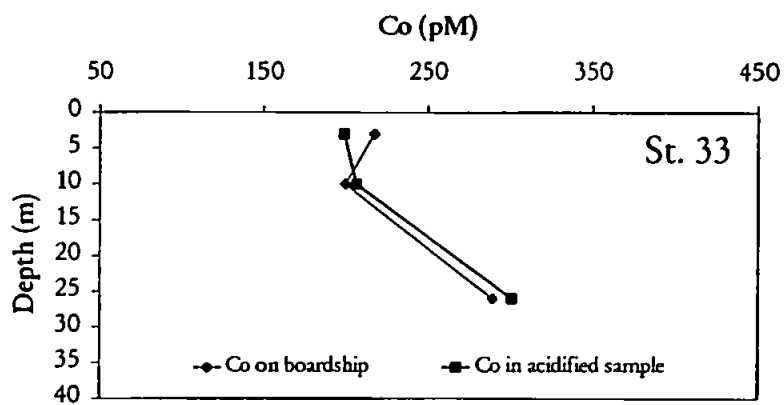
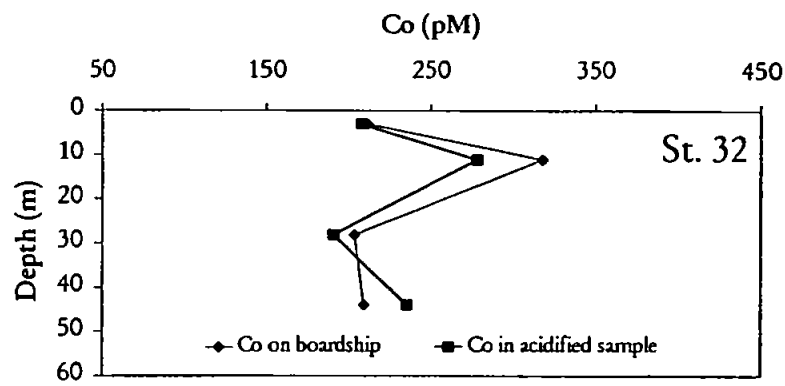


Figure 5.12: Depth profiles of dissolved Co (stations 32, 33, and 34). Land-based Co determination using acidified (pH 2) samples and FI-CL detection on land (RSD comprises between 3.9 and 5.8 %), and shipboard Co determination in samples at natural pH (7.9–8.1).

5.3.3 Distribution of dissolved Mn

In Figure 5.13 three areas have been identified, using depth averaged Mn concentrations. Zone A where the concentrations of Mn range between 7.5 and 14 nM with the exception for station 5, 6 and 8 (Mn > 14 nM). Zones B and D with lower Mn(II) values ranging between 4 and 8 nM. Zone C with relatively high concentrations of dissolved Mn ranging between 6 and 22 nM. At station 8 the increase in Mn concentration appear to have been due to the influence of fresh Humber water input, as indicated by value over 25 nM in waters adjacent to the Humber mouth (salinity 30.7). Figure 5.14 shows a contour plot for dissolved surface Mn(II) in the western North Sea. The distribution of Mn is different from Co. The Humber is an important source of Mn in the North Sea, but there are offshore areas where the Mn concentrations have similar values to the Humber mouth. In Figure 5.15, the Mn(II) depth profiles for all the stations are reported. The concentrations of Mn(II) ranged from a minimum of 3.9 nM at 55 m depth at station 21 to a maximum of 23.8 nM at 22 m depth at station 31.

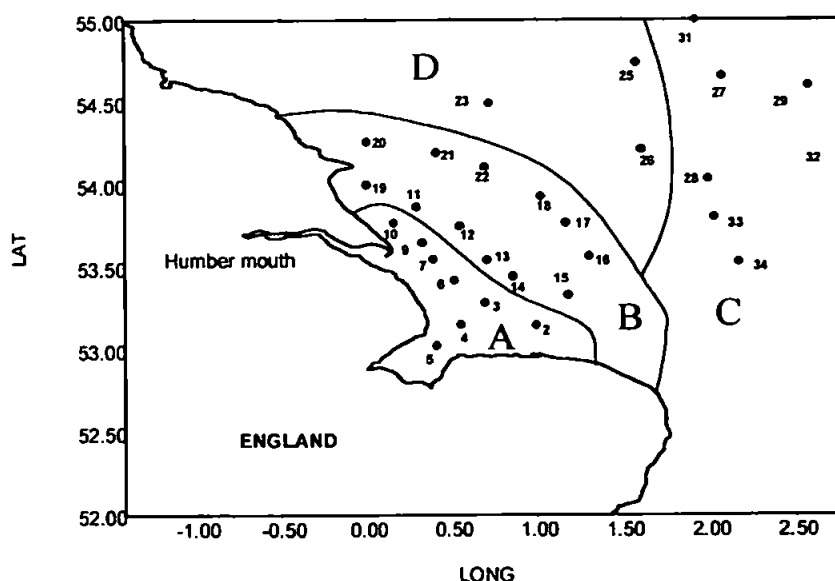


Figure 5.13: Distribution of dissolved manganese in the western North Sea (depth averaged).

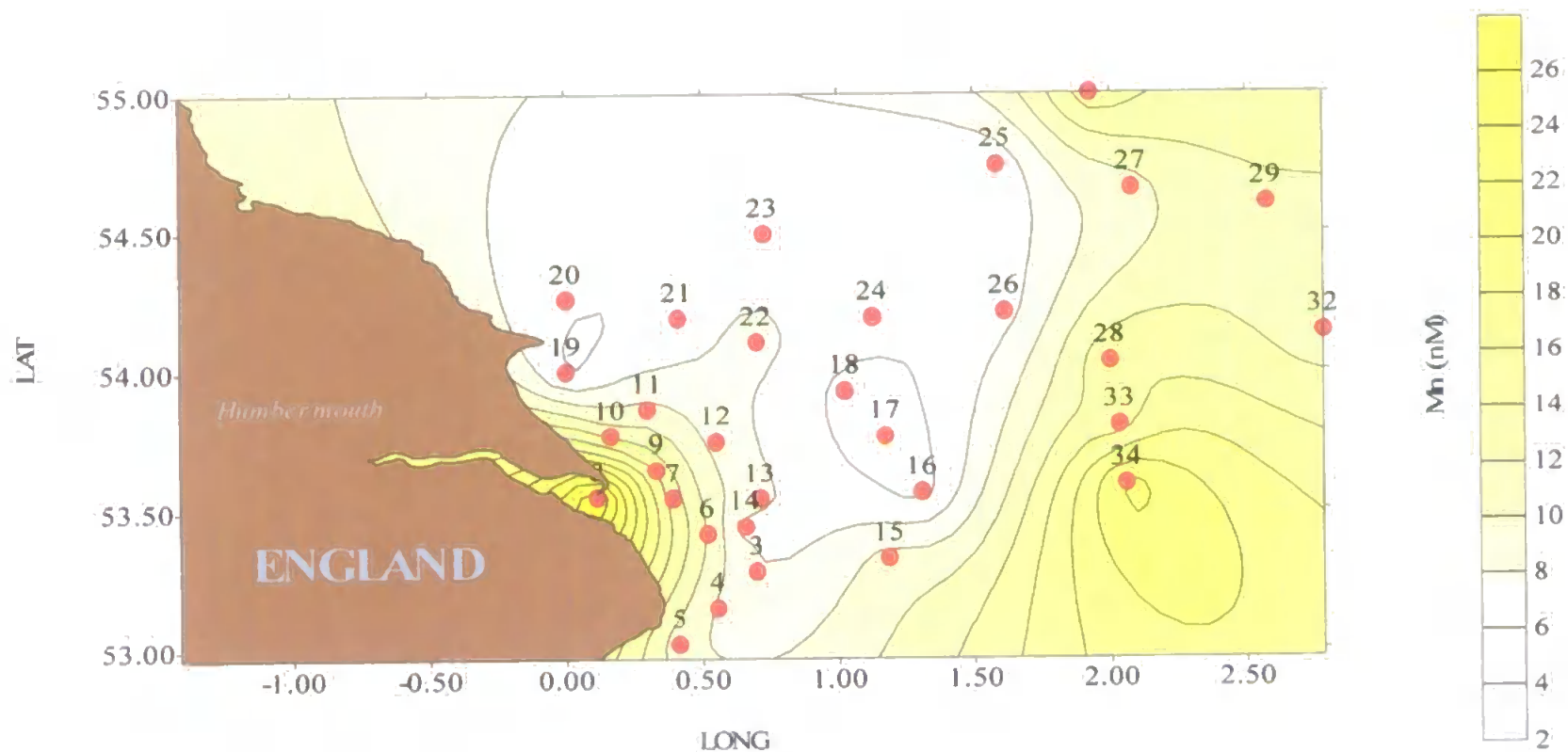


Figure 5.14: Surface distribution (4 m depth) of dissolved Mn in the North Sea (Stations 1 and 2 have not been considered due to suspected contamination; the value for dissolved Mn at station 8 was the value at ebb tide).

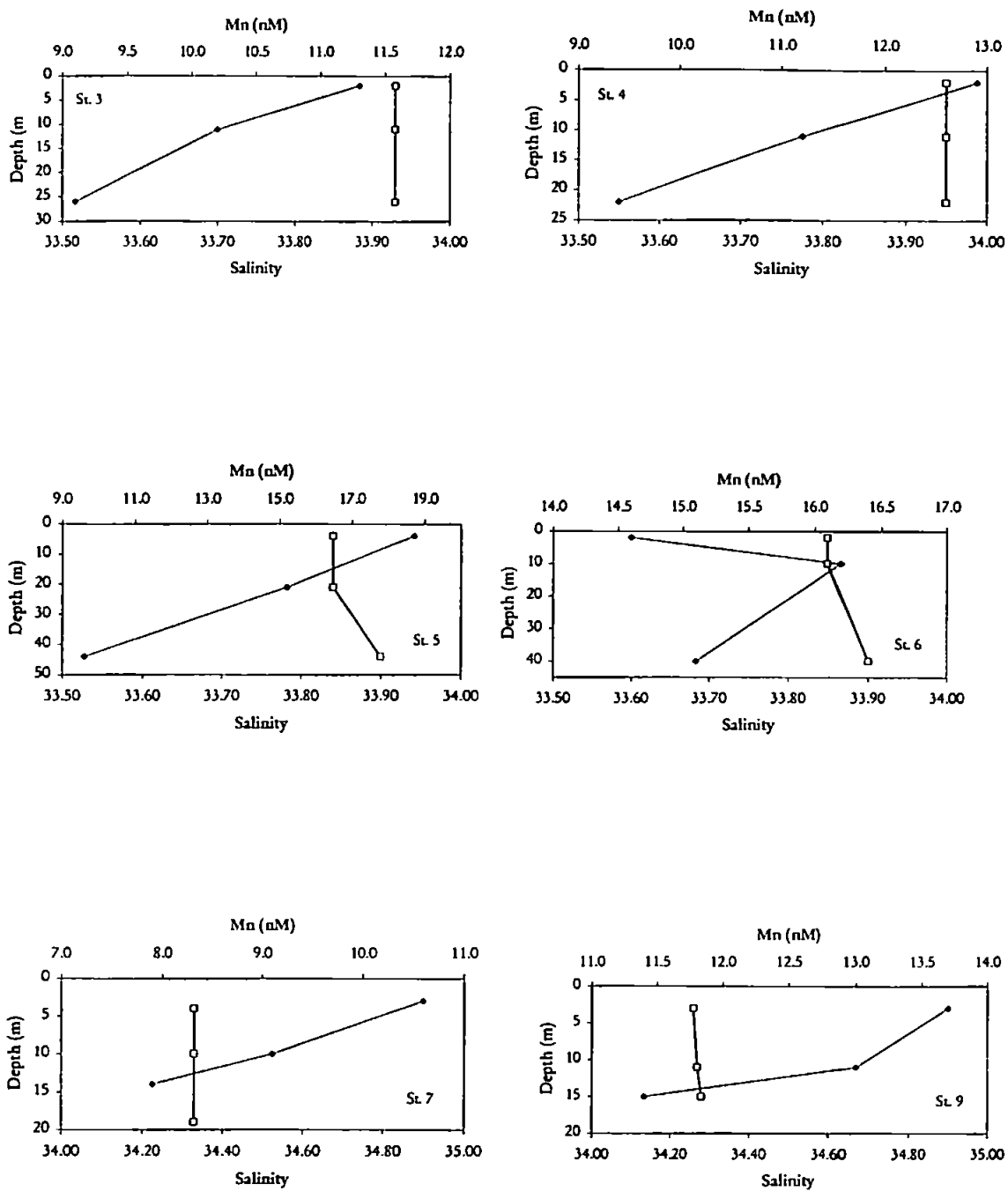


Figure 5.15: Depth profiles at the IMPACT stations (--- represents Salinity; -◆- represents Mn; RSD comprises between 4.2 and 6.6 %)

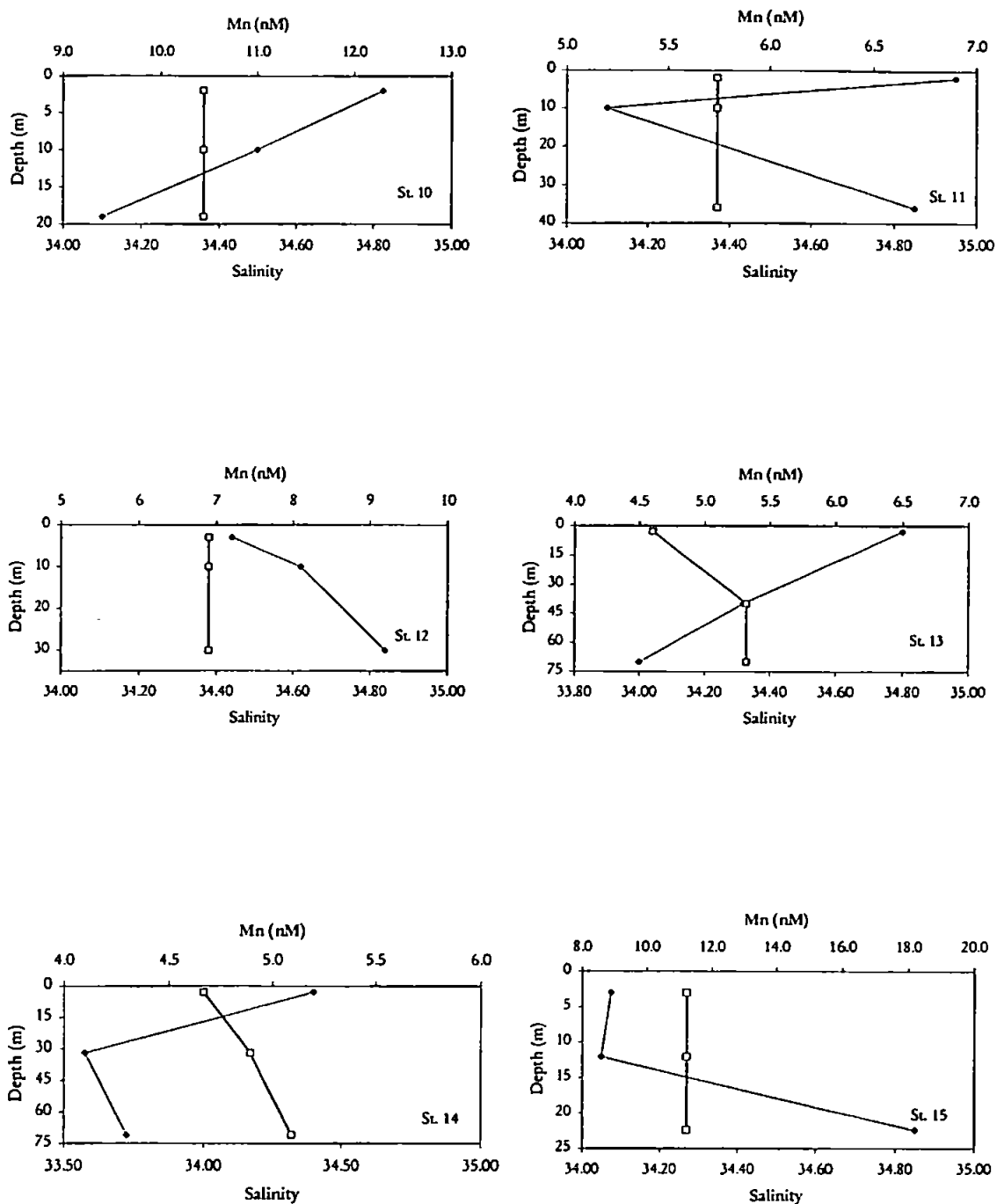


Figure 5.15 (continued): Depth profiles at the IMPACT stations (--- represents Salinity; -◆- represents Mn; RSD comprises between 4.2 and 6.6 %)

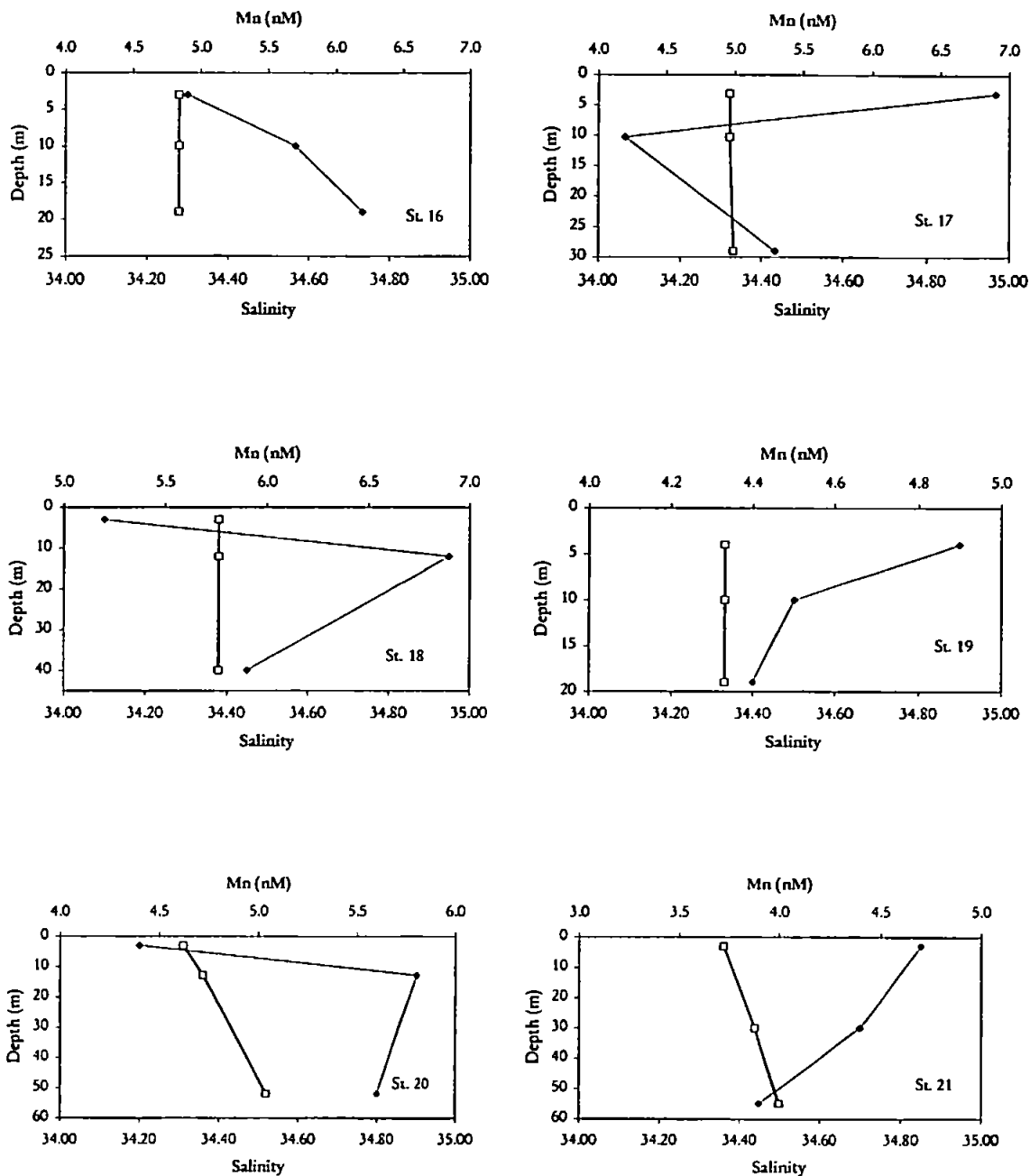


Figure 5.15 (continued): Depth profiles at the IMPACT stations (--- represents Salinity; -◇- represents Mn; RSD comprises between 4.2 and 6.6 %)

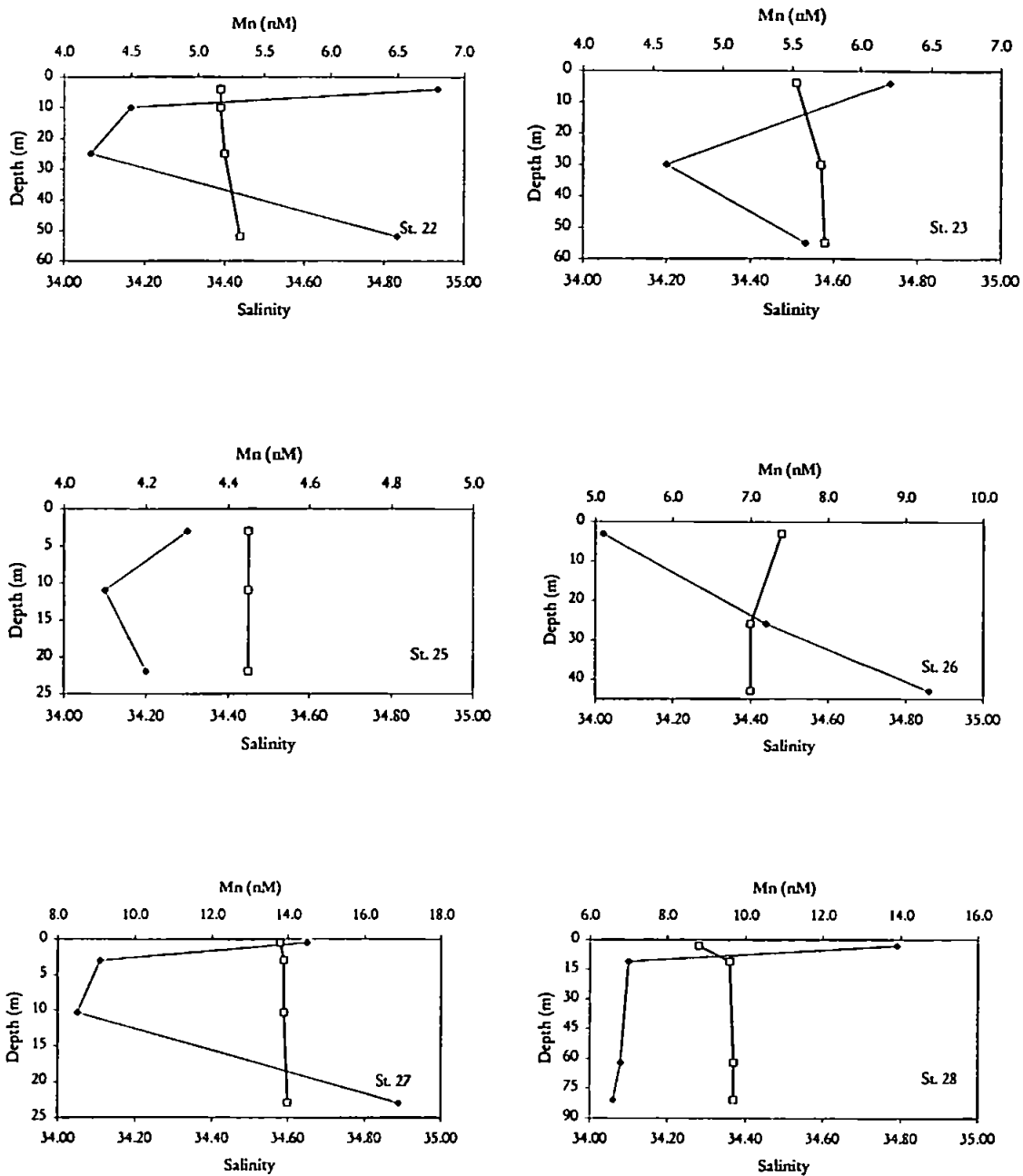


Figure 5.15 (continued): Depth profiles at the IMPACT stations (--- represents Salinity; -◆- represents Mn; RSD comprises between 4.2 and 6.6 %)

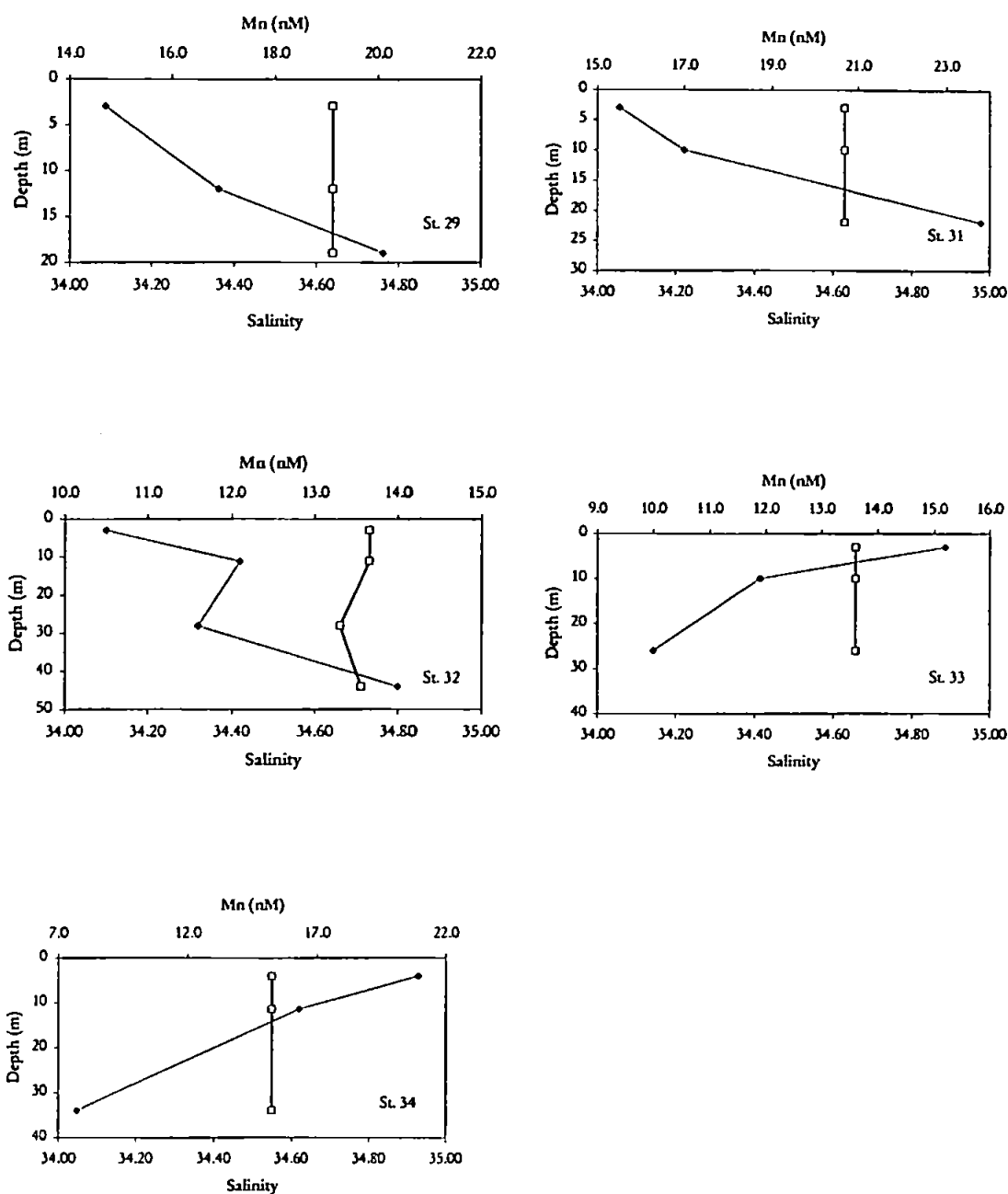


Figure 5.15 (continued): Depth profiles at the IMPACT stations (-- represents Salinity; -◇- represents Mn; RSD comprises between 4.2 and 6.6 %)

5.3.4 Co and Mn in North Sea waters

A comparison of our data with those from other authors is important as a first approach for data quality. However the trace metal concentrations in shelf waters and especially in large estuaries are variable due to variability in freshwater discharges and metal inputs to the system, tidal influences, and therefore comparisons between the various data sets is often difficult. In addition, differences in exact sampling locations and states of the tide will have an important effect on the observed trace metal concentration in marine systems, and will impair our abilities to compare data sets from different surveys. Nevertheless, previously reported values are included in the discussion as an indication of the overall accuracy of the results from this study. Concentrations of Co and Mn are reported in Table 5.2 for coastal waters around UK. The data obtained in this study are generally in good agreement with data from the literature, and suggest good data quality and that the concentrations of Co and Mn have remained within a relatively narrow concentration range over the last decade. Our measurements show that the dominant process determining cobalt concentration is dilution of high concentration river water inputs by low concentration Atlantic surface waters, indicating also that the shelf waters contained elevated cobalt levels relative to the geochemical "norm" (vertical distributions of Co in the open ocean are at a maximum in surface waters, ca. 4-50 pM, and depleted to less than 20 pM at depth) (Donat and Bruland, 1995). Cobalt is a particle reactive metal, and will therefore be scavenged by suspended particulate matter in estuarine and coastal areas. This mechanism probably contributed to the reduction in Co(II) concentrations in offshore waters. Possible evidence of benthic inputs can be found in the near coastal area of the Humber.

Table 5.2: Co and Mn concentrations in coastal waters

Typical levels of Mn (nM) and location	Typical levels of Co (nM) and location
Not measured	0.33 ^{a)} (maximum value) Humber
Not measured	0.58 ^{a)} (maximum value) Tees
Not measured	0.15 ^{a)} (maximum value) Tyne
6.2 ± 7.0 ^{b)} Central Southern North Sea	0.16 ± 0.10 ^{b)} Central Southern North Sea
8.0 – 13.8 ^{c)} Dogger Bank, Central North Sea	0.11 - 0.59 ^{c)} Dogger Bank, Central North Sea
3.9 – 24.6 ^{d)} North Sea	0.04 - 0.47 ^{d)} North Sea
3 – 40 ^{e)} Central North Sea	0.06 – 1.00 ^{e)} Central North Sea
10.1 ± 3.6 ^{f)} Irish Sea	0.14 ± 0.03 ^{f)} Irish sea
6.5 ± 1.7 ^{g)} Celtic Sea and English Channel	0.13 ± 0.04 ^{g)} Celtic Sea and English Channel
6.1 ± 1.3 ^{h)} Scottish Coast	0.07 ± 0.03 ^{h)} Scottish Coast
11.0 ± 13.8 ^{g)} Strait of Dover	0.32 ± 0.21 ^{g)} Strait of Dover
4.01 ± 1.51 ^{h)} English Channel	0.30 ± 0.32 ^{h)} English Channel
2.3 – 5.0 ⁱ⁾ English Channel	0.08 - 0.71 ⁱ⁾ English Channel
8 – 16 ^{j)} European Shelf area	Not measured

a) Achterberg et al., 1999; b) Burton and Statham, 1988; c) Fileman, et al., 1991; d) Hydes and Kremling, 1993; e) Kremling et al., 1987; f) Kremling and Hydes, 1988; g) Statham et al., 1993; h) Statham et al., 1999; i) Tappin et al., 1993; j) Kremling, 1985.

Anoxic and suboxic conditions in the sediments may therefore result in benthic inputs of dissolved Co and both of this process and particle scavenging will weaken the Co-salinity relationship.

An important result is that significant concentration gradients across the thermocline were not observed, probably due the relatively high “background” levels (compare with open ocean values) (Wong et al., 1995), the shallow depths and relatively rapid turn-over of the water-column.

Distributions of Mn near to land are mainly determined by riverine, atmospheric and sediment inputs, desorption-adsorption on particles, and redox chemistry of the metal (Burton et al., 1993; Tappin et al., 1995). An important factor in the biogeochemical cycle of Mn is the solubilisation of aerosol-bound manganese on contact with coastal seawater (Statham and Chester, 1988). Atmospheric fluxes are often less important (Chester et al., 2000; Tappin et al., 1993; Williams et al., 1998) compared with riverine and sediment fluxes. The sediments appear to be an important source, with rivers contributing to enhanced Mn concentrations in nearshore waters. Dehairs et al. (1989) reported that suspended particulate matter collected in the North Sea was enriched in manganese after the spring bloom period relative to the preceding winter. The enrichment was driven by a benthic flux of dissolved manganese into the water column and subsequent removal of manganese to particles. The sedimentary flux of manganese was initiated by aerobic demineralisation of sedimented spring bloom material at the sediment surface; subsequent oxygen depletion was then followed by dissolution of solid manganese phases (Dehairs et al., 1989). It has been reported (Tappin et al., 1993) that the occurrence of elevated concentrations of manganese above the thermocline is not a common phenomenon in European shelf waters. Kremling

et al. (1987) did not observe similar surface Mn enrichment for stratified regions of the North Sea. Our Mn data shows strong evidence of riverine Mn inputs to nearshore coastal waters. Nearshore stations showed clear surface maxima of Mn, which coincided to a slight minimum of salinity (e.g. stations 3, 5, 7, 9, 10, 11, and 13). Therefore the Mn signal can be attributed to a freshwater source. The near surface minima can also be partly caused by strong atmospheric Mn inputs in this part of the western North Sea. Evidence of benthic Mn inputs was observed at offshore deep stratified stations. For example, at stations 20, 22, 26, and 32 enhanced bottom waters Mn concentrations were evident, with values reaching ca. 14 nM in bottom waters at station 32. The thermocline at these stations forms a physical limit against mixing, and consequently surface Mn values are much lower than bottom waters values. Furthermore, other stations situated in the central North Sea (27, 29, and 31) also showed an increase in Mn concentrations with depth, indicating a benthic source. Stations closer to land, indifferent to the immediate impact of the Humber plume, showed evidence of atmospheric Mn inputs (stations 17, 18, 22, 23, 25, 27, 28, 33, and 34). This suggests that the atmosphere forms are additional and important sources of Mn to coastal waters of the western and central North Sea.

The observation of the trace metal data in relation with salinity values shows a lack of correlation with salinity and between Co and Mn:

$$\text{Mn} = 0.48 \text{ Sal} - 7.29; \text{Co} = -0.075 \text{ Sal} + 2.78; \text{Co} = 0.0025 \text{ Mn} + 0.188.$$

These observations are most likely due to the dynamic nature of the coastal waters of the North Sea, with diverse riverine, benthic, atmospheric inputs, biological, particle-scavenging removal processes and in some areas strong tidal currents (Charnock et al., 1994). All the input and removal process are highly dynamic on a temporal and spatial scale, complicating the interpretation of

coastal trace metal behaviour. However, it appears that Mn and Co have a different behaviour in the coastal water of the North Sea, with benthic and atmospheric inputs being more important for Mn.

The large difference in concentrations of the two metals investigated between shelf waters of high salinity and river waters entering the southern North Sea is exemplified looking at the concentrations of surface dissolved Co and Mn in the central zone of the southern North Sea and in the Humber Estuary (Table 5.3).

Table 5.3: Concentrations of Co(II) and Mn(II) in the Central southern North Sea and in the Humber Estuary (concentration given for the central zone of the southern North Sea is the mean, with standard deviation).

	Co (pM)	Mn (nM)
Central southern North Sea (S > 33.8)	203.2 ± 16.9	9.4 ± 1.2
Humber Estuary (S = 30.1 – 32.8)	184.6 - 1021.0	7.7 - 26.8

5.3.5 Tidal cycle study in the Humber estuary

At Station 8 (53° 32` 8" N, 0° 05` 5" E) in the mouth of the Humber a tidal cycle was undertaken (sampling period: 13 hours). Table 5.4 shows tidal state at our station during its occupation.

For many pollutants the Humber is a main source for the North Sea (Robson and Neal, 1997; Vice, 1993). The Humber estuary receives pollutant loads from industrial and domestic discharges (National Rivers Authority, 1995).

Table 5.4: Different states of tide at Station 8

GMT	Tidal state
2:30	Max flood
4:10	High water
7:00	Max Ebb
10:30	Low water
12:30	Ebb

The catchment of the Humber is the largest of any UK estuary, covering ca. 20% of the area of England ($26 \times 10^3 \text{ km}^2$). The strong influence of the rivers discharging waters with enhanced cobalt and manganese concentrations into the Humber is shown in Figure 5.16. The data are plotted in the sequence in which they were obtained. Cobalt values reached a maximum of 0.102 nM at a salinity of 30.5; a maximum manganese concentration of more 25 nM and Total Oxidisable Nitrogen (TON) of 80 μM (Gardolinski, personal communication) were observed at the same tidal state. Similar results have been observed during the same tidal cycle study for total dissolved Cr (Achterberg et al., 1999). Our results indicate that highest Co, Mn and TON concentrations were found at low salinity and lowest contaminant concentrations at high salinity (flood tide). This shows the importance of riverine/estuarine contaminant inputs into the western North Sea.

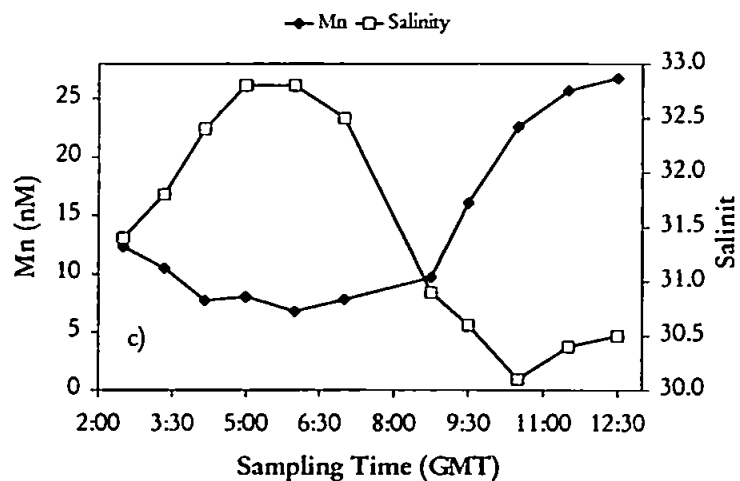
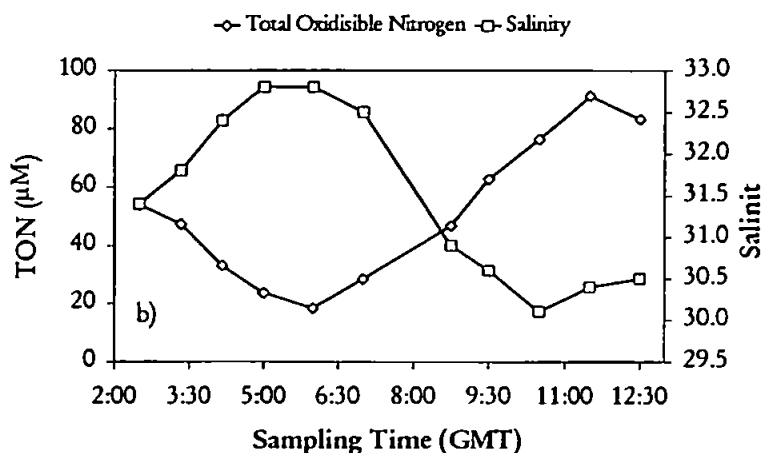
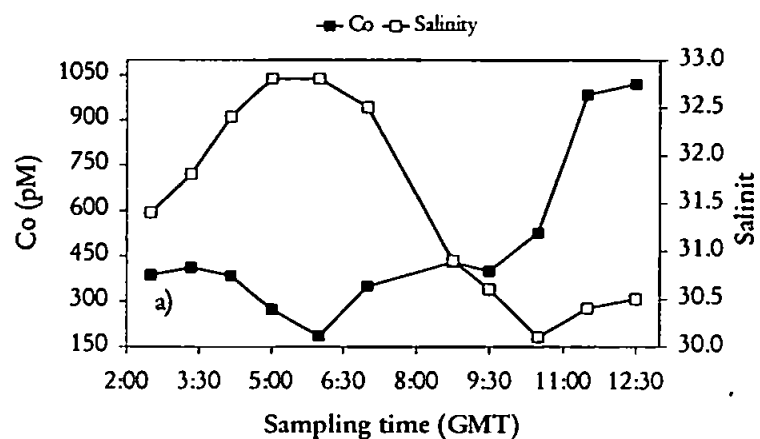


Figure 5.16: a) concentration of dissolved Co, b) Total Oxidisable Nitrogen (TON) and c) concentration of dissolved Mn during a tidal cycle at the Humber mouth (RSD <7%).

5.4 CONCLUSIONS

FI-CL manifold based on the pyrogallol reaction can be used for the determination of Co in seawater. The FI-CL instrumentation was sufficiently rugged and portable to be deployed on-board ship. FI-CL manifold based on the TCNQ-O₂-Eosin Y-DDAB reaction can be used for the determination of Mn in seawater. As a result of the development of an accurate and precise method for the determination of low concentrations of dissolved Co and Mn, it is possible to achieve a good understanding of the concentrations at which these metals occur in coastal waters. The processes, however, which control the distribution of dissolved cobalt and manganese in shelf waters are not well understood. Many data have been gained from single deep ocean station profiles (Sakamoto-Arnold and Johnson, 1987; Knauer et al., 1982; Johnson et al., 1988; Coale, 1991; de Jong et al., 2000; Klinkhammer, 1994; Sunda and Huntsman, 2000; Yeats et al., 1992). In contrast, in coastal waters the different processes controlling metal distributions tend to be superimposed – inputs can be from rivers, sediments, atmospheric and in situ degradation of material; removal can be by biological uptake, sorption in or on particulate and by flushing with ocean water. The dissolved cobalt and manganese concentrations obtained during the CH 148 cruise compared well with other cited literature values. This work shows the importance of riverine and benthic inputs. For Co, the Humber is an important source to the western North Sea, with a decrease in Co concentrations in an offshore direction. For Mn, the Humber posed an important source, but in addition benthic manganese resulted in enhanced Mn concentrations in deep waters at stratified stations. Atmospheric inputs were evident for Mn.

CHAPTER 6

INTERCOMPARISON OF ANALYTICAL METHODOLOGIES FOR THE DETERMINATION OF COBALT AND MANGANESE IN SEAWATER.

6.1 INTRODUCTION

It is important to be able to determine trace metal concentrations in marine (and freshwater) environments in order to monitor compliance with legislation and ensure good water quality (Worsfold et al., 2000). The challenge of determining trace metals in seawater environments is compounded by the potential interference from matrix constituents, particularly the major ions.

Boyle et al. (1977) stated that results for the determination of trace metals in seawater should not be accepted unless they meet at least one of the following three criteria: oceanographic consistency, interlaboratory agreement using the Certified Reference Materials (CRMs) such as the Canadian seawater trace metal standards (NASS, CASS and SLEW), and comparison of different analytical methodologies. The International Organisation for Standardisation (ISO) defines reference materials as follows:

Reference Material (RM) - material or substance one or more of whose properties are sufficiently homogeneous and well established to be used for the calibration of an apparatus, the assessment of a measurement method, or for assigning values to materials.

Certified Reference Material (CRM) - reference material, accompanied by a certificate, one or more of whose property values are certified by a procedure which establishes its traceability to an accurate realisation of the unit in which

the property values are expressed by and uncertainty at a stated level of confidence.

Reference materials are one of the cornerstones in producing reliable chemical measurements and, as such, have a wide range of applications in the laboratory. These include: method validation, instrument calibration, verification of instrumentation, laboratory and analyst performance, uncertainty estimation and internal quality control. In general, reference materials should be used on a regular basis within the framework of a sound quality assurance system. When used in this manner, the analyst can feel confident that the analytical system is under statistical control and is producing results that are fit for purpose.

An evaluation of the accuracy of the FI-CL analytical methods developed for cobalt and manganese has been carried out by determination of the concentrations of dissolved Co(II) and Mn(II) in seven samples from the Scheldt estuary using two additional analytical techniques. Co(II) concentrations have been determined by Adsorptive Cathodic Stripping Voltammetry (AdCSV). Mn(II) concentrations have been measured by Inductively Coupled Plasma - Mass Spectrometry (ICP-MS). Furthermore, Co(II) has been determined by FI-CL (using the oxidation of pyrogallol with hydrogen peroxide in an alkaline medium) with the Luminometer FS900CDT as detector at the Universite Libre de Bruxelles. The accuracy of the methods was ascertained by analysis of CRMs such as CASS-3 and SLEW-2.

6.1.1 Study Site

The Scheldt flows through northern France, western Belgium and the south-west of the Netherlands. Its hydrographic basin covers an area of 20,000 km² in one of the most populated and industrialised areas of Europe. Concentrations of dissolved Pb, Hg, Zn, Cu and Cd in the estuarine waters are about 2 times higher than in the marine waters of the Belgian coastal zone (which forms part of the Southern Bight of the North Sea) and an order of magnitude higher than oceanic concentrations (Baeyens, 1998; Baeyens et al., 1987). Therefore, for pollution control, a better understanding of the respective biogeochemical cycles of heavy metals in the Scheldt estuary with emphasis on the basic governing processes is important. Geophysical (water and sediment circulation) and biological (production and biodegradation) processes are important to estuarine environments. Human activities such as discharging of liquid waste and dredging of sludge are superimposed on the natural processes and, moreover, interfere with them. Four aspects make the Scheldt estuary very peculiar and distinct from other estuaries: (1) the Scheldt is a tide-governed estuary due to the low river flow which leads to large residence times; (2) the upper estuary receives large inputs of biodegradable organic matter inducing anoxic conditions in the water column during summer; (3) considerable and direct supply of toxic pollutants occurs in the upper estuary as a result of the diverse activities of industries around Antwerp; (4) the anoxic zone, the area of pollutant inputs and the zone of maximum turbidity coincide geographically, making it very difficult to distinguish between their individual effects on the metal distribution and behaviour. The river Scheldt is a lowland-river, which rises in the northern part of France (St. Quentin), and flows into the North Sea near Vlissingen (the Netherlands). The total length of the river is 355 km, the fall over the total river

length is at most 100 meters and the mean depth of the Scheldt estuary is about 10 m. The river Scheldt (Figure 6.1) as well as all its branches are rain-fed. The discharge of these rivers varies considerably with minimal discharges occurring in summer and in autumn, and maximum ones in winter and spring. During winter and spring, the lower riverine part from Gent to Antwerp is a tidal fresh water river. During summer and autumn, on the contrary, when the discharge of the river is reduced, the water becomes brackish between an Antwerp and the Rupel mouth. In the total river basin of the Scheldt live approximately 7 million people. Urban areas with population densities of over 1000 inhabitants per km² are found near Lille (France), Gent, Brussels and Antwerp. The largest industrial areas are concentrated near Lille, Antwerp, along the canal from Gent to Terneuzen, and near Vlissingen. The river Scheldt and its branches are used as a major drain for industrial and domestic wastes. A substantial part of these is not treated in a waste water treatment plant. This gives rise to very poor water quality in the larger part of the river and the eastern part of the estuary (Baeyens et al., 1998a; Baeyens et al., 1998b).

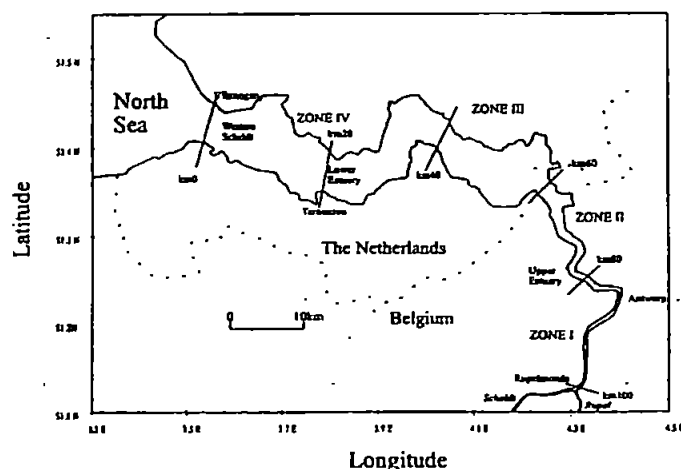


Figure 6.1: Map of the Scheldt Estuary. Lower estuary (km 0-km 60). Upper estuary (km 60-km 100) (reproduced from Baeyens et al., 1998c).

Four sections (see Figure 6.1) can be distinguished in the Scheldt river basin: the non-tidal fresh water river corresponding to the upper-Scheldt and a considerable part of the branches; the mostly fresh water tidal river extending from Gent to Rupelmonde with the lower parts of some tributaries; the upper estuary (brackish) or the Sea Scheldt between Rupelmonde and the Belgian-Dutch border; and the lower estuary (brackish and salt) called the Western Scheldt. The predominant factors determining the hydrological characteristics of the Scheldt river are the fresh water flow rate and the tidal influence. The mean discharge rate of the Scheldt, determined at Schelle (90 km from the mouth), amounted to $104 \text{ m}^3 \text{ s}^{-1}$. However, since the Scheldt is a typical rain-river, the actual discharge rate is highly dependent on the season. Over the total catchment area about 30% of the rainfall drains into the surface water, but in densely populated areas such as Brussels and Antwerp this value increases to 45%. During winter, the average discharge rate amounts to $180 \text{ m}^3 \text{ s}^{-1}$ with exceptional values of up to $600 \text{ m}^3 \text{ s}^{-1}$.

Average summer values decrease to $60 \text{ m}^3 \text{ s}^{-1}$ with minimal values down to $20 \text{ m}^3 \text{ s}^{-1}$ (Paucot et al., 1997). The major tributaries of the Scheldt river are the Dender, the Durme, and the Rupel (including Nete, Zenne and Dijle) accounting respectively for about 27, 6, 10 and 56 (17, 12, 27)% of the total fresh water input into the upper estuary. In addition, fresh water supply to the Western Scheldt occurs through the canal Gent-Terneuzen ($15 \text{ m}^3 \text{ s}^{-1}$), the discharge-sluice of lake 'Zoommeer' near Bath ($11 \text{ m}^3 \text{ s}^{-1}$) and some minor discharges from polders ($20 \text{ m}^3 \text{ s}^{-1}$). The Western Scheldt, the Sea Scheldt and the river Scheldt up to Gent and the lower parts of some tributaries are influenced by the tide.

The tidal range varies throughout the estuary and the tidal rivers, and this variability is paralleled by the volumes of water transported by the tide. In

Vlissingen the mean vertical tide is 3.8 m, whereas it is 5.0 m in Antwerp and 2.0 m in Gent. The flood volumes are respectively $1000 \cdot 10^6$ and $62 \cdot 10^6 \text{ m}^3$ per tide in Vlissingen and Antwerp. Hence, the Scheldt estuary is vertically well-mixed. Only in the neighbourhood of Antwerp, occasionally a small vertical stratification may occurs (Wollast et al., 1978). Since the residence time increases quickly with increasing vertical mixing due to dilution of fresh water in a large body of seawater, the residence time of fresh water in the Scheldt estuary is high (two to three months). The longitudinal salinity profile of the Scheldt (the transition between fresh and salt water is particularly smooth) is primarily determined by the magnitude of the river discharge. The tidal action, on the contrary, contributes to a lesser degree (the salinity during shift a tidal period is much smaller than the salinity change between low and high river discharge) (Bayens et al., 1998c).

6.2 EXPERIMENTAL

6.2.1 Sampling

Seven estuarine water samples were collected during part of a tidal cycle from the Scheldt estuary at a single geographic site near Antwerp (Belgium) on an ebb tide on the 25th July 2000 between 10:53 am and 16:53 pm by M. S. Charles and M. S. Yunus, Universite` Libre de Bruxelles (see Figure [Error! Not a valid link.](#)). Salinity was measured *in situ* using a home made salinometer. Filtration was undertake after a 20 min sedimentation period in an acid-cleaned plastic container through an acid cleaned (1 M HCl, 24 h) $0.45 \text{ }\mu\text{m}$ polycarbonate membrane filter (Sartorius), in a field-laboratory situated on a pontoon in the estuary. Samples were then acidified to pH 1.5 with 200 μl of HNO_3 (65 %

Suprapur, Merck Eurolab) per 100 ml of sample and stored in a refrigerator at approximately 5°C prior to analysis.



Figure 6.2: The sampling station

6.2.2 Reagents

6.2.2.1 FI-CL, AdCSV, and ICP-MS Reagents

For the determination of Co by chemiluminescence with the luminometer detector (in Brussels) the following reagents were used without further purification and prepared in UHP water (the reagents were prepared as reported in Chapter 3); pyrogallol (ACS grade, Aldrich), methanol, cetyltrimethylammonium bromide (CTAB, Microselect 99%, Fluka), hydrogen peroxide 30% (Merck, BDH).

For the determination of Mn by TCNQ-DDAB-Eosin Y chemiluminescence, the following reagents were used: DDAB, Eosin Y, NaOH, and TCNQ (obtained from Fluka) and NaOH (BDH; AnalaR). All reagents were prepared in UHP water (the reagents were prepared as reported in Chapter 4).

The reagents for the analysis of Co by AdCSV were dimethylglyoxime (DMG); (Aldrich 99+%; 200 μ M, final concentration in cell) and borate buffer (Merck, BDH Aristar, 10 mM final concentration in cell) at pH 8.5. The acidified samples were neutralised to pH 8 with ammonia (purified using isopiestic distillation). H_2O_2 for the UV-digestion step was 30% v/v (Merck, BDH Aristar). For the analysis of Mn by ICP-MS, HNO_3 (2% v/v) was used to rinse the ICP-MS system between two subsequent analyses.

6.2.2.2 Cobalt and Manganese Standards

A 179 μ M Co(II) stock standard was prepared by dilution of a 1000 mg l^{-1} (17.9 mM) Co(II) atomic absorption standard solution ($\text{Co}(\text{NO}_3)_2$, BDH Merck, SpectrosoL), in 0.5 M nitric acid. Other standards were prepared daily in 0.05 M sub-boiled, quartz distilled hydrochloric acid (Q-HCl) by serial dilution.

A 182 μ M Mn(II) stock standard was prepared by dilution of a 1000 mg l^{-1} (18.2 mM) Mn(II) atomic absorption standard solution ($\text{Mn}(\text{NO}_3)_2$, BDH Merck, SpectrosoL), in 0.5 M nitric acid. Other standards were prepared daily in 0.05 M Q-HCl by serial dilution.

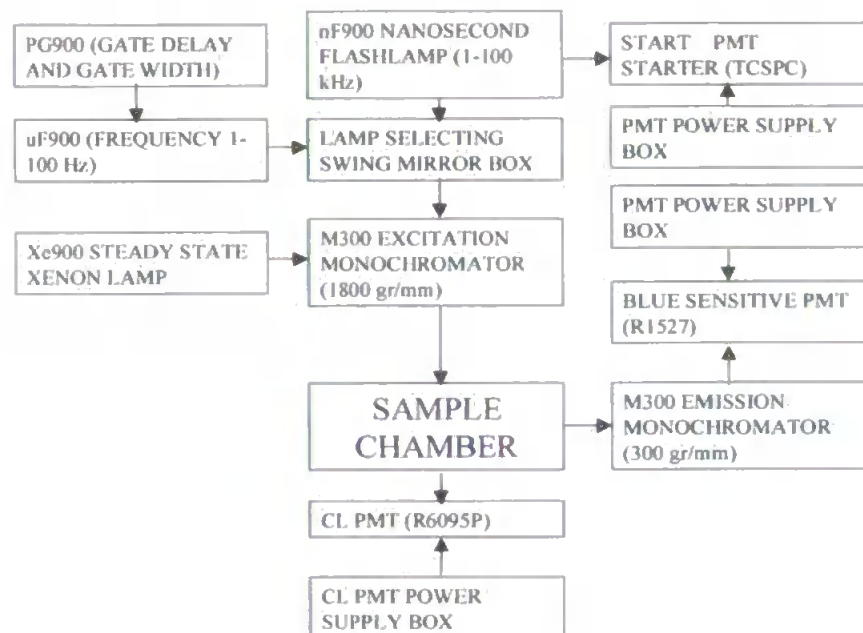
6.2.3 The Luminometer FL/FS 900

The luminometer is a modified version of a commercial instrument (FL/FS 900 from Edinburgh Analytical Instruments) capable of monitoring fluorescence (FL) and room temperature phosphorescence (RTP) decay curves after pulsed excitation, FL and RTP steady state signals and transient chemiluminescence (CL) emission with a T geometry. The specific features of the instrument are the following. Emission can be monitored at 90° to the excitation beam for FL and RTP. A flipping mirror is incorporated to select the appropriate light source in

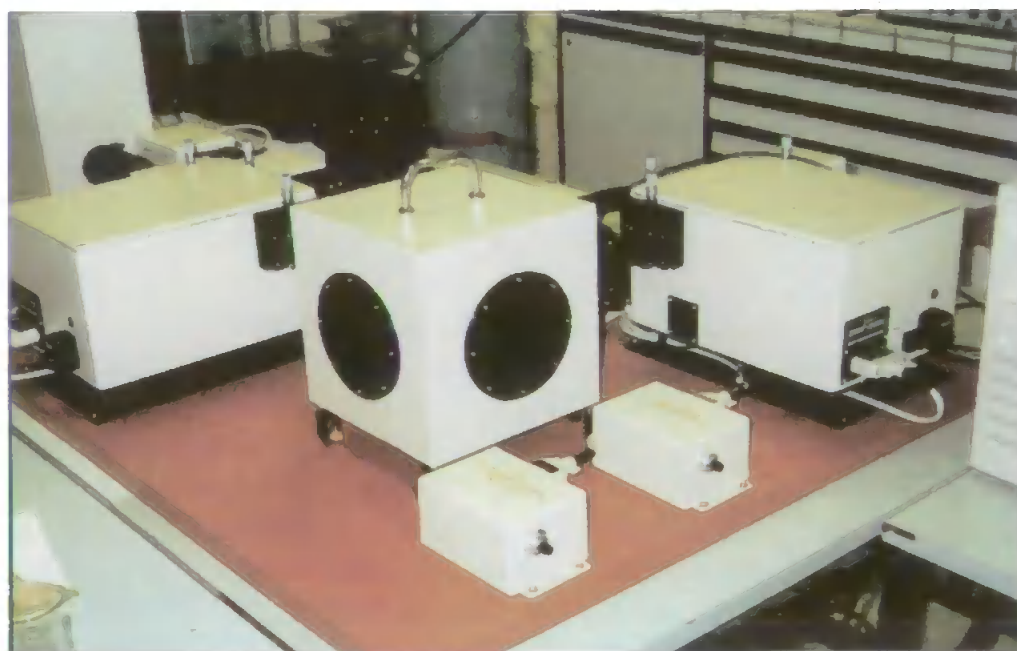
front of the excitation monochromator and a special cell compartment for CL measurements is added. Excitation wavelengths (200-750 nm) can be selected by a 300 mm focal length grating (G318 HO μ 25) blazed at 250 nm. Emission wavelengths (200-900 nm) can be selected by a second monochromator equipped with a grating (G318HO μ 5) blazed at 500nm. A Hamamatsu R1527 PMT is used to measure light intensities in the photon counting mode.

The excitation source used for steady state FL is a continuous 450 W Xe-arc (Xe 900; 230-2000 nm). The light source used to record time-resolved fluorescence emission is a nF 900 nanosecond flashlamp filled with hydrogen. The source emitted approximately 10^8 photons per pulse in the wavelength range 110-850 nm with a FWHM of 0.8 ns. Its power output was > 5W at 100 Hz; its frequency can be adjusted between 1-100 Hz and its FWHM was in the range 1.5-3 μ s. The pulses are viewed by a 9661B Electron Tubes PMT in the Time Correlated Single Photon Counting (TCSPC) technique. A μ F 900 us flashlamp serves as an excitation source for monitoring RTP spectra and decay profiles. The delay and gate times are 0.05 ms and the excitation and emission slits are set at 10 and 20 nm, respectively. CL signals are measured with a R 6095 Hamamatsu PMT. A PC controls the luminometer. Data acquisition and analysis are performed by the FS900 CDT Edinburgh Instruments Software for CL and steady state FL and RTP emissions. Data acquisition and analysis in the TCSPC mode are performed with the FL 900 CDT and FLA 900 level 2 software packages.

For our investigations, a photon multiplier assembly was positioned on the luminometer, with a transparent PTFE flow cell mounted in front of the PMT. A block diagram of the instrumentation is shown in Figure [Error! Not a valid link.](#) together with a photograph of the arranged FI-CL set-up for cobalt determination used during the analyses of the Scheldt samples in Brussels.



a)



b)

Figure 6.3: a) General optical arrangement of the FS900CDT spectrometer; b) photograph of the FS900CDT spectrometer.

6.2.4 Methodology

A detailed description of the FI-CL manifolds for the determination of Co and Mn is contained in Chapter 3 and in Chapter 4, respectively. The operating conditions were as follows. For the determination of Co using the FI-luminometer in Brussels, the Scheldt samples were diluted 1:4 with UHP water. A preconcentration time of 120 s on the 8-HQ column was used prior to analysis (Figure 6.4 shows the adapted manifold).

The determination of Mn by FI-CL (see Chapter 4) in Scheldt samples was undertaken after 1:16 dilution with UHP water. Samples were preconcentrated for 6 min onto the 8-HQ column prior to analysis.

The voltammetric equipment for the AdCSV analysis was a Hanging Mercury Drop Electrode (HMDE) Metrohm VA Stand 663, connected to a μ Autolab voltammeter (Ecochemie) via an interface for the mercury electrode (IME, Ecochemie). The whole system was PC controlled. The analysis of Co(II) with AdCSV was carried out by Dr. C. Braungardt. The acidified samples were UV-irradiated for 4 h prior to analysis in the presence of 0.05% v/v of H_2O_2 with a 400 W medium pressure mercury lamp (Photochemical Reactors Ltd). Sample temperature during UV digestion was ca. 70 °C. After filling the voltammetric cell with 10 ml of sample, the reagents were added, and the solution was de-aerated for 4 min using N_2 . Subsequently the Co-DMG complex was collected onto the HMDE for 50 s, at a deposition potential of -1.0 V. The AdCSV method used square wave modulation at 50 Hz and the scan was from -1 to -1.3 V.

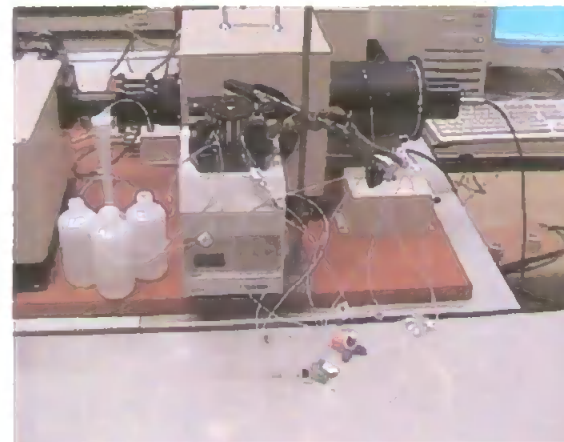
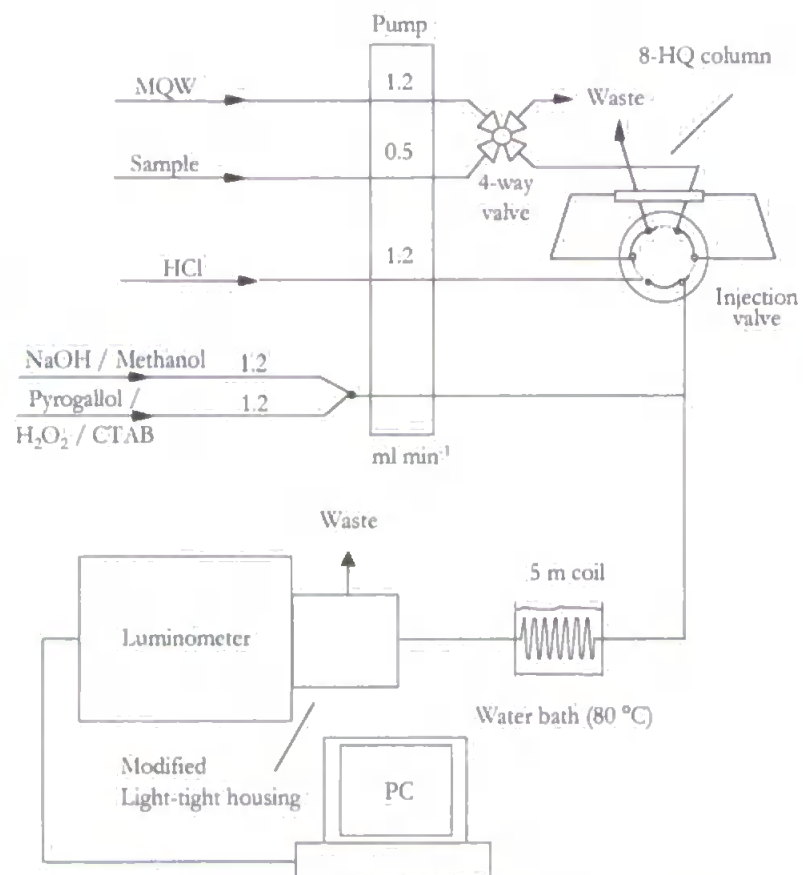


Figure 6.4: FI-CL manifold for the determination of Co(II) with the luminometer detector. Inset: Photograph of the arranged manifold for the measurement of Co by FI-CL analysis.

A commercially available ICP-MS instrument was used (Plasmaquad PQ-2) for the determination of Mn in Scheldt samples.

The operating conditions and main acquisition parameters are summarised in Table 6.1. For the determination of Mn by ICP-MS the samples were diluted 1:4 with UHP water and analysed through direct injection.

Table 6.1: Instrumental ICP-MS conditions and measurement parameters

ICP-MS Plasmaquad PQ-2	Operating conditions
Forward power (W)	1350
Reflected power (W)	4
Gas flow rates:	
Plasma (L/min)	13
Auxiliary (L/min)	1.0
Nebulizer flow rate (L/min)	0.85
Nebulizer pressure (psi)	40
Sample depth	(8-10) mm
Acquisition mode	Peak jumping
Sample cone	Ni, 1.0 mm orifice
Skimmer cone	Ni, 0.4 mm orifice
Dwell time	320 ms
Washing solution	HNO ₃ 2% v/v
Flow rate	1 ml/min

6.3 RESULTS AND DISCUSSION

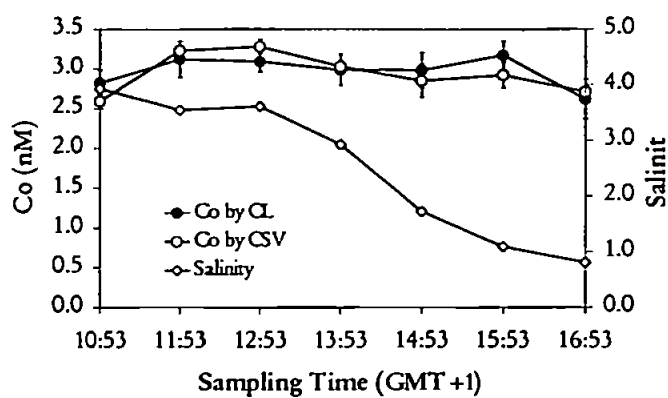
Table 6.2 shows the results for the analyses of the Scheldt samples, using the different analytical methods. The salinity ranged between 0.1810 and 3.926. The Mn concentrations ranged between 310 and 522 nM (ICP-MS analysis), whereas the Co concentrations ranged between 2.59 and 3.28 nM (AdCSV analysis). Previous workers (Paucot et al., 1997) reported a much higher Mn concentrations (4000 nM at salinity 5) in the upper part of the Scheldt estuary. Co(II) concentrations observed in this study are in good agreement with values reported by Zhang ranging between 2 and 5 nM (Zhang et al., 1989). The dissolved Co concentrations in the Scheldt are lower compared with other estuarine systems. Co concentrations in the range of 7-11 nM were observed in the Tamar estuary at salinities 6-10 (Cannizzaro et al., 1999). The dissolved Mn concentrations in the Scheldt are similar to other estuarine systems (Burton et al., 1993). Mn concentrations in the range of 330-460 nM were observed in the Rhine estuary at salinities 2.4-7.6. For both Mn and Co, there is no clear correlation with salinity (see Figure 6.5a,b). Cobalt and manganese therefore showed a non-conservative behaviour for the dissolved phase, indicating a weak removal mechanism in the Scheldt. It must be noted that our sampling approach resulted in samples with a narrow salinity range and this limits our ability to fully interpret geochemical parameters affecting Co and Mn in the Scheldt. Similar results have been obtained for the measurement of Cd by fluorescence (performed by M. S. Charles and M. S. Yunus from the Université Libre de Bruxelles, see Figure Error! Not a valid link.c). The Cd-salinity relationship was linear ($r^2 = 0.95$) and is assigned to the formation of CdCl_2 complexes following the desorption of cadmium from suspended solid matters, due to the

increasing concentration of chloride at high tide during the mixing of freshwater with seawater.

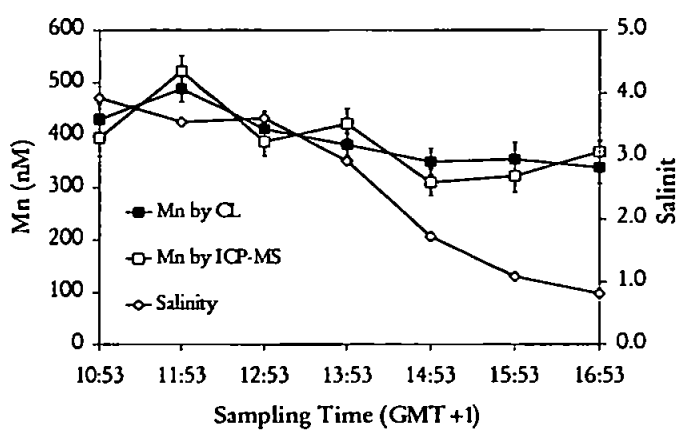
It could be argued that the values for Mn concentrations determined by ICP-MS should be higher than the values obtained by FI-CL. The reason for that is ICP-MS measures the total amount of Mn in solution. However Mn(II) is the main specie in seawater (see Table 1.2).

Table 6.2: Data obtained for Co and Mn for the analyses of the Scheldt samples with the different methods, and salinity (all the concentrations are expressed in nM).

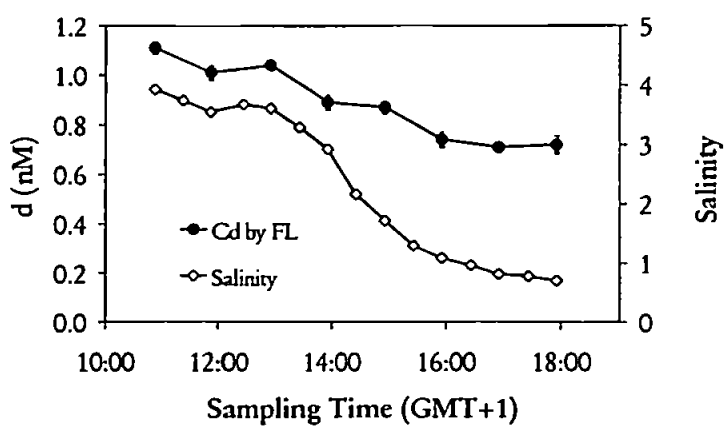
Time (GMT+1)	Mn (ICP-MS)	Mn (FI-CL)	Co (AdCSV)	Co (FI-CL-Luminometer)	Salinity
10:53	395 ± 35	430 ± 30	2.59 ± 0.09	2.82 ± 0.17	3.926
11:53	522 ± 30	488 ± 25	3.23 ± 0.06	3.12 ± 0.23	3.546
12:53	388 ± 27	412 ± 34	3.28 ± 0.09	3.09 ± 0.13	3.607
13:53	422 ± 29	382 ± 22	3.03 ± 0.07	2.99 ± 0.20	2.925
14:53	310 ± 26	349 ± 26	2.85 ± 0.21	2.98 ± 0.22	1.722
15:53	322 ± 31	354 ± 33	2.92 ± 0.16	3.17 ± 0.18	1.086
16:53	368 ± 22	338 ± 31	2.71 ± 0.07	2.62 ± 0.25	0.810



a)



b)



c)

Figure 6.5: Mn, Co, Cd and salinity data for the Scheldt estuary samples during tidal cycle: a) Co by AdCSV and FI-CL with luminometer detector; b) Mn by ICP-MS and FI-CL; c) Cd by fluorescence.

6.3.1 CRM results

Table 6.3 illustrates the reliability of all the considered techniques producing observed values within the range of the certified concentrations for Co and Mn. By applying a pooled *t*-test on the different analytical populations no significant statistical difference (95% confidence limits) were found between the various techniques for Co and Mn.

Another confirmation of accuracy can be obtained by using different analytical methods on the samples, with a statistical test to verify analytical agreement. The results of two different analytical methods may be compared using the *t*-test in order to evaluate if they differ significantly. The *t*-value for the determination in the Scheldt samples of manganese by FI-CL and ICP-MS and cobalt by FI-CL and AdCSV are respectively 0.29 and 0.39. The critical value of $|t|$ ($P=0.05$) at 6 degrees of freedom is 2.45 (Miller and Miller, 1993). Since the experimental value of $|t|$ is less than the reference value, the difference between the two results is insignificant at the 5% level confirming a good agreement between experimental results for the different methods for the determination of Mn and Co.

Table 6.3: Accuracy of applied techniques for the determination of Mn(II) and Co(II) in seawater CRMs with AdCSV, FI-CL, and ICP-MS (all the concentrations are expressed in nM).

Metal analysed	Observed AdCSV	Observed FI-CL	Observed ICP-MS	Certified value (CRM)
Mn(II)	-	47.9 ± 5.7	-	45.68 ± 6.55 (CASS-3)
Mn(II)	-	73.2 ± 4.9	70.6 ± 3.7	70.98 ± 5.46 (SLEW-2)
Co(II)	0.92 ± 0.13	-	-	0.87 ± 0.21 (SLEW-2)

6.4 CONCLUSIONS

The project offered the opportunity to bring together four laboratories with complementary experience in analytical chemistry, flow-injection methods, instrumentation, marine sciences, organic compound synthesis, optical and time-dependent luminescence techniques. Our contribution has resulted in the development and optimisation of the FI-CL chemistries for Co and Mn (together with Fe and Cu, by other researchers) in seawater. The FI-CL approach has been successfully applied for laboratory studies of Co and Mn in coastal waters (Scheldt estuary). The Plymouth contribution has resulted in the transfer of the technology to Brussels and Oviedo.

As it appears, a high level of integration of the different tasks was achieved; yet provision was allowed for the development of each partner's own independent instrumentation. The analytical and technological know-how developed by the partners was integrated in a single multi-technique optical equipment in the coordinator laboratory. The common equipment was successfully applied to specific cation monitoring and can integrated chemiluminescence, fluorescence and room temperature phosphorescence based detection system. It is a first step towards multi-analyte, multi-detection instrumentation.

A project server was created as a World Wide server accessible by Internet and supporting technical data can be found at the MEMOSEA website <http://www.ulb.ac.be/sciences/cop/MAST-III/main.htm>.

CHAPTER 7

CONCLUSIONS AND FUTURE WORK

7.1 General conclusions

The need to accurately assess and continuously monitor the input of trace metals into rivers, estuaries and the sea is a fundamental responsibility of society. By developing and establishing more efficient and reliable monitoring techniques the scientific community will be in a better position to study the fate of trace metals and to judge the effects of trace metals pollution on marine ecosystems.

This project gives support to current EU legislation concerning water, e.g. "Pollution caused by certain dangerous substances discharged into the aquatic environment of the Community" (76/464/EEC) and "Convention for the prevention of marine pollution from land-based sources" (75/437/EEC).

The potential direct economic benefits are considerable. Application of the new monitoring techniques remove the need for expensive and labour intensive sample collection, processing and analysis in the laboratory. High resolution data would be available immediately and could be used for law enforcement in the case of calamities, or the data could be used for water quality modelling purposes. The new monitoring strategy is environmentally friendly. Ship-board analysis eliminated the need for use and subsequent disposal of plastic sample containers. Also toxic organic solvents are not used for extraction/preconcentration (as in current practices) hence there is no longer

associated costs for waste solvent disposal. Inter-laboratory collaboration within the EU and beyond will be encouraged in order to promote and transfer new technologies. The economic and possible social impacts are linked to the high potential for multisectorial industrial applications of the instrumentation constructed.

- The attraction of the flow injection (FI) approach with chemiluminescence (CL) detection for monitoring of Co and Mn in marine systems was the simplicity, robustness and portability of instrumentation coupled with the excellent detection limits (nM to pM) and rapid response (minutes) that made it ideally suited to shipboard operation. These methodologies generated validated trace metal data at sea with high spatial and temporal resolution.
- The 8-HQ resin was perfectly suitable for the preconcentration of trace metals in seawater. It was also very efficient for seawater matrix removal. The effect of the sample pH on the chelation ability of the resin is the most important parameter to know in order to predict a reliable use of the resin. Most of the transition metals of environmental interest (e.g. Cu(II), Ni(II), Co(II), Fe(III)) could be retained in the resin at pH 5 and higher with the only exception of Cr(III). The new jacket column permitted an easy replacement of the resin within a few minutes. The column was easily integrated in FI systems and the dimensions chosen (size 10 mm length by 2.5 mm i.d.) gave the best results in terms of accuracy and sample throughput.

- The method for the determination of dissolved Co at the picomolar level based on a flow injection technique coupled with pyrogallol chemiluminescence detection has been improved in terms of LOD and preconcentration time compared with previous methods. A practical limit of detection of 5 pM was achieved with a preconcentration time of 60 s. One analytical cycle could be completed within 8 min, making this system suitable for real-time analyses. The reproducibility of the system was in the range 2-6%.
- The method for the determination of dissolved Mn by exploiting the Mn(II) catalysis of the oxidation of 7,7,8,8- tetracyanoquinodimethane (TCNQ)-O₂-OH-Eosin Y in presence of didodecyldimethylammonium bromide (DDAB) was fully developed. A practical limit of detection of 3 nM was achieved with a preconcentration time of 6 min. One analytical cycle could be completed within 26 min. The reproducibility of the system was in the range 3-7%.
- Shipboard results confirm the feasibility of using a flow injection-chemiluminescence method for Co and Mn in seawater. Environmental data on the distribution of Co and Mn in the western North Sea was successfully acquired. The data were obtained using FI-CL methods at the sea and in the lab. The dissolved cobalt and manganese concentrations obtained compared well with literature values. The work showed the importance of riverine and benthic inputs and the complex biogeochemistry of these metals in coastal marine environments.
- The chemiluminescence technique was combined with the luminometer as a detector and good statistical agreement (by *t*-test) was found for the

measurements of the concentrations of Co and Mn with other analytical methods such as AdCSV, and ICP-MS respectively.

7.2 SUGGESTIONS FOR FUTURE WORK

7.2.1 Speciation

The overall goal of the environmental metal speciation studies is to provide the data required for environmental impact assessment of trace metals by determining their chemical speciation, distribution, properties and fluxes. The impact assessment of trace metals in the natural environment is ultimately concerned with how these metals directly or indirectly affect the biota.

Each CL reaction reported in this thesis is selective towards Co(II) and Mn(II) species. Historical modelling papers report that Co is mainly inorganically bound in seawater (main complexes are Co^{2+} , CoCO_3 , CoCl^+), however more recent studies showed that a variable percentage of Co(II) (between 40 and 70%) is organically bound in seawater. The incorporation of an in-line U.V. photo-oxidation unit (using lamps with different powers, e.g. 120 or 400 W, and/or adding chemical reagents such as H_2O_2) for breakdown of organically bound Co complexes would enable a series of studies to be performed aimed at resolving the speciation of Co in seawater (although this technique has not always proven 100% effective in completely destroying organic complexes). The primary dissolved form of Mn is thought to be Mn(II). The main form of Mn(II) in seawater is computed to be free hydrated ion (58%) and chloride complexes (37%) (Turner et al., 1981), although some workers (von Langen et al., 1997) suggest that there may be some soluble Mn(III) complexes in natural waters, they are likely to be present only as meta-stable intermediates, and most of the Mn(III) is also present as particulate oxides. Therefore the next stage in

the development of the current FI-CL technique is the validation of a new analytical method which employs pre-treatment steps (acidification, reduction) which may alter species composition (FIA-CL has been already used to assess copper complexation in seawater by Zamzow et al., 1998).

7.2.2 The preconcentration/matrix removal step

On-line matrix separation and preconcentration by flow injection analysis with sorbent packed minicolumns has been shown to be very useful in the determination of trace metals. A number of chelating resins containing aminocarboxylic acid groups, iminodiacetic acid, and many others are today commercially available or easy to synthesise. It is of interest to prepare new chelating resins having specificity for a selected metal ion (the specificity or selectivity of a chelating resin is usually correlated to that of the monomeric compound corresponding to the functional group). For example 4-methyl-8-quinolinol is almost twice as selective for Co than the 8-quinolinol (8-HQ). Moreover the properties of chelating sorbents and their analytical possibilities depend on many factors and the most important one is the nature of chemically active groups capable forming complexes with the metal ions in solution. Also essential is the nature of the polymeric matrix, as well as the methods of synthesis of sorbents. To characterise the properties of chelating sorbents it is necessary to investigate their acidic and basic properties, complexing capacities, and selectivity with respect to metal ions, depending on conditions, kinetic properties, and possibilities of regeneration.

7.2.3 In-line Standard Addition(s)

The application of the FI-CL technique reported in this thesis relies on an internal standard addition method for quantification of Co and Mn in the sample. The reason for adopting such a procedure was to eliminate any possible change in calibration sensitivity that may have resulted from a change in sample matrix. One possible improvement to this method would be to incorporate a multi-port valve for standards and mixing loop, which would enable an automated in-line standard addition to be performed, reducing operator time and risk of sample contamination.

7.2.4 Multi-element FI-CL Technique

Advantages of field monitors using FI coupled with CL detection include rapid analysis, high sensitivity, robustness, minimal sample handling, compatibility with automated data acquisition facilities and low maintenance and running costs. As discussed in this thesis, the potential of CL-based analytical techniques for trace metals has been documented in numerous papers over the past decade. Such methods lend themselves to marine applications, although relatively few have actually been exploited for practical shipboard use. The next generation of FI-CL monitors could be based upon novel CL chemistries for the determination of a variety of trace metal in seawater. Since the instrumentation is generic, in the future it may be possible to adapt the current FI-CL monitor for the simultaneous, selective determination of two or more species (e.g. Mn, Co, Cu, Cr) based on different reaction chemistries. The success of such a multi-element monitor, however, will depend on an ingenious design of flow configuration to eliminate any interfering effect of one reaction on another.

7.2.5 Upgrade of Instrumentation

Since the onset of this research, there have been a number of commercial developments concerning the instrumentation used in the FI-CL monitor. The current detection system is based upon a high voltage photomultiplier unit, which possesses excellent sensitivity and has proved successful during the fieldwork reported in this thesis, but remains relatively large and somewhat fragile. The next generation of CL detectors is based on a miniature, low voltage (12 V) and more robust design. The incorporation of such a detection system into the current instrumentation will reduce the size of the current monitor and additionally, due to the nature of the output signals from such detectors, aid in the PC acquisition of CL signal. Such portable analytical monitors may then be controlled using user-friendly graphical programming operating and acquisition systems (e.g. LabVIEW®, National Instruments) run using notebook computers. A two dimensional CCD detector can be used to rapidly acquire chemiluminescence spectra from batch and continuous flow reactions with high spectral resolution and signal-to-noise ratio. This provides an excellent means of determining the spectral properties of chemiluminescence emitting species, which in turn can facilitate identification and mechanistic elucidation. Full spectral information can be obtained, allowing for enhanced data manipulation, e.g. multicomponent deconvolution.

7.2.6 Submersible FI-CL and sampling campaign

The use of discrete sampling methods to investigate pollution and biogeochemical processes can miss important concentration changes because of restrictions in sampling frequency. For example sunlight plays a crucial role in the formation of bioavailable manganese, since it drives the redox cycling of Mn

in oxic environmental systems. Bacterially mediated Mn(II) oxidation is suppressed by light and reduction of Mn(III, IV) is enhanced by light (through reductive dissolution of particulate Mn(III, IV)-(hydr)oxides).

Due to logistical limitations, only a limited amount of discrete samples can be collected from a research vessel using samplers (Go-Flo, Niskin) attached to hydrowire or rosette. In addition, discrete samples have to be stored and preserved until returned to a land based laboratory. Storage and sample preservations are critical steps with respect to metal contamination, and both sample bottles and acids need to be ultraclean. Furthermore, to minimise the contamination risk during sample handling, the vessel needs to have a clean room or container with filtered air. A much longer term goal for FI-CL trace metal monitoring would be the development of truly in situ (i.e. submersible) units. Such systems have already been designed and successfully deployed at sea for macro-nutrients based on spectrophotometry, although it would be a considerable challenge to modify the instrumentation for submersible CL detection. However, such a monitor would possess numerous advantages, eliminating the need for remote sample collection, minimising contamination problems and increasing the temporal and spatial resolution of a real-time data set. Deployments could be buoy or CTD mounted and accommodate several chemistries in tandem with sophisticated automation and communication technologies. One interesting application of such a unit would be the in situ deployment at km depths for mapping and tracing of species in hydrothermal vent plumes (e.g. Fe, Mn). Balls (1989) highlighted that exchange reactions with sediment would tend to absorb the impact of increased anthropogenic inputs making it difficult to see changes by monitoring the dissolved concentration of metals in coastal regions.

High-resolution and high-quality data are absolutely necessary to deconvolute the complex temporal and spatial behaviour of metals in coastal and estuarine waters.

REFERENCES

- Achterberg, E.P., Colombo, C., and van den Berg, C.M.G. *The distribution of dissolved Cu, Zn, Ni, Co and Cr in English coastal surface waters*. Cont. Shelf Res. 1999. **19**, 537 - 558.
- Albrecht, A., Reichert, P., Beer, J., and Luck, A. *Evaluation of the importance of reservoir sediments as sinks for reactor-derived radionuclides in riverine systems*. Journal of Environmental Radioactivity. 1995. **28**, 239 - 269.
- Albrecht, H.O. *Über die Chemilumineszenz des Aminophthasaurehydrazids*. Zeitschrift für physikalische Chemie. 1928. **136**, 321 - 330.
- Alexandrova, A. and Arpadjan, S. *Determination of trace elements in analytical-reagent grade sodium-salts by atomic-absorption spectrometry and inductively-coupled plasma-atomic emission-spectrometry after preconcentration by column solid-phase extraction*. Analyst. 1993. **118**, 1309 - 1312.
- Alwarthan, A.A. and Townshend, A. *Chemiluminescence determination of iron(II) and titanium(III) by flow injection analysis based on reactions with and without luminol*. Analytica Chimica Acta. 1987. **196**, 135 - 140.
- Alwarthan, A.A., Almuaibed, A., and Townshend, A. *Chemiluminescence determination of titanium(IV) by flow injection analysis using a Jones reductor column online*. Analytical Sciences. 1991. **7**, 623 - 625.
- Alwarthan, A.A., Habib, K.A.J., and Townshend, A. *Flow injection ion-exchange preconcentration for the determination of iron(II) with chemiluminescence detection*. Fresenius Journal of Analytical Chemistry. 1990. **337**, 848 - 851.
- Andrew, K.N., Blundell, N.J., Price, D., and Worsfold, P.J. *Flow injection techniques for water monitoring*. Analytical Chemistry. 1994. **66**, A 916 - A 922.
- Apte, S.C. and Batley, G.E. *Trace metal speciation: non electrochemical approach* in "Metal speciation and bioavailability in aquatic systems". Eds. Tessier A. and Turner D.R. Chichester, Wiley. 1995.
- Arimoto, R., Duce, R.A., and Ray B.J. *Concentrations, sources and air exchange of trace elements in the atmosphere over the Pacific Ocean* in "Chemical oceanography". Eds. Riley, J.P., Duce, R.A., and Chester, R. Academic Press, London - SEAREX: The sea/air exchange program. 1989. 107 - 149.
- Atanasova, D., Stefanova, V., and Russeva, E. *Co-precipitative pre-concentration with sodium diethyldithiocarbamate and ICP-AES determination of Se, Cu, Pb, Zn, Fe, Co, Ni, Mn, Cr and Cd in water*. Talanta. 1998a. **47**, 1237 - 1243.

- Atanasova, D., Stefanova, V., and Russeva, E. *Preconcentration of trace elements on a support impregnated with sodium diethyldithiocarbamate prior to their determination by inductively coupled plasma-atomic emission spectrometry*. Talanta. 1998b. **45**, 857 - 864.
- Azeredo, L.C., Sturgeon, R.E., and Curtius, A.J. *Determination of trace-metals in seawater by graphite-furnace atomic-absorption following online separation and preconcentration*. Spectrochimica Acta Part B-Atomic Spectroscopy. 1993. **48**, 91 - 98.
- Azubel, M., Fernandez, F.M., Tudino, M.B., and Troccoli, O.E. *Novel application and comparison of multivariate calibration for the simultaneous determination of Cu, Zn and Mn at trace levels using flow injection diode array spectrophotometry*. Analytica Chimica Acta. 1999. **398**, 93 - 102.
- Baeyens, W. *Evolution of trace metal concentrations in the Scheldt estuary (1978-1995). A comparison with estuarine and ocean levels*. Hydrobiologia. 1998. **366**, 157 - 167.
- Baeyens, W., Elskens, M., Van Ryssen, R., and Leermakers, M. *The impact of the Scheldt input on the trace metal distribution in the Belgian coastal area (results of 1981-1983 and 1995- 1996)*. Hydrobiologia. 1998a. **366**, 91 - 108.
- Baeyens, W., Gillain, G., Ronday, F., and Dehairs, F. *Trace metals in the eastern part of the North Sea. II: Flows of Cd, Cu, Hg, Pb and Zn through the coastal area*. Oceanol. Acta 1987. **10**, 301 - 309.
- Baeyens, W., Monteny, F., Van Ryssen, R., and Leermakers, M. *A box model of metal flows through the Scheldt (1981-1983 and 1992- 1995)*. Hydrobiologia. 1998b. **366**, 109 - 128.
- Baeyens, W., van Eck, B., Lambert, C., Wollast, R., and Goeyens, L. *General description of the Scheldt estuary*. Hydrobiologia. 1998c. **366**, 1 - 14.
- Baeyens, W.R.G., De Keukeleire, D., Korkidis, K., (Eds.) *Luminescence Techniques in chemical and Biochemical Analysis*, Dekker, New York. 1991.
- Balcerowicz, D., Balcerowicz, K., Slawinska, D., and Slawinska, J. Chem. Anal., (Warsaw). 1970. **15**, 479.
- Balls P.W. *The partitioning of trace metals between dissolved and particulate phases in European coastal waters: a compilation of field data and comparison with laboratory studies*. Neth. J. Sea Res. 1989. **23**, 7 - 14.
- Balls P.W. *Trace metals in the Northern Sea*. Mar. Pollut. Bull. 1985. **16**, 203 - 207.
- Batterham, G.J., Munksgaard, N.C., and Parry, D.L. *Determination of trace metals in seawater by inductively coupled plasma mass spectrometry after off-line dithiocarbamate solvent extraction*. Journal of Analytical Atomic Spectrometry. 1997. **12**, 1277 - 1280.
- Baturin G.N. *The Geochemistry of Mn and manganese nodules in the ocean*. Ed. D. Reidel. 1988.

- Baturin, G.N., Dmitriyev, L.V., Rakovsky, E.E., and Kersky, A.N. *On geochemistry of iron-manganese crusts from the bottom of the south-atlantic*. Geokhimiya. 1989. 592 - 596.
- Beere, H.G. and Jones, P. *Investigation of chromium(III) and chromium(VI) speciation in water by ion chromatography with chemiluminescence detection*. Analytica Chimica Acta. 1994. **293**, 237 - 243.
- Bender, M.L., Klinkhammer, G.P., and Spencer, D.W. *Manganese in seawater and the marine manganese balance*. Deep-Sea Res. 1977. **24**, 799 - 812.
- Benkhedda, K., Infante, H.G., Ivanova, E., and Adams, F.C. *Trace metal analysis of natural waters and biological samples by axial inductively coupled plasma time of flight mass spectrometry (ICP-TOFMS) with flow injection on-line adsorption preconcentration using a knotted reactor*. Journal of Analytical Atomic Spectrometry. 2000. **15**, 1349 - 1356.
- Berg, E.W. *Physical and chemical methods of separation*. McGraw-Hill Book Company, New York. 1963.
- Bewers, J.M., Sundby, P.A., and Yeats, P.A. *The distribution of trace metals in the Western North Atlantic off Nova Scotia*. Geoch. et Cosmoch. Acta. 1976. **40**, 687 - 696.
- Beynon, R.J., and Easterby, J.S. *Buffer solutions*. Oxford University Press. 1996.
- Birks, J.W. *Photophysical and Photochemical Principles in "Chemiluminescence and photochemical reaction detection in chromatography"*. Ed. Birks J.W. VCH Publishers Inc. 1989
- Blain, S., Appriou, P., and Handel, H. *Preconcentration of trace-metals from sea-water with the chelating resin chelamine*. Analytica Chimica Acta. 1993. **272**, 91 - 97.
- Bloxham, M.J., Hill, S.J., and Worsfold, P.J. *Determination of trace-metals in sea-water and the online removal of matrix interferences by flow-injection with inductively-coupled plasma-mass spectrometric detection*. Journal of Analytical Atomic Spectrometry. 1994. **9**, 935 - 938.
- Bowen, E.J. and Lloyd, R.A. *Chemiluminescence from dissolved oxygen*. Proc. Chem. Soc. (London). 1963.
- Bowie, A.R., Achterberg, E.P., Mantoura, R.F.C., and Worsfold, P.J. *Determination of sub-nanomolar levels of iron in seawater using flow injection with chemiluminescence detection*. Analytica Chimica Acta. 1998. **361**, 189 - 200.
- Bowie, A.R., Fielden, P.R., Lowe, R.D., and Snook, R.D. *Sensitive determination of manganese using flow injection and chemiluminescent detection*. Analyst. 1995. **120**, 2119 - 2127.
- Bowie, A.R., Sanders, M.G., and Worsfold, P.J. *Analytical applications of liquid-phase chemiluminescence reactions - a review*. Journal of Bioluminescence and Chemiluminescence. 1996. **11**, 61 - 90.

- Boyle, E.A., Sclater, F.R., and Edmond, J.M. *The distribution of dissolved copper in the Pacific. Earth Planet. Earth and Planetary Science Letters.* 1977. **37**, 38-54.
- Bradford, G.R. and Bakhtar, D. *Determination of trace-metals in saline irrigation drainage waters with inductively coupled plasma optical-emission spectrometry after preconcentration by chelation solvent- extraction.* Environmental Science & Technology. 1991. **25**, 1704 - 1708.
- Brasil, J.C., DoNascimento, P.V.B., and Santelli, R.E. *Flow injection spectrophotometric determination of cobalt in silicate rocks employing cobalt-nitroso-R complex retention on activated alumina minicolumn.* Quimica Analitica. 1996. **15**, 135 - 139.
- Brewer, P.G. *Trace elements in seawater* in "Chemical Oceanography". Eds. Riley, J.P. and Skirrow, G. Academic Press, New York 1975. 2nd, vol. **1**, 415 - 496.
- Bruland, K.W. and Franks, R.P. *Mn, Ni, Cu, Zn and Cd in the western North Atlantic* in "Trace Metals in Seawater". Eds. Wong, C.S., Boyle, E.A., Bruland, K.W. and Goldberg, E.D. Plenum Press, New York. 1983a. 395 - 414.
- Bruland, K.W. *Trace Elements in Sea-water* in "Chemical Oceanography". Eds. Riley, J.P. and Chester, R. Academic Press. 1983b.
- Buckley, P.J.M. and van den Berg, C.M.G. *Copper complexation profiles in the Atlantic Ocean.* Marine Chemistry. 1986. **19**, 281 - 296.
- Burdo, T.G. and Seitz, W.R. Anal.Chem. 1975. **47**, 1639.
- Burton, J.D. and Statham, P.J. *Trace metals as tracers in the ocean.* Philosophical Transactions of the Royal Society of London. 1988. **325**, 127 - 145.
- Burton, J.D., Althaus, M., Millward, G.E., Morris, A.W., Statham, P.J., Tappin, A.D., and Turner, A. *Processes influencing the fate of trace metals in the North Sea.* Phil. Trans. R. Soc. London. 1993. **343A**, 557 - 568.
- Campbell, A.K. *Chemiluminescence.* 1988. Ellis Horwood, Chichester.
- Cannizzaro, V., Bowie, A.R., Sax, A., Achterberg, E.P., and Worsfold, P.J. *Determination of cobalt and iron in estuarine and coastal waters using flow injection with chemiluminescence detection.* Analyst. 1999. **125**, 51 - 57.
- Carruthers J.N. *The water movements in the southern North Sea - Part I: The surface currents.* 1925. 1 - 114.
- Chang, H.J., Sung, Y.H., and Huang, S.D. *Determination of ultra-trace amounts of cadmium, cobalt and nickel in sea-water by electrothermal atomic absorption spectrometry with on-line preconcentration.* Analyst. 1999. **124**, 1695 - 1699.
- Chapin, T.P., Johnson, K.S., and Coale, K.H. *Rapid determination of manganese in sea water by flow-injection analysis with chemiluminescence detection.* Analytica Chimica Acta. 1991. **249**, 469-478

- Charnock, H., Dyer, K.R., Huthnance, J.M., Liss, P.S., Simpson, J.H., and Tett, P.B. *Understanding the North Sea System*. Eds. Chapman, A.H. and Hall, G.E.M. London. 1994.
- Chen, G.N., Duan, J.P., and Hu, Q.F. *Flow-injection chemiluminescent detection of trace Co(II) with dibromoalizarin violet-H₂O₂-CTMAB system*. Mikrochimica Acta. 1994. **116**, 227 - 238.
- Chen, H., Wei, D.B., An, T.C., and Fang, Y.J. *The determination of Mn(II) in water by reversed flow injection spectrophotometry*. Analytical Letters. 1999. **32**, 787 - 797.
- Chester, R. *Marine Geochemistry*. Unwin Hyman. London. 2000. 1st Ed.
- Chester, R., Nimmo, M., Fones, G.R., Keyse, S., and Zhang, Z. *Trace metal chemistry of particulate aerosols from the UK mainland coastal rim of the NE Irish sea*. Atmospheric Environment. 2000. **34**, 949 - 958.
- Chin, C.S., Johnson, K.S., and Coale, K.H. *Spectrophotometric determination of dissolved manganese in natural- waters with 1-(2-Pyridylazo)-2-Naphthol - application to analysis in situ in hydrothermal plumes*. Marine Chemistry. 1992. **37**, 65 - 82.
- Coale, K.H., Johnson, K.S., Stout, P.M., and Sakamoto, C.M. *Determination of copper in seawater using a flow-injection method with chemiluminescence detection*. Analytica Chimica Acta. 1992. **266**, 345-351.
- Colombo, C., vandenBerg, C.M.G., and Daniel, A. *A flow cell for on-line monitoring of metals in natural waters by voltammetry with a mercury drop electrode*. Analytica Chimica Acta. 1997. **346**, 101 - 111.
- Cotton, A.A. and Wilkinson, G. *Advanced inorganic chemistry*. John Wiley and Sons. New York, 1980. 4th Ed.
- Cullen, J.T. and Sherrell, R.M. *Techniques for determination of trace metals in small samples of size-fractionated particulate matter: phytoplankton metals off central California*. Marine Chemistry. 1999. **67**, 233 - 247.
- Danielsson, L.G. *Cadmium, cobalt, copper, iron, lead, nickel and zinc in Indian Ocean Water*. Marine Chemistry. 1980. **8**, 199 - 215.
- de Jong, J.T.M., Boye, M., Schoemann, V.F., Nolting, R.F., and de Baar, H.J.W. *Shipboard techniques based on flow injection analysis for measuring dissolved Fe, Mn and Al in seawater*. Journal of Environmental Monitoring. 2000. **2**, 496 - 502.
- de Jong, J.T.M., den Das, J., Bathmann, U., Stoll, M.H.C., Kattner, G., Nolting, R.F., and de Baar, H.J.W. *Dissolved iron at sub-nanomolar levels in the Southern Ocean as determined by shipboard analysis*. Analytica Chimica Acta. 1998. **377**, 113 - 124.
- Dedeurwaeder, H.L., Baeyens, W.F., and Dehairs, F.H. *Estimates of dry and wet deposition of several trace metals in the southern Bight of the North Sea*. 1985. **1**, 135 - 137.

- Dehairs, F., Baeyens, W., and Vangansbeke, D. *Tight coupling between enrichment of iron and manganese in North Sea suspended matter and sedimentary redox processes - evidence for seasonal variability*. Estuarine Coastal and Shelf Science. 1989. **29**, 457 - 471.
- Dierssen, H., Belzer, W., and Landing, W.M. *Simplified synthesis of an 8-hydroxyquinoline chelating resin and a study of trace metal profiles from Jellyfish Lake, Palau*. Marine Chemistry. 2001. **73**, 173 - 192.
- Donat, J.R. and Bruland, K.W. *Direct determination of dissolved cobalt and nickel in seawater by differential pulse cathodic stripping voltammetry preceded by adsorptive collection of their nioxime complexes*. Analytical Chemistry. 1988. **60**, 240-244 .
- Donat, J.R. and Bruland, K.W. *Trace Elements in the Oceans* in "Trace Metals in Natural Waters". Eds. Salbu, B. and Steinners, E. CRC Press, Boca Raton, FL (USA). 1995. 247 - 281.
- Economou, A., Fielden, P.R., and Efstathiou, C.E. *Virtual instrumentation for stripping voltammetry on the rotating disk electrode*. Instrumentation Science & Technology. 2000. **28**, 379 - 386.
- Eisma, D., and Kalf, J. *Dispersal, concentration and deposition of suspended matter in the North Sea*. J. of the Geological Soc. of London. 1987. **144**, 161 - 178.
- Elinany, G.A, Ebeid, F.M, Zahara, A.M. and Ziedan, F.I. J. Electroanal. Chem. 1976. **72**, 363.
- Ellwood, M.J. and van den Berg, C.M.G. *Determination of organic complexation of cobalt in seawater by cathodic stripping voltammetry*. Marine Chemistry. 2001. **75**, 33 - 47.
- Elrod, V.A., Johnson, K.S., and Coale, K.H. *Determination of subnanomolar levels of iron(II) and total dissolved iron in seawater by flow injection analysis with chemiluminescence detection*. Analytical Chemistry. 1991. **63**, 893 - 898.
- Encyclopaedia of Analytical Sciences, Academic Press, London. Vol. 2 and Vol. 5. 1995
- Emerson, S., Kalhorn, S., Jacobs, L., Tebo, B.M., Nealson, K.H., and Rosson, R.A. *Environmental oxidation rate of manganese(II): bacterial catalysis*. Geochimica et Cosmochimica Acta. 1982. **46**, 1073-1079.
- Emmenegger, L., King, D.W., Sigg, L., and Sulzberger, B. *Oxidation kinetics of Fe(II) in a eutrophic Swiss lake*. Abstracts of Papers of the American Chemical Society. 1997. **213**, 95 - GEOC.
- Escobar, R., Garcia-Dominguez, M.S., Guiraum, A., and Delarosa, F.F. *Determination of Cr(III) in urine, blood serum and hair using flow injection chemiluminescence analysis*. Fresenius Journal of Analytical Chemistry. 1998. **361**, 509 - 511.

- Escobar, R., Lin, Q., Guiraum, A., and Delarosa, F.F. *Determination of trivalent, and hexavalent chromium in waste water by flow injection chemiluminescence analysis*. International Journal of Environmental Analytical Chemistry. 1995. **61**, 169 - 175.
- Escobar, R., Lin, Q.X., Guiraum, A., and Delarosa, F.F. *Flow injection chemiluminescence method for the selective determination of chromium(III)*. Analyst. 1993. **118**, 643 - 647.
- Falk, H., Geerling, R., Hattendorf, B., Krenzel Rothensee, K., and Schmidt, K.P. *Capabilities and limits of ICP-MS for direct determination of element traces in saline solutions*. Fresenius Journal of Analytical Chemistry. 1997. **359**, 352 - 356.
- Fang Z., Xu S., and Zhang S. *Fundamental and practical considerations in the design of on-line column preconcentration for flow-injection atomic spectrometric systems*. Analytica Chimica Acta. 1987. **200**, 35 - 49.
- Fang, Z. *Flow injection separation and preconcentration*. VCH, New York. 1993.
- Field, M.P., Cullen, J.T., and Sherrell, R.M. *Direct determination of 10 trace metals in 50 μ l samples of coastal seawater using desolvating micronebulization sector field ICP-MS*. Journal of Analytical Atomic Spectrometry. 1999. **14**, 1425 - 1431.
- Fileman, C.F., Althaus, M., Law, R.J., and Haslam, I. *Dissolved and particulate trace-metals in surface waters over the Dogger Bank, central North Sea*. Marine Pollution Bulletin. 1991. **22**, 241 - 244.
- Fritz J.S. *Analytical solid-phase extraction*. John Wiley and Sons, New York. 1999.
- FTNS *Flushing times of the North Sea*. Co-operative Research Report 123, International Council for the Exploration of the Sea, Copenhagen. 1983
- Fukai, R. *A spectrophotometric method for determination of cobalt in sea-water after enrichment with solid manganese dioxide*. J. Oceanographical Society, Japan. 1967. **24**, 265 - 274.
- Gao, H.W. *Analysis of cobalt solution with m-chloroazoantipyline and determination of trace amounts of cobalt by beta-correction spectrophotometry*. Canadian Journal of Applied Spectroscopy. 1996. **41**, 113 - 118.
- Garrels, R.M. and Christ, C.L. *Solutions, Minerals and Equilibria*. Harper and Row. 1965.
- Gassama, N., Sarazin, G., and Evrard, M. *the distribution of Ni and Co in a eutrophic lake - an application of a square-wave voltammetry method*. Chemical Geology. 1994. **118**, 221 - 233.

- Ghoneim, M.M., Hassanein, A.M., Hammam, E., and Beltagi, A.M. *Simultaneous determination of Cd, Pb, Cu, Sb, Bi, Se, Zn, Mn, Ni, Co and Fe in water samples by differential pulse stripping voltammetry at a hanging mercury drop electrode*. Fresenius Journal of Analytical Chemistry. 2000. **367**, 378 - 383.
- Gledhill, M., Nimmo, M., Hill, S.J., and Brown, M.T. *The toxicity of Cu(II) species to marine algae, with particular reference to macroalgae*. Journal of Phycology. 1997. **33**, 2 - 11.
- Gollnick, K., and Kuhn, H.J., in H.H., Wasserman and R.W., Murray (Eds.). *Singlet Oxygen*. Academic, New York. 1979. Chap. 8, p. 290.
- Goto, K., Taguchi, S., Miyabe K., and Haruyama K. *Effect of cationic surfactant on the formation of ferron complexes*. Talanta. 1982. **29**, 569 - 575.
- Grasshoff, K., Ehrhardt, M., and Kremling, K. *Methods of Seawater Analysis*. Weinheim Verlag Chemie. 1983.
- Grotti, M., Leardi, R., Gnecco, C., and Frache, R. *Determination of manganese by graphite furnace atomic absorption spectrometry: matrix effect control by multiple linear regression model*. Spectrochimica Acta Part B-Atomic Spectroscopy. 1999. **54**, 845 - 851.
- Haraldsson, C., Lyven, B., Pollak, M., and Skoog, A. *Multielement speciation of trace-metals in fresh-water-adapted to plasma source-mass spectrometry*. Analytica Chimica Acta. 1993. **284**, 327 - 336.
- Harris D.C. *Quantitative chemical analysis*. 4th Edition Freeman W.H.C. New York. 1995.
- Hartenstein, S.D., Ruzicka, J., and Christian, G.D. *Sensitivity enhancements for flow-injection analysis inductively coupled plasma atomic emission-spectrometry using an online preconcentrating ion-exchange column*. Analytical Chemistry. 1985. **57**, 21 - 25.
- Hashemi, P. and Olin, A. *Equilibrium and kinetic properties of a fast iminodiacetate based chelating ion exchanger and its incorporation in a FIA-ICP-AES system*. Talanta. 1997. **44**, 1037 - 1053.
- Heggie, D., Klinkhammer, G., and Cullen, D. *Manganese and copper fluxes from continental-margin sediments*. Geochimica et Cosmochimica Acta. 1987. **51**, 1059 - 1070.
- Hering, R. *Chelatbildende Ionenaustauscher*. Akademie-Verlag. Berlin. 1967.
- Herreramelian, J.A., Hernandezbrito, J., Geladocaballero, M.D., and Perezpena, J. *Direct determination of cobalt in unpurged oceanic seawater by high-speed adsorptive cathodic stripping voltammetry*. Analytica Chimica Acta. 1994. **299**, 59 - 67.
- Hewitt, C.N. and Nicholas D.J. *Cations and anions: Inhibitions and interactions in metabolism and enzyme activity*. in "Metabolic inhibitors" Academic, Eds. R.M. Hochster and J.H. Questel. 1963. **vol. 2.**, 311 - 436.

- Hinze, W.L., Riehl, T.E., Singh, H.N., and Baba, Y. *Micelle-enhanced chemiluminescence and application to the determination of biological eductants using lucigenin*. *Analytical Chemistry*. 1984a. **56**, 2180 - 2191.
- Hinze, W.L., Singh, H.N., Baba, Y., and Harvey, N.G. *Micellar enhanced analytical fluorimetry*. *Trac-Trends in Analytical Chemistry*. 1984b. **3**, 193 - 199.
- Hirata, S., Aihara, M., Hashimoto, Y., and Mallika, G.V. *On-line column preconcentration for the determination of cobalt in sea water by flow-injection chemiluminescence detection*. *Fresenius Journal of Analytical Chemistry*. 1996. **355**, 676 - 679.
- Hirata, S., Umezaki, Y., and Ikeda, M. *Determination of chromium(III), titanium, vanadium, iron(III), and aluminium by inductively coupled plasma atomic emission-spectrometry with an online preconcentrating ion-exchange column*. *Analytical Chemistry*. 1986. **58**, 2602 - 2606.
- Hopkins, D.M. *An analytical method for hydrogeochemical surveys - inductively coupled plasma-atomic emission-spectrometry after using enrichment coprecipitation with cobalt and ammonium pyrrolidine dithiocarbamate*. *Journal of Geochemical Exploration*. 1991. **41**, 349 - 361.
- Howard, A.G. and Statham, P.J. *Inorganic trace analysis: philosophy and practice*. Wiley. 1993.
- Hughes, D.M., Chakrabarti, C.L., Goltz, D.M., Gregoire, D.C., Sturgeon, R.E., and Byrne, J.P. *Seawater as a multicomponent physical carrier for ETV-ICP-MS*. *Spectrochimica Acta Part B-Atomic Spectroscopy*. 1995. **50**, 425 - 440.
- Hydes, D. *Seasonal variation in dissolved aluminium concentrations in coastal waters and biological limitation of the export of the riverine input of aluminium to the deep sea*. *Continental Shelf Res.* 1989. **9**, 919 - 929.
- Hydes, D.J. and Kremling, K. *Patchiness in dissolved metals (Al, Cd, Co, Cu, Mn, Ni) in North Sea surface waters: seasonal differences and influence of suspended matter*. *Continental Shelf Research*. 1993. **13**, 1083-1101.
- Hydes, D.J. *Continuous-flow determination of manganese in natural-waters containing iron*. *Analytica Chimica Acta*. 1987. **199**, 221 - 226.
- Hydes, D.J., Elly-Gerreyn, B.A., Gall, A.C., and Rector, R. *The balance of supply of nutrients and demands of biological production and denitrification in a temperate latitude shelf sea - a treatment of the southern North Sea as an extended estuary*. *Marine Chemistry*. 1999. **68**, 117 - 131.
- Igarashi, S., Aihara, T., and Yotsuyanagi, T. *Flow injection spectrophotometric determination of ng ml⁻¹ levels of cobalt(II) using the photochemical decomposition of a cadmium(II)-water-soluble porphyrin complex*. *Analytica Chimica Acta*. 1996. **323**, 63 - 67.
- Imdadullah *Development of new hybrid analytical methods based on the combination of solvent-extraction with reversed micellar-mediated*

- chemiluminescence detection and their application to the trace determination of precious metals.* Bunseki Kagaku (Japan Analyst). 1994. **43**, 363 - 364.
- Imdadullah, Fujiwara, T., and Kumamaru, T. *Chemiluminescence from the reaction of chloroauric acid with luminol in reverse micelles.* Analytical Chemistry. 1991. **63**, 2348 - 2352.
- Isshiki, K. and Nakayama, E. *Determination of ultratrace amounts of cobalt by catalysis of the tiron hydrogen-peroxide reaction with an improved continuous-flow analysis system.* Talanta. 1987. **34**, 277 - 281.
- Jarvie, H.P., Neal, C., and Tappin, A.D. *European land-based pollutant loads to the North Sea: an analysis of the Paris Commission data and review of monitoring strategies.* Sci. of the Total Environment. 1997. **194/195**, 39-58.
- Jickells, T.D., Church, T.M., and Deuser, W.G. *Global Biogeochemical Cycles.* 1987. **1**, 117 - 130.
- Johnson, K.S., Stout P.M., Berelson, W.M., and Sakamoto-Arnold, C.M. *Cobalt and copper distributions in the waters of Santa Monica Basin, California.* Nature. 1988. **332**, 527 - 530.
- Jones, P. and Beere, H.G. *Ion chromatography determination of trace silver ions using hydrophilic resins with chemiluminescence detection.* Analytical Proceedings. 1995. **32**, 169 - 171.
- Jorgensen, S.S., Petersen, K.M., and Hansen, L.A. *A simple multifunctional valve for flow-injection analysis.* Analytica Chimica Acta. 1985. **169**, 51 - 57.
- Kantipuly, C., Katragadda, S., Chow, A., and Gesser, H.D. *Chelating polymers and related supports for separation and preconcentration of trace-metals.* Talanta. 1990. **37**, 491 - 517.
- Karlberg, B. and Pacey, G. *Flow Injection Analysis - a practical guide.* Elsevier, Amsterdam. 1989.
- Kearns, D.R., in H.H., Wasserman and R.W., Murray (Eds.). *Singlet Oxygen.* Academic, New York. 1979. Chap. 4, p. 120.
- Kenawy, I.M.M. and Hafez, M.A.H. *Preconcentration and multielement determination in different water samples using cellulose-sodium sulphide and/or the thiourea system with atomic absorption spectrometry.* Analisis. 1996. **24**, 275 - 280.
- Kendrick, K.D., May, M.T., Plishka, M.J., and Robinson, M.J. *Metals in biological systems.* Ellis Horwood: Chichester. 1992. 71 - 79.
- King, D.W., Lounsbury, H.A., and Millero, F.J. *Rates and mechanism of Fe(II) oxidation at nanomolar total iron concentrations.* Environmental Science and Technology. 1995. **29**, 818 - 824.
- Klemm, W., Bombach, G., and Becker, K.P. *Investigations of trace elements in high salinity waters by ICP-MS.* Fresenius Journal of Analytical Chemistry. 1999. **364**, 429 - 432.

- Klinkhammer G.P. and Bender M.L. *The distribution of manganese in the Pacific Ocean*. Geoch. Cosmoch. Acta. 1980. **46**, 361 - 384.
- Klinkhammer, G., Bender M., and Weiss, R.F. *Hydrothermal manganese in the Galapagos Rift*. Nature. 2000. **269**, 319 - 320.
- Klinkhammer, G.P. *Fiber optic spectrometers for in-situ measurements in the oceans - the zaps probe*. Marine Chemistry. 1994. **47**, 13 - 20.
- Klinkhammer, G.P., Rona, P., Greaves, M., and Elderfield, H. *Hydrothermal manganese plumes in the Mid-Atlantic ridge rift valley*. Nature. 1991. **314**, 727 - 731.
- Klopf, L.L. and Nieman, T.A. *Effect of iron(II), cobalt(II), copper(II), and manganese(II) on the chemiluminescence of luminol in the absence of hydrogen peroxide*. Analytical Chemistry. 1983. **55**, 1080 - 1083.
- Knauer, G.A., Martin, J.H., and Gordon, R.M. *Cobalt in north-east Pacific waters*. Nature. 1982. **297**, 49 - 51.
- Kobayashi, M. and Shimizu, S. *Cobalt proteins*. European Journal of Biochemistry. 1999. **261**, 1 - 9.
- Komatsu, T., Ohira, M., Yamada, M., and Suzuki, S. *Analytical use of luminescence induced ultrasonically in solution. Part 1. Sonic chemiluminescence of luminol for determination of cobalt(II) at sub-pg levels by flow-injection and continuous-flow methods*. Bulletin of the Chemical Society of Japan. 1986. **59**, 1849 - 1855.
- Koshino, Y. and Narukawa, A. *Determination of manganese, iron and copper in sodium by chemical modification graphite-furnace atomic-absorption spectrometry*. Talanta. 1993. **40**, 799 - 803.
- Kostka, J.E., Luther, G.W., and Nealson, K.H. *chemical and biological reduction of Mn(III)-pyrophosphate complexes - potential importance of dissolved Mn(III) as an environmental oxidant*. Geochimica et Cosmochimica Acta. 1995. **59**, 885 - 894.
- Kremling, K. and Hydes D. *Summer distribution of dissolved Al, Cd, Co, Cu, Mn, and Ni in surface waters around the British Isles*. Continental Shelf Research. 1988. **8**, 89 - 105.
- Kremling, K. *The distribution of cadmium, copper, nickel, manganese, and aluminum in surface waters of the open atlantic and european shelf area*. Deep-Sea Research Part A-Oceanographic Research Papers. 1985. **32**, 531 - 555.
- Kremling, K., Wenck, A., and Pohl, C. *Summer distribution of dissolved Cd, Co, Cu, Mn, and Ni in Central North Sea Waters*. Dtsch. Hydrogr. Z. 1987. **40**, 102 - 114.
- Kryszewski, M., Ciesielski, W., and Pecherz, J. Acta Polymer. 1981. **32**, 524.
- Kumagai, H., Yamanaka, M., Sakai, T., Yokoyama, T., Suzuki, T.M., and Suzuki, T. *Determination of trace metals in sea-water by inductively coupled plasma mass spectrometry interfaced with an ion chromatographic separation*

- system: effectiveness of nitrilotriacetate chelating resin as the column stationary phase for preconcentration and elimination of matrix effects.* Journal of Analytical Atomic Spectrometry. 1998. **13**, 579 - 582.
- Kunitake, T., and Okahata, Y. J. of American Chemical Soc. 1977. **99**, 3860.
- Kyaw, T., Fujiwara, T., Inoue, H., Okamoto, Y., and Kumamaru, T. *Reversed micellar mediated luminol chemiluminescence detection of iron(II, III) combined with on-line solvent extraction using 8- quinolinol.* Analytical Sciences. 1998. **14**, 203 - 207.
- Laevastu, T. *Serial atlas of the marine environment.* 1963.
- Lamoureux, M.M., Gregoire, D.C., Chakrabarti, C.L., and Goltz, D.M. *Modification of a commercial electrothermal vaporizer for sample introduction into an inductively-coupled plasma-mass spectrometer: 2. performance evaluation.* Analytical Chemistry. 1994. **66**, 3217 - 3222.
- Lan, C.R. and Yang, M.H. *Synthesis, properties and applications of silica-immobilized 8- quinolinol. Part 2. Online column preconcentration of copper, nickel and cadmium from seawater and determination by Inductively-Coupled Plasma-Atomic emission-Spectrometry.* Analytica Chimica Acta. 1994. **287**, 111 - 117.
- Landing, W.M. and Bruland, K.W. *The contrasting biogeochemistry of iron and manganese in the Pacific Ocean.* Geochimica et Cosmochimica Acta. 1987. **51**, 29 - 43.
- Landing, W.M. and Lewis, B.L. *Thermodynamic modelling of trace metal speciation in the Black Sea.* NATO-ASI Symposium series "Black Sea oceanography". 1991. 125 - 160.
- Landing, W.M., Haraldsson, C., and Paxeus, N. *Vinyl polymer agglomerate based transition metal chelating ion- exchange resin containing the 8-Hydroxyquinoline functional group.* Analytical Chemistry. 1986. **58**, 3031-3035 -
- Lee, A.J. *North Sea: physical oceanography.* 1980. 467 - 492.
- Lewis, B.L. and Landing, W.M. *The biogeochemistry of manganese and iron in the black-sea.* Deep-Sea Research Part A-Oceanographic Research Papers. 1991. **38**, S773 - S803.
- Lewis, S.W., Price, D., and Worsfold, P.J. *Flow injection assays with chemiluminescence and bioluminescence detection - a review.* Journal of Bioluminescence and Chemiluminescence. 1993. **8**, 183 - 199.
- Li, X.J., Schramel, P., Wang, H.Z., Grill, P., and Kettrup, A. *Determination of trace metal ions Co, Cu, Mo, Mn, Fe, Ti, V in reference river water and reference seawater samples by inductively coupled plasma emission spectrometry combined with the third phase preconcentration.* Fresenius Journal of Analytical Chemistry. 1996. **356**, 52 - 56.

- Li, Y.H. *Distribution patterns of the elements in the ocean - a synthesis*. *Geochimica et Cosmochimica Acta*. 1991. **55**, 3223 - 3240.
- Lin, J.M. and Hobo, T. *Flow-injection analysis with chemiluminescent detection of sulphite using $\text{Na}_2\text{CO}_3\text{-NaHCO}_3\text{-Cu}^{2+}$ system*. *Analytica Chimica Acta*. 1996. **323**, 69 - 74.
- Lin, P.H., Danadurai, K.S.K., and Huang, S.D. *Simultaneous determination of cobalt, nickel and copper in seawater with a multi-element electrothermal atomic absorption spectrometer and microcolumn preconcentration*. *Journal of Analytical Atomic Spectrometry*. 2001. **16**, 409 - 412.
- Lin, Q.X., Guiraum, A., Escobar, R., and Delarosa, F.F. *Flow-injection chemiluminescence determination of cobalt(II) and manganese(II)*. *Analytica Chimica Acta*. 1993. **283**, 379 - 385.
- Makita, Y., Suzuki, T., Yamada, M., and Hobo, T. *Flow injection determinations of cobalt(II) and iron(II) based on chemiluminescence induced by the catalytic decomposition of peroxomonosulfate*. *Nippon Kagaku Kaishi*. 1994. 701 - 706.
- Makita, Y., Umebayashi, H., Suzuki, T., Masuda, A., Yamada, M., and Hobo, T. *New analytical chemiluminescence system using peroxymonosulfate as oxidant*. *Chemistry Letters*. 1993. 1575 - 1578.
- Malahoff, A., Kolotyrkina, I.Y., and Shpigun, L.K. *Shipboard determination of dissolved cobalt in sea-water using flow injection with catalytic spectrophotometric detection*. *Analyst*. 1996. **121**, 1037 - 1041.
- Malamas, F., Bengtsson, M., and Johansson, G. *Online trace-metal enrichment and matrix-isolation in atomic-absorption spectrometry by a column containing immobilized 8-quinolinol in a flow-injection system*. *Analytica Chimica Acta*. 1984. **160**, 1 - 10.
- Manheim F.T. *Marine cobalt resources*. *Science*. 1986. **232**, 600 - 608.
- Mantoura, R.F.C., Dickson, A., and Riley, J.P. *The complexation of metals with humic materials in natural waters*. *Estuar. Coast. Mar. Sci.* 1978. **6**, 387-408.
- Marshall, M.A. and Mottola, H.A. *Performance studies under flow conditions of silica-immobilized 8-quinolinol and its application as a preconcentration tool in flow-injection atomic-absorption determinations*. *Analytical Chemistry*. 1985. **57**, 729 - 733.
- Martell, A.E. and Smith, R.M. *Critical Stability Constants*. 1974. Plenum.
- Martin, J.H. and Knauer, G.A. *Lateral transport of Mn in the Northeast pacific gyre oxygen minimum*. *Nature*. 1985a. **314**, 524 - 526.
- Martin, J.H. *Iron and cobalt in NE Pacific waters*. *EOS*. 1985b. 1291.
- Martin, J.H., Fitzwater, S.E., Gordon, R.M., Hunter, C.N., and Tanner, S.J. *Iron, primary production and carbon nitrogen flux studies during the JGOFS north-atlantic bloom experiment*. *Deep-Sea Research Part II-Topical Studies In Oceanography*. 1993. **40**, 115 - 134.

- Martin, J.H., Gordon, R.M., Fitzwater, S., and Broenkow, W.W. *VERTEX: Phytoplankton/iron studies in the Gulf of Alaska*. Deep-Sea Research Part A-Oceanographic Research Papers. 1989. **36**, 649 - 680.
- Martin, J.-M. and Windom, H.L. *Present and future roles of ocean margins in regulating marine biogeochemical cycles of trace elements*. 1991. Wiley.
- Measures, C.I., Yuan, J., and Resing, J.A. *Determination of iron in seawater by flow injection-analysis using in-line preconcentration and spectrophotometric detection*. Marine Chemistry. 1995. **50**, 3 - 12.
- Meluzova, G.B. and Vassilev, R.F. *Stoichiometry of chemiluminescent oxidation of pyrogallol by oxygen in aqueous solutions*. Mol. Photochem. 1970. **2**, 251 - 257.
- Merenyi, G., Lind, J., and Eriksen, T.E. *Luminol chemiluminescence - chemistry, excitation, emitter*. Journal of Bioluminescence and Chemiluminescence. 1990a. **5**, 53 - 56.
- Merenyi, G., Lind, J., Shen, X., and Eriksen, T.E. *Oxidation potential of luminol - is the autoxidation of singlet organic-molecules an outer-sphere electron-transfer*. Journal of Physical Chemistry. 1990b. **94**, 748 - 752.
- Miller, J.C. and Miller, J.N. *Statistics for analytical chemistry*. 1988.
- Miller, R.J. and Ingle, J.D. *Determination of cobalt by pyrogallol chemiluminescence*. Talanta. 1982. **29**, 303 - 311.
- Millero, F.J. and Sotolongo, S. *The oxidation of Fe(II) With H₂O₂ in seawater*. Geochimica et Cosmochimica Acta. 1989. **53**, 1867 - 1873.
- Millero, F.J., Gonzalez-Davila, M., and Santana-Casiano, J.M. *Reduction of Fe(III) with sulfite in natural waters*. Journal of Geophysical Research-Atmospheres. 1995a. **100**, 7235 - 7244.
- Millero, F.J., Yao, W.S., and Aicher, J. *The speciation of Fe(II) and Fe(III) in natural waters*. Marine Chemistry. 1995b. **50**, 21 - 39.
- Mittal, K.L. and Fendler, E.J. *Solution behaviour of surfactants: theoretical and applied aspects*. 1982. Plenum.
- Moffett, J.W. *The importance of microbial Mn oxidation in the upper ocean: a comparison of the Sargasso Sea and equatorial Pacific*. Deep-Sea Research I. 1997. **44**, 1277 - 1291.
- Moody, J.R. and Beary, E.S. *Purified reagents for trace metals analysis*. Talanta. 1982. **29**, 1003 - 1010.
- Morel, F.M.M. *Principles of aquatic chemistry*. Wiley, New York. 1983.
- Morel, F.M.M., Reinfelder, J.R., Roberts, S.B., Chamberlain, C.P., Lee, J.G., and Yee, D. *Zinc and carbon co-limitation of marine-phytoplankton*. Nature. 1994. **369**, 740 - 742.

- Morley, N.H., Fay, C.W., and Statham, P.J. *Design and use of a clean shipboard handling system for seawater samples*, in *Advances in Underwater Technology, Ocean Science and Offshore Engineering*. Graham & Trotman: 1988. 16th Edition, 283-289.
- Morris, A.W. *Seasonal variation of dissolved metals in inshore waters of the Menai Straits*. Mar. Pollut. Bull. 1974. **5**, 54 - 59.
- Morris, A.W., Bale, A.J., and Howland, R.J.M. *The dynamics of estuarine manganese cycling*. Est. Coastal and Shelf Sciences. 1982. **14**, 174 - 192.
- Mundschenk, H. *Occurrence and behaviour of radionuclides in the Moselle River. 2. Distribution of radionuclides between aqueous phase and suspended matter*. Journal of Environmental Radioactivity. 1996. **30**, 215 - 232.
- Murray, A.P., Spell, B., and Paul, B. *The contrasting geochemistry of Mn and Cr in the eastern tropical Pacific Ocean*, in "Trace metals in seawater". Nato Conference Series 4. Mar. Sci. N. 13. Plenum. 1983. 643 - 669.
- Muto, S., Deguchi, K., Kobayashi, E., Kaneko, E., and Meguro K. J. Coll. and Interface Sci. 1970. **33**, 475.
- Muto, S., Deguchi, K., Shimazaki, Y., Aono, Y., and Meguro, K. Bulletin of The Chemical Society of Japan. 1971. **44**, 2087.
- Myasoedova, G.V. and Savvin, S.B. *Chelating sorbents in analytical-chemistry*. CRC Critical Reviews in Analytical Chemistry. 1986. **17**, 1 - 63.
- Nakahara, S., Yamada, M., and Suzuki, S. *Chemiluminescence for the determination of traces of cobalt(II) by continuous-flow and flow-injection methods*. Analytica Chimica Acta. 1982. **141**, 255 - 262.
- Nakahara, S., Yamada, M., and Suzuki, S. *Chemiluminescence for the determination of traces of cobalt(II) by continuous-flow and flow-injection methods*. Analytica Chimica Acta. 1982. **141**, 255 - 262.
- Nakamura, T., Oka, H., Ishii, M., and Sato, J. *Direct atomisation atomic-absorption spectrometric determination of Be, Cr, Fe, Co, Ni, Cu, Cd, and Pb in water with zirconium hydroxide coprecipitation*. Analyst. 1994. **119**, 1397 - 1401.
- Nakano, S., Fukuda, M., Kageyama, S., Itabashi, H., and Kawashima, T. *Flow-injection determination of chromium(III) by pyrogallol chemiluminescence*. Talanta. 1993. **40**, 75 - 80.
- Nakano, S., Tanaka, K., Oki, R., and Kawashima, T. *Flow-injection spectrophotometry of manganese by catalysis of the periodate oxidation of 2,2'-aziaobis(3- ethylbenzothiazoline-6-sulfonic acid)*. Talanta. 1999. **49**, 1077 - 1082.
- Nakayama, E., Isshiki, K., Sohrin, Y., and Karatani, H. *Automated-determination of manganese in seawater by electrolytic concentration and chemiluminescence detection*. Analytical Chemistry. 1989. **61**, 1392 - 1396.

- National Rivers Authority *Contaminants entering in the Sea*. 1995. Report n. 24. Water Quality Series, Bristol.
- Ngoc, L.H. and Whitehead, N.E. *Ni and Co determination in the North Western Mediterranean by differential pulse cathodic stripping voltammetry*. *Oceanologica Acta*. 1986. **9**, 433 - 438.
- Nickson, R.A., Hill, S.J., and Worsfold, P.J. *Behaviour of matrix cations (Ca^{2+} , K^+ , Mg^{2+} and Na^+) during on-line preconcentration and atomic spectrometric detection of trace metals in natural waters*. *Analytica Chimica Acta*. 1997. **351**, 311 - 317.
- Nickson, R.A., HILL, S.J., and Worsfold, P.J. *Field preconcentration of trace metals from seawater and brines coupled with laboratory analysis using flow injection and ICP- AES detection*. *International Journal of Environmental Analytical Chemistry*. 1999. **75**, 57 - 69.
- Nicolai, M., Rosin, C., Tousset, N., and Nicolai, Y. *Trace metals analysis in estuarine and seawater by ICP-MS using on line preconcentration and matrix elimination with chelating resin*. *Talanta*. 1999. **50**, 433 - 444.
- Nikokavouras, J., Vassilopoulos, G., and Paleos, C.M. *Chemiluminescence in oriented systems - chemi-luminescence of lucigenin in model-membrane structures*. *Journal of the Chemical Society - Chemical Communications*. 1981. 1082 - 1083.
- Nimmo, M. and Chester, R. *The chemical speciation of dissolved nickel and cobalt in Mediterranean rainwaters*. *Science of the Total Environment*. 1993. **135**, 153 - 160.
- Nimmo, M. and Fones, G.R. *The potential pool of Co, Ni, Cu, Pb and Cd organic complexing ligands in coastal and urban rain waters*. *Atmospheric Environment*. 1997. **31**, 693 - 702.
- Nimmo, M., Fones, G.R., and Chester, R. *Atmospheric deposition: A potential source of trace metal organic complexing ligands to the marine environment*. *Croatica Chimica Acta*. 1998. **71**, 323 - 341.
- Nolting, R.F. and de Jong, J.T.M. *Sampling and analytical methods for the determination of trace- metals in surface seawater*. *International Journal of Environmental Analytical Chemistry*. 1994. **57**, 189 - 196.
- Obata, H., Karatani, H., and Nakayama, E. *Automated determination of iron in seawater by chelating resin concentration and chemiluminescence detection*. *Analytical Chemistry*. 1993. **65**, 1524 - 1528.
- Okamura, K., Gamo, T., Obata, H., Nakayama, E., Karatani, H., and Nozaki, Y. *Selective and sensitive determination of trace manganese in sea water by flow through technique using luminol hydrogen peroxide chemiluminescence detection*. *Analytica Chimica Acta*. 1998. **377**, 125 - 131.
- Orians, K.J. and Boyle, E.A. *Determination of picomolar concentrations of titanium, gallium and indium in sea-water by inductively-coupled plasma-*

- mass spectrometry following an 8-hydroxyquinoline chelating resin preconcentration. *Analytica Chimica Acta*. 1993. **282**, 63 - 74.
- Ozturk, D.B., Filik, H., Tutem, E., and Apak, R. *Simultaneous derivative spectrophotometric determination of cobalt(II) and nickel(II) by dithizone without extraction*. *Talanta*. 2000. **53**, 263 - 269.
- Pacyna, J.M. *Estimation of the atmospheric emissions of trace-elements from anthropogenic sources in Europe*. *Atmospheric Environment*. 1984. **18**, 41 - 50.
- Palaroan, W.S., Bergantin, J., and Sevilla, F. *Optical fiber chemiluminescence biosensor for antioxidants based on an immobilized luminol/hematin reagent phase*. *Analytical Letters*. 2000. **33**, 1797 - 1810.
- Paucot, H., and Wollast, R. *Transport and transformation of trace metals in the Scheldt Estuary*. *Marine Chemistry*. 1997. **58**, 229 - 244.
- Pelizzetti, E. and Pramauro, E. *Analytical applications of organised molecular assemblies*. *Anal. Chim. Acta*. 1985. **169**, 1 - 29.
- Perrin D.D. *Masking of chemical reactions*. in "Chemical Analysis". Wiley, New York. 1970. p. 211.
- Pesavento, M. and Baldini, E. *Study of sorption of copper(II) on complexing resin columns by solid phase extraction*. *Analytica Chimica Acta*. 1999. **389**, 59 - 68.
- Porta, V., Abollino, O., Mentasti, E., and Sarzanini, C. *Determination of ultra-trace levels of metal-ions in sea-water with online preconcentration and electrothermal atomic-absorption spectrometry*. *Journal of Analytical Atomic Spectrometry*. 1991. **6**, 119 - 122.
- Porta, V., Sarzanini, C., Mentasti, E., and Abollino, O. *Online preconcentration system for inductively coupled plasma atomic emission-spectrometry with quinolin-8-ol and amberlite XAD-2 resin*. *Analytica Chimica Acta*. 1992. **258**, 237 - 244.
- Powell, K.J. *Application of flow injection analysis adsorption-elution protocols for aluminium fractionation*. *Analyst*. 1998. **123**, 797 - 802.
- Prandle, D. *A modelling study of the mixing of ^{137}Cs in the seas of the European continental shelf*. *Phil. Trans. R. Soc. London*. 1984. **A310**, 407 - 436.
- Price, N.M. and Morel, F.M.M. *Cadmium and cobalt substitution for zinc in a marine diatom*. *Nature*. 1990. **344**, 658 - 660.
- Pyrzynska, K. and Jonca, Z. *Multielement preconcentration and removal of trace metals by solid-phase extraction*. *Analytical Letters*. 2000. **33**, 1441 - 1450.
- Qian, J., Xue, H.B., Sigg, L., and Albrecht, A. *Complexation of cobalt by natural ligands in freshwater*. *Environmental Science & Technology*. 1998. **32**, 2043 - 2050.
- Qin, W., Zhang, Z.J., and Liu, H.J. *Chemiluminescence flow sensor for the determination of vitamin B-12*. *Analytica Chimica Acta*. 1997. **357**, 127 - 132.

- Qin, W., Zhang, Z.J., Li, B.X., and Liu, S.N. *Chemiluminescence flow-sensing system for hydrogen peroxide with immobilized reagents*. *Analytica Chimica Acta*. 1998. **372**, 357 - 363.
- Quinby-Hunt, M.S., and Wilde, P. *Modelling of dissolved elements in seawater*. *Ocean Science and Engineering*. 1986. **11**, 153 - 251.
- Radziszewski B. *Chem. Ber.* 1877. **10**, 70.
- Ramis Ramos, G., Garcia Alvarez-Coque, M.C., Berthod, A., and Winefordner, J.D. *Fluorescence in microemulsions and reversed micelles, A review and new results*. *Anal. Chim. Acta*. 1988. **208**, 1 - 19.
- Rao, C.R.M. *Selective preconcentration of gallium using muromac A-1 ion exchange column*. *Analytica Chimica Acta*. 1995. **318**, 113 - 116.
- Resing, J.A., and Mottl, M.J. *Determination of manganese in seawater using flow-injection analysis with online preconcentration and spectrophotometric detection*. *Analytical Chem.* 1992. **64**, 2682 - 2687.
- Robards, K. and Worsfold, P.J. *Analytical applications of liquid-phase chemiluminescence*. *Analytica Chimica Acta*. 1992. **266**, 147 - 173.
- Robertson, A. *The distribution of cobalt in oceanic waters*. *Geochimica et Cosmochimica Acta*. 1970. **34**, 553 - 567.
- Robson, A.J., and Neal, C. *A summary of regional water quality for eastern UK rivers*. *Sci. of the Total Environment*. 1997. **194/195**, 15-37.
- Roitz, J.S. and Bruland, K.W. *Determination of dissolved manganese(II) in coastal and estuarine waters by differential pulse cathodic stripping voltammetry*. *Analytica Chimica Acta*. 1997. **344**, 175 - 180.
- Ruzicka, J. and Hansen, E.H. *Flow Injection Analysis*. Wiley, New York. 1988. 2nd Edition.
- Ryan, M.A., Miller J.D., and Ingle, J.D. *Anal. Chem.* 1978. **50**, 1772.
- Saager, P.M. *On the relationships between dissolved trace metals and nutrients in seawater*. PhD Thesis 1992.
- Safavi, A. and Baezzat, M.R. *Flow injection chemiluminescence determination of pyrogallol*. *Analytica Chimica Acta*. 1998. **368**, 113 - 116.
- Saito, M.A. and Moffett, J.W. *Complexation of cobalt by natural organic ligands in the Sargasso Sea as determined by a new high-sensitivity electrochemical cobalt speciation method suitable for open ocean work*. *Marine Chemistry*. 2001. **75**, 49 - 68.
- Saitoh, K., Hasebe, T., Teshima, N., Kurihara, M., and Kawashima, T. *Simultaneous flow injection determination of iron(II) and total iron by micelle enhanced luminol chemiluminescence*. *Analytica Chimica Acta*. 1998. **376**, 247 - 254.

- Sakai, H., Tsubota, H., Nakai, T., Ishibashi, J., Akagi, T., Gamo, T., Tilbrook, B., Igarashi, G., Kodera, M., Shitashima, K., Nakamura, S., Fujioka, K., Watanabe, M., Mcmurtry, G., Malahoff, A., and Ozima, M. *Hydrothermal activity on the summit of Loihi Seamount, Hawaii*. *Geochemical Journal*. 1987. **21**, 11 - 21.
- Sakamoto-Arnold, C.M. and Johnson, K.S. *Determination of picomolar levels of Cobalt in seawater by flow injection analysis with chemiluminescence detection*. *Analytical Chemistry*. 1987. **59**, 1789-1794.
- Saleh, M.A. and Wilson, B.L. *Analysis of metal pollutants in the Houston Ship Channel by inductively coupled plasma/mass spectrometry*. *Ecotoxicology and Environmental Safety*. 1999. **44**, 113 - 117.
- Samuelson, O. *Ion-exchange separations in analytical chemistry*. John Wiley and Sons Inc., New York. 1963.
- Schrauzer, G.N. *Cobalt*. in "Metals and their compounds in the environment: occurrence, analysis and biological relevance". Ed. E. Merian. VCH 1991. 872 - 892.
- Segawa, T., Ishikawa, H., Kamidate, T., and Watanabe, H. *Micelle-enhanced fluorescein chemiluminescence catalyzed by horseradish-peroxidase for the determination of hydrogen-peroxide*. *Analytical Sciences*. 1994. **10**, 589 - 593.
- Seitz, W.R. and Hercules, D.M. *Chemiluminescence analysis for trace elements*. in "Chemiluminescence and Bioluminescence". Eds. Cormier, M.J., Hercules, D.M., and Lee, J. Plenum Press, New York. 1973. 427 - 449.
- Sengupta, J.G. and Bouvier, J.L. *Direct determination of traces of Ag, Cd, Pb, Bi, Cr, Mn, Co, Ni, Li, Be, Cu and Sb in environmental waters and geological-materials by simultaneous multielement graphite-furnace atomic-absorption spectrometry with zeeman-effect background correction*. *Talanta*. 1995. **42**, 269 - 281.
- Shiller, A.M. *Dissolved gallium in the Atlantic Ocean*. *Marine Chemistry*. 1998a. **61**, 87 - 99.
- Shiller, A.M., Mao, L.M., and Cramer, J. *Determination of dissolved vanadium in natural waters by flow-injection analysis with colorimetric detection*. *Limnology and Oceanography*. 1998b. **43**, 526 - 529.
- Shimizu, T., Izawa, M., Ichikawa, K., and Shijo, Y. *Graphite-furnace AAS determination of cobalt in natural-water after preconcentration with minicolumn chelating resin*. *Bunseki Kagaku*. 1991. **40**, 45 - 47.
- Sillanpaa, M., Orama, M., Ramo, J., and Oikari, A. *The importance of ligand speciation in environmental research: a case study*. *Science of the Total Environment*. 2001. **267**, 23 - 31.
- Sillen, L.G. *Stability Constants of Metal-Ion Complexes*, Special Publications no. 17. 1964. 2nd, 597 - 599.
- Slawinska, D. and Slawinska, J. *Chemiluminescent flow method for determination of formaldehyde*. *Anal. Chem*. 1975. **47**, 2101 - 2109.

- Slawinska, J. *Chemiluminescence in the process of oxidative ring-opening of purpurogallinquinones*. Photochem. and Photobiology. 1971. **13**, 489 - 497.
- Sperling, M., Yin, X.F., and Welz, B. *Flow-injection online separation and preconcentration for electrothermal atomic-absorption spectrometry. Part 2. Determination of ultra-trace amounts of cobalt in water*. Journal of Analytical Atomic Spectrometry. 1991. **6**, 615 - 622.
- Statham, P.J. and Burton, J.D. *Dissolved manganese in the North Atlantic Ocean, 0-35°N*. Earth and Planetary Science Letters. 1986. **79**, 55-65.
- Statham, P.J. and Chester, R. *Dissolution of manganese from marine atmospheric particulate into seawater and rainwater*. Geochim. Cosmochim. Acta. 1988. **52**, 2433 - 2437.
- Statham, P.J., Auger, Y., Burton, J.D., Choisy, P., Fischer, J.-C., James, R.H., Morley, N.H., Ouddane, B., Pushkaric, E., and Wartel, M. *Fluxes of Cd, Co, Cu, Fe, Mn, Ni, Pb, and Zn through the Strait of Dover into the southern North Sea*. Oceanologica Acta. 1993. **16**, 541-552.
- Statham, P.J., Burton, J.D., and Hydes, D.J. *Cd and Mn in the Alboran Sea and adjacent North Atlantic: geochemical implications for the Mediterranean*. Nature. 1985. **313**, 565-567.
- Statham, P.J., Leclercq, S., Hart, V., Batte, M., Auger, Y., Wartel, M., and Cheftel, J. *Dissolved and particulate trace metal fluxes through the central English Channel, and the influence of coastal gyres*. Continental Shelf Research. 1999. **19**, 2019 - 2040.
- Steffan, I. and Vujicic, G. *Determination of cobalt, molybdenum and vanadium in Austrian mineral waters by ICP-AES after ion-exchange separation and preconcentration*. Mikrochimica Acta. 1993. **110**, 89 - 94.
- Stieg, S., and Nieman, T.A. *Determination of trace amount of cobalt(II) and other metals by the chemiluminescent oxidation of gallic acid*. Anal. Chem. 1977. **49**, 1322 - 1325.
- Sunda, W.G. and Huntsman, S.A. *Cobalt and zinc interreplacement in marine phytoplankton: Biological and geochemical implications*. Limnol. Oceanogr. 1995. **40**, 1404 - 1417.
- Sunda, W.G. and Huntsman, S.A. *Effect of sunlight on redox cycles of manganese in the southwestern Sargasso Sea*. Deep-Sea Research. 1988. **35**, 1297-1317.
- Sunda, W.G. and Huntsman, S.A. *Effect of Zn, Mn, and Fe on Cd accumulation in phytoplankton: Implications for oceanic Cd cycling*. Limnology and Oceanography. 2000. **45**, 1501 - 1516.
- Sunda, W.G. and Huntsman, S.A. *The use of chemiluminescence and ligand competition with EDTA to measure copper concentration and speciation in seawater*. Marine Chemistry. 1991. **36**, 137 - 163.

- Sundby, B., Anderson, L.G., Hall, P.O., Iverfeldt, A., Rutgers van der Loeff, M.M., and Westerlund, S.F.G. *The effect of oxygen on release and uptake of cobalt, manganese, iron and phosphate at the sediment-water interface*. *Geochimica et Cosmochimica Acta*. 1986. **50**, 1281-1288.
- Sung, Y.H., Liu, Z.S., and Huang, S.D. *Automated on-line preconcentration system for electrothermal atomic absorption spectrometry for the determination of copper and molybdenum in sea-water*. *Journal of Analytical Atomic Spectrometry*. 1997a. **12**, 841 - 847.
- Sung, Y.H., Liu, Z.S., and Huang, S.D. *Use of Muromac A-1 chelating resin for determination of copper and molybdenum in seawater by atomic absorption with on-line preconcentration*. *Spectrochimica Acta Part B-Atomic Spectroscopy*. 1997b. **52**, 755 - 764.
- Suzuki, A., Nakadai, F., Itagaki, M., and Watanabe, K. *Catalytic analysis of trace manganese(II) using stilbazo in the presence of ethylenediamine and hydrogen peroxide*. *Bunseki Kagaku*. 1997. **46**, 891 - 894.
- Tappin, A.D., Hydes, D.J., Burton, J.D., and Statham, P.J. *Concentrations, distributions and seasonal variability of dissolved Cd, Co, Cu, Mn, Ni, Pb and Zn in the English Channel*. *Continental Shelf Research*. 1993. **13**, 941-969.
- Tappin, A.D., Millward, G.E., Statham, P.J., Burton, J.D., and Morris, A.W. *Trace metals in the Central and Southern North Sea*. *Estuarine, Coastal and Shelf Science*. 1995. **41**, 275-323.
- Tebo, B.M. and Lee, Y. *Bioleaching Processes*. 1993. 695 - 704.
- Tebo, B.M., Nealson, K.H., Emerson, S., and Jacobs, L. *Microbial mediation of Mn(II) and Co(II) precipitation at the O₂/H₂S interfaces in two anoxic fjords*. *Limnology and Oceanography*. 1984. **29**, 1247 - 1258.
- Tercier, M.L., Buffle, J., and Graziottin, F. *Novel voltammetric in-situ profiling system for continuous real-time monitoring of trace elements in natural waters*. *Electroanalysis*. 1998. **10**, 355 - 363.
- Trautz M. and Schorigin P. *Über Chemilumineszenz*. *Z. Wiss. Photogr. Photochem.* 1905. **3**, 121 - 129.
- Tsukada, S., Miki, H., Lin, J.M., Suzuki, T., and Yamada, M. *Chemiluminescence from fluorescent organic compounds induced by cobalt(II) catalyzed decomposition of peroxomonosulfate*. *Analytica Chimica Acta*. 1998. **371**, 163 - 170.
- Turner, D.R., Whitfield, M., and Dickson, A.G. *The equilibrium speciation of dissolved components in freshwater and seawater at 25 °C and 1 atm pressure*. *Geochimica et Cosmochimica Acta*. 1981. **45**, 855-881.
- Twort, A.C., Law, F.M., Crowley, F.W., and Ratnayaka, D.D. *Water Supply*. 1994. Ed. Edward Arnold. 4th Edition
- US Department of Energy. *Subsurface Science Program: Program overview US DOE*. 1994.

- Valcarcel, M. and Luque de Castro, M.D. *Flow Injection Analysis: principles and applications*. Ellis Horwood, Chichester. 1987.
- van Beusekom, J.E.E. *Distribution of dissolved aluminium in the North Sea: Influence of suspended matter*. 1988. Mitteilungen Geologische-Palaeontologisches Institut Universitat, 117 - 136.
- van Paggé S.A. and Postma L. *North Sea pollution: the use of modelling techniques for the assesment of waste inputs*. 1987. Werkgroep Noodzee, Proceedings Second North Sea Seminar 86, 97 - 113.
- Vega, M. and vandenBerg, C.M.G. *Determination of cobalt in seawater by catalytic adsorptive cathodic stripping voltammetry*. Analytical Chemistry. 1997. **69**, 874 - 881.
- Vice North Sea quality status report 1993 Oslo and Paris Commissions, London. Report: North Sea Task Force. 1993. 132.
- Viseu, M.I., Velazquez, M.M., Campos, C.S., Garcia-Mateos, I., and Costa, S.M.B. *Structural transitions in a bicationic amphiphile system studied by light-scattering, conductivity, and surface tension measurements*. Langmuir. 2000. **16**, 4882 - 4889.
- von Langen, P.J., Johnson, K.S., Coale, K.H., and Elrod, V.A. *Oxidation kinetics of manganese (II) in seawater at nanomolar concentrations*. Geochimica et Cosmochimica Acta. 1997. **61**, 4945 - 4954.
- Watanabe, H., Goto, K., Taguchi, S., McLaren, J.W., Berman, S.S., and Russell, D.S. *Preconcentration of trace-elements in seawater by complexation with 8-hydroxyquinoline and adsorption on C-18 bonded silica-gel*. Analytical Chemistry. 1981. **53**, 738 - 739.
- Watanabe, K. and Rokugawa, K. *Catalytic analysis of trace manganese(II) using catechol and ethylenediamine*. Bunseki Kagaku. 1994. **43**, 303 - 309.
- Watanabe, K., Miyamoto, H., and Itagaki, M. *Determination of zinc(II) using the micellar enhanced chemiluminescence of 1,10-phenanthroline*. Bunseki Kagaku (Japan Analyst). 1999. **48**, 705 - 710.
- Wells, M.L. and Bruland, K.W. *An improved method for rapid preconcentration and determination of bioactive trace metals in seawater using solid phase extraction and high resolution inductively coupled plasma mass spectrometry*. Marine Chemistry. 1998. **63**, 145 - 153.
- Westerlund, S. and Ohman, P. *Cadmium, copper, cobalt, nickel, lead, and zinc in the water column of the Weddell Sea, Antarctica*. Geochimica et Cosmochimica Acta. 1991. **55**, 2127-2146.
- Westerlund, S., Anderson, L.G., Hall, P.O., Iverfeldt, M.M., van der Loeff, M.M.R., and Sundby, B. *Benthic fluxes of cadmium, cobalt, nickel, lead and zinc in the coastal environment*. Geochimica et Cosmochimica Acta. 1986. **50**, 1289 - 1296.

- Whitfield, M. *The mean oceanic residence time (MORT) concept: a rationalisation*. Marine Chemistry. 1979. **8**, 101 – 123.
- Whitfield, M. and Turner, D.R. *The role of particles in regulating the composition of seawater*. in "Aquatic surface chemistry". Ed. Stumm W.J. Wiley & Sons, New York. 1987. p. 457.
- Williams, D.R. *The solution chemistry of metal ion in biological systems* in "The metals of life". Van Nostrand Reinhold Co. 1971.
- Williams, M.R., Millward, G.E., Nimmo, M., and Fones, G. *Fluxes of Cu, Pb and Mn to the northeastern Irish Sea: The importance of sedimental and atmospheric inputs*. Marine Pollution Bulletin. 1998. **36**, 366 - 375.
- Willie, S.N., Iida, Y., and McLaren, J.W. *Determination of Cu, Ni, Zn, Mn, Co, Pb, Cd, and V in seawater using flow injection ICP-MS*. Atomic Spectroscopy. 1998. **19**, 67 - 72.
- Withfield, M. and Turner D.R. *Chemical periodicity and the speciation and cycling of the elements*. In "Trace metals in seawater". (Eds.) C.S. Wong, E. Boyle, K.W. Bruland, J.D. Burton, and E.D. Goldberg. New York Plenum Press. 1983. 719 - 750.
- Wollast, R. and Peters, J.J. *Biogeochemical properties of an estuarine system: the river Scheldt*. In: Biogeochemical of Estuarine Sediments. Proc. UNESCO/SCOR Workshop. Meilreux, 1976, 279 - 293.
- Wollast, R. *The Scheldt Estuary*. In Pollution of the North Sea: an assessment Springer Berlin. 1988. 183 - 193.
- Wong, G.T.F., Pai, S.C., and Chung, S.W. *Cobalt in the western Philippine Sea*. Oceanologica Acta. 1995. **18**, 631 - 638.
- Worsfold, P.J., Achterberg, E.P., Bowie, A.R., Sandford, R.C. and Mantoura, R.F.C., Flow injection with chemiluminescence detection for the shipboard monitoring of trace metals, in Varney, M.S. (Ed.), *Chemical Sensors in Oceanography*, Gordon and Breech, Amsterdam, Netherlands, (2000), pp. 71-94.
- Xie, Z.H., Zhang, F., and Pan, Y.S. *Chemiluminescence detection of trace amounts of cobalt(II) with the 2,6,7-trihydroxy-9-(4'-chlorophenyl)-3-fluorone-hydrogen peroxide-cetyltrimethylammonium bromide system*. Analyst. 1998. **123**, 273 - 275.
- Yamada, M. and Suzuki, S. *Micellar enhanced chemiluminescence of 1,10-phenanthroline for the determination of ultratraces of copper(II) by flow-injection method*. Analytical Letters Part A - Chemical Analysis. 1984. **17**, 251 - 263.
- Yamada, M., Kamiyama, S., and Suzuki, S. *Eosin Y-sensitized chemiluminescence of 7,7,8,8-tetracyanoquinodimethane in surfactant vesicles for determination of manganese(II) at sub-nanogram levels by flow-injection method*. Chemistry Letters. 1985. 1597 - 1600.

- Yamada, M., Komatsu, T., Nakahara, S., and Suzuki, S. *Improved chemiluminescence determination of traces of cobalt(II) by continuous-flow and flow-injection methods*. *Analytica Chimica Acta*. 1983. **155**, 259 - 262.
- Yeats, P.A., Dalziel, J.A., and Moran, S.B. *A Comparison of Dissolved and Particulate Mn And Al Distributions in the Western North Atlantic*. *Oceanologica Acta*. 1992. **15**, 609 - 619.
- Yebrabiurrun, M.C., Bermejobarrera, A., Bermejobarrera, M.P., and Barcielaalonso, M.C. *Determination of trace-metals in natural-waters by flame atomic-absorption spectrometry following online ion-exchange preconcentration*. *Analytica Chimica Acta*. 1995. **303**, 341 - 345.
- Yee, D. and Morel, F.M.M. *In vivo substitution of zinc by cobalt in carbonic anhydrase of a marine diatom*. *Limnology and Oceanography*. 1996. **41**, 573 - 577.
- Yuzefovsky, A.I., Lonardo, R.F., Wang, M.H., and Michel, R.G. *Determination of ultra-trace amounts of cobalt in ocean water by laser-excited atomic fluorescence spectrometry in a graphite electrothermal atomizer with semi online flow-injection preconcentration*. *Journal of Analytical Atomic Spectrometry*. 1994. **9**, 1195 - 1202.
- Zamzow, H., Coale, K.H., Johnson, K.S., and Sakamoto, C.M. *Determination of copper complexation in seawater using flow injection analysis with chemiluminescence detection*. *Analytica Chimica Acta*. 1998. **377**, 133 - 144.
- Zhang, H., van den Berg, C.M.G., and Wollast, R. *The determination of interactions of cobalt(II) with organic compounds in seawater using cathodic stripping voltammetry*. *Marine Chemistry*. 1990. **28**, 285-300.
- Zhang, L.P. and Terada, K. *Spectrophotometric determination of cobalt(II) in water after preconcentration by sorption of its nitroso complex with poly(chlorotrifluoroethylene) resin*. *Analytical Sciences*. 1994. **10**, 161 - 165.
- Zhang, Q.B., Minami, H., Inoue, S., and Atsuya, I. *Determination of ultra-trace amounts of cobalt in seawater by graphite furnace atomic absorption spectrometry after pre- concentration with Ni/8-quinolinol/1-nitroso-2-naphthol complex*. *Analytica Chimica Acta*. 2000. **407**, 147 - 153.
- Zhou, Y.X. and Zhu, G.Y. *Rapid automated in-situ monitoring of total dissolved iron and total dissolved manganese in underground water by reverse-flow injection with chemiluminescence detection during the process of water treatment*. *Talanta*. 1997. **44**, 2041 - 2049.
- Zhuang, Z.X., Wang, X.R., Yang, P.Y., Yang, C.L., and Huang, B.L. *Flow-injection online Co-APDC coprecipitation preconcentration and determination of lead and copper in seawater with graphite- furnace atomic-absorption spectrometry*. *Canadian Journal of Applied Spectroscopy*. 1994. **39**, 101 - 107.
- Zuehlke, R.W., D.R. and Kester, D.R. *Development of Shipboard Copper Analyses by Atomic Absorption Spectroscopy*. in "Mapping Strategies in Chemical Oceanography". Ed. Zirino, A. American Chemical Society, Washington D.C. 1985. 117 - 137.